

Basic Performance, Optimization, and Safety and Risk Evaluation of Next-Generation Refrigerants and Refrigerating and Air Conditioning Technologies

Part 2: Safety and Risk Evaluation of Next-Generation Refrigerants

Year 2020 Progress Report

June 1, 2021

Disclaimer

The Japan Society of Refrigerating and Air Conditioning Engineers (JSRAE) prepared the information contained in this Report with utmost care based on the latest technical information available at that time. Nevertheless, we do not guarantee the accuracy of the information contained in this Report. Additionally, the Society and the authors shall not be held responsible or liable for any damage whatsoever arising from such actions as the utilization or usage of the information and materials contained in this Report.

Copyright

The copyright of this Report is held by its authors. This Report may not be reproduced or copied in whole or in part without permission.

Basic Performance, Optimization, and Safety and Risk Evaluation of Next-Generation Refrigerants and Refrigerating and Air Conditioning Technologies

Part 2: Safety and Risk Evaluation of Next-Generation Refrigerants

Year 2020 Progress Report

June 1, 2021

Edited by the Research Committee on Next-Generation Refrigerants, JSRAE

Published by the Japan Society of Refrigerating and Air Conditioning Engineers

Nihonbashi-Otomi Bldg. 5F, 13-7 Nihon-bashi Odenma-cho,
Chuo-ku, Tokyo, 103-0011 Japan

TEL +81-3-5652-3223 FAX +81-3-5623-3229

Table of contents

Table of contents	2
Chapter 1 Introduction.....	5
1.1 Outline of the NEDO Project.....	5
1.2 Activities of WG II of the Research Committee for Next-Generation Refrigerants.....	7
1.3 About this Report.....	9
References.....	9
Chapter 2 Progress achieved at the University of Tokyo.....	10
2.1 Introduction.....	10
2.2 Refrigerant leakage from a residential split air conditioner.....	10
2.2.1 Method of numerical fluid analysis.....	10
2.2.2 Validation study of the simulation model through refrigerant leakage experiments.....	13
2.2.3 Numerical calculation-based consideration of the maximum allowable charge for flammable refrigerants.....	15
2.2.4 Summary.....	17
2.3 Refrigerant leakage from a commercial refrigerated display cabinet.....	17
2.3.1 Numerical fluid analysis method.....	17
2.3.2 Validation of the simulation model using refrigerant leakage experiments.....	18
2.3.3 Effects of fan operation on the scale of flammable region.....	22
2.3.4 Summary.....	24
2.4 Suppression of diesel explosions at the pump-down of residential air conditioners.....	24
2.4.1 Experimental apparatus and conditions.....	25
2.4.2 Experimental results.....	27
2.4.3 Summary.....	30
References.....	30
Chapter 3 Progress achieved at Suwa University of Science.....	32
3.1 Introduction.....	32
3.2 Structure of the present study.....	32
3.3 Extraction of ignition sources and an evaluation method for their ignition capability.....	33
3.4 Evaluation of the ignition possibility of R290 due to electric sparks.....	34
3.4.1 Evaluation of the ignition possibility due to electric sparks from contact relays.....	34
3.4.2 Evaluation of the ignition possibility due to electric sparks from brush motors.....	37
3.4.3 Evaluation of the ignition possibility due to electric sparks from light switch operations.....	37
3.4.4 Evaluation of the ignition possibility due to electric sparks from power plugging in and unplugging.....	41
3.4.5 Evaluation of the ignition possibility due to electrostatic sparks.....	44
3.5 Ignition hazard of R290 due to various electrical appliances.....	46
3.6 Ignition possibility of R290 due to high-temperature hot surfaces.....	47
3.6.1 Study outline and flow.....	47
3.6.2 Experimental outline.....	47
3.6.3 Experimental results and discussion.....	49
3.7 Summary and future works.....	50
3.7.1 Evaluation of the ignition possibility due to electric sparks.....	50
3.7.2 Evaluation of ignition hazard due to high-temperature surfaces.....	51
References.....	51
Chapter 4 Progress achieved at the Research Institute of Science for Safety and Sustainability, AIST.....	53
4.1 Introduction.....	53
4.2 Ignitability evaluation of real devices present in flammable concentration regions.....	53
4.2.1 Appliances selected for evaluation and experimental method.....	53

4.2.2	Results of ignitability evaluation experiments	53
4.2.3	Summary and plan for ignitability evaluation	55
4.3	Diffusion behavior measurement and physical hazard evaluation of room air-conditioner indoor unit	55
4.3.1	Case studies of refrigerant leakage accidents and determination of leakage conditions	56
4.3.2	Experimental method for the measurement of leakage and diffusion behaviors in the room air conditioner indoor unit	56
4.3.3	Experimental results of the measurement of leakage and diffusion behaviors in the room air conditioner indoor unit	57
4.3.4	Experimental method for full-scale physical hazard evaluation of the room air conditioner indoor unit	59
4.3.5	Experimental results of the full-scale physical hazard evaluation of the room air conditioner indoor unit	60
4.3.6	Summary of the full-scale physical hazard evaluation of the room air conditioner indoor unit	60
4.4	Diffusion behavior measurement and physical hazard evaluation of reach-in display cabinet	61
4.4.1	Experimental method for the measurement of leakage and diffusion behaviors in the reach-in refrigerated display cabinet	61
4.4.2	Experimental results of the measurement of leakage and diffusion behaviors in the reach-in refrigerated display cabinet	61
4.4.3	Experimental method for the full-scale physical hazard evaluation of the reach-in refrigerated display cabinet	62
4.4.4	Experimental results of the full-scale physical hazard evaluation of the reach-in refrigerated display cabinet	62
4.4.5	Summary of the full-scale physical hazard evaluation of the reach-in refrigerated display cabinet	64
	References	64
Chapter 5	Progress achieved at the Research Institute for Sustainable Chemistry, AIST	65
5.1	Introduction	65
5.2	Evaluation of flammability limits of low GWP blend refrigerant	65
5.3	Evaluation of burning velocity of low GWP blend refrigerant	68
5.4	Evaluation of the quenching distance for low-GWP blend refrigerants	70
5.5	Evaluation of the fundamental flammability of conventional blend refrigerants	72
	References	74
Chapter 6	Progress of risk assessment of mini-split air conditioners using A3 refrigerant conducted by JRAIA75	75
6.1	Introduction	75
6.2	The risk assessment outline	75
6.2.1	Scope of the risk assessment	75
6.2.2	The structure of this report	76
6.2.3	Risk assessment method	76
6.2.4	Air conditioners covered by the risk assessment	77
6.2.5	Tolerable values of the risk assessment	78
6.3	Accident occurrence probability	78
6.3.1	Temporal encounter probability	78
6.3.2	Summary about accident occurrence probabilities	80
6.4	Indoor ignition sources	81
6.4.1	Foreseeable indoor ignition sources	81
6.4.2	Open flames	81
6.4.3	High-temperature surfaces	82

6.4.4	Sparks.....	82
6.4.5	Summary of potential ignition sources.....	84
6.4.6	Ignition-source heights.....	84
6.4.7	Indoor flammable region due to refrigerant leakage.....	86
6.4.8	Identification of ignition sources.....	88
6.4.9	Summary of indoor ignition sources.....	88
6.5	Simulation of outdoor refrigerant leak.....	90
6.5.1	Installation condition of outdoor unit.....	90
6.5.2	Simulation of outdoor refrigerant leakage.....	90
6.5.3	Outdoor ignition sources.....	93
6.5.4	Study results of outdoor unit risk from refrigerant leakage simulations.....	93
6.5.5	Possible safety measures for outdoor unit.....	93
6.6	Consideration and proposal for events beyond the assumptions of the risk assessment.....	94
6.6.1	Beyond the assumptions in the risk assessment.....	94
6.6.2	Proposal for unassumed events in risk assessment.....	95
6.7	Summary.....	96
	References.....	96
Chapter 7 Progress of risk assessment of refrigerated display cabinets using A3 refrigerant conducted by JRAIA		
97		
7.1	Introduction.....	97
7.2	Main revision points of International Standard IEC60335-2-89.....	97
7.2.1	Maximum refrigerant charge.....	97
7.2.2	Minimum room floor area.....	97
7.2.3	Refrigerant leak test.....	97
7.3	Refrigerant leak analysis.....	98
7.3.1	Leakage from the refrigerated space of a reach-in refrigerated display cabinet.....	98
7.3.2	Leakage from outside the refrigerated space of a horizontal refrigerated display cabinet.....	102
7.3.3	Leakage from the refrigerated space of a vertical open refrigerated display cabinet.....	104
7.4	Condition and method for risk assessment.....	106
7.4.1	Process of risk assessment and calculation of ignition probability.....	106
7.4.2	Setting of risk model for built-in refrigerated display cabinet.....	106
7.4.3	Life stage of built-in refrigerated display cabinet and scenario for each stage.....	107
7.4.4	Setting of tolerable level.....	110
7.4.5	Refrigerant leak rate.....	111
7.4.6	Refrigerant leak probability.....	111
7.5	Japanese law (High Pressure Gas Safety Act).....	112
7.5.1	Disposal of refrigerant.....	113
7.5.2	Recovery of refrigerant.....	113
7.5.3	Refrigerant charge to refrigerating equipment.....	113
7.6	Japanese Standard.....	114
7.6.1	Maximum refrigerant charge.....	114
7.6.2	Surface temperature.....	114
7.6.3	Measurement exemption time and leakage test exemption.....	114
7.6.4	Refrigerant leak rate.....	115
7.6.5	Ensuring safety while working.....	115
7.7	Task for risk assessment.....	115
7.8	Summary.....	115
	References.....	116

Chapter 1 Introduction

1.1 Outline of the NEDO Project

Under the designated product system of the Freon Emission Control Law, each sector is required to encourage the broader use of low GWP refrigerants. However, no established safety evaluation/risk evaluation methods exist for highly flammable refrigerants, such as hydrocarbons. Accordingly, it is essential to understand the basic characteristics of next-generation refrigerants and to establish concurrently safety/risk evaluation methods for the challenges inherent in next-generation refrigerants, including the development of standards and domestic safety standards as well as international standardization. This will support the development of refrigerating and air-conditioning equipment and the like charged with next-generation refrigerants for achieving energy-saving and low greenhouse effects. Considering such circumstances, this Project aims to lay the development foundation for energy-saving refrigerating and air-conditioning equipment running on next-generation refrigerants and to contribute to achieving the market launch of refrigerants and refrigerating and air-conditioning equipment products by 2026. For this purpose, this Project is geared toward establishing a safety/risk evaluation method for next-generation refrigerants for use in small and medium-size refrigerating and air-conditioning equipment, including industrial-use refrigeration and cold storage equipment and residential air-conditioning equipment.

The NEDO project “Development of Refrigerants and Refrigerating and Air Conditioning Technologies and Evaluation Methods for Achieving Energy-Saving and Low-Greenhouse Effects” includes, among others, a development theme entitled “Development of safety/risk evaluation methods for next-generation refrigerants,” which was jointly proposed by and commissioned to the University of Tokyo, the Suwa University of Science, and the National Institute of Advanced Industrial Science and Technology (AIST) (Research Institute of Science for Safety and Sustainability). The following lists the research themes commissioned to the three institutions for the safety evaluation of fires associated with flammable refrigerants:

[University of Tokyo]

- Evaluation of risks associated with flammable refrigerant leakage
- Evaluation of the severity of harm from indoor fires caused by flammable refrigerants

[Suwa University of Science]

- Screening and modeling of ignition sources
- Physical risk assessment of various ignition sources

[National Institute of Advanced Industrial Science and Technology (Research Institute of Science for Safety and Sustainability)]

• Case studies of accidental refrigerant leakage from refrigerating and air-conditioning equipment and modeling of leakage conditions

- Evaluation of fire-causing abilities of devices in flammable concentration regions
- Diffusion behavior measurement and physical hazard evaluation of small-amount, long-term leakage
- Diffusion behavior measurement and physical hazard evaluation of rapid leakage inside indoor units

Independent of the joint proposals of the three institutions, the National Institute of Advanced Industrial Science and Technology (Research Institute for Sustainable Chemistry) was commissioned by NEDO with the aim of performing a safety evaluation of low-GWP low-flammability mixed refrigerants. The research themes were as follows:

[National Institute of Advanced Industrial Science and Technology (Research Institute for Sustainable Chemistry)]

- Evaluation of the flammability of mixed refrigerants
- Evaluation of practical combustion safety of mixed refrigerants

R-Map, a method for evaluating the risk presented by home appliances, maps out risks as a 6×5 matrix plotting six levels of likelihood and five degrees of harm. This evaluation method was developed by the Union of Japanese Scientists and Engineers under the supervision of the Ministry of Education, Culture, Sports, Science, and Technology. Figure 1-1 shows an example of a typical R-Map.¹⁻¹⁾ Area-A (pink area) corresponds to products that require a recall. Area-B (yellow area) requires that the level of likelihood be reduced to that of the minimum risk. Area-C (blue area) is for

products that present only negligible risks and can be distributed as is. Regarding the likelihood of accidents, the criteria indicate that consumer products such as household appliances can be regarded as safe (deemed as Area-C) even if one fatal accident occurs in 100 years. For example, if one hundred million units of a product have been distributed, as is the case with room air conditioners in Japan, the acceptable likelihood of accidents is 10^{-10} (cases/unit/year). Figure. 1-1 shows an example of the likelihood associated with one hundred million distributed units.

Thus, accident likelihood evaluation and harm severity evaluation must be performed to evaluate the product risk. For a flammable refrigerant leak from refrigerating or air-conditioning equipment to cause a fire, the three conditions (rapid refrigerant leakage, flammable space existence, and ignition source existence) shown in Fig. 1-2 must co-occur. Assuming that the three conditions are independent events, the probability of a fire occurring is obtained as the product of the occurrence probability of rapid refrigerant leakage multiplied by that of the existence of flammable space and that of the existence of ignition source. Therefore, to obtain the probability of a fire occurring, the occurrence probability must be determined for each of the three factors.

Likelihood →		Risk				
		0	I	II	III	IV
Frequently	10^{-4}					Not acceptable
Some time	10^{-5}					
Rare	10^{-6}					
Usually not	10^{-7}					
Very difficult	10^{-8}					
Extremely difficult	10^{-9}					
Near zero	10^{-10}					
Allowable frequency of fire events: 10^{-2} case/year						
Room air conditioner in Japan: 10^8 units						
Allowable frequency of fire events per unit: $10^{-2}/10^8 = 10^{-10}$ case/unit/year						
		Severity →				
		No damage	Minor damage (smoke from product)	Light damage (fire from product, light injury)	Major damage (fire, human injury)	Lethal damage (permanent injury, death, burn down house)

Fig. 1-1 R-Map for consumer products when one hundred million units are distributed.¹⁻¹⁾

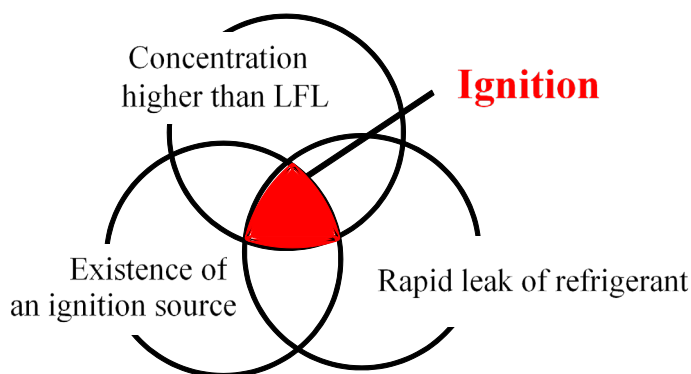


Fig. 1-2 Conditions for fire accident occurrence.

The NEDO project sets out to address the frequency of fires and investigate the severity of the associated damage. Using propane as the refrigerant, we first set out to examine fires associated with refrigerant leakage from room air conditioners and stand-alone display cabinets. Figure 1-3 shows the relationship between the research themes adopted by the three institutions. The three institutions are to undertake their research through mutual cooperation. The final risk evaluation will be conducted through cooperation with the Japan Refrigeration and Air Conditioning Industry Association (JRAIA).

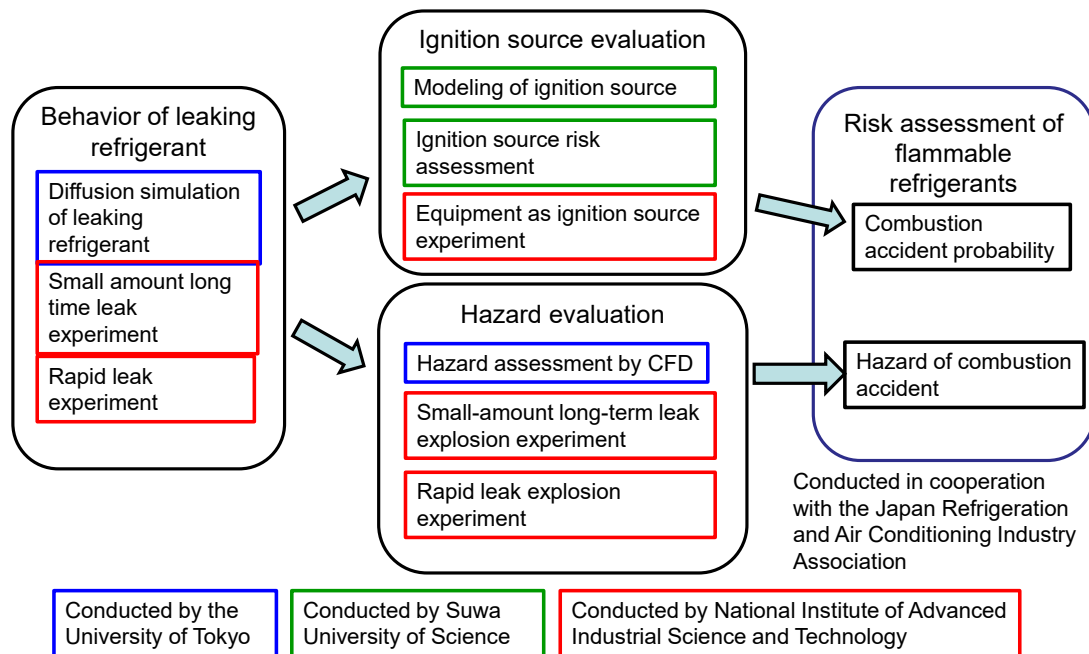


Fig.1-3 Research flows in this project.

1.2 Activities of WG II of the Research Committee for Next-Generation Refrigerants

To encourage the wider adoption of low-GWP refrigerants, which are highly flammable, stakeholders in the industry have highlighted the need for scientific knowledge-based risk evaluation of flammable refrigerants. Research addressing the safety of refrigerants is currently undertaken by various parties, namely the Suwa University of Science, the University of Tokyo, and the National Institute of Advanced Industrial Science and Technology, as part of the New Energy and Industrial Technology Development Organization (NEDO) project “Development of Refrigerants and Refrigerating and Air Conditioning Technologies and Evaluation Methods for Achieving Energy-Saving and Low-Greenhouse Effects” (2018 to 2020). On the other hand, in 2016, JRAIA started to evaluate the risks associated with applying highly flammable refrigerants (A3 refrigerants) to refrigerating and air-conditioning equipment. JRAIA separately discussed the influence of the installation conditions and the existence of ignition sources. To compile the knowledge gained from the above project and perform an objective evaluation from a third-person perspective, the “Research Committee on Next-Generation Refrigerants” was set up in 2018 as a NEDO investigation project within the Japan Society of Refrigerating and Air Conditioning Engineers (JSRAE). Deliberations on the safety of flammable refrigerants and an associated risk evaluation are currently undertaken by the Investigation Committee’s Working Group II (WG II). The WG II deliberation system is built on an industry–government–academia partnership as shown in Fig. 1-4. The breakdown of the Committee membership is shown in Table 1-1:

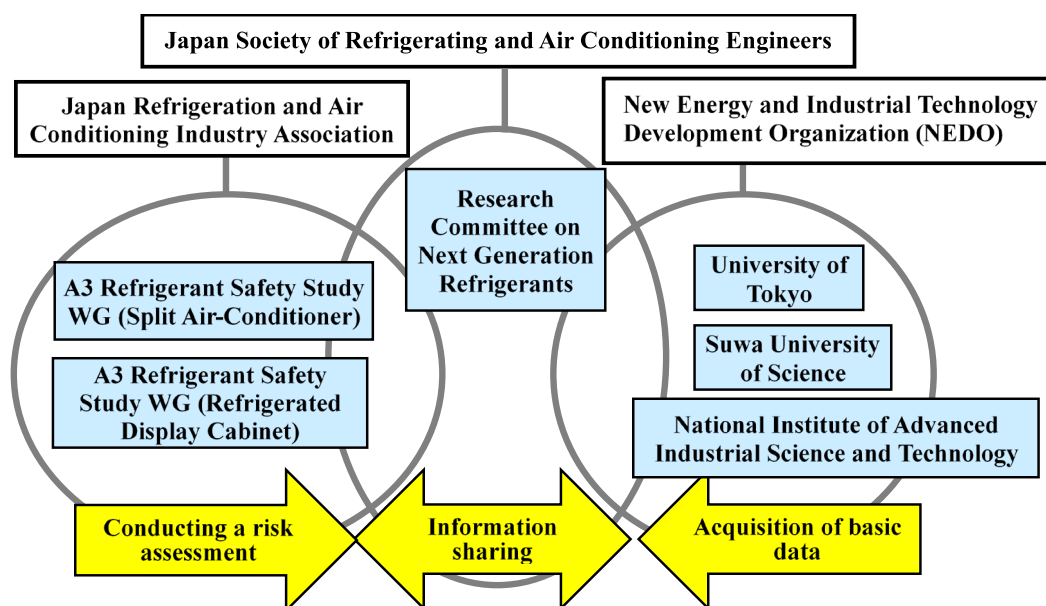


Fig. 1-4 Deliberation system for risk assessment of flammable refrigerants.

Table 1-1 Investigation Committee on Next-Generation Refrigerants, WG II Committee List as of March 1, 2021

	Affiliation	Department	Title	Name	
Chair	National Institution for Academic Degrees and Quality Enhancement of Higher Education	Department of Research and Development	Specially Appointed Professor	Eiji HIHARA	
Committee member	Suwa University of Science	Department of Mechanical-Electrical Engineering, Faculty of Engineering	Associate Professor	Tomohiko IMAMURA	
	National Institute of Advanced Industrial Science and Technology	Research Institute for Sustainable Chemistry	Chief Researcher	Kenji TAKIZAWA	
	National Institute of Advanced Industrial Science and Technology	Research Institute of Science for Safety and Sustainability	Chief Researcher	Hiroumi SHIINA	
Observer	Japan Refrigeration and Air Conditioning Industry Association	Panasonic Corporation		Koji MUROZONO	
		Panasonic Corporation		Kenji TAKAICHI	
		Okamura Corporation		Toshimasa KATOH	
		Mitsubishi Electric Corporation		Koji YAMASHITA	
		Toshiba Carrier Corporation		Hiroichi YAMAGUCHI	
		Daikin Industries, Ltd.		Satoru FUJIMOTO	
		Daikin Industries, Ltd.		Shigeharu TAIRA	
		Hitachi-Johnson Controls Air Conditioning, Inc.		Toshiharu SASAKI	
		Mitsubishi Heavy Industries Thermal Systems, Ltd.		Kenji MATSUDA	
		Engineering Department	Department Manager/Councilor	Takeshi SAKAI	
			Councilor	Kazuhiro HASEGAWA	
		University of Tokyo	Graduate School of Frontier Sciences	Associate Professor	Chaobin DANG
				Specially Appointed Researcher	Makoto ITOH
		Suwa University of Science	Department of Mechanical-Electrical Engineering, Faculty of Engineering	Lecturer	Kyoko KAMIYA
		Tokyo University of Marine Science and Technology	Department of Marine Electronics and Mechanical Engineering	Professor	Norihiro INOUE
	National Institute of Advanced Industrial Science and Technology	Research Institute of Science for Safety and Sustainability	Research Group Leader	KUBOTA Shiro	
	New Energy and Industrial Technology Development Organization	Department of Environment	Senior Chief Researcher	Satoshi FUJIGAKI	
			Chief Researcher	Masamichi ABE	
			Specialist Researcher	Tatsuhiko TAKAHASHI	
			Chief	Makoto GOCHO	
			Senior staffer	Yoko NISEKI	
Secretariat	Japan Society of Refrigerating and Air Conditioning Engineers		Secretary-General	Kenji MATSUDA	
				Shigehiro UEMURA	
				Akira NISHIGUCHI	

1.3 About this Report

This Report presents a summary of the achievements made in FY2020 by Working Group II of the Research Committee on Next-Generation Refrigerants. The authors are grateful to the New Energy and Industrial Technology Development Organization for their economic support of the activities conducted by this Study Group. Additionally, the authors thank the Committee members and authors' collaborators for the cooperation they extended to the authors.

This Report is a publication. Its copyright belongs to the joint authors. Those making reference to this Report are asked to indicate their respective sources.

Table 1-2 Author list

Chapter	Author
Chapter 1 Introduction	Eiji HIHARA (National Institution for Academic Degrees and Quality Enhancement of Higher Education)
Chapter 2 Progress achieved at the University of Tokyo	Chaobin DANG (University of Tokyo), Shizuo SAITOH, and Makoto ITOH
Chapter 3 Progress achieved at Suwa University of Science	Tomohiko IMAMURA (Suwa University of Science)
Chapter 4 Progress achieved at the National Institute of Advanced Industrial Science and Technology Research Institute of Science for Safety and Sustainability	Hiroumi SHIINA (National Institute of Advanced Industrial Science and Technology), Yoshiaki TAKAHASHI, Ryo MATSUKI, Tei SABURI, and Shiro KUBOTA
Chapter 5 Progress achieved at the National Institute of Advanced Industrial Science and Technology Research Institute for Sustainable Chemistry	Kenji TAKIZAWA (National Institute of Advanced Industrial Science and Technology)
Chapter 6 Progress in the risk evaluation of room air conditioners using A3 refrigerant by the Japan Refrigeration and Air Conditioning Industry Association	Kenji TAKAICHI (Panasonic Corporation)
Chapter 7 Progress in the risk evaluation of built-in refrigerated display cabinets using A3 refrigerant by the Japan Refrigeration and Air Conditioning Industry Association	Koji YAMASHITA (Mitsubishi Electric Corporation)

References

1-1) Risk Assessment Handbook (Practice), Ministry of Economy, Trade and Industry, June 2011.

Chapter 2 Progress achieved at the University of Tokyo

2.1 Introduction

The University of Tokyo received a commissioned study on the combustion of flammable refrigerants and risk evaluation. This study consisted of the following three themes: the risk associated with flammable refrigerant leakage from a split air conditioner (indoor unit), the risk associated with flammable refrigerant leakage from a commercial refrigerated display cabinet, and the suppression of diesel explosions at the pump-down operation of split air conditioners.

The first two study themes aim to simulate the concentration diffusion of a flammable refrigerant as it leaks indoors from a room air conditioner or a commercial display cabinet and to calculate the change over time in the flammable-gas volume. The obtained results enabled the calculation of the probability of ignition as the flammable refrigerant leaks indoors. Leakage experiments were first conducted using carbon dioxide and other safe, low-GWP gases, and the obtained results were then used to validate the simulation model. Then, we performed a simulation of the leakage from a room air conditioner indoor unit to evaluate the validity of the regulated maximum charge amount for flammable refrigerants.

For flammable-refrigerant leakage from a commercial refrigerated display cabinet, we first performed a leakage experiment using carbon dioxide and compared the obtained results with the simulated results to examine the validity of the simulation model. After that, we simulated the leakage from a refrigerated display cabinet to evaluate the maximum charge amounts of flammable refrigerants.

A possible accident during the pump-down operation performed for refrigerant recovery from a heat pump is self-ignition combustion (diesel explosion), which occurs when air is mixed with a gaseous mixture of refrigerant and lubricating oil, and the temperature increases because of adiabatic compression. Additionally, there have been reports of broken room air conditioner outdoor units from accidents during refrigerant recovery. R290, R1234yf, and R32, known as low GWP refrigerants, are flammable and are feared to cause diesel explosions more easily than conventional, non-flammable refrigerants R410A. An experimental setup that assumed diesel explosions was built to investigate the addition of a combustion-inhibiting substance to lubricating oil as a method of suppressing diesel explosions.

2.2 Refrigerant leakage from a residential split air conditioner

2.2.1 Method of numerical fluid analysis

We numerically calculated the diffusion of leaked refrigerant gas (from an air conditioner indoor unit) while it is mixed with indoor air. The basic equations for a 3D-space mixture advection-diffusion problem are the mass conservation equation (2-1), the Navier-Stokes equations (2-2), the advection-diffusion equation (2-3), and the equation of state of an ideal gas (2-4). For numerical calculations, we used ANSYS Fluent 18.1. Table 2-1 shows a summary of the calculation conditions.

$$\frac{\partial \rho}{\partial t} + \frac{\partial}{\partial x_j} (\rho u_j) = 0 \quad (2-1)$$

$$\frac{\partial \rho u_i}{\partial t} + \frac{\partial}{\partial x_j} (\rho u_j u_i - \tau_{ij}) = -\frac{\partial p}{\partial x_i} + g_i (\rho - \rho_o) \quad (2-2)$$

$$\frac{\partial}{\partial t} (\rho Y_m) + \frac{\partial}{\partial x_j} \left(\rho u_j Y_m - \rho Y_m \frac{D}{X_m} \nabla X_m \right) = 0 \quad (2-3)$$

$$\rho = \frac{p}{RT \left(\frac{Y_A}{M_A} + \frac{Y_B}{M_B} \right)} \quad (2-4)$$

where τ_{ij} is the stress tensor; X_m is the molar concentration; Y_m , Y_A , and Y_B are mass concentrations; M_A and M_B are the

molecular weight; and D is the diffusion coefficient.

Additionally, using Eq. (2-5)^[2-1], we calculated the molecular diffusion coefficient during refrigerant diffusion and regarded it as a constant, irrespective of temperature and pressure:

$$D_{AB} = \frac{1.5 \times 10^{-5} T^{1.81}}{p(T_{CA} \cdot T_{CB})^{0.1405} \cdot (V_{CA}^{0.4} + V_{CB}^{0.4})^2} \cdot \sqrt{\frac{1}{M_A} + \frac{1}{M_B}} \quad (2-5)$$

where T_{CA} and T_{CB} are critical temperatures in K; and V_{CA} and V_{CB} are the critical specific volume in cm³/mol.

Table 2-2 shows the diffusion coefficients for the refrigerant-air mixtures used in the present study.

Table 2-1 Simulation outline

	Room	Display cabinet
Software	ANSYS Fluent 18.1	ANSYS Fluent 2019 R1
Simulation	Unsteady and compressible flow	Unsteady and incompressible flow
Species transport	2 components (Air - Refrigerant)	2 components (Air - Refrigerant)
Turbulence model	Realizable k-ε	(Ditto)
Solver	SIMPLE	Coupled
Scheme	2nd order upwind	(Ditto)

Table 2-2 Diffusion coefficient

	R290-Air	R32-Air	R744-Air
Diffusion coefficient [m ² /s]	1.11 × 10 ⁻⁵	1.35 × 10 ⁻⁵	1.59 × 10 ⁻⁵

A summarized outline of our laboratory model is shown in Fig. 2-1 and Table 2-3. The size of this calculation model was equivalent to that of the laboratory model built for the refrigerant experiment to be explained later. The model had dimensions of 3800 × 2400 × 2550 mm, a 100-mm diameter air vent opposite the air conditioner, and a door undercut measuring 900 × 7 mm. A finer mesh was set near the boundaries. Based on IEC 60335-2-40:2018^[2-2], the leak rate was set to discharge the total amount of refrigerant indoors within 4 min. R290 and R32 were the target refrigerants in the calculation. For comparison with the refrigerant leakage experiments, we used carbon dioxide (R744) instead of R290. To prevent fire occurrence, especially during an experiment using R290, we chose to use R744 as a replacement because it possesses similar physical properties to R290.

The details of the wall-mounted indoor unit and those of the floor-mounted indoor unit are shown in Fig. 2-2 and Fig. 2-3, respectively. Both indoor units had an air intake and an air outlet. The boundary conditions applied to their air intake and set to their air outlet were a free outflow condition and a uniform flow velocity condition, respectively. No calculations were performed for the inside of the indoor units.

The conditions under which the indoor unit fan started to stir the indoor air after refrigerant leakage are summarized in Table 2-4. The fan air flow rate was calculated using Eq. (2-6).^[2-3] The fan air flow rate for R290 was 185 m³/h. For the wall-mounted indoor unit, the fan wind velocity was 0.75 m/s. The fan was set to start 30 s after leakage onset. As its structural component, the indoor unit included an air intake and an air outlet. When refrigerant was discharged from the air outlet, indoor air was drawn in from the air intake. As a result, the refrigerant from the air outlet was mixed with the drawn-in air. Based on the experimentally measured values, the refrigerant concentration at the air outlet was set to 50% for this analysis.

$$Q_{min} = 3600 \frac{5Y \sqrt{A_0} \dot{m}_{leak}^{3/4}}{h_0^{1/8} [LFL(1-F)]^{5/8}} \quad (2-6)$$

where Q_{min} is the required air flow rate in m^3/h ; Y is a constant equal to 1; A_0 is the air flow opening area in m^2 ; \dot{m}_{leak} is the refrigerant flow rate in kg/s ; LFL is the lower flammability limit in kg/m^3 ; and F is a constant equal to 0.5.

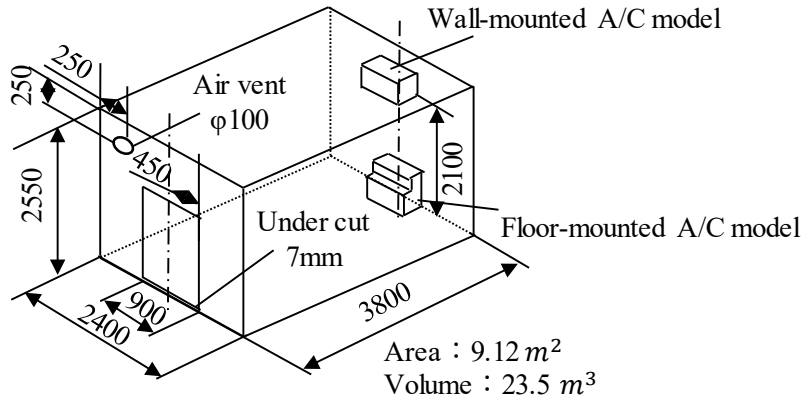


Fig. 2-1 Modeled room.

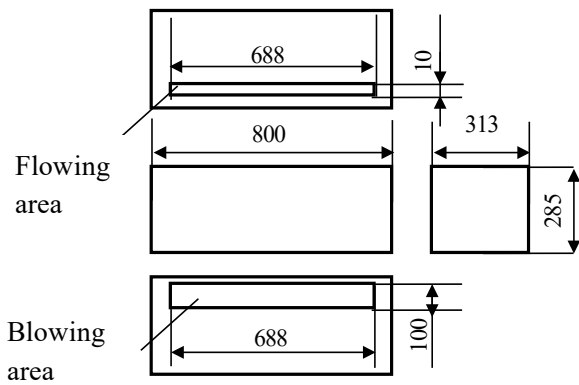


Fig. 2-2 Details of wall-mounted indoor unit model.

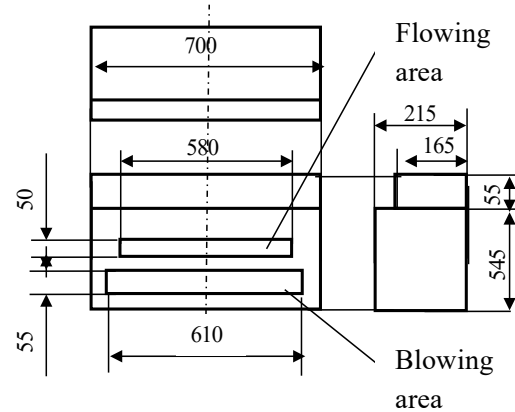


Fig. 2-3 Details of floor-standing indoor unit model.

Table 2-3 Simulation condition

Refrigerant	R290 and R32
Leak amount	Evaluated
Leak time	4 min
Boundary of A/C model	1 outlet and 1 inlet
Floor Area	Evaluated
Ventilation	Exist (Vent and Door gap)

Table 2-4 Fan condition

Flow rate	Equation (2-6)
Direction	Vertical direction for wall-mounted unit, horizontal direction for floor-mounted unit
Process	Process 1: 0 - 30 s: Refrigerant leak Process 2: 30 - 240 s: Refrigerant leak with fan operation Process 3: 240 s - : Fan operation

2.2.2 Validation study of the simulation model through refrigerant leakage experiments

In the present study, to examine the model’s validity, we performed concentration distribution measurement using refrigerant leak tests and compared the measured results with the refrigerant concentrations numerically calculated for the same points. The dimensions of the constructed laboratory is shown in Fig. 2-1. We fitted heat-insulating boards on the walls as a precaution for preventing drifts. The refrigerants used were R32 and R744. The refrigerant supply system is shown in Fig. 2-4. The specifications of the equipment used in this study are summarized in Table 2-5. The mass flow controller was intended for R32. Hence, the flow rate coefficient was calibrated via the experiment using R744. We conducted experiments to discharge refrigerant only from the wall-mounted indoor unit. To simplify the internal structure and ensure a uniform refrigerant discharge from the air outlet, we built a model. Figure 2-5 shows a detailed drawing of this model. The air outlet measured 688 mm × 100 mm. With no air intake provided, 100% pure refrigerant was discharged at a uniform rate. To measure refrigerant concentrations, we used oximeters to estimate the refrigerant concentrations based on the decrease in oxygen concentration, with the aim of using more than one type of refrigerant. The refrigerant concentration X_{ref} was calculated using Eq. (2-7) from the oxygen concentration X_{O_2} and the initial oxygen concentration $X_{O_2,atm}$:

$$X_{ref} = \frac{X_{O_2,atm} - X_{O_2}}{X_{O_2,atm}} \tag{2 - 7}$$

All the 14 oximeters were calibrated by checking them against the R744 concentration calculated using Eq. (2-7) from an R744 concentration reading from an oximeter, and we confirmed that they measured refrigerant concentrations with an accuracy of ± 2% of full scale. These oximeters were installed at the 14 points shown in Fig. 2-6. The experimental conditions are summarized in Table 2-6.

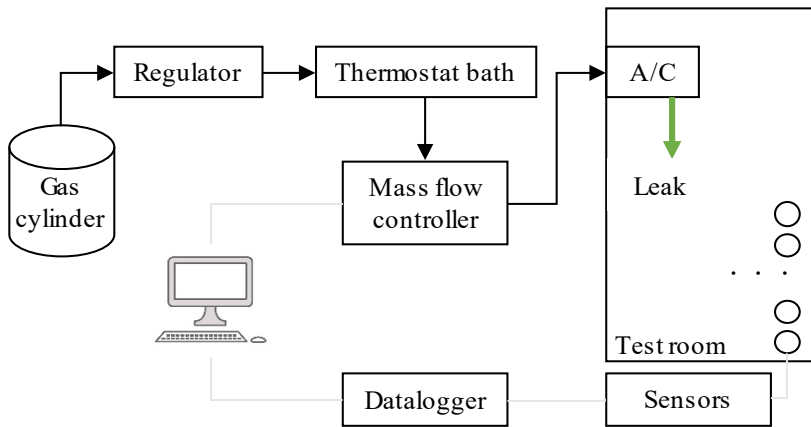


Fig. 2-4 Schematic of experimental setup.

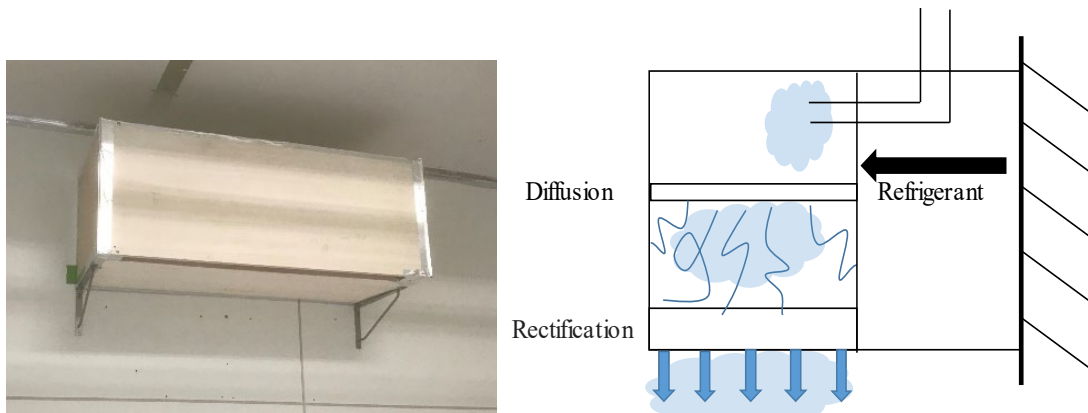


Fig. 2-5 Internal structure of wall-mounted air conditioner.

Table 2-5 Equipment specification

Name	Type	Specifications
Mass flow controller	Fujikin (FCST1500)	Gas: R32 Range: 0 - 250 L/min Accuracy: $\pm 2\%$ of full scale.
Oximeters	ICHINEN JIKO (JKO-O ₂ Ver.3)	Gas: Oxygen Principle: Galvanic battery type Resolution: 0.01% Accuracy: $\pm 0.5\%$ (≥ 10 vol%), $\pm 0.01\%$ (< 10 vol%)

Table 2-6 Experimental conditions for validation of CFD model

No.	Refrigerant	Air vent	Refrigerant amount (g)
1-1			200
1-2	R744	exist	300
1-3			400
1-4			500
2			R744
3	R32	exist	500

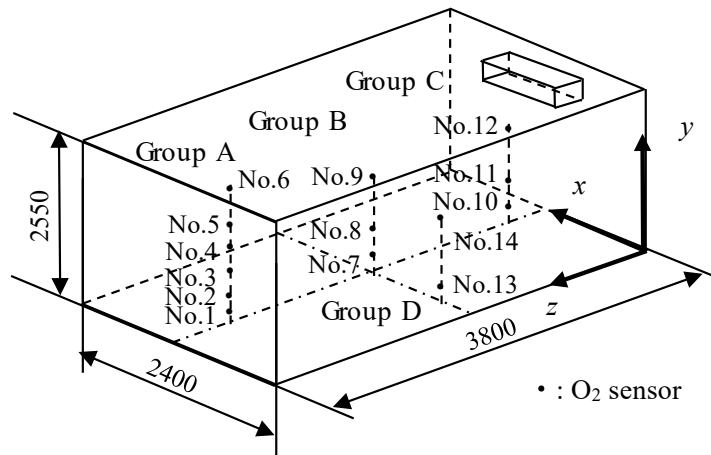


Fig. 2-6 Concentration measurement points.

As shown in Fig. 2-7, we compared the calculated and measured values for Group A measurement points under test conditions No. 1-4, No. 2, and No. 3 (Table 2-6). The ordinate axis represents the test gas concentration, and the abscissa axis represents the elapsed time. The figure shows that the refrigerant concentration continuously increased at each point from the start to the end of refrigerant leakage (240 s) and then gradually decreased after 240 s had elapsed. In the early phase of the experiment, we observed discrepancies between the measured and calculated values. After reducing the mesh sizes near the air conditioner indoor unit's air outlet, near the ventilating opening, and near the door undercut and improving the shapes of the walls to allow gas to flow smoothly in or out, we observed fewer and smaller discrepancies. In the final phase of the experiment, as shown in Fig. 2-7, the measured and calculated values agreed with each other with reasonable accuracy and appeared to be successful reproductions of actual physical phenomena, thus validating our calculation model.

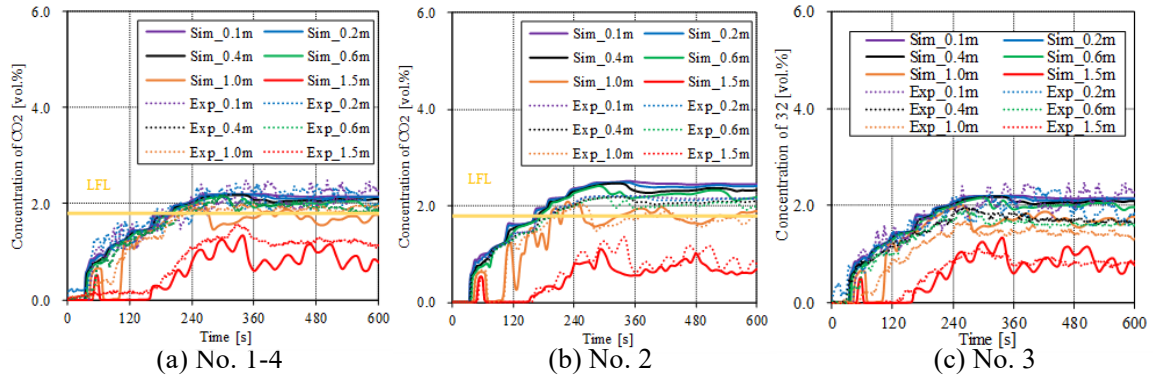


Fig. 2-7 Validation of calculation model.

(Comparisons of concentrations between calculation and measurements)

2.2.3 Numerical calculation-based consideration of the maximum allowable charge for flammable refrigerants

Using the validated numerical calculation method, we performed numerical calculations of the behavior of refrigerants leaked from the following air conditioners: wall-mounted and floor-mounted indoor units. Because regulations stipulate a maximum charge amount for flammable refrigerants, we evaluated this value using the equation specified in IEC 60335-2-40:2018 [2-2]:

$$m_{max} = 2.5 \times LFL^{(5/4)} \times A^{1/2} \times h_0 \quad (2-8)$$

and an equation that assumes the air conditioner fan operates during refrigerant leakage[2-3]:

$$m_{max} = F \times LFL \times A \times 2.2 \quad (2-9)$$

(1) Leakage from the wall-mounted indoor unit

From the simulated results, we calculated the flammable-gas volume V_{FL} as a function of time. When the refrigerant charge amount was small, the flammable-gas volume disappeared immediately after leakage ceased (240 s). However, with a larger charge amount, the flammable-gas volume persisted even after leakage ceased. We determined this limit in the refrigerant charge amount as the maximum allowable charge amount for each floor area and compared it with the values from Eq. (2-8) and Eq. (2-9) for R290 and R32. The results are shown in Fig. 2-8. The circles (○) in the figure represent the maximum charge amount with which the flammable gas disappeared immediately after refrigerant leakage ceased. If a refrigerant charge amount lies above this symbol, then the flammable gas remains even after refrigerant leakage ceases. As shown in Fig. 2-8, the calculated values lie above the line representing Eq. (2-8) for both R290 and R32, meaning that Eq. (2-8) provides a reasonable estimation. An evaluation of Eq. (2-9) reveals that this equation makes conservative estimates for R32 regardless of the floor area. However, in the case of R290, Eq. (2-9) makes risky estimates for floor areas of 7.5 m² or more because the green line lies above the symbols. Therefore, in this case, using the indoor unit fan becomes necessary. With the indoor unit fan operating at the air flow rate given by Eq. (2-6), the flammable volume was observed to disappear upon the cessation of refrigerant leakage.

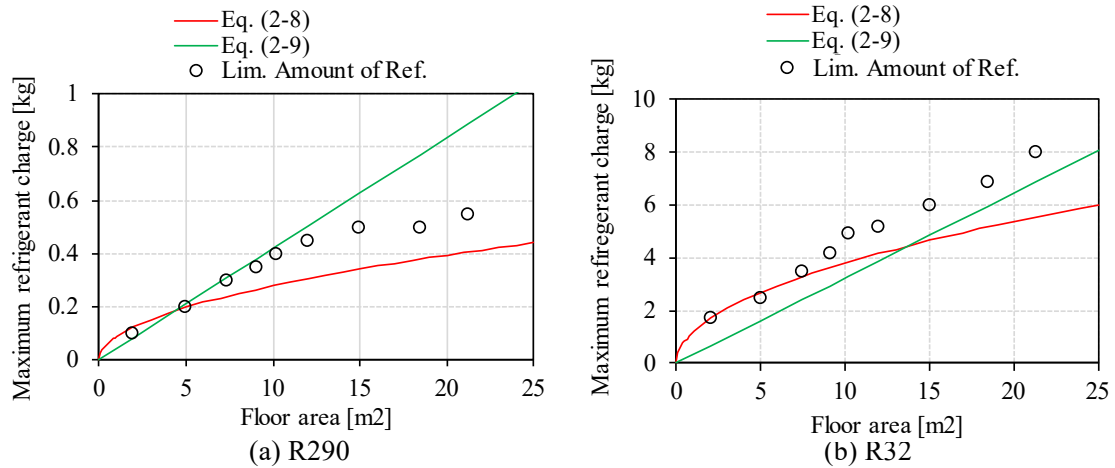


Fig. 2-8 Comparison of maximum allowable refrigerant charge.
(Wall-mounted air conditioner)

(2) Leakage from the floor-mounted indoor unit

For the floor-mounted indoor unit, we calculated the maximum allowable charge amount for each floor area and compared it with the values from Eq. (2-8) and Eq. (2-9) for both R290 and R32. The results are shown in Fig. 2-9. The calculated results for R290 were compared with the line representing Eq. (2-8), revealing that Eq. (2-8) provides reasonable estimations. For R32, the line representing Eq. (2-8) remained below the calculated values at all floor areas, indicating that Eq. (2-8) provides safe estimations. For both R290 and R32, much of the line representing Eq. (2-9) remained well above the calculated values, indicating that Eq. (2-9) provides dangerous estimations.

On the basis of the above results, we determined, by calculation, the effects of fan operation on the flammable-gas concentration for each floor area for R290 and R32. With the indoor unit fan in operation, the flammable-gas volume gradually decreased over a long time, unlike the case with the wall-mounted air conditioner. When the floor area 5 m² (R290), 9.12 m² (R290), and 12 m² or less (R32), the flammable gas completely disappeared when the fan was in operation. However, when the floor area was 15 m² or more (R290) and 21.28 m² (R32), a small amount of the flammable gas remained for a while even after the cessation of refrigerant leakage.

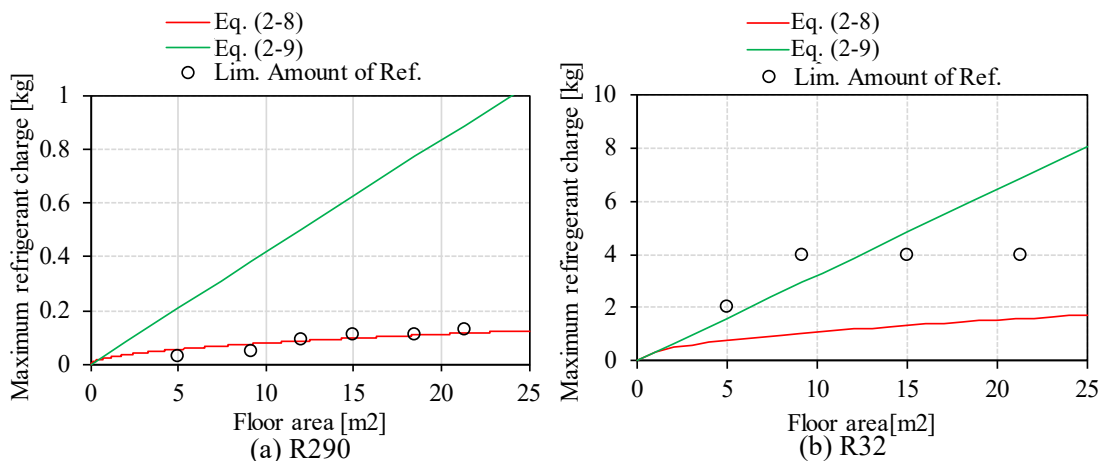


Fig. 2-9 Comparison of maximum allowable refrigerant charge.
(Floor-mounted air conditioner)

2.2.4 Summary

To evaluate the indoor leakage risk of R290, one of the next-generation refrigerant candidates for residential air conditioners, the maximum allowable charge was evaluated using numerical fluid dynamics analysis. This study provided the following findings:

- 1) The results of the numerical fluid dynamics analysis were compared with those of the refrigerant leakage experiments conducted using R744 and R32. The comparison showed that the concentration distributions of the refrigerants were highly reproducible, thereby validating the calculation method.
- 2) Regarding the maximum allowable charge, Eq. (2-8) was appropriate for wall-mounted air conditioners using R290 and R32. Regarding floor-mounted air conditioners, R32 was sufficiently safe, but R290 had an inadequate safety margin.
- 3) Regarding the maximum allowable charge, for wall-mounted air conditioners, the flammable gas disappeared immediately after the fan operated. Hence, fan operation was very effective in reducing risk. For floor-mounted air conditioners, the flammable gas existed locally even after the fan was started, as long as the refrigerant continued to leak. However, the volume of the refrigerant flammable gas immediately disappeared at the cessation of refrigerant leakage. This study revealed that an indoor unit fan that starts upon detecting leakage was necessary for assured safety and that a small volume of residual flammable gas remained in a large room even if the fan started operating 30 s after the onset of leakage.

2.3 Refrigerant leakage from a commercial refrigerated display cabinet

2.3.1 Numerical fluid analysis method

The numerical calculation method used was the same as that explained in 2.2.1. Details of the model laboratory room is shown in Fig. 2-10. The size of the calculation model was equivalent to that of the laboratory built for the refrigerant leakage experiment described later. This model had dimensions of $5600 \times 3800 \times 2550$ mm and an air vent (100 mm in diameter) in a wall adjacent to the wall with a mounted model display cabinet. A finer mesh was set near the boundaries. The initial indoor conditions were a gauge pressure of 0 Pa and a temperature of 300 K. For the ventilation opening, pressure boundary conditions were set. The selected refrigerant was R290. For comparison with the experiment, a calculation based on non-flammable R744 was performed separately. To reduce computational cost, such as computation time and memory usage, the center plane of the room was defined as the plane of symmetry.

Details of the model commercial display cabinet are shown in Fig. 2-11. This display cabinet had two door leaves, both intended to open simultaneously in the leak test. A condensing unit was provided at the bottom or top of the display cabinet. When the condenser fan was in operation, uniform velocity fields were assumed upstream and downstream of the fan. The fan was assumed to run continuously. As shown in Fig. 2-11, the condensing unit was installed at the bottom of the display cabinet. The centerline of the display cabinet enclosure was in alignment with that of the laboratory model and 100 mm off from the wall surface. For the condition in which multiple units were arranged side by side, a closing plate was provided at each end of the clearance to the wall. Therefore, when sucked in from the front into the bottom fan, gas passed through the clearance behind and returned to the indoor space from the level of the enclosure top face. A similar structure designed to suck gas in from the bottom was employed for the case in which the fan was set to blow forward. R290 was used as the refrigerant for the normal calculation. In accordance with the applicable IEC standards, the swing door was set to rotate by 60° every 3 s. The parameters used were the position, air outlet orientation, and wind velocity of the condenser fan.

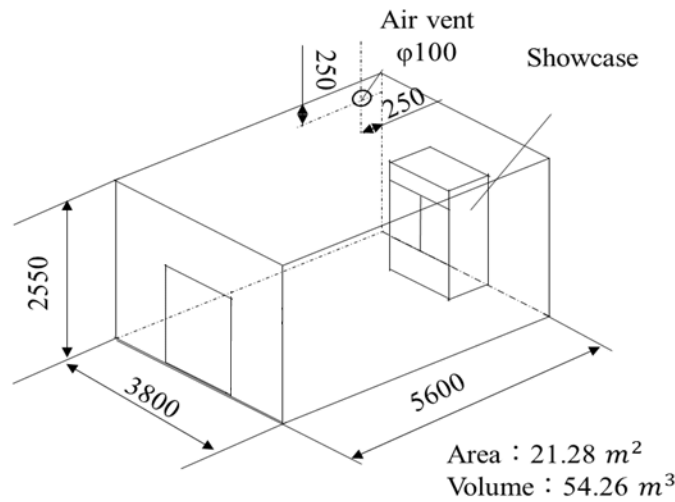


Fig. 2-10 Modeled room.

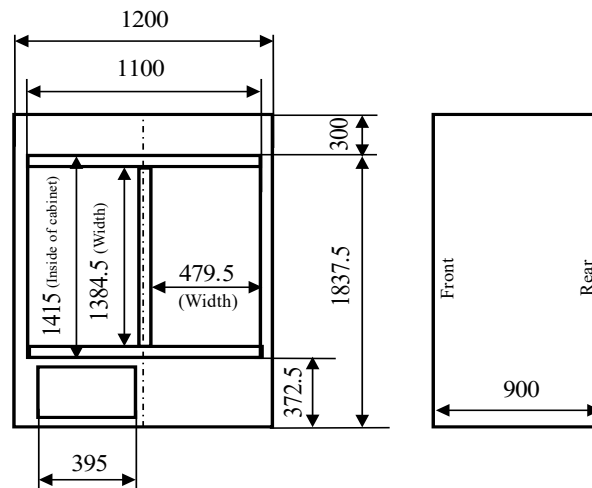


Fig. 2-11 Details of display cabinet.

2.3.2 Validation of the simulation model using refrigerant leakage experiments

In the present study, we performed concentration distribution measurements using refrigerant leak tests and compared the numerically calculated and experimental results to examine the validity of the calculation model. The shape of the laboratory was the same as that of the calculation model (Fig. 2-10). The laboratory walls were covered with heat-insulating material on the side exposed to external walls to reduce heat conduction from the outside air. Additionally, a skylight in the laboratory allowed light in from the lighting installed outside to reduce the number of heat sources inside. The general view of the refrigerant supply system is the same as shown in Fig. 2-4. The gas used for the experiment was R744.

The locations of installed oximeters are shown in Table 2-7 and Fig. 2-12. A total of 12 oximeters were installed at 6 points out of those specified in the IEC 60335-2-89 and at another 6 points to measure the indoor refrigerant concentration. The latter six sensors were divided into two groups: one at the three levels (100 mm, 400 mm, and 1000 mm) above point A (500 mm from the wall opposite to the enclosure) and the other at the same levels above point B (center of the room). In the validation study of the model, a comparison was made between the calculated and measured concentration at these 12 points over time.

We built a model display cabinet, as shown in Fig. 2-13. The display cabinet was hollow inside. A linear actuator was fitted on each two-door leaves to open the door. The actuators had a stroke of 300 mm and a maximum speed of 100

mm/s, and they were adjusted to open the door by 60° every 3 s using PWM control. To reduce leakage during gas filling (before the door was opened), cushioning material was stuck around the perimeter of the main body opening so as to be compressed by the actuators during door closure.

As shown in Fig. 2-13, a hose was installed at the rear bottom to fill the cabinet with refrigerant R744. The cabinet had to be bled of air while it was filled with the refrigerant. Because refrigerant R744 is denser than air, it remained in the lower part of the cabinet. Therefore, air was removed from the upper part. The removed gas was guided through the hose and released out of the laboratory to prevent its leakage to the inside of the laboratory. After refrigerant filling, a fan installed inside the cabinet was used to stir the internal gas and the outlet was closed via the solenoid valve. As a result, the composition of the internal gas was as uniform as possible.

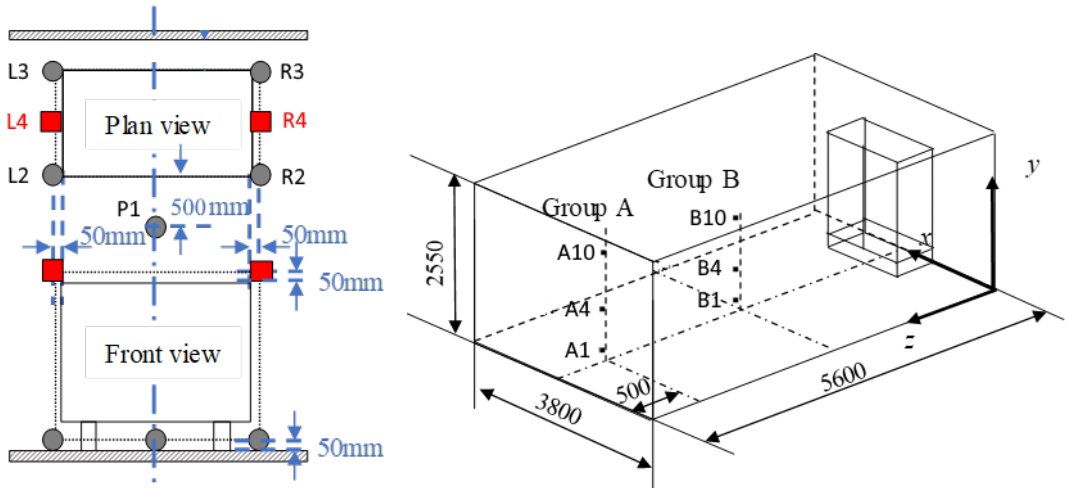


Fig. 2-12 Concentration measurement points.

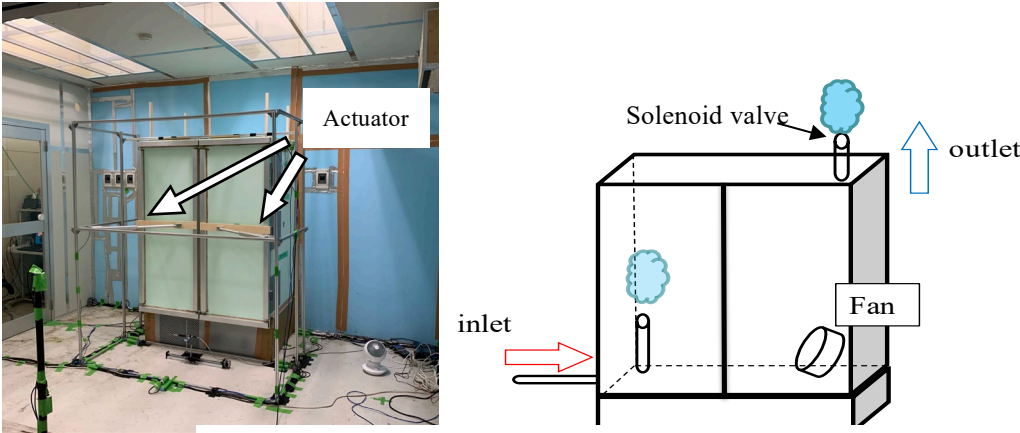


Fig. 2-13 Internal structure of showcase model.

The maximum charge amount for flammable refrigerants is stipulated in IEC60335-2-89: 2019. For split systems, this value is 150 g, and for systems with a built-in motor compressor, this value is 13 times the lower flammable limit (LFL) or 1.2 kg, whichever is lower. For R290, the LFL is 0.038 kg/m³, resulting in a maximum charge of 494 g. Therefore, the refrigerant leakage amount for our experiment was set to 494 g. To ensure safety during the experiment, the refrigerant was replaced with R744, which is similar to R290 in density and is non-flammable.

The results obtained with no condenser fan and those obtained with the condenser fan blowing forward from the bottom at 1.3 m/s are shown in Figs. 2-14 and 2-15, respectively. In both figures, the left-side graph shows the results at the measurement points specified in IEC60335-2-89: 2019, and the right-side graph shows the values at the points inside the laboratory. With no fan in operation, the refrigerant concentration reached a maximum value approximately 10 s after the door was opened at positions P1, L2, and R2 near the front side, and this value gradually decreased in an oscillating manner until approximately 120–180 s. With the fan in operation, the differences in concentration rapidly

diminished, the oscillation in concentration disappeared after 60 s, and the concentration was more uniform. Moreover, a significant difference was observed between P1 and B1 because the experiment used actual equipment and positioned the fan to the left side (Fig.2-11), whereas the fan was positioned at the center of the calculation model to maintain the symmetry plane, thus exposing the measurement point directly to fan-blown air. Additionally, the sensor response time was probably the main cause for the longer durations of rapid concentration rise immediately after the door was opened in the experiment.

The validity of this model was demonstrated because the calculation results generally matched the experimental values in terms of both behavior and values. Therefore, we proceeded with the calculation for R290.

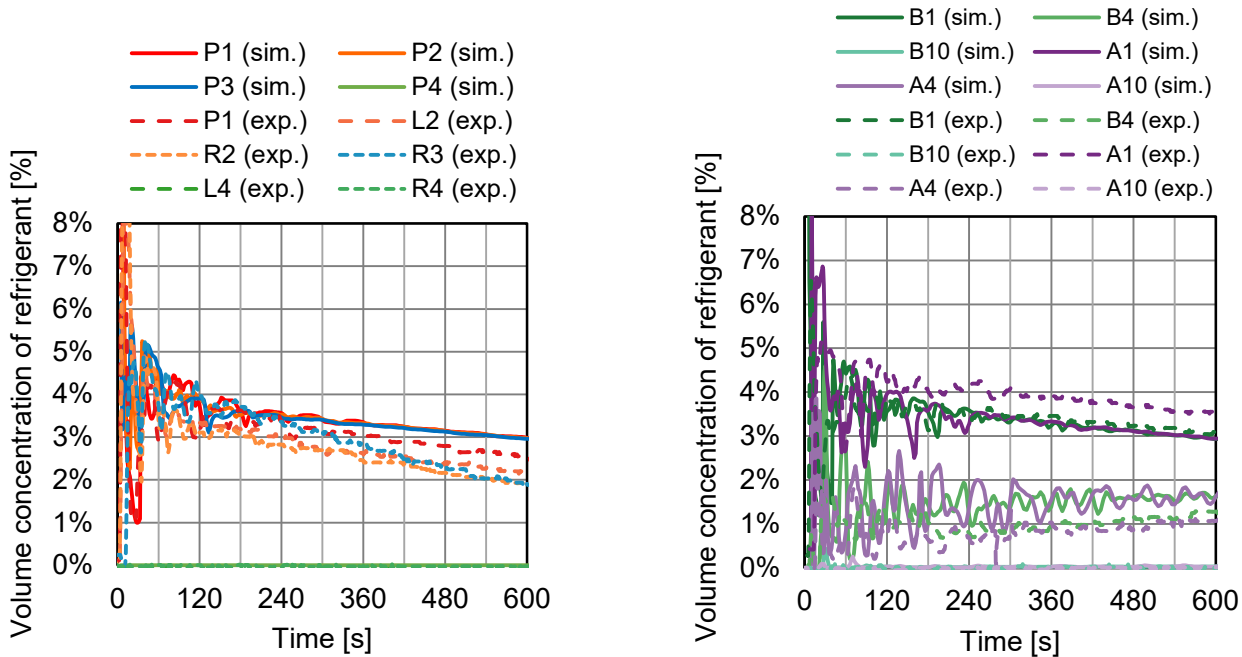


Fig. 2-14 Comparison of simulation and experiment without fan when 494 g of R744 is released.

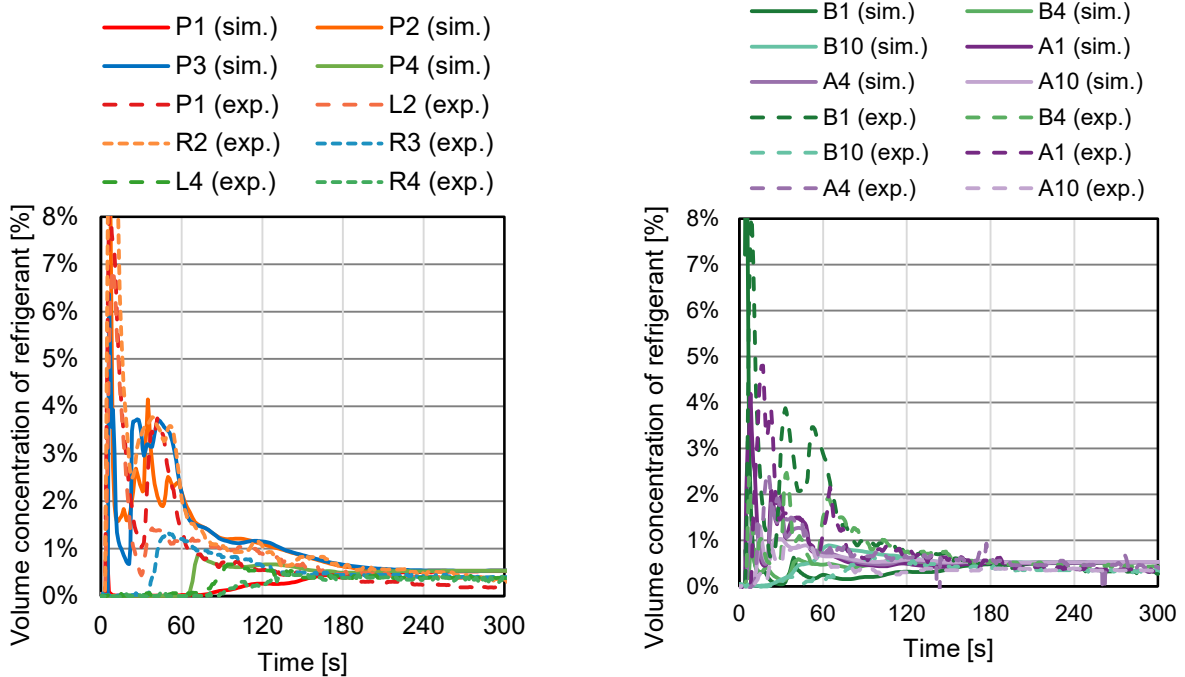


Fig. 2-15 Comparison of simulation and experiment with a fan (wind speed of 1.3 m/s at the bottom) when 494 g of R744 is released.

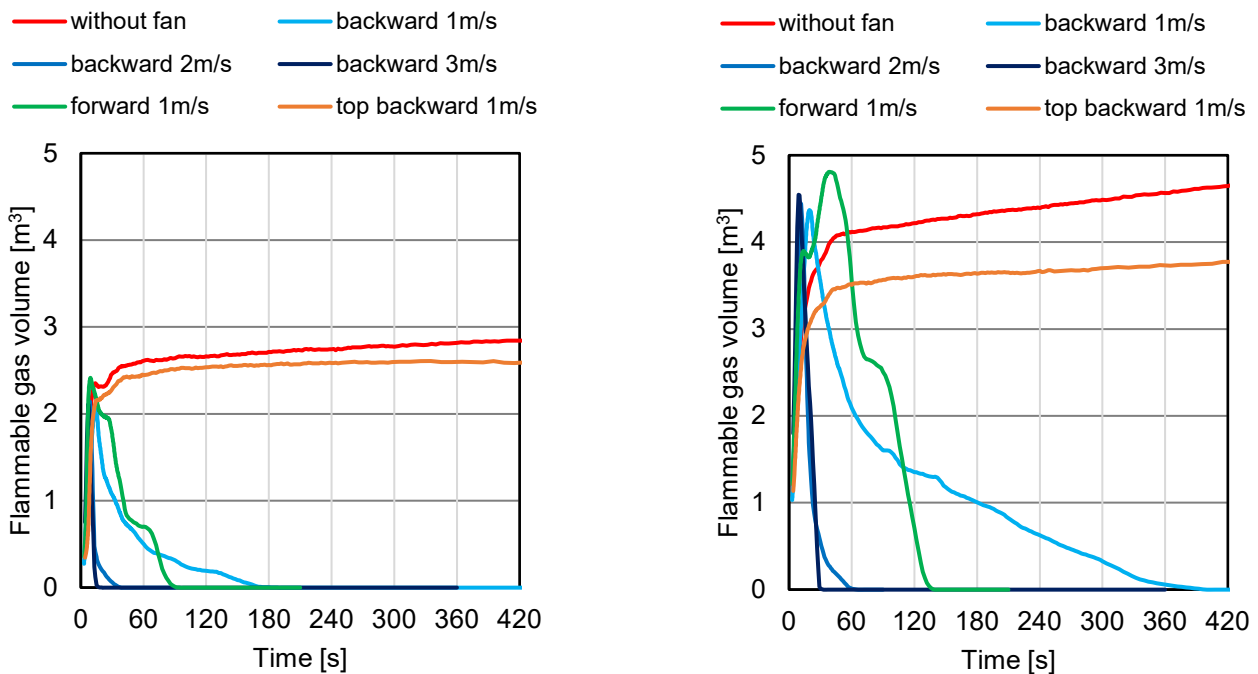
2.3.3 Effects of fan operation on the scale of flammable region

The obsolete version of IEC 60335-2-89 specifies $m_{max} = 150$ g as the condition for ensuring safety without activating any supplementary safety device. As a result of the revision made in 2019, the current IEC 60335-2-89:2019^[2-4] includes a formula for the maximum allowable charge amount for flammable refrigerants, assuming that the air conditioner fan starts upon refrigerant leakage:

$$m_{max} = 13 \times LFL \tag{2 - 10}$$

R290 has an LFL of 0.038 kg/m^3 , which translates into a maximum refrigerant charge amount of 494 g. Additionally, Annex CC of the same standard requires that at all eight measurement points around the enclosure, the measured concentrations decrease to below 50% of the LFL within 5 min. Therefore, we decided to investigate the effects of fan operation. In the case of commercial refrigerated display cabinets, the condensing unit is expected to be installed at either of two locations, the upper and lower units. Hence, our investigation on the concentration and residence time of flammable gas covered both the upper and lower units and the whole area inside, including all the areas not covered by the measurement points.

Figure 2-16 shows the change in flammable gas volume as a function time with 494 g of released R290 and the bottom-mounted fan operating at different wind velocities. The left graph of Fig. 2-16 shows the results of calculating the gas volume in the concentration range between LFL and the upper flammable limit (UFL) as the flammable gas volume; the right graph shows the results of evaluating the gas volume with a concentration of 0.5 LFL or more as the flammable gas volume. With the fan blowing backward at 1 m/s, the flammable region disappeared after 180 s, and the region of 0.5 LFL or more also disappeared after approximately 405 s. With the fan blowing backward at 2 m/s, the flammable region disappeared after 40 s. With the fan blowing forward at 1 m/s, the region of 0.5 LFL or more disappeared after 140 s. In contrast, with the top-mounted fan blowing backward at a wind velocity of 1 m/s, the flammable volume saw no significant decrease and disappeared only after 1620 s had elapsed; this trend was comparable to that observed for the fan-less condition.



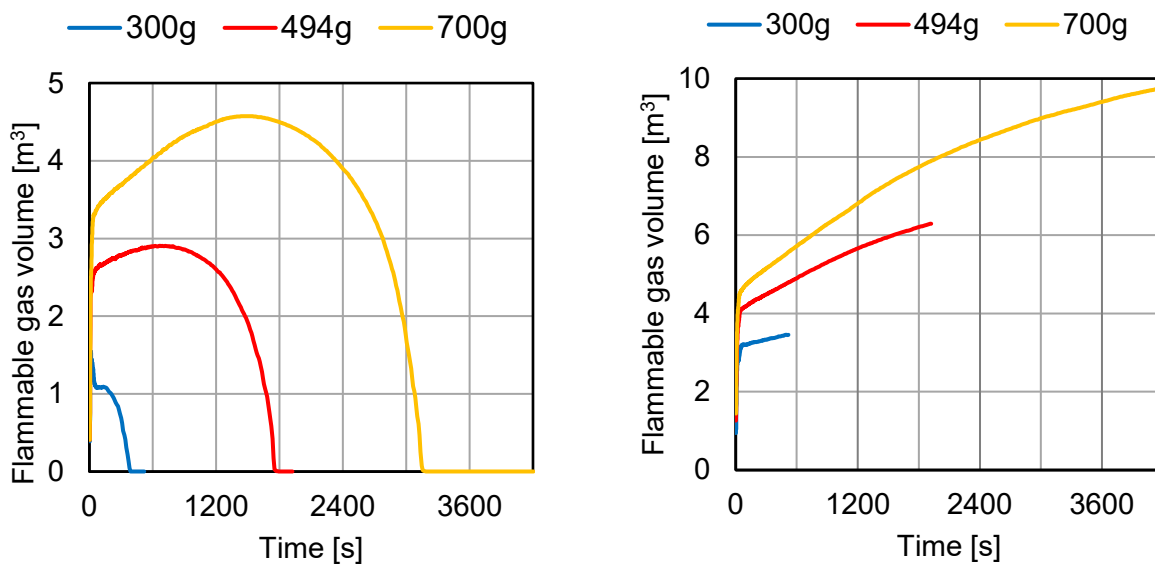
(a) A gas in the concentration range of LFL to UFL is defined as flammable gas.

(b) A gas with a concentration of 0.5 LFL or higher is defined as flammable gas.

Fig. 2-16 Effect of condenser fan on flammable gas volume when 494 g of R290 is released.

Figure 2-17 shows the change in the flammable gas volume when the refrigerant charge amount changed under the fan-less condition. As explained earlier, a charge amount of 494 g was excessive because it was determined assuming that a fan was in operation. The flammable gas volume gradually increased to 2.91 m³ after 670 s had elapsed and then decreased. The flammable region remained until 1800 s had elapsed. A comparison with Fig. 2-16 revealed that the bottom fan reduced the residence time of the flammable region by 90% or more. By increasing the refrigerant charge amount to 700 g, it took 50 min or more for the flammable gas to disappear. By reducing the refrigerant charge amount to 300 g, the flammable gas volume disappeared after approximately 6 min had elapsed. Therefore, the refrigerant charge amount significantly affects safety with no fan in operation. When the concentration range of flammable gas was defined as LFL to UFL, the time-integrated values of the flammable gas volume for the refrigerant discharge amounts of 300, 494, and 700 g under the fan-less condition were 24.4, 4345, and 1.21×10⁵ m³s, respectively. When the flammable gas was defined as a gas with a concentration of 1/2 LFL or more, the time-integrated value with the refrigerant charge of 494 g was as high as 10,150 m³s, which was reached when the calculation was discontinued after 1920 s had elapsed.

Figure 2-18 shows the time-integrated value of flammable gas volume with the bottom-mounted fan in operation. A positive value for wind speed indicates backward blowing, whereas a negative value indicates forward blowing. As shown in Fig. 2-16, at 1 m/s, the two ranges differed in change over time but were similar in the size of the flammable space-time product. Comparing the front blowout and the rear blowout at a wind speed of 1 m/s, the time variations of the flammable gas volume (Fig. 2-16) were different, but the time-integral of the flammable volume was similar.



(a) A gas in the concentration range of LFL to UFL is defined as flammable gas.

(b) A gas with a concentration of 0.5 LFL or higher is defined as flammable gas.

Fig. 2-17 Effect of refrigerant charge on flammable gas volume without fan.

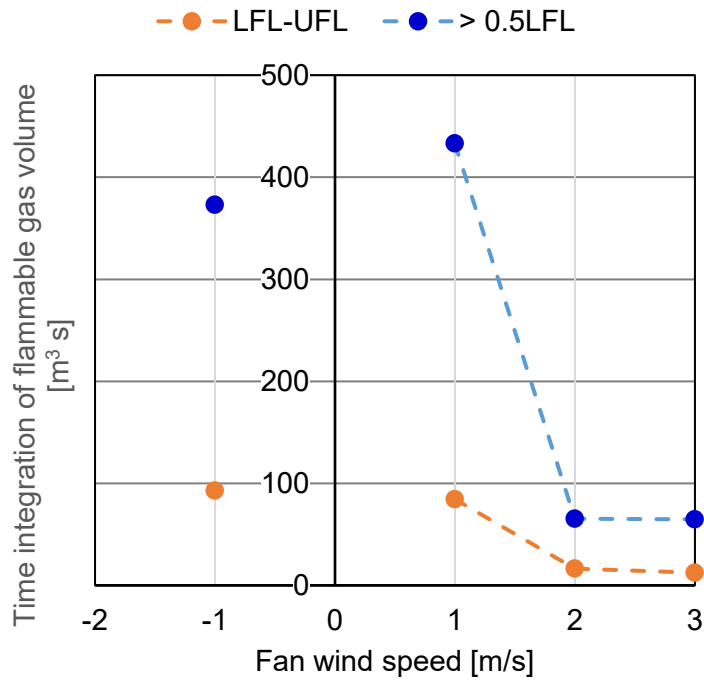


Fig.2-18 Difference in time integration of flammable gas volume depending on fan wind direction.

From the above results, we expect that a condenser fan in operation at the bottom will have a significant effect on reducing the risk arising from leakage and will be effective above a certain level regardless of whether the fan blows forward or backward. To ensure safety, we consider it more desirable to use bottom-mounting condenser units.

2.3.4 Summary

To assess the risk of indoor leakage of R290, a next-generation refrigerant candidate for commercial refrigerated display cabinets, the effects of refrigerant charge and fan operation on the flammable region scale were evaluated using numerical fluid dynamics analysis. This study provided the following findings:

- 1) To examine the validity of the method employed for the numerical fluid dynamics analysis, a model display cabinet was built in a room with a floor area of 21 m² for refrigerant leakage experiments using R744. Assuming leakage into the display cabinet, the indoor concentration distribution was measured as a function of time with the door open after the refrigerant was introduced and stirred. This study examined the validity of the accuracy for approximately 5 min from leakage occurrence, which is expected to be important in risk evaluation and subsequent accuracy.
- 2) The size of the flammable region was evaluated as the refrigerant charge increased without the condenser fan in operation. When 494 g of R290 was released, the combustible gas region remained for 30 min or more.
- 3) For each installation position, air velocity, and wind direction of the condenser fan, the changes in the volume of the flammable region and the time-integrated value of flammable gas volume were evaluated to investigate the effect of fan operation on the flammable gas region. For example, with the condenser fan installed at the bottom of the cabinet, the wind direction (forward or backward) made almost no difference on flammable gas dissipation.
- 4) With the condenser fan installed at the top of cabinet, the effect of refrigerant gas stirring was almost negligible.

2.4 Suppression of diesel explosions at the pump-down of residential air conditioners

Refrigerant-related air-conditioner compressor ruptures are frequently reported. An air-conditioner compressor explodes when its internal pressure becomes abnormally high during the work (called “pump-down”) performed for refrigerant-gas recovery into the outdoor unit before relocation or disposal of the air conditioner. Considering that the inclusion of air is a necessary factor for compressor rupture, Higashi et al.^[2-5] compressed a gas mixture of air, refrigerant, and lubricating oil in a model engine simulating a compressor to determine the conditions that caused diesel

explosions. They reported that in the low refrigerant concentration range, combustion occurs with a pressure rise and requires lubricating oil. Moreover, Higashi et al.^{[2-6][2-7]} performed diesel explosion experiments with different lubricating oils and investigated the effects of additives in lubricating oils. They demonstrated that the flammability of the lubricating oil affected the conditions for explosions and reported that polyolester oil (POE), lower in flammability, was less prone to explosive combustion than polyalkylene glycol oil (PAG), indicating that its additives reduced the flammable range. In the present study, we performed a compression combustion experiment using a mixed gas of refrigerant, air, and lubricating oil in a model engine simulating an air-conditioner compressor to investigate the effects of combustion-inhibitor concentration on combustion.

A lubricating oil is required in compressors of refrigerating and air-conditioning equipment to provide lubricity. Moreover, the lubricating oil should be compatible with the refrigerant and have long-term stability. The function of lubricating oils is maintained by the additives in the oil (base oil). There are many types of additives, such as oxidation inhibitors, stabilizers, or anti-wear agents, to suit the intended use. Our earlier studies have shown that oil (base oil) combustion propagates to the refrigerant, causing a further increase in pressure. Successful inhibition of lubricating oil combustion can reduce or prevent damage caused by compressor ruptures. Ignited oil generates radicals and induces oxidizing chain reactions, thereby leading to sustained combustion. Additives are expected to inhibit such chain reactions by capturing radicals or intermediate products. Hence, earlier studies used a lubricating oil (POE) containing a phenol-based oxidation inhibitor (A1) and an epoxy-based stabilizer (A2). These studies indicated that additives have a combustion-inhibiting effect and can reduce the probability of compressor explosions occurring. In the present study, we focused on the combustion-inhibiting effect of a phenol-based oxidation inhibitor (A1), an epoxy-based stabilizer (A2), and a phosphorus-based anti-wear agent (P1). We experimentally investigated the effects of additive concentration and additive-refrigerant combinations on diesel-explosion inhibition.

2.4.1 Experimental apparatus and conditions

Figure 2-19 shows a schematic of the experimental apparatus used to simulate the conditions of a compressor rupture that occurs during the pump-down of an air conditioner. This apparatus consisted mainly of a refrigerant compressor and its driving system, a refrigerant supply system, an air supply system, a lubricating oil supply system, and a measurement and control system. The refrigerant compressor was simulated using a small model engine (ENYA R155-4C: 4-cycle modified engine) (hereafter called the “simulated compressor”) and driven by an electric motor (Mitsubishi Electric General-Purpose AC servo: HP-JP203) directly connected to the engine crankshaft.

The refrigerant supply system supplied refrigerant from the refrigerant cylinder via a mass flow controller and through the piping to the simulated compressor. In the air supply system, compressed air was supplied from the air compressor via a mass flow controller (manufactured by Kofloc: MODEL 8550MC-0-0-1-1) and a dehumidifier to flow through the piping to the simulated compressor. The refrigerant and the air blended into a mixture in the middle of the pipeline. The mixture was heated up to the designated temperature using an electric heater and supplied to the simulated compressor. In the lubricating oil supply system, lubricating oil was supplied from a tank, pressurized using a hydraulic pump, and then injected from the injector of an oil injection system (fuel injection system manufactured by FC Design) into the intake pipe of the simulated compressor. An encoder and a stroke sensor read the piston phase and injected oil at the piston phase angle of 90° (relative to the top dead center angular position of 0° for aspiration). The equivalence ratio (ϕ) was defined as the ratio of the actual mass of the oil to the mass of the oil completely burned with the engine's stroke volume of air. The theoretical air-to-fuel ratio was determined from the mass fraction (CHO ratio) of carbon, hydrogen, and oxygen in the oil. With an oil injection pressure of 100 MPa, the relationship between oil injection time and oil mass was premeasured and calibrated. The motor was controlled via a servo amplifier using a personal computer. The internal pressure of the engine was converted into an electric signal using a piezoelectric pressure sensor (manufactured by Kistler: 6045A), and the exhaust gas temperature was measured using a K-type sheath thermocouple (0.5 mm OD) provided on the exhaust pipe. The electric signals for pressure and temperature and the oil injection system signals (encoder, stroke sensor, and oil injection signals) were recorded in the personal computer via a data logger. The lubricating oil was a POE of viscosity grade 68. In the present study, A1, A2, and phosphorus anti-wear agent P1 were used as additives. The refrigerants were R290, R1234yf, R32, and R22. Tables 2-7 and 2-8 show the experimental conditions and the physical properties of the lubricating oil and the additives, respectively.

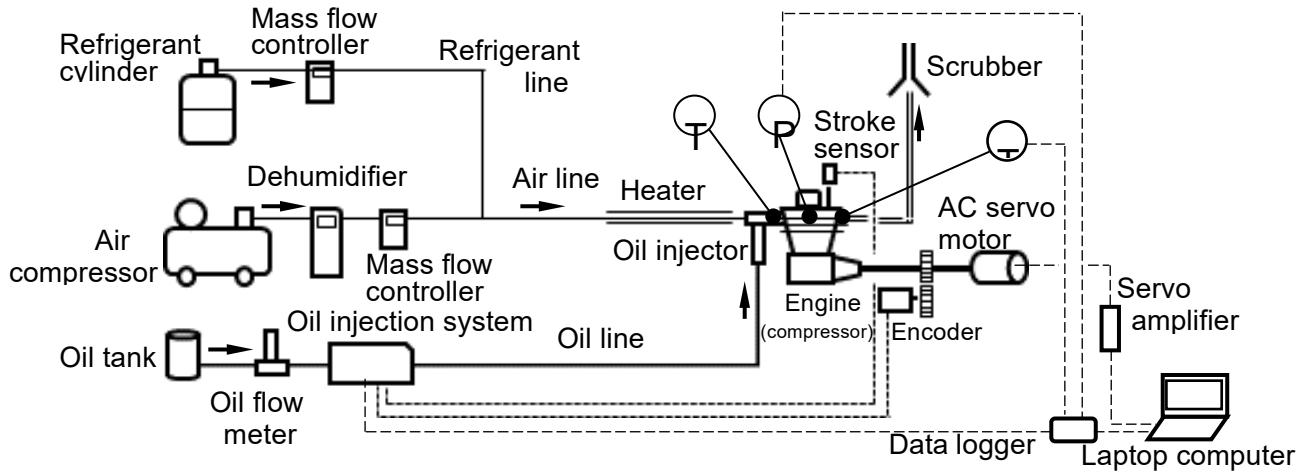


Fig. 2-19 Experimental apparatus.

Table 2-7 Experimental conditions

Compressor	Model engine (4 stroke engine) ENYA R155-4C(modified)
Compression ratio [-]	16
Stroke volume [cc]	25
Engine revolution [rpm]	1500
Mixture gas flow rate [L min ⁻¹]	18.8
Oil injection timing [°]	90 (at crank angle)
Inlet gas temperature [°C]	260±5
Oil equivalent ratio [-]	1
Refrigerat concentration [vol%]	0-64.9

Table 2-8 Properties of lubricant and additives

Lubricating oil	Polyolester (POE)
Viscosity grade	68
Ignition point [°C]	408
CHO ratio [mass%]	70.1:10.8:19.1
Theoretical air-fuel ratio [kg kg ⁻¹]	10.91
Additive	A1: Phenolic antioxidant A2: Epoxy stabilizer P1: Phosphorus anti-wear agent
Concentration of additive [wt%]	0, 1, 5

We conducted an experiment in the following sequence of steps: supply the specified amount of air to the simulated compressor operating at an engine speed of 50 rpm; increase the voltage of the electric heater wound around a pipe until the air temperature at the inlet of the simulated compressor reaches the designated temperature; flow the designated amount of refrigerant after the temperature stabilizes; change the engine speed of the simulated compressor to 1500 rpm and then start the oil injection system to inject oil; and start to record data to the personal computer immediately after oil injection until several seconds have elapsed. This experiment was conducted using different refrigerants and additives at different concentrations, and a lubricating oil (POE) with an equivalence ratio (ϕ) of 1.

2.4.2 Experimental results

(1) Pressure rise during lubricating oil combustion

To investigate the effects of additive concentration on lubricating oil combustion, we performed a compression ignition experiment using a mixed gas of air and lubricating oil ($\phi = 1$). The additive concentrations were 0, 1, and 5 wt%. Under these conditions, the mixed gas of lubricating oil and air burned by self-ignition. Due to the resulting calorific value, a significant pressure rise occurred. Figure 2-20 shows the average value of pressure rise obtained from 8 to 16 tests performed for each additive concentration. The ordinate axis in the figure represents the maximum pressure of the mixed gas divided by that of a mixed gas containing no additives, and the abscissa axis represents the additive concentration. The value of $P_{\max, \text{baseoil}}$ was 6.76 MPa. Although the maximum pressure decreased with an increase in additive concentration, the greatest decrease occurred with additive A2 at the concentration of 1%, similarly to the decrease at 5%.

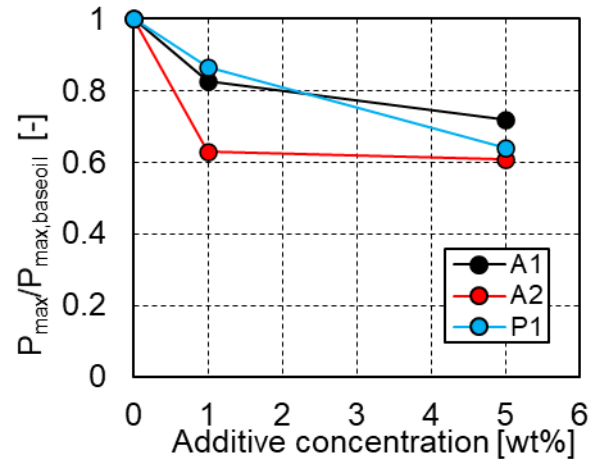
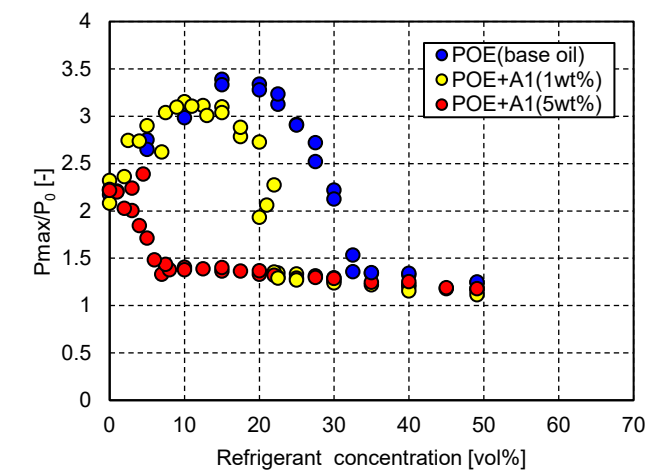


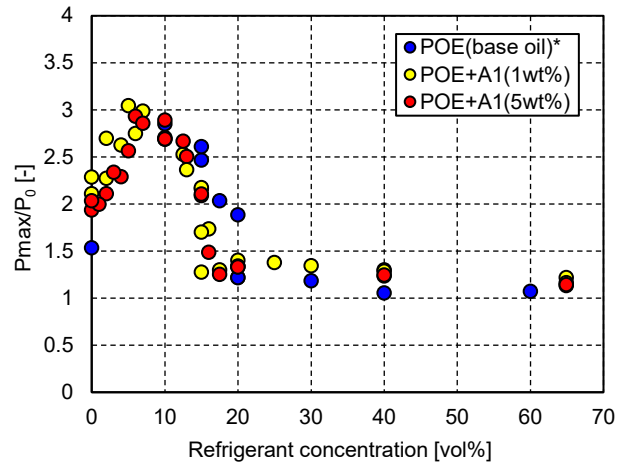
Fig. 2-20 Relationship between maximum pressure of mixed gas and additive concentration.

(2) Addition of the phenol oxidation inhibitor (A1)

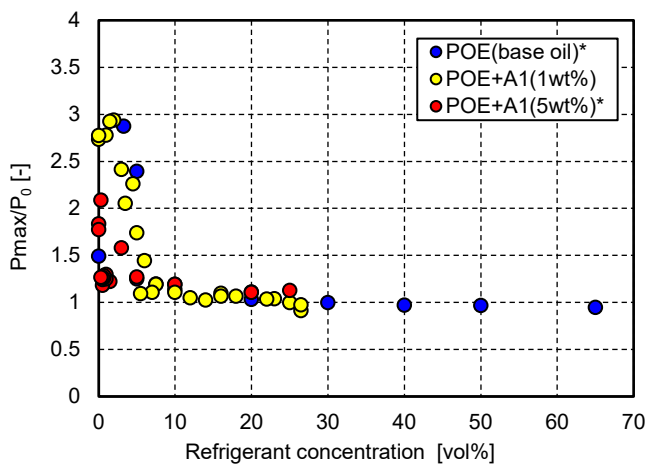
Using the additive concentration as the parameter, Fig. 2-21 shows the non-dimensional maximum pressure relative to refrigerant concentration for each of the refrigerants R22, R32, R1234yf, and R290. The value P_0 , which was used to de-dimensionalize pressure, is the measured maximum value of pressure from air-only compression with the inlet gas temperature set to 260 °C. The maximum pressure changes with an increase or decrease in clearance caused by factors such as a worn engine cylinder inner wall. Therefore, P_0 was measured at the beginning of each test and was used as the reference for non-dimensional pressure rise. The measured P_0 was approximately 2 to 2.3 MPa. A comparison of the UFL of refrigerant R22 is shown in Fig. 2-21 (a); the value was 32 vol% with no additive (0 wt% = base oil), and it was 22 vol% and 5 vol% with 1 wt% and 5 wt% of additive A1, respectively. Therefore, the UFL decreased with an increase in additive concentration. The flammable range was observed to narrow remarkably with an increase in additive concentration. Additionally, the non-dimensional maximum pressure was 3.4 with 0 wt% of additive A1, 3.2 with 1 wt% addition, and 2.3 with 5 wt% addition. Therefore, the maximum pressure decreased with an increase in additive concentration. The flammable range was 0–20 vol% for R32, which was narrower than R22’s range of 0–30 vol% and wider than R1234yf’s range of 0–6 vol%. In other words, the refrigerants differed from each other in their flammable range. For R32 and R1234yf, the influence of the additive concentration was unclear, although the additive concentration was observed to slightly reduce the flammable range. R290 showed a narrow flammable range of 0–2.5 vol% and a non-dimensional maximum pressure of 3.3 with 0 wt% of the additive, 2.7 with 1 wt% addition, and 2.4 with 5 wt% addition. Therefore, the maximum pressure decreased with an increase in additive concentration.



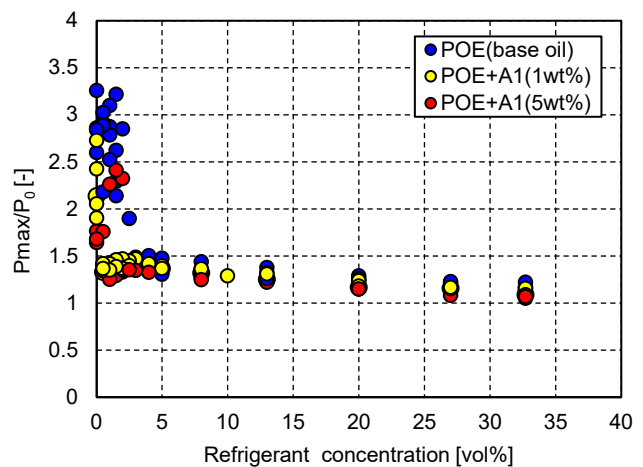
(a) R22



(b) R32



(c) R1234yf



(d) R290

Fig. 2-21 Relationship between the maximum pressure of mixed gas and the refrigerant concentration for additive A1.

(3) Addition of the epoxy stabilizer (A2)

Using the additive concentration as the parameter, Fig. 2-22 shows the non-dimensional maximum pressure relative to refrigerant concentration for each of the refrigerants R22, R32, R1234yf, and R290. A comparison of the UFL of refrigerant R22 was made (Fig. 2-22(a)); the UFL was 32 vol% with no additive (0 wt% = base oil), and it was 22 vol% and 18 vol% with 1 wt% and 5 wt% of additive A2, respectively. Therefore, the UFL decreased with an increase in additive concentration. Another comparison showed that the upper-limit concentration of the R32 refrigerant in its flammable range changed as follows: 20 vol% with no additive, 10 vol% with 1 wt% of additive, and a disappearance of the flammable range with 5 wt% of additive. The upper-limit concentration of the R1234yf refrigerant in its flammable range did not show a particularly systematic tendency. For R290, the flammable range disappeared even at an additive concentration of 1%.

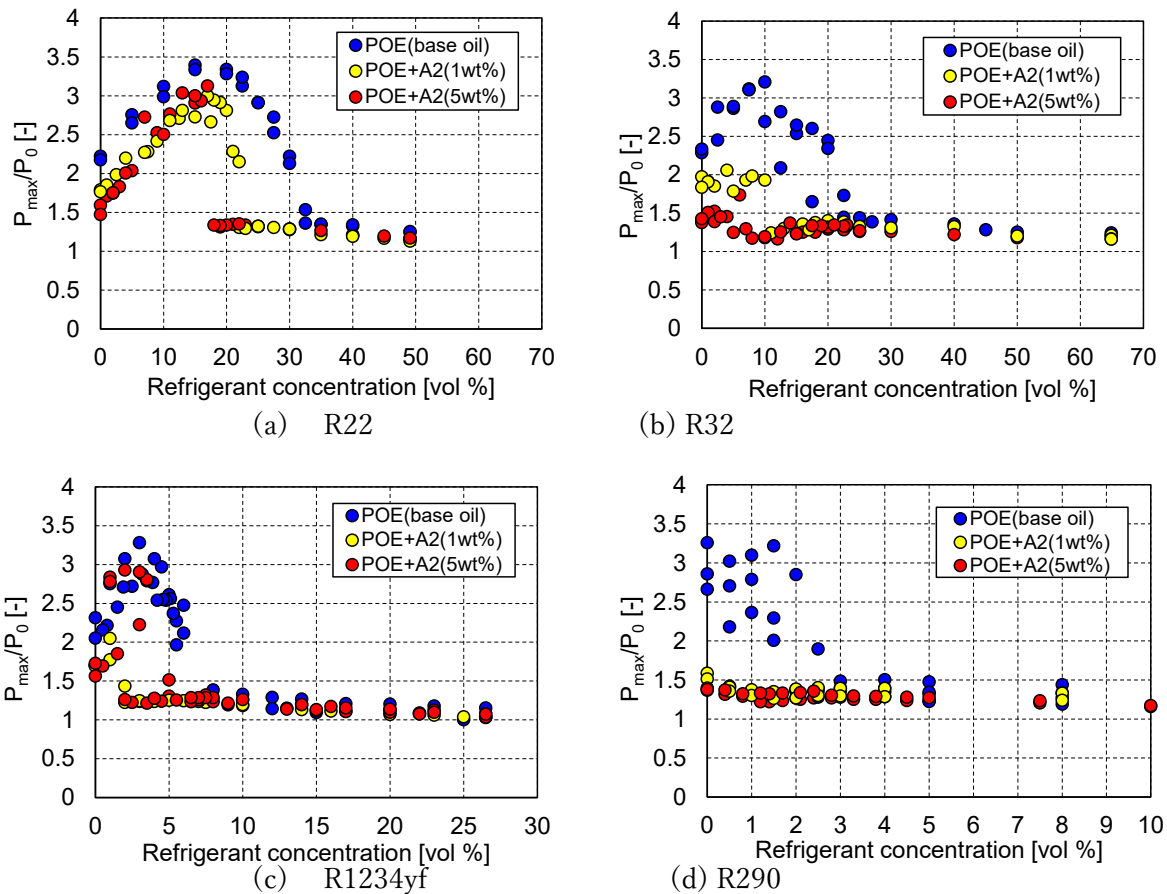


Fig. 2-22 Relationship between the maximum pressure of mixed gas and the refrigerant concentration for additive A2.

(4) Addition of the phosphorus anti-wear agent (P1)

Figure 2-23 shows the experimental results for additive P1. The effect of additive P1 concentration on combustion was similar to that of additive A1. A comparison of the UFL of refrigerant R22 was made for each additive concentration, revealing that the UFL was 32 vol% with no additive (0 wt%, base oil), and it was 25 vol% and 20 vol% with 1 wt% and 5 wt% of additive P1. Therefore, the UFL and non-dimensional maximum pressure decreased with an increase in additive concentration. However, the combustion- and pressure-inhibiting effects of additive P1 were than those of additive A1. In the presence of R32 and R290, the combustion- and pressure-inhibiting effects of additive P1 was approximately comparable with those of additive A1.

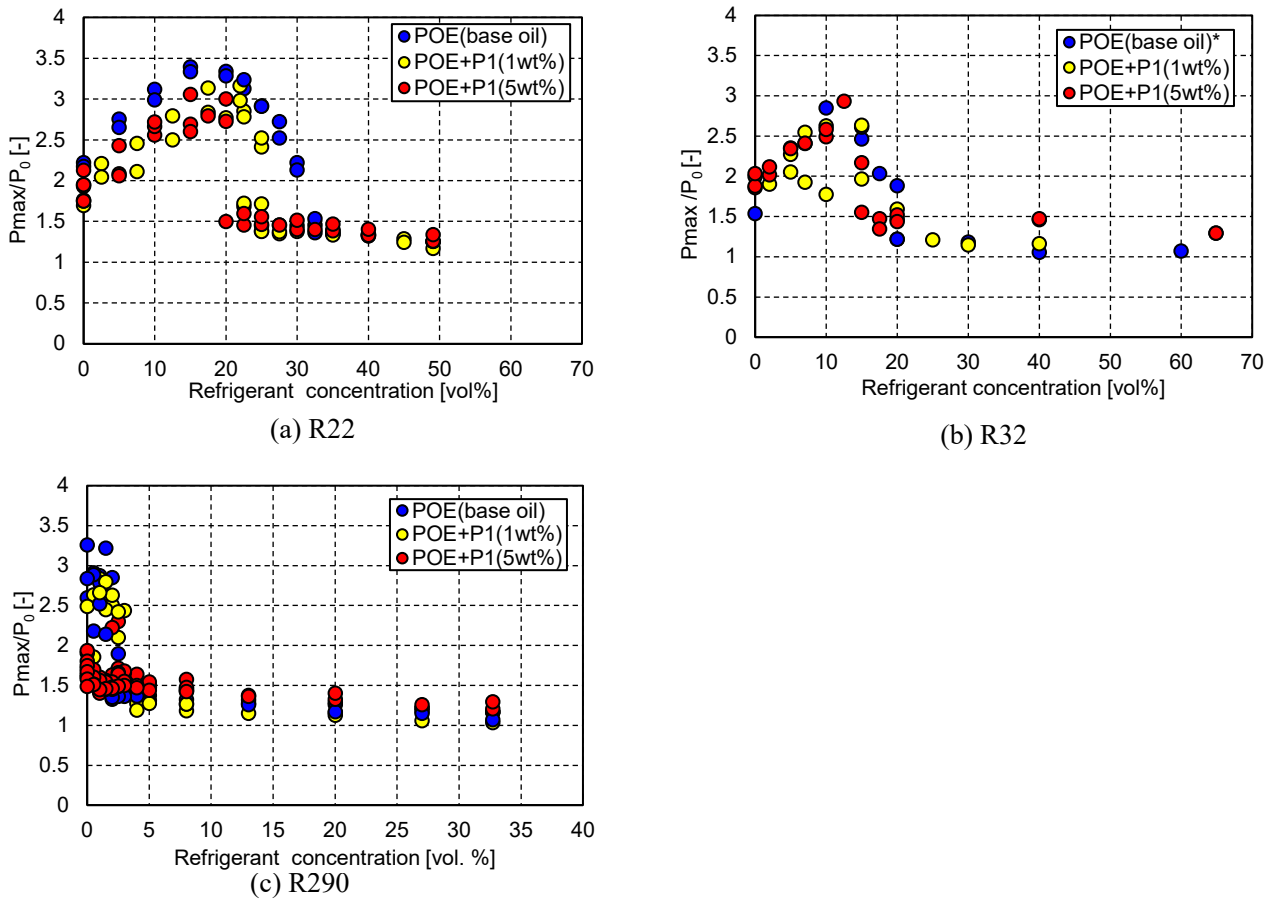


Fig. 2-23 Relationship between the maximum pressure of mixed gas and the refrigerant concentration for additive P1.

2.4.3 Summary

Using combinations of a lubricating oil (POE) containing additives with refrigerants R22, R32, R1234yf, and R290, we conducted a diesel compression experiment. The additives used were a phenol-based oxidation inhibitor A1, an epoxy-based stabilizer A2, and a phosphorus-based anti-wear agent P1, and they were added in concentrations of 0, 1, and 5 wt%, respectively. From the experimental results, we obtained the following findings:

- 1) Additives affect the flammable range and the maximum pressure. As the additive concentration increased, the flammable range became narrower and the maximum pressure decreased. Therefore, an increased additive concentration, which increases the combustion-inhibiting effect and reduces the destructive force of explosions, is expected to reduce the probability of compressor explosions occurring and the scale of the resulting damage.
- 2) The combustion-inhibiting effect varied depending on the combination of the refrigerant and the additive. Additive A2 showed an inhibitory effect on many refrigerants, even when added at a concentration of 1%. For R290 and R1234yf in particular, the concentration range for the occurrence of diesel explosions was significantly reduced.
- 3) For R22, its explosion was difficult to inhibit with small amounts of additives. The cause for the wide concentration range in which non-flammable R22 causes a diesel explosion is to be explored in the future.

References

- 2-1) Kirk, R.E. and Othmer, D.F., 1999. Concise Encyclopedia of Chemical Technology, Wiley.
- 2-2) IEC 60335-2-40: 2018. Household and similar electrical appliance - Safety - Part 2-40: Particular requirements for electrical heat pumps, air-conditioners and dehumidifiers. I.E.C.
- 2-3) IEC 60335-2-40 61D/421/CD, 2019. Amendment 1 – Household and similar electrical appliances – Safety – Part 2-40: Particular requirements for electrical heat pumps, air-conditioners and dehumidifiers (f1). I.E.C.

- 2-4) IEC 60335-2-89, "Household and similar electrical appliance –Safety- Part 2-89: Particular requirements for commercial refrigerating appliances and ice-makers with an incorporated or remote refrigerant unit or motor-compressor", International Electrotechnical Commission, (2019).
- 2-5) Higashi, T., Saitoh, S., Dang, C., Hihara, E., 2017. Diesel combustion of oil and refrigerant mixture during pump-down of air conditioners. *Int. J. Refrigeration* 75, 300-310.
- 2-6) Higashi, T., Tamai, S., Saitoh, S., Dang, C., Hihara, E., 2017. Effect of lubricating oil on explosion accidents of compressor during pump-down of air conditioner. *Trans of the JSRAE* 34(3), 181-191. Doi: <https://doi.org/10.11322/tjsrae.17-17>.
- 2-7) Higashi, T., Tamai, Dang, C., Hihara, E., Shitara, Y., 2018. Effect of additives to suppress the combustion of oil on pump-down accidents, JRAIA International Symposium on New Refrigerants and Environmental Technology.

Chapter 3 Progress achieved at Suwa University of Science

3.1 Introduction

Following the 2016 Kigali revision to the Montreal Protocol,³⁻¹⁾ Japan is required to reduce its HFC emissions by 85% of that in FY2011-13. Japan is expected to fall short of this target value by 2029 if the currently used refrigerants are applied without change.³⁻²⁾ Thus, HFC-emissions reduction should be promoted immediately. To this end, realistic consideration must be given to replacing the currently used refrigerants with next-generation refrigerants, such as propane (R290), as a fundamental countermeasure. However, many of these next-generation refrigerants are highly flammable. For their practical use, it is necessary to develop countermeasures assuming realistic scenarios of fire/explosions due to leakage of such a gas as R290 and to reduce the physical risks involved to socially acceptable levels. From this perspective, we started a research and development study titled “Establishment of a physical risk assessment method for next-generation refrigerant combustion through consideration of ignition sources in real use environments,” aiming to develop an evaluation method for devices and phenomena that may become potential ignition sources during the use of next-generation refrigerant-charged home-use air-conditioning equipment and industrial-use refrigeration and cold storage equipment for built-in refrigerated display cabinets. The obtained results are expected to allow more precise evaluations of ignition probabilities, i.e., more critical than in previous risk assessment methods intended to be applied to next-generation refrigerants. For the years from FY2018 to 2020, we focused particular attention on the hydrocarbon-based natural refrigerants of next-generation refrigerants. So far, we have evaluated, through bibliographic and website surveys and experiments, the possibilities that R290-air mixed gases leaked and pooled from air conditioning equipment may catch fire arising from the normal use of general household appliances and other electrical appliances or other causes, such as smoking. In this Report, we present an outline of these efforts.

The ignition sources used were selected with full consideration of the risk assessment results for home-use air-conditioning equipment and industrial-use refrigeration and cold storage equipment by the General Corporate Judicial Person, Japan Refrigeration and Air Conditioning Industry Association (hereafter “JRAIA”). The present study is currently undertaken as part of the NEDO Project “Development of Refrigerants and Refrigerating and Air Conditioning Technologies and Evaluation Methods for Achieving Energy-Saving and Low-Greenhouse Effects.” In this study, we endeavor to improve the accuracy and reliability of the experimental data and the physical risk assessment method to be developed through close collaboration with the other co-proposing institutions, i.e., the University of Tokyo, the National Institute of Advanced Industrial Science and Technology (hereafter the “AIST”), and the Research Institute of Science for Safety and Sustainability.

3.2 Structure of the present study

The present study consists of the following two subthemes:

- (1) Screening and modeling of ignition sources likely to pose a problem during the use of equipment

Identifying devices and phenomena likely to become ignition sources in real usage situations, assuming that refrigerants for home-use air-conditioning equipment and industrial-use refrigeration and cold storage equipment are replaced with extremely flammable hydrocarbon-based natural refrigerants regarded as promising next-generation refrigerants. The ignition sources thus identified shall be classified according to mechanism of ignition into categories, and an ignition mechanism model (hereafter “ignition source model”) for each category shall be developed.

The progress achieved so far is as follows: Assuming mainly the usage situations of home-use air-conditioning equipment, we identified and classified devices and phenomena regarded as potential ignition sources on the basis of JRAIA’s risk assessment results. First, using bibliographic and website survey results, a model of the ignition potential of electric sparks to ignite R290-air mixed gases was established, including an explicit mechanism of ignition, and was evaluated by comparison with the minimum ignition energy for R290. From the results thus obtained and the disassembly investigation results of the household appliances identified earlier, the ignition potential of each electrical appliance was evaluated. Similarly, for ignition due to static electricity or hot surfaces, ignition mechanism

models were developed on the basis of fundamental scientific theories.

(2) Physical risk assessment of next-generation refrigerants by means of various ignition sources

On the basis of the ignition source models developed in (1), data on the hazard of ignition shall be obtained and accumulated mainly through experiments. Closely cooperating with our co-proposers, i.e., the University of Tokyo and the AIST Research Institute of Science for Safety and Sustainability, we shall share knowledge and findings. On the basis of the obtained data and analytical results, a scientifically generalizable evaluation method shall be established for the ignition characteristics of next-generation refrigerants, including hydrocarbon-based natural refrigerants and mildly flammable HFC-based/HFO-based refrigerants.

The progress achieved so far is as follows: From the results of the classification in (1), we selected various types of potential ignition sources in the categories of electric sparks and hot surfaces. Then, we experimentally investigated the ignition possibility of R290-air mixed gas in the presence of these selected ignition sources: (i) electric sparks during contact relay opening/closing operations, (ii) wall-mounted light switches, (iii) plugging in and unplugging, and (iv) high-temperature hot surfaces represented by cigarettes.

3.3 Extraction of ignition sources and an evaluation method for their ignition capability

The JRAIA conducted a risk assessment relating to R290 introduced into home-use air-conditioning equipment and industrial-use refrigeration and cold storage equipment and made a list of devices requiring more detailed investigations regarding the risk of ignition. We first classified these devices, on the basis of their inherent mechanisms of ignition, into the major categories of “electric sparks,” “high-temperature hot surfaces,” and “open flames,” and investigated the ignition mechanism of each device. Then, we tagged the potential ignition sources of the electrical appliances and phenomena under each major category, and we decided to evaluate the ignition hazard on the basis of the ignition mechanism model of each major category. Table 3-1 shows the list of ignition sources selected for evaluation.

Table 3-1 List of selected ignition sources used in general life for R290/air mixture.

Major Category	Middle Category	End Category
Electric spark	Electric relay	Refrigerator, Washing machine, Hair dryer, Rice cooker, Microwave oven, Dehumidifier, Vacuum cleaner, Electric carpet, Oven, Fan, Television, Printer, Air cleaner, Audio & Video, Telephone, Facsimile
	Thermostat	Refrigerator, Electric stove, Oven toaster, Electric kettle, Electric Kotatsu table, Iron, Hair dryer
	Human operation	Plugging in and unplugging, Wall-mounted lighting switch
	Brush motor	Vacuum cleaner, Hair dryer, Electric razor
	Charge	Printer, Electrostatic spark discharge
Hot Surface		Electric heater, Hot plate for cooking, Burnt cigarette
Open flame		Burnt cigarette and lighter, Candles

Generally speaking, the ignition hazard of flammable gas can be evaluated by considering whether a flammable gaseous mixture is formed around an energy supply source and whether that source has sufficient energy to ignite the flammable gaseous mixture. The former is evaluated using a physical quantity called the flammable range, and the latter is evaluated from the (minimum) ignition energy. The reason the word “minimum” is in round parentheses here is that an evaluation based exclusively on the minimum ignition energy may result in an overestimation of the ease of ignition because of the dependence of ignition energy on the concentration of the flammable gaseous mixture. The minimum ignition energy is generally measured using a capacitive spark discharge in a calm flammable gas. For example, Lewis and Elbe³⁻³⁾ estimated the duration of spark discharge to range from 10^{-8} to 10^{-7} s. Strehlow³⁻⁴⁾ reported that in spontaneous discharge using an air capacitor for the experimental determination of the minimum ignition energy, up to approximately 90% of the stored energy is discharged in the form of sparks within 10^{-5} s.

For instance, a flammable gas-air mixture is ignited with several mJ of energy, such as static electricity. However, the mixture will not be ignited even if subjected via a Nichrome wire at the Joule heat equivalent of that energy. Additionally, electric sparks cannot generally ignite kerosene, wood chips, or the like in a chamber. The difference between the first and

the subsequent cases is the apparent ignition process. Nevertheless, these cases have the actual ignition process in common,^{3-5,3-6} which is approximately as follows:

Ignition is the onset of a sustained combustion reaction. A combustion reaction consists of chain reactions. Therefore, the combustion field must contain many active chemical species, such as the chain carriers OH and H. When energy (heat) is applied to the flammable gaseous mixture and the temperature rises, the number of active chemical species increases. At the same time, the flammable gaseous mixture loses heat and active chemical species to the surroundings. In other words, the balance between the heat generation rate and the heat loss rate determines the number of active chemical species. The heat generation rate is generally given by the Arrhenius equation:

$$\dot{q}_1 = QVC^n B \exp\left(-\frac{E}{RT}\right) \tag{3-1}$$

where V is the reaction system volume (m^3), Q is the reaction volume's substantive calorific value (kJ/m^3), C^n is the concentration term in the reaction rate equation, C is the number of moles per unit volume (mol/m^3), n is the order of the reaction, B is the rate constant, E is the activation energy (kJ/mol), R is the gas constant ($kJ/molK$), and T is the temperature (K).

Meanwhile, the heat loss rate is given by the Newtonian cooling principle as follows:

$$\dot{q}_2 = hS(T - T_0) \tag{3-2}$$

where h is the heat transfer rate (kW/m^2K), S is the system's boundary area (m^2), T is the system's internal temperature (K), and T_0 is the system's boundary temperature (K). Fig. 3-1 shows the plot of the two equations with respect to temperature. In other words, if $\dot{q}_1 > \dot{q}_2$, the system's temperature rises with no end and hence necessarily leads to ignition. Meanwhile, if $\dot{q}_1 < \dot{q}_2$, i.e., the heat release rate is greater, the temperature does not rise enough to cause ignition. Accordingly, where an instantaneous local high temperature is formed (heat release action can be ignored) as is the case with electric sparks, ignition will occur if a flame kernel and a concurrent mass of hot gas are formed between the electrodes and if this flame kernel has sufficient energy for steady-state flame propagation.

On the other hand, where a mixed gas is gradually heated as with a cooking hot plate, the effects of heat release cannot be ignored. Additionally, the initial low-temperature stage involves almost no reactive heat generation. Therefore, the ignition is governed by the externally supplied heating energy (or power). The required energy is larger than the minimum ignition energy produced by electric sparks – by one order of magnitude. In other words, as far as hot-surface ignitions are concerned, it is not appropriate to discuss the ignition possibility with a comparison of the minimum ignition energy defined above.

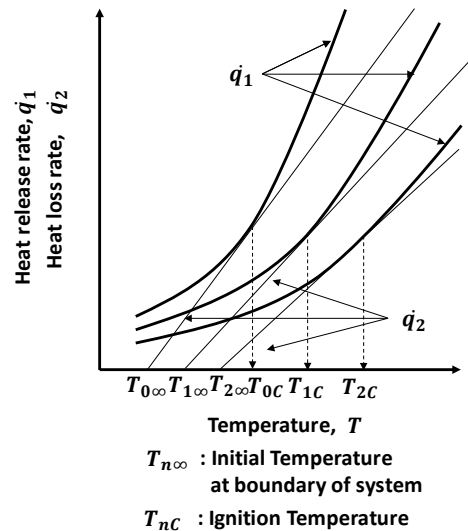


Fig. 3-1 Schematic diagram of the relationship between the balance of heat release and heat loss and ignition³⁻⁵.

3.4 Evaluation of the ignition possibility of R290 due to electric sparks

3.4.1 Evaluation of the ignition possibility due to electric sparks from contact relays

(1) Ignition model

In the case of electric sparks from contact relays, ignition depends on the balance between the heat generation rate and the heat loss rate, as explained above. Hence, it follows that the magnitude of discharge duration significantly affects the ignition energy. In other words, ignition may be possible if a characteristic time during which the effects of heat loss can be ignored exists from the start of energy supply until a certain point in time, and if the energy generated within that duration is sufficient for a sustained combustion reaction (minimum ignition energy). Kinoshita³⁻⁷ calls this duration the “critical ignition time” and estimates its duration to be approximately 100 μs (10^{-7} s).

⁴ s). As supporting evidence, Kinoshita quotes the Schlieren photographic observation results presented by Strehlow³⁻⁸⁾ for R290-air mixed gas flames, even after considerable time (approximately 10^{-4} s) has elapsed since the occurrence of a spark discharge: the initial flame resulting from a spark discharge developed into a full-fledged flame, which can propagate by itself if the energy was at or above a certain critical value, and if otherwise, the heat from the initial flame was lost to the electrodes, resulting in the termination and extinction of flame propagation. Additionally, many other studies have been reported, including those investigating the mechanism of electric discharge independently of combustion, to the same effect that OH radicals, the combustion-governing chain carriers, have a time constant of approximately $100 \mu\text{s}$.³⁻⁹⁻³⁻¹³⁾

However, contact relays used in household appliances are supposed to take approximately 10^{-3} to 10^{-2} s to release their discharge energy.³⁻⁷⁾ On the other hand, the minimum ignition energy is usually measured using a capacitive discharge with a discharge duration of 10^{-8} to 10^{-7} s.³⁻³⁾ The longer the discharge duration, the greater the heat release amount. Hence, ignition due to an electric discharge from a contact relay is estimated to require a considerably larger amount of energy than the required minimum ignition energy. However, to simplify the evaluation while assuming the worst situations, we decided to perform an evaluation on the premise that ignition is likely to occur when the minimum ignition energy is exceeded by the discharge energy produced between the contact relay contacts within $100 \mu\text{s}$. Additionally, in the fiscal year 2020, to investigate the effects of circuit load characteristics on discharge energy and ignition, we configured and experimentally evaluated circuits with variable resistance, inductance, and capacitance, and then installed and turned ON and OFF relays with exposed contacts in R290-air mixed gas to see if ignition would occur.

(2) Ignition possibility evaluations in the existing literature

Ohtori et al.³⁻¹⁴⁾ conducted arc energy measurements using a circuit consisting of a telephone relay, a carbon lamp (resistive load), and a 48-VDC power supply. According to their report, the arc duration is approximately $100 \mu\text{s}$ or below with a contact current below 1.4 A, which means that substantially all discharge energy can contribute to ignition. Though dependent on the material of the contacts, a contact current of approximately 0.6 A or above can produce an amount of energy (~ 0.5 mJ) exceeding the minimum ignition energy for R290-air mixed gas. However, because the ignition energy produced by electric sparks draws a downward convex curve with respect to fuel concentration, the above value is not necessarily sufficient for ignition at any concentration in the flammable range, and the fuel concentration range for an ignitable R290-air mixed gas is limited to the range from 3.0 to 6.9 vol% at the highest.

On the basis of the voltage/current measurement results reported in the literature³⁻¹⁵⁻³⁻¹⁷⁾, we measured the amounts of energy produced within $100 \mu\text{s}$ after the start of electric discharge for power relays and electromagnetic contactors with a controlling current exceeding 2 A. Some of these devices produced approximately 6 to 7 mJ of energy. These cases were ignitable over the entire flammable range for R290-air mixed gases because their ignition energy at the upper and lower flammability limits was approximately 4 mJ.

From the above, it follows that when an arc discharge occurs from the contact element of an electrical part, the amount of discharge energy alone cannot serve to deny the hazard of ignition. Electrical parts with a control capacity of 2 A or higher, in particular, can lead to ignition over the entire flammable range.

(3) Actual measurements of the discharge energy from contact relays

We performed the following experiments to demonstrate the investigation results described above:

(a) Experimental outline

We used two different types of commercially available contact relays (OMRON MK2P and G7J). The relays were connected to their respective loads, and for each of the contact closing and opening operations, the voltage across the contacts and the current flowing through the circuit were measured using a probe and recorded on a chart recorder. Fig. 3-2 shows the circuit diagram and photo of the apparatus. The loads used as actual devices were two different types of hair dryers, two different types of electric screwdrivers, and a single type of LED bulb. The loads used as model circuits were the following three different types: a resistor-only circuit (R circuit), a variable resistor-coil combination circuit (RL circuit), and a variable resistor-coil-capacitor combination circuit (RLC circuit) (Table 3-2).

Considering that the available AC power supply frequency was 60 Hz at the location of the experiment, we repeated the measurement 60 times per load type-relay type combination.

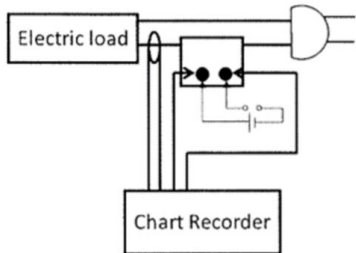


Fig. 3-2 Schematic diagram of experimental electrical circuit.

Table 3-2 Specifications of test devices.

Type of relay	Type of Electrical Load				Consumption Power (W)
Type 1	Inductive & Resistance	Hair dryer	Type A	HIGH	840
				MIDDLE	440
			LOW	40	
		Type B	HIGH	1050	
			MIDDLE	1000	
			LOW	700	
Capacitive & Resistance	Screwdriver	Type A	130		
		Type B	210		
Resistance	Electric bulb			50	
	Type 2	Inductive & Resistance	Hair dryer	Type A	HIGH

(b) Results

(i) Tests with actual devices

Regardless of the load device used, the discharge energy released within 100 μs had a value exceeding the minimum ignition energy. The amount of energy was larger at the closing of the relay than at its opening. The discharge energy tended to increase with higher power consumption (Fig. 3-3).

(ii) Tests with the model circuits

Fig. 3-4 summarizes the relationship between the element values and the energy produced within 100 μs after the start of electric discharge for each circuit element. First, for the R circuit, the discharge energy decreased as the circuit resistance increased. For the RL circuit and the RLC circuit, the discharge energy decreased as the coil inductance and capacitor capacity increased. These results allowed us to relate the amount of discharge energy to the value of the current flowing through the circuit, thus revealing that the resulting energy increased as the current values increased.

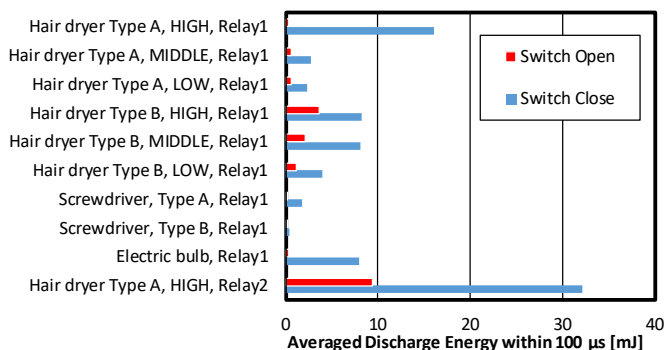


Fig. 3-3 Average discharging energy within 100 μs from the commencement of discharge in each condition of electrical relays and electrical loads.

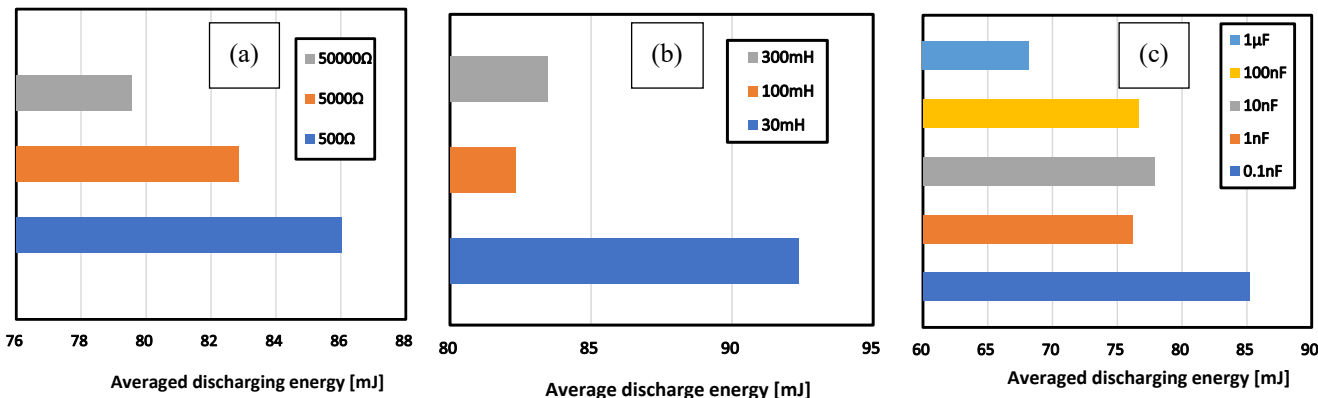


Fig. 3-4 Averaged energy of spark discharge at the gap of electrical contact with various characteristic values of an electrical circuit.

(a) R-only circuit (b) RL circuit (c) RLC circuit

(4) Ignition experiment

(a) Experimental outline

As shown in Fig. 3-5, a relay (OMRON MK2P) with its contact protection cover removed to expose its contacts was installed in a combustion chamber (plastic case), into which R290 was introduced to form an R290-air pre-mixed gas. Then, we operated the contacts to see if ignition would occur. Note that the plastic hood cover protecting the electrical contact was removed and the electrical contact was exposed to R290/air mixture for the ignition test. The top of the chamber was sealed with aluminum foil, which would be ruptured to provide an opening for pressure release at the occurrence of ignition. The R290 concentration inside the combustion chamber was set to 5.2 vol%. From the subsection immediately above, it turned out that the current's magnitude significantly governed the discharge energy. However, due to the small-rated capacity of the circuit elements, the resistor would be damaged if directly applied with 100 VAC. Then, using a 10- Ω resistor, we configured a circuit with a variable voltage transformer, which was used to adjust the supply voltage within the rated capacity of the circuit elements to provide a current on the order of amperes. The set voltages were 55, 60, and 70 ACV. The number of contact opening/closing operations was specified as 60 times at the maximum. The inverse of the required number of opening/closing operations for ignition was defined as the ignition frequency.

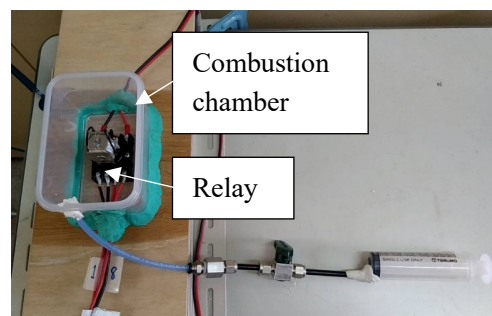


Fig. 3-5 Photo of experimental setup for ignition test by open/close of the mechanical relay with electrical contact.

(b) Results

In this experiment, ignition was observed in several cases. An electric discharge from the contacts caused a flame to propagate throughout the entire chamber, break through the aluminum foil, and propagate to the outside air. Fig. 3-6 shows the relationship between the nominal current (value of supply voltage divided by resistance) and the ignition frequency. The ignition frequency showed a tendency to increase exponentially as the current values increased. Therefore, it was suggested that the ignition frequency could be evaluated using the circuit current as an index. Incidentally, evaluating the ignition frequency from the circuit current was proposed because in the case of AC discharges, the current-voltage waveform significantly varies depending on the initial phase at the time of energization, thereby making it difficult to define the discharge energy. However, phenomenologically speaking, ignition is considered to be governed by the energy supplied to the unburned gas (or the energy per time). Hence, the challenge for the next fiscal year is to establish an organizing method more in line with scientific knowledge.

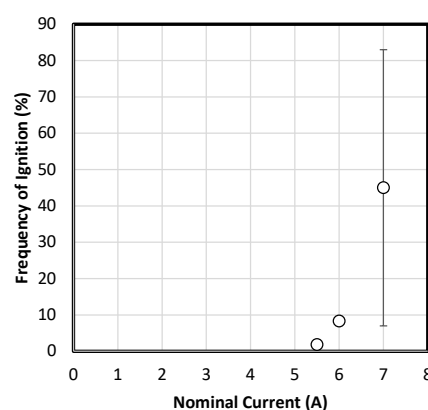


Fig. 3-6 Relationship between the ignition frequency and nominal value of current.

3.4.2 Evaluation of the ignition possibility due to electric sparks from brush motors

An approach similar to the case with electric sparks from contact relays helps to consider what governs ignition due to electric sparks from brush motors. Among the examples of measurements taken of brush motors' electric discharge waveforms is a study conducted by Isato³⁻¹⁸⁾ on the commutation phenomena and brush wear in DC motors during high-speed rotation. In the mentioned paper, the author observed current-voltage waveforms and rounded up the obtained results into a relationship linking arc duration, arc voltage, residual current, and rotational speed. According to the reported results, the arc duration and the residual current reached a minimum value at approximately 3000 rpm and then increased, whereas the arc voltage remained almost constant with the rotational speed. The current, the voltage, and the arc duration were measured at the rotational speed of 3000 rpm, at which the resulting amount of energy would be the smallest, and were read to be 17 V, 0.55 A, and 37 μ s, respectively. Therefore, the energy was 0.35 mJ. Since the arc duration was 100 μ s, we expected that all this energy would contribute to ignition and hence might ignite R290 depending on its concentration, albeit the possibility is not as high as with the cases of power relays or electromagnetic contactors described above.

3.4.3 Evaluation of the ignition possibility due to electric sparks from light switch operations

(5) Study outline

As one of the assumed scenarios for possible ignition due to electric sparks, we considered the case of turning on or off a light using a wall-mounted switch in an indoor environment where a flammable gaseous mixture was formed from R290 refrigerant leaked from home-use air-conditioning equipment. As shown in Fig. 3-7, wall-mounted switches contain contacts around which an arc discharge may occur and cause ignition. Accordingly, we conducted experimental evaluation of the ignition possibility due to switch operation, both qualitatively and quantitatively. Additionally, although many countries, including Japan and the United States, use voltages of 100 to 110 V, 16 of the 20 major countries³⁻¹⁹⁾ use 200 to 230 V. Hence, we experimented with the supply voltage set to 100 VAC and 230 VAC.

(6) Study flow

First, to determine if an R290-air mixed gas within the flammable range was formed near the switching contacts, the assumed ignition source, we measured the R290 concentration in the testing space and the casing containing the contacts (hereafter “contact casing”) (Test A). Next, we operated each switch under an air atmosphere, measured the voltage across the contacts and the circuit current, and determined the discharge energy to evaluate its ignition hazard (Test B). On the basis of the results thus obtained, we conducted the ignition experiment: We operated each switch with an R290-air flammable gaseous mixture formed in the testing space, visually observed the discharge and ignition behaviors around the contacts, and, at the same time, measured the amount of discharge energy and the distance to the light-emitting portion to quantitatively investigate their relationship to the occurrence/non-occurrence of ignition (Test C).

(7) Experimental outline

(a) Test A (concentration measurement experiment)

We built a 1-m cubic acrylic pool and cut holes in its wall to install the main body of each switch, including its contact casing, and a switch box supporting it. The switches used were the two types shown in Fig. 3-7 (Type A: Panasonic, WNP5101MW; Type B: Panasonic, WTP50011WP), both accounting for an estimated total domestic market share of 90% or more. For each switch, the installed heights were 787.75, 505, and 222.25 mm from the pool bottom, approximately corresponding to the heights of 3/4H, 1/2H, and 1/4H (H = pool height of 1000 mm), respectively. Hereafter in this Report, this notation is used to express the switch location. Allowing R290 to leak vertically downward in this pool, we measured the intra-pool R290 concentration at five different points along the height direction using an ultrasonic gas analyzer (US-II-T-S, Daiichi Nekken Co., Ltd.). The five leakage points were at the heights of 0, 100, 300, 500, 1000 mm from the floor, where the concentration was measured. Although the leak rate was set to 10 g/min, the leak amounts used were 41 g and 87 g, whose full-amount leakage and uniform diffusion into the pool resulted in an in-pool R290 concentration amounting to the lower flammability limit (LFL, 2.1 vol%) or the upper flammability limit (UFL, 9.5 vol%), respectively. However, to ensure safety, instead of R290, we allowed carbon dioxide to leak. The latter has nearly the same molecular weight as R290 and is supposed to resemble R290 in leakage behavior. The R290 concentrations were obtained from the carbon dioxide and R290 concentration calibration curves measured beforehand using an ultrasonic gas analyzer.



Fig. 3-7 Photos of test switches for lighting.
Upper: Body Middle: Button
Low: Electrical contacts
Left: Type A, Right: Type B

(b-1) Test B-1 (discharge energy measurement experiment: 100 V)

Using the setup shown in Fig. 3-8, we measured the amounts of discharge energy from the light switch contacts. The loads used were the following resistive loads: incandescent light bulbs (40, 60, and 100 W) and an LED bulb (60 W). A current monitor was placed between the light switch and each load to observe the current waveform during energization while measuring the voltage across the switch using an oscilloscope. The switching action was performed via remote control with a jig fitted on a motorized slider. To observe the conditions of the contacts in the contact casing, we drilled a hole in the casing for a high-speed camera to record the electric discharging process from vertically downward. The surroundings around the contacts were placed under an air atmosphere to perform the switch press action ten times per load. For each load type, the product of the obtained current and voltage waveforms was time-integrated to determine the amount of discharge energy.

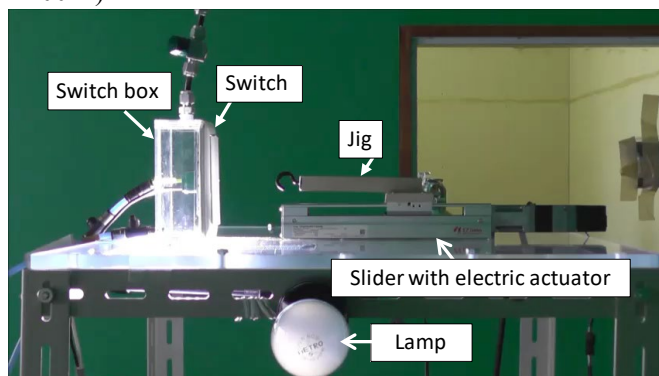


Fig.3-8 Photo of setup used to measure the discharge energy of wall-mounted light switches.

(b-2) Test B-2 (discharge energy measurement experiment: 100 and 230 V)

Using a circuit similar to the one in (b-1), we measured the amounts of discharge energy from the light switch contacts. The loads used were the following resistive loads: six different types of incandescent light bulbs (40, 60, and 95 W bulbs, one for each wattage, and three different types of 100 W bulbs) and a Hf fluorescent lamp (32 W). The applied voltages were 100 V and 230 V, and the switch used was a Type A switch (Fig. 3-7). The atmosphere around the switch contacts was air. The switch press action was performed 60 times per load. The amounts of discharge energy were determined similarly to the case of (b-1).

(c-1) Test C-1 (ignition experiment: 100 V)

The ignition experiment setup used was the same as in Fig. 3-8. To ensure safety, R290 was introduced only into the switch box. The concentration measurement results above showed that the concentrations inside the switch box and the contact casing were approximately the same. Hence, we assumed that if the switch box contained an R290-air mixed gas within the flammable concentration range, R290 would flow into the casing through the hole in the contact casing. Predetermined amounts of R290 were measured out into syringes in advance and introduced through the inlet port on the switch box. The amounts introduced were 12 mL and 21 mL, which, if wholly diffused into the switch box, resulted in an in-box concentration amounting to the LFL or the stoichiometric concentration, respectively. In this test, the only circuit load used was an incandescent light bulb (60 W), and the only type of switch used was a Type B switch. The methods used to check the occurrence/non-occurrence of ignition were a video camera and eye-sight observation. The amounts of discharge energy from opening/closing the light switch were determined similarly to the case of (b) above.

(c-2) Test C-2 (ignition experiment: 230 V)

The combustion chamber used for the ignition experiment was a pool built from 10-mm-thick acrylic boards to an inner capacity of $150 \times 150 \times 150$ mm. This chamber had its top sealed with aluminum foil, which would be ruptured to release pressure at the occurrence of combustion. The pool had a small fan installed inside. The socket for the switch was provided vertically along the chamber's outer wall, with the switch contact casing positioned inside the pool. The circuit was configured the same as in Test B. The contact casing had an opening cut to allow R290 gas to flow in between the switch electrodes. The R290 gas was introduced into the acrylic pool and stirred to a uniform concentration by the small fan for 1 min. The in-pool R290 gas concentration was set to approximately 4%, which corresponded to the stoichiometric concentration. A hole was cut in the bottom of the contact casing for a high-speed camera to record the electric discharging process. The loads used were the 100 W incandescent light bulbs and the Hf fluorescent lamp (32 W). Both produced large amounts of discharge energy in Test B. The applied voltage was set to 230 V. The switch press action was performed 50 times per load. The amounts of discharge energy were determined similarly to that in Test B.

(8) Results and discussion

(a) Flow of flammable gaseous mixture into the contact casing

In both Type A and Type B, regardless of the leak height, an R290-air mixed gas with a composition in the flammable range was observed to flow into the contact casings of the switches installed at the heights of 1/2H and 1/4H. The R290 probably flowed into the switch box through the gap between the switch plate and the main body of the switch and then into the contact casing through the hole in it.

(b) Discharge energy from the contacts

As a result of the experiment, we obtained the following findings:

- (i) In some cases, a single switching action caused more than one electric discharge.
- (ii) Larger amounts of discharge energy were observed at circuit opening operations than at circuit closing operations. Note, although the discharge duration itself was longer during circuit opening operations than circuit closing operations, as far as the critical ignition time was concerned, the amount of discharge energy was greater during circuit closing. Nevertheless, in some cases, both circuit operations were observed to generate energy exceeding the minimum ignition energy.
- (iii) The light bulbs showed an arc discharge voltage distribution spreading over an approximate range from 10 to 20 V, regardless of the applied voltage. Larger amounts of discharge energy occurred with the applied voltage of 100 V, from which a higher maximum current resulted during an electric discharge.
- (iv) Generally, an alternating current arc discharge shows its maximum voltage when the phase angle is nearly 90°. However, regardless of the applied voltage, large amounts of voltage were observed with the fluorescent lamp when the phase was within the range from 20° to 90°. The probable cause was the effects of the ballast inside the fluorescent light fixture. The discharge energy was higher with the applied voltage of 230 V.
- (v) The above tendencies did not depend on the load type.

It follows from these findings that there is no denying the hazard that an R290-air mixed gas of a flammable composition may form near the light switch contacts and the possibility that discharge energy from the contacts may occur in amounts exceeding the minimum ignition energy, thus indicating that the possibility of ignition cannot be excluded.

(c) Ignition experiment

On the basis of the above, we conducted the following ignition experiments: 60 repeated switching actions (100 V) under each concentration condition and 200 repeated switching actions (230 V) at an R290 gas concentration of approximately 4%. Notably, we did not observe ignition during these experiments. The high-speed camera images of the captured electric discharging process showed that the distance to the light-emitting portion was approximately 0.1 to 0.4 mm. This value corresponds to approximately 1/10 to 1/4 times the quenching distance (1.7 mm^{3-20}) of R290. The diameter of the contacts was approximately 2.0 mm, which was also larger than the inter-contact distance by one order of magnitude. Therefore, there are two probable reasons for the absence of ignition. First, because the size of the discharge kernel was below the quenching distance, the discharge kernel suffered heat loss due to its contact with the contacts and failed to develop into a sustainable flame. Second, the discharging power by arc discharge was small because the current through the circuit of the lighting device (electric load) was small.

However, the IEC standard³⁻²¹⁾ prescribes a criterion called “3 mm gap” as a general technical reference for switching contacts. Hence, the contacts are separated from each other by at least 3 mm. It follows then that if an electric discharge occurs over the full gap length to form a flame kernel, the resulting flame will pass through the gap and propagate throughout.

Accordingly, we considered the relationship between gap length and dielectric breakdown voltage. A voltage V_s that causes dielectric breakdown (i.e., electric discharge) in a gas is a function of the product of gas pressure p and electrode distance d , as expressed by the following equation (Paschen’s law):

$$V_s = \frac{Bpd}{K + \ln(pd)}, K = \ln \left\{ \ln \left(1 + \frac{1}{\gamma} \right) \right\} \quad (3-3)$$

where B and K are constants and γ is the cathode secondary electron emission coefficient, which can be deemed as $\gamma = 0.01$ in the case of air atmosphere. Generally, the dielectric breakdown voltage in air is 330 V. Hence, the

corresponding gap length d determined using Eq. (3-3) under atmospheric pressure conditions is 0.01 mm. For a gap length of 3 mm, the dielectric breakdown voltage will exceed 12 kV. For a gap length of 1.7 mm, i.e., the quenching distance, the value will be approximately 7.8 kV. Because such large amounts of voltage are unlikely to be generated by light-switch operation, the gap length during an electric discharge is estimated to be below the quenching distance at the maximum. Therefore, we consider that the ignition possibility due to arc discharges from light switch contacts is negligible.

3.4.4 Evaluation of the ignition possibility due to electric sparks from power plugging in and unplugging

(9) Study outline

With basic knowledge alone, including electric spark energy, it is difficult to evaluate the ignition hazard due to electric sparks from plugging in and unplugging to and from the socket (mainly unplugging). In addition, no research reports have been published on this issue. Therefore, we decided to reproduce this action experimentally to evaluate its effect on ignition. Incidentally, some of the results of this study were orally presented in FY 2019.³⁻²²⁾ In the fiscal year 2020, bearing in mind application of overseas products, we performed ignition possibility evaluation using an SE Type (Type C) socket plug, which is 230 VAC-compatible and used in more than half of all countries around the world.

(10) Study flow

An R290-air mixed gas of a predetermined concentration was introduced into a combustion chamber mounted with a power socket, into which the power plug of a load was plugged to observe the occurrence/non-occurrence of ignition via high-speed photography. We attempted a quantitative evaluation of the ignition behavior by measuring fluctuations in the current and voltage across the plug during plugging in and unplugging.

(11) Experimental outline

(a) Adaptability experiment for 100 VAC products (Type A)

In the internal space of a 150-mm cubic chamber with its top sealed with aluminum foil (Fig. 3-9), a commercially available Type A power socket (Fig. 3-10) was vertically installed for the ignition experiment. Built with no partition between its inside and the prong insertion holes, the socket housing allowed gas, if it had infiltrated, to diffuse and reside all over inside. We conducted the following two patterns of tests: ① repeating the plugging in and unplugging action 200 times (Test ①) and ② repeating only the unplugging action 100 times (Test ②). In Test ①, the R290 gas that was introduced into the chamber was replaced every time ignition was observed. Meanwhile, in Test ②, the gas was replaced every time, regardless of ignition. In both tests, the R290 concentration of 5.18 vol%, at which the minimum ignition energy is supposedly encountered, was selected as the observational target concentration to ensure the most rigorous evaluation possible. The voltage across the power plug and the circuit current were measured using a probe and recorded on the chart recorder. The loads used were household

Table 3-3 List of test device specifications.

Type of Electrical Load				Consumption Power (W)
Inductive & Resistance	Hair dryer	Type A	HIGH	810
			MIDDLE	420
		Type B	HIGH	1040
			MIDDLE	700
Capacitive & Resistance	Screwdriver	Type A	200	
		Type B	80	
Inductive & Capacitance	Vacuum cleaner	Type A	1000	
		Type B	970	

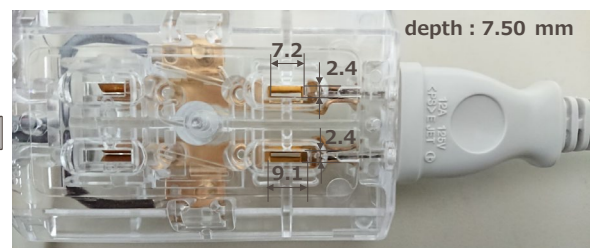
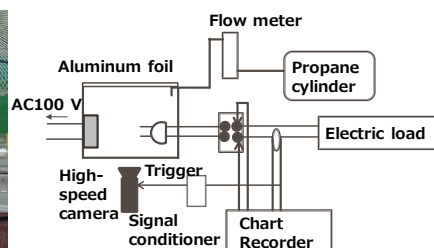
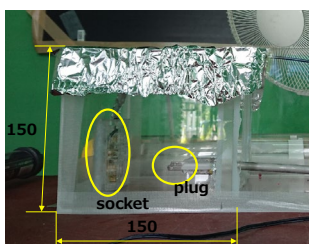


Fig. 3-9 Photo of setup for the ignition test of propane/air mixture by plugging in or unplugging the power cable of general electric appliances.

Fig. 3-10 Photo of the electrical socket.

appliances (hair dryer, electric screwdriver, and vacuum cleaner) that were commercially available; their specifications are shown in Table 3-3.

(b) Adaptability experiment for 230 VAC products (SE Type)

Fig. 3-11 shows the socket in its normal condition (Left) and one with its cover portion cut out as much as possible for use in the experiment (Right). As shown in Fig. 3-12, we installed the socket for the experiment in the internal space of a 200-mm cubic polycarbonate pool with its top sealed with aluminum foil. We cut the socket's cover portion smaller to expose the socket's inside to the R290 gas atmosphere. The R290 gas concentration inside the chamber was adjusted to approximately 4%. The applied voltage was 230 V. A variable resistor was used to provide two different loads (50 Ω and 300 Ω). The plugging in and unplugging actions were performed at two different speeds (quick and slow). The loads thus caused were measured using a force gauge and adjusted until constant. We repeated the measurement 50 times per case and recorded the voltage and current between the socket and the plug using an oscilloscope to calculate the discharge energy.

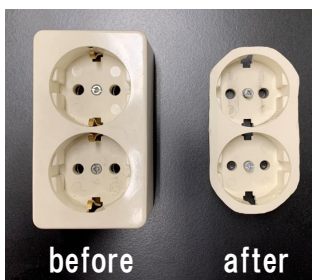


Fig. 3-11 Photo of electrical plug socket (SE type)

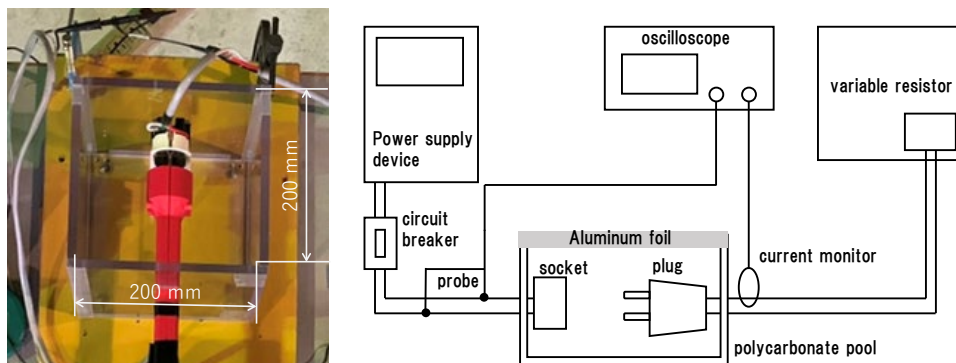


Fig. 3-12 Photo of setup for the ignition test of propane/air mixture by plugging in or unplugging the power cable.

(12) Results and discussion

(d) Adaptability experiment for 100 VAC products

(a-1) Ignition probability

In Test ②, no ignition was observed, even once, whichever of the two loads was used. This result suggests that ignition requires a certain number of repeated plugging in and unplugging. As shown in Fig. 3-13, the ignition probability showed a tendency to increase by and large as the power consumption increased.

(a-2) Ignition and flame propagation mechanisms

Fig. 3-14 shows the high-speed color photographs of the socket and its vicinity with the Type B hair dryer used as the load. In the figure, *t* stands for the elapsed time from the start of electric discharge (when the emitted light was observed). The images in Fig. 3-14(a) and (b) show highly similar behaviors. In both cases, the discharge duration (duration of this emitted light) ranged from 4.3 to 4.5 ms, and approximately 100 to 130 ms after removing the plug from the socket, a flame gushed out a different socket (upper socket). The resulting discharge energy was approximately 4.5 mJ, a sufficient amount of energy to cause ignition. Considering the width of the socket's plug prong insertion hole (~ 2.4 mm) and the quenching distance of an R290 flame (1.70 mm), repeated plugging in and unplugging should lead to the R290-air mixed gas infiltrating from outside the socket into the socket's housing to catch fire from sparks during unplugging, resulting in a gush of flame out the upper socket.

On the other hand, Fig. 3-14(c) shows a somewhat different view. After the emission of light inside the socket, a flame was observed to occur near the prongs at a significantly earlier stage than in Fig. 3-14(a) and (b), which

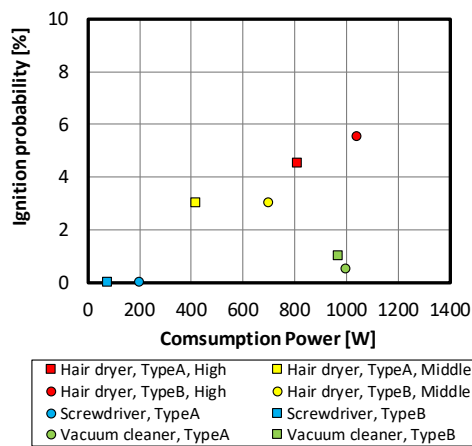


Fig. 3-13 Dependence of the ignition probability by plugging in/unplugging on the consumption power.

propagated in concentric circles within approximately 6 ms. Because the flame was seen to propagate from near the prongs toward the socket, the probable mechanism of ignition, in this case, involved ignition occurring outside the socket and the flame propagating to the unburned gas mixture in the chamber, unlike the cases in Fig.3-14(a) and (b). We surmised that the responsible factor for the ignition was an electrostatic discharge produced either between the prongs and dust particles whirled up in the chamber due to repeated plugging in and unplugging or between the prongs and the metal powder particles entrained from inside the socket during plugging in and unplugging. However, the present experiment alone did not provide us with conclusive evidence. Additionally, load conditions, such as inductance, capacitance, and resistance, showed no definitive effects on the ignition possibility. As explained earlier, the ignition possibility depended almost exclusively on power consumption.

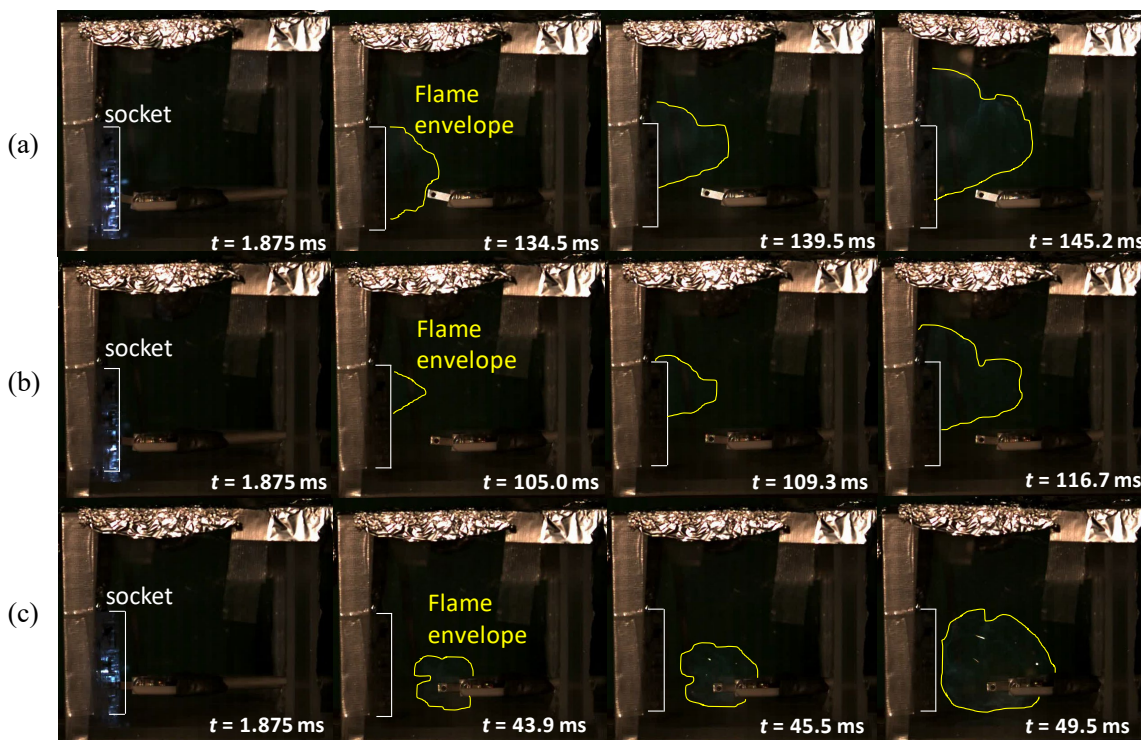


Fig. 3-14 High-speed images of test space around an electrical socket. Electrical load: hair dryer (type B)

(e) Adaptability experiment for 230 VAC products

Fig. 3-15 shows images of the plug near the socket, which captured the moments of light emission inside the socket for the 300 Ω -OFF quick action (Fig. 3-15(a)) and the 50 Ω -OFF quick and slow actions (Fig.3-15(b) and (c)). In the 300 Ω -OFF quick action, the light emission range was minute. The only observable case of light emission was the one shown in the photo. In the 50 Ω -OFF quick and slow actions, bluish-white light was observed to occur over a wider range than in Photo (a). This result suggests that the light emission observed during the 300 Ω -OFF quick action was probably due to an electric discharge. Meanwhile, during the 50 Ω -OFF action, an instantaneous flash of yellow and bluish-white light was observed through the gap between the housing and the switch box (Fig. 3-15(b) and (c)). This phenomenon

was observed for 20/50 of the 50 Ω -OFF quick actions and for 8/50 of the 50 Ω -OFF slow actions. This phenomenon might be an example of ignition due to a trace amount of R290-air mixed gas present in the portions of the plug and socket making electrical

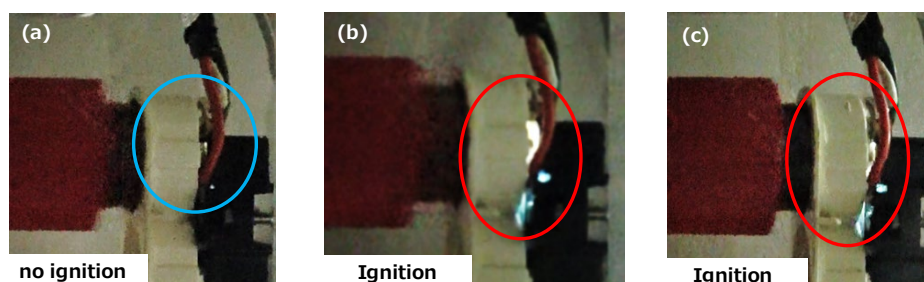


Fig. 3-15 Photo of test space around an electrical socket and plug. (a) 300 Ω -OFF quick, (b) 50 Ω -OFF quick, (c) 50 Ω -OFF slow

contact. However, no changes were observed, such as the aluminum foil getting blown off from the top of the acrylic pool. Moreover, the video images did not capture any flame propagating to the R290 gas inside the acrylic pool. The discharge energy of ignition fell in the range from 63 to 328 mJ, and no light emissions of this kind were observed in the range of 50 mJ or below, still well above the minimum ignition energy of R290 (0.7 mJ).

3.4.5 Evaluation of the ignition possibility due to electrostatic sparks

(13) Study outline and flow

To evaluate the ignition possibility due to electrostatic sparks, we considered everyday-life electrostatic charge scenarios and human body electrostatic discharge scenarios in line with the risk assessment conducted by the JRAIA. On the basis of the obtained results, we estimated electrostatic potentials, energy amounts, and the effects of humidity on these parameters through bibliographic surveys and other methods. The scenario development process required a comprehensive consideration covering, among other factors, the positional relationship of the static discharge and flammable concentration region and the occurrence probability of static discharges.

(14) Outline and results of the evaluation

(f) Electrostatic charge scenario

Probable causes of the human body's electrostatic charges in everyday life include walking/shuffling, standing up from sofas/chairs, undressing, blanket folding, and hair brushing. As scenarios of static discharge from the human body (statically charged from such sources), we considered two cases: ① static discharge while touching a doorknob and ② static discharge while undressing.

(g) Types of static discharge and scientific classification of ignition capabilities

Electrostatic discharge mainly occurs as spark discharge, corona discharge, brush discharge, creeping discharge, cone discharge, and lightning-like discharge. The characteristics of these types of static discharges are as follows:³⁻²³⁾

(i) Spark discharge:

A static discharge that occurs between conductors. Its discharge energy is relatively large and can be calculated using $E = (1/2)CV^2$ (C : capacitance (F) and V : voltage (V)). According to a guideline, this static discharge can ignite flammable gas with a minimum ignition energy of 100 mJ or less and hence is a potential ignition source. The relationship between electrostatic potential and capacitance is shown in Fig. 3-16. Spark discharges are likely to occur when a conductor has a maximum electrostatic potential exceeding 330 V.

(ii) Corona discharge

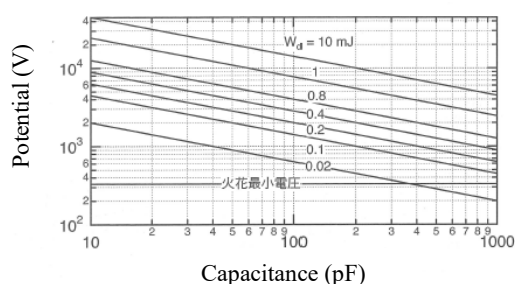


Fig. 3-16 Relationship between the electrostatic potential and capacitance at each energy by spark discharge³⁻²²⁾.

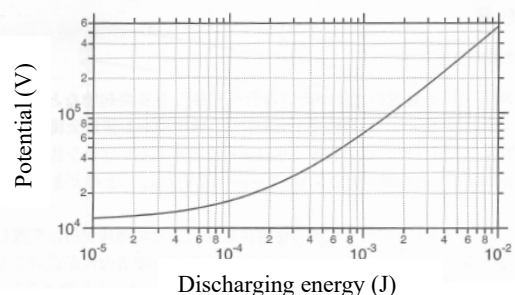


Fig. 3-17 Relationship between the charge potential and discharging energy by brush discharge³⁻²²⁾.

A static discharge that occurs in the presence of a high local electric field, which is an unequal electric field formed near a pointed needle electrode, a thin wire electrode, or an electrode with an extremely small curvature radius. Generally, this static discharge occurs with an electrode with a curvature radius of 5 mm or less. Nevertheless, this static discharge is relatively low in energy and generally does not pose a risk as an ignition source of flammable gases other than those with an extremely low minimum ignition energy, such as hydrogen.

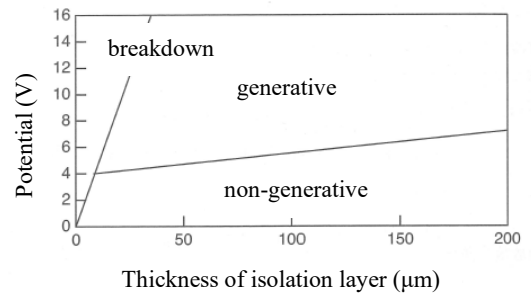


Fig. 3-18 Criteria for the generation of creeping discharge³⁻²²).

(iii) Brush discharge

A static discharge that occurs mainly when a high-curvature grounding metal, a fingertip, or the like approaches an electrically charged insulant. Positive-polarity discharges are known to pose a higher risk of ignition. A brush discharge has an energy ranging from 1 to 3 mJ without exceeding 4 mJ, but it poses a risk as a potential ignition source of flammable gases. Fig. 3-17 shows the relationship between the average electric potential of an insulant's surface and the discharge energy of a brush discharge (for the case of a grounding conductor sphere with a radius of 20 mm).

(iv) Creeping discharge

An insulating body with a small thickness has electric double layers on both of its sides, which enables it to sustain a higher surface charge. A static discharge that occurs along the surface of such an insulant is a creeping discharge. In some cases, this static discharge has an energy of approximately 10 J and poses a risk as a potential ignition source of flammable gases. However, as shown in Fig. 3-18, creeping discharge occurs on an insulating body when the thickness is 8 mm or less and its insulating layer's electric potential reaches 4 kV or more.

(v) Cone discharge

A static discharge that occurs on the surface of a cone-shaped field where electrically charged powder particles build up during the pneumatic conveyance of powder with insulating properties.

(vi) Lightning-like discharge

A lightning-like discharge occurs in an installed silo or a tank where charged clouds form in the presence of electrically charged powder particles or mist vapors during powder loading or delivery into a silo or the like, jet cleaning inside a tank, or other similar situations. However, this static discharge requires an electric field as high as 500 kV/m and hence usually does not occur.

(h) Ignition hazard due to static discharge while touching a doorknob

The static discharge, in this case, corresponds to the "spark discharge" listed above in (b). An electrostatic potential of 4 kV or more in the human body is necessary for the occurrence of visibly observable static discharge light. This electric potential corresponds to the intensity of an electric shock "that feels like being stuck deep with a needle and causes a slight pain in the finger." This description³⁻²⁴) seems to apply to static electricity in general living environments. Hence, the electrostatic potential used for estimations here is 4 kV. Generally, the capacitance of the human body is 100 pF.³⁻²⁴) Using these values, the energy of a spark discharge is $E = 0.80$ mJ. The possibility of ignition due to static discharge of this kind cannot be excluded when the discharge is simply evaluated using this energy value exclusively.

(i) Ignition possibility due to a static discharge while undressing

The static discharge, in this case, corresponds to the "brush discharge" listed above in (b). According to the literature, an electrostatic potential generated from undressing is approximately 4.0 to 5.0 kV. In this case, from Fig. 3-17, the discharge energy is in the order of $<10^{-5}$ J and hence falls short of igniting R290-air mixed gas. Therefore, we consider that the ignition possibility due to an electrostatic discharge involved in undressing is negligible.

3.5 Ignition hazard of R290 due to various electrical appliances

Section 3.4 presented a list of cases where a contact relay was one of the electrical parts used. If the vicinity of the electric discharge contains R290-air mixed gas, ignition might occur depending on the gas concentration. We surmised that the discharge energy might be large enough to ignite the gas regardless of its concentration, especially near the contacts of a relay with a control capacity exceeding 2 V. On the basis of these observations, we performed disassembly investigations of some general household appliances used in everyday life and, at the same time, evaluated some of them in terms of ignition possibility using photographs of disassembled devices posted on websites.

(i) Ink jet printers

A commercially available ink jet printer (EPSON, EP-806AR) was disassembled to check for any electrical parts that might be a potential ignition source, as explained in Section 3.4. The printer was found to contain two sheet-feeding brush motors and an ink cartridge-driving brush motor. This printer uses contact relays for both of its two electronics boards, one for ink discharge control and the other for sheet feed control. It follows from the foregoing that the brush motors used inside an ink jet printer may ignite R290 vapors.

(ii) Electric fan

A commercially available electric fan (Mitsubishi Electric, Summer Life R30C-W) was disassembled to check for any electrical parts that might be a potential ignition source. This appliance contains a brushless motor, which has a low possibility of ignition. The fan's operating switch part includes contacts, between which electric discharges are likely to occur, similar to an electromagnetic contactor or a contact relay. Hence, the possibility of ignition due to these contacts cannot be excluded. Incidentally, the electric fan subjected to disassembly investigation this time happened to be an older model. Unlike this one, newer models of electric fans in wide distribution nowadays are equipped with electronic control of their operation. Such models are supposed to have a built-in electronics board, which, if mounted with a contact relay, may become an electric discharge source that ignites R290 vapors. This hazard cannot be excluded.

(iii) Microwave oven

A commercially available microwave oven (SANYO, EM-LP1) was disassembled to check for any parts that may be a potential ignition source. We first identified a turn table-driving motor. This motor is rated to run at 6 rpm. At this number of revolutions, arc discharges are unlikely to occur. Moreover, the motor is directly connected to a plastic gear and is unlikely from this point of view to cause ignition-capable electric discharges. Apart from this motor, the oven was equipped with an inside thermostat. This thermostat is a bi-metal contact switch. In the past, cases were reported of the ignition of ethyl ether due to sparks from thermostats. Additionally, the oven was found to have contact parts fitted inside. Accordingly, the thermostat inside a microwave oven may be a potential ignition source of R290. This hazard cannot be excluded.

(iv) Vacuum cleaner

A commercially available vacuum cleaner (TWINBIRD, FW3K167) was disassembled to check for any parts that may be a potential ignition source. The vacuum cleaner tested contains a universal motor. The motor's commutator and brush cause arc discharges or mechanical sparks. When operated, this universal motor was seen to emit electric discharges in the air. Additionally, when checking for photographs³⁻²⁵⁾ of another disassembled vacuum cleaner on the Internet, we found that the vacuum cleaner has a relay mounted on its circuit board. This circuit board is located near the motor and has poor air-tightness. It follows from the foregoing that a vacuum cleaner may ignite R290 vapors due to such factors as arc discharges from its brush motor or electric discharges from the relay on its circuit board. This hazard cannot be excluded.

(v) Washing machine

Using photographs³⁻²⁶⁾ of disassembled washing machines (TOSHIBA's AW70DG and National's NA-F50Z8) posted on the Internet, we made educated guesses about the electrical and electronic parts used in them. In both washing machines, the control panel had beneath it an electronics board mounted with a contact relay, and the electronics board was water-proofed by filling it with resin to prevent electric leakage. The photos posted on the Internet suggest that electrical parts were not wholly covered with resin but had high air-tightness. Accordingly, contact relays used in washing machines are unlikely to become an ignition source.

(vi) Dehumidifier/air purifier

Using a photograph³⁻²⁷⁾ of a disassembled dehumidifier (CORONA, CD-J107X) posted on the Internet and the results of actual disassembly of air purifiers (SHARP's KC-Y65 and KC-B50, and Panasonic's f-vxe60), we made educated guesses about the electrical and electronic parts used in them. As in the washing machines investigated, these appliances contained, beneath the control panels, an electronics board, which appeared to be mounted with both contact and non-contact relays. Unlike the washing machines, these appliances did not appear very well waterproofed. Accordingly, the ignition of R290 vapors may occur due to the contact relays on the electronics board in these kinds of appliances. This possibility cannot be excluded.

(vii) Hair dryer

Using photographs^{3-28), 3-29)} of disassembled hair dryers (National's EH534 and Tescom's Nobby NB1902) posted on the Internet, we made educated guesses about the electrical and electronic parts used in them. A circuit board, along with a contact relay on it, was found in the handle of each hair dryer. Moreover, a brush motor was also identified. It follows from the foregoing that a hair dryer may ignite R290 vapors. This hazard cannot be excluded.

(viii) Electric dispensing pot

Using a photograph³⁻³⁰⁾ of a disassembled electric dispensing pot (Tiger, PDK-G) posted on the Internet, we made educated guesses about the electrical and electronic parts used in it. A circuit board, along with a contact relay on it, was found in the bottom part of the product. Electric dispensing pots and electric kettles often have poor air-tightness at the bottom and may contain a thermostat or a thermistor. It follows from the foregoing that the ignition of R290 vapors may occur due to an electric dispensing pot. This hazard cannot be excluded.

(ix) Electric rice cooker

Using photographs³⁻³¹⁾ of disassembled electric rice cookers (National's SR-SS18A and Tiger's JAQ-A550) posted on the Internet, we made educated guesses about the electrical and electronic parts used in them. A circuit board, along with a contact relay on it, was found in the bottom part of each product. It follows from the foregoing that the ignition of R290 vapors may occur due to an electric rice cooker. This hazard cannot be excluded.

(x) Electrically heated floor mat

In general, electrically heated floor mats often have a floor-mounted control unit. Photographs of some products posted on the Internet³⁻³²⁾ showed control units containing a relay inside. With a hot wire inside to warm its whole body, a floor mat of this kind has a high overall circuit resistance and is likely to cause electric discharges between its contact elements. Additionally, many products use a temperature control thermostat, which has led to cases of flammable-gas fire accidents. Hence, the ignition of R290 vapors may occur due to an electrically heated floor mat. This hazard cannot be excluded.

3.6 Ignition possibility of R290 due to high-temperature hot surfaces

3.6.1 Study outline and flow

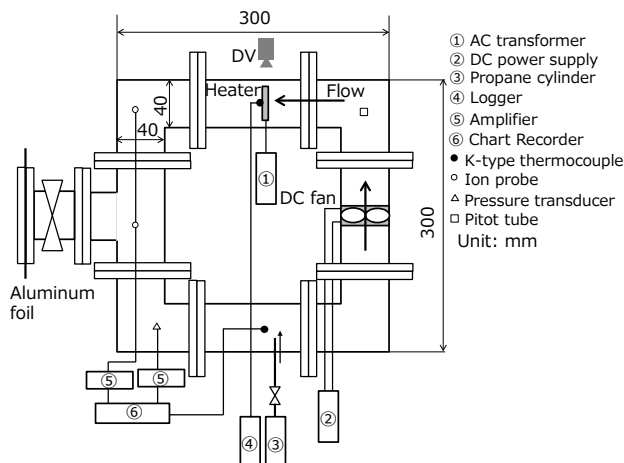
The preceding sections mainly described the ignition possibility due to electric sparks. This section presents the results of our experimental investigation on the ignition hazard due to high-temperature hot surfaces, such as lit cigarettes, electric heaters (electric stove heaters), and cooking hot plates. First, we built an apparatus capable of reproducing the situation of a flammable gas flowing at a certain flow velocity impinging a heated wall. While changing the concentration of the gas, the applied voltage to the heated wall, and the flow velocity of the gas, we observed if ignition would occur and measured the temperature at the moment of ignition and the required time from the start of heating until the occurrence of ignition. On the basis of the ignition mechanism presented in Section 3.3, we derived a relationship for the supply voltage and ignition energy to explain our experimental results. At the same time, we uncovered the gas flow velocity/concentration dependence of the minimum ignition energy and the supply power contributing thereto. We recommend consulting references³⁻³³⁻³⁶⁾ for detailed descriptions of this section.

3.6.2 Experimental outline

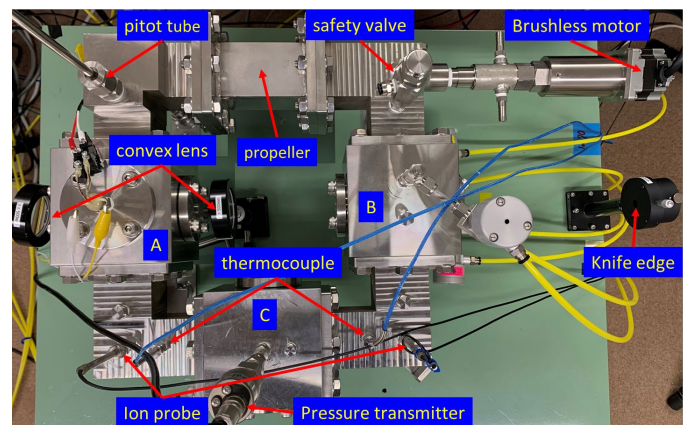
In this experiment, we used two different loop-type combustion chambers: one acrylic and the other stainless steel (loop

line 40 mm × 40 mm across and 340 mm long), as shown in Fig. 3-19(a) and Fig. 3-19(b), respectively. We used two different types of chambers because we initially used the acrylic chamber to facilitate visualization of the inside, but its quick deterioration from heating forced us to use the stainless steel chamber instead. Regardless of the chamber used, the specifications and dimensions of the rest of the apparatus remained unchanged, albeit with variable experimental conditions. The flow of the flammable gaseous mixture was caused by a brushless fan in the chamber. Two square-shaped ceramic heaters, one 25 mm × 25 mm across and the other 10 mm × 10 mm across, were mounted in the chamber facing against the flow direction and were used as heating surfaces by applying a predetermined voltage via a variable voltage transformer. The temperature of each heating surface was measured using a platinum-rhodium thermocouple with a built-in heater. In the test using the stainless steel chamber, the ignition behaviors around the heating surfaces were captured using a high-speed camera and the Schlieren technique through a 20-mm-diameter observation window in the chamber. In the test using the acrylic chamber, a normal-speed digital video camera was used to record the ignition behaviors.

We allowed the experimental conditions to vary within the following ranges: flow velocity within 0.0 to 4.0 m/s, R290 concentration within 2.1 to 9.5 vol%, and voltage within 50 to 90 V (25 mm × 25 mm heater) and 21 to 25 V (10 mm × 10 mm heater). The occurrence/non-occurrence of ignition was comprehensively determined from information such as visual changes around the heating surfaces, increases in the chamber's internal pressure, ion probes' responses, and increases in temperature. The heating time was set to a maximum of 10 min, and the number of testing times was set to a maximum of 10 times per combination of flow velocity, voltage, and concentration. If ignition occurred even once in this duration, we considered the conditions applied as responsible for the ignition. Additionally, the minimum voltage observed to cause ignition was defined as the minimum ignition voltage.



(a) Schematic diagram of acrylic chamber



(b) Photo of SUS chamber

Fig. 3-19 Schematic diagram and photo of closed-loop combustion chamber.

3.6.3 Experimental results and discussion

- (15) Relationship between the required ignition time and the supply power

We examined the relationship between the required time from the start of heating until the occurrence of ignition (t_{ig}) and the supply power (P) per heater unit area (A). Regardless of the heater dimensions, an increase in P/A resulted in a shorter t_{ig} and a difference originated from the difference of flow velocity. Conversely, a decrease in P/A caused an exponential increase in t_{ig} to infinity (i.e., non-ignition). Considering that ignition occurred when a heat flux slightly above the P/A value for the required ignition time of infinity was supplied from the wall surface to the unburned gas, we hereafter call this value the critical ignition heat flux $q_{w,c}$. The increase in $q_{w,c}$ was dependent on the flow velocity. In Fig. 3-20, one curve extends for each flow velocity regardless of the heater dimensions, suggesting that the concentration effects were minor. Note, however, that $q_{w,c}$ took a significantly larger value with the 10 mm \times 10 mm heater, although the required ignition time was sorted out by the supply power per unit area.

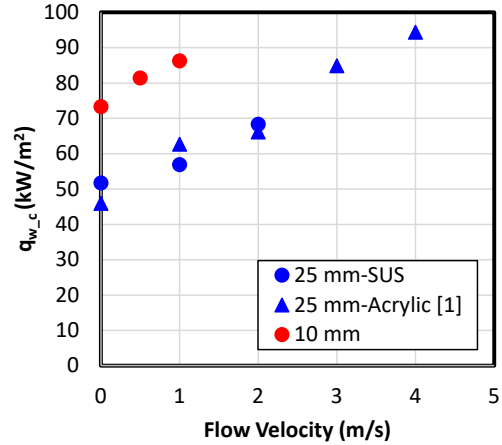


Fig. 3-20 Dependence of $q_{w,c}$ on the flow velocity.

- (16) Behavior of the critical ignition heat flux

Here, let q_w be the heat flux flowing from the heater to the unburned gas, let C be the heater's heat capacity, let T_w be the heater's temperature, and let t be time. Then, the following equation holds:

$$q_w = \frac{P}{A} - \frac{C}{A} \cdot \frac{dT_w}{dt} \quad (3.4)$$

The occurrence of ignition holds true for the condition of $q_w > q_{w,c}$. Let us assume from the results presented in (1) that $q_{w,c}$ remains constant for each flow velocity and independent of the concentration. Then, if P/A is relatively larger than $q_{w,c}$, $q_{w,c}$ is easily exceeded even when the second term on the right side (i.e., dT_w/dt) is a little too large. Hence, ignition will occur at an early phase. Conversely, if P/A slightly exceeds $q_{w,c}$, ignition will not occur until the second term on the right side is sufficiently small. Hence, t_{ig} will become long, with a correspondingly increased ignition temperature. Therefore, we plotted the relationship between P/A and dT_w/dt at the time of ignition and defined the intercept value for $dT_w/dt = 0$ as $q_{w,c}$. Fig. 3-20 shows the relationship between $q_{w,c}$ and the flow velocity. Regardless of the heater dimensions, $q_{w,c}$ increases monotonically with the increase in flow velocity. In other words, the figure shows that ignition becomes more difficult at higher flow velocities, regardless of the heater dimensions. This observation is empirically sound and agrees with the results we obtained by numerically solving the basic energy and mass conservation equations assuming that our experimental system was a one-dimensional potential flow.³⁻³⁴⁾

According to a dimensional analysis that assumed a one-dimensional potential flow to model our experimental system,³⁻³⁶⁾ the non-dimensional critical ignition heat flux $q_{w,c}^*$ is expressed by the following equation:

$$q_{w,c}^* = \frac{q_{w,c}}{\rho c s \Delta T} = f\left(\frac{\lambda}{\rho c D}, \frac{\rho c s^2}{a \lambda}\right) \quad (3.5)$$

where ρ is the density, c is the specific heat, s is the laminar flow burning velocity, ΔT is the temperature difference, D is the diffusion coefficient, a is the elongation-contraction rate, and λ is the thermal conductivity. The first term on the right side is the Lewis number (the ratio between material diffusion rate and temperature diffusion rate), and the second term is the Damköhler number (the ratio of the chemical reaction's characteristic time and presence time). In the case of pre-mixed gas combustion, the Lewis number is often assumed to equal 1. Hence, we also assumed the same here. It follows then that $q_{w,c}^*$ depends exclusively on the Damköhler number. Here, the elongation-contraction rate a should be related to the flow's vertical stress acting on the heater. Therefore, assuming that the relationship can be expressed as $a \propto u/L$ (where u = flow velocity and L = length of heater's side), Eq. (3.5) can be rewritten as

follows:

$$q_{w_c}^* = f \left\{ \frac{\lambda}{\rho c D}, \frac{\rho c s^2}{(u/L)\lambda} \right\} \quad (3.6)$$

A look at the relationship between $q_{w_c}^*$ obtained by applying Eq. (3.5) to the experimental results and the Damköhler number reveals that $q_{w_c}^*$ is almost inversely proportional to the square root of the Damköhler number and generally agrees well with the theoretical analysis results. This result suggests that a smaller wall size leads to a reduced elongation-contraction rate and therefore an increased critical ignition heat flux, that the degree of the increase is estimated using the Damköhler number, and that the effects of the burning velocity are offset from both sides and cease to be apparent.

(17) Evaluation of the ignition possibility due to cigarettes

Using Fourier's law, we estimated the heat flux from the cigarette's hot surface to the unburned gas mixture to investigate if the ignition of the R290-air pre-mixed gas occurs due to a lit cigarette's hot surface. Assuming that the heat transfer thickness is 1 mm, the heat flux is approximately 17 kW/m². When this relationship is plotted along those in Fig. 3-20, the resulting value is even smaller than the critical ignition heat fluxes for the 25 mm × 25 mm squares. Because a cigarette has a diameter of approximately 7 mm, the critical ignition heat flux corresponding to this dimension can be assumed to be even larger than the results for the 25 mm × 25 mm squares. Accordingly, we estimated the ignition possibility due to a cigarette's hot surface would be extremely small.

3.7 Summary and future works

3.7.1 Evaluation of the ignition possibility due to electric sparks

So far, we have uncovered the following findings:

- (18) On the basis of the dependence of ignition on the balance between the heat generation rate and the heat release rate, we devised a simplified method to screen possible ignition sources by comparing the discharge energy generated within a specific duration with the minimum ignition energy. Using this method, we screened everyday-life household appliances regarding their ignition possibility.
- (19) From the experiments conducted to determine the ignition hazard due to arc discharges from contact relays, we demonstrated that the increase in discharge energy depends on power consumption, that a larger discharge energy occurs when a switch is closed than when it is opened, and that discharge energy occurs in amounts exceeding the minimum ignition energy of R290-air mixed gas. Additionally, from the experiments using model circuits, we demonstrated that the circuit current affects the discharge energy, thus enabling the use of circuit current as an index to predict ignition frequency.
- (20) We experimentally investigated the operation of a wall-mounted switch for lighting in the presence of an R290-air mixture as an ignition hazard. The flammable gaseous mixture flowed into the contact casings of the switches. Additionally, the discharge energy from the contacts reached or exceeded that of the minimum ignition energy. Hence, it has been conventionally assumed that the ignition hazard cannot be excluded. However, not even once did our experiment detect the occurrence of ignition. The likely cause was that the contact-to-contact distance was too small for a flame to become sufficiently large for steady propagation.
- (21) We experimentally investigated the action of plugging in and unplugging in the presence of an R290-air pre-mixed gas as an ignition hazard. Ignition occurred upon the plugging in of some general household appliances (hair dryers). Similarly, ignition occurred with some overseas standard-compliant (230 VAC) products. In both cases, the measured discharge energy exceeded the minimum ignition energy by approximately two to three orders of magnitude.
- (22) For the ignition risk due to electrostatic discharge, we studied scenarios and compared the ignition risk due to known discharge characteristics. We found that the ignition hazard due to a discharge from the contact between an electrically charged human body and a doorknob is undeniable, whereas the ignition hazard due to static electricity caused by undressing is negligible.

On the basis of these findings, we include the following in the list of remaining challenges:

- (23) Conducting ignition experiments of operating relays in the presence of flammable gaseous mixtures, using various

kinds of actual load devices and varying the operating current, to accumulate ignition/non-ignition and ignition frequency data and to clarify the relationship between current and power consumption and ignition frequency, thereby refining the ignition hazard evaluation. Moreover, we will configure a measurement circuit that is able to maintain a constant discharge energy and to change the discharge duration only, with the aim of establishing an ignition hazard evaluation index usable for the evaluation of ignition hazard due to electric discharges from contact relays. The reason is that differences in the supply energy per unit time due to a significant difference in discharge duration (approximately 10^3 to 10^5 s) are probably among the causes responsible for the cases of non-ignition despite the availability of discharge energy that is sufficiently higher than the minimum ignition energy.

- (24) Investigating the ignition hazard due to arc discharges or spark discharges from brush motors. First, we will conduct ignition experiments using actual devices in a flammable gaseous mixture to evaluate their ignition capability. If any device is evaluated to have ignition capability, we will configure a circuit with variable capacitance, inductance, and resistance values as we did in (1) to accumulate and quantitatively evaluate discharge energy data, thereby identifying the factors governing discharge energy.

3.7.2 Evaluation of ignition hazard due to high-temperature surfaces

So far, we have uncovered the following findings:

- (25) A clear correlation exists between the supply power and ignition time. The influence of concentration on this correlation was small. In addition, the ignition time became infinite (i.e., non-ignition) at a certain level of supply power, which means that a critical ignition heat flux governing ignition or non-ignition existed and its value increased with an increase in flow rate (in other words, reduced flammability) (Fig.3-2). Although this tendency was not affected by the heater dimensions, the critical ignition heat flux was significantly intensified when the heater was small.
- (26) By expressing the non-dimensional critical heat flux $q_{w,c}^*$ as a function of the Damköhler number, we found that the critical ignition heat flux can be predicted for various heater dimensions.
- (27) Considering the critical ignition heat flux values obtained through the model experiment and theoretical analysis and the dependence on heater size, the ignition possibility of hot surfaces such as cigarettes was probably extremely minimal.

References

- 3-1) Fluoride Gases Management Office, Manufacturing Industries Bureau, Ministry of Economy, Trade and Industry: "On the Outline of the Montreal Protocol and the Kigali Revision," https://www.env.go.jp/press/y067-07/ref01_5.pdf, (2017).
- 3-2) Fluoride Gases Management Office, Manufacturing Industries Bureau, Ministry of Economy, Trade and Industry: "On the Response to the Montreal Protocol and the Kigali Revision and the Recent Trends Therein," http://www.meti.go.jp/shingikai/sankoshin/seizo_sangyo/kagaku_busshitsu/pdf/005_07_00.pdf (2018).
- 3-3) Lewis, B., and von Elbe, G. "Combustion, Flame and Explosions of Gases," p. 346, Academic Press, New York and London, (1961).
- 3-4) Strehlow, R.A., Mizutani, Y. (trans.): "Fundamentals of Combustion" (Japanese trans.), p. 211, Morikita Publishing, Tokyo (1972).
- 3-5) Hirano, T.: "Combustion Science - Combustion Phenomena and Their Control -" (in Japanese), Kaibundo, pp. 93-140 (1986).
- 3-6) Niioka, T., Kono, M., and Sato, J. (Eds.): "Fundamentals of Combustion Phenomena" (in Japanese), Ohmsha, pp. 121-149 (2001).
- 3-7) Kinoshita, K.: "A Study on Fire Accidents Due to Electrical Sparks and Heating" (in Japanese), Ph.D. dissertation submitted to Kogakuin University, p. 58 (1997).
- 3-8) Strehlow, R.A., Mizutani, Y. (trans.): "Fundamentals of Combustion" (Japanese trans.), p.215, Morikita Publishing, Tokyo (1972).
- 3-9) Chang Jen-Shih: "Physics and Chemistry of Atmospheric Plasmas," Journal of Plasma and Fusion Research, 82(10), pp. 682-692 (2006).
- 3-10) Watanabe, M., Hotta, E., Tanoue, K., Ushimaru, K., Kuboyama, T., and Moriyoshi, Y.: "Radical Measurements and Ignition Characteristics of Repetitive Nano-Pulse Discharges Plasma" (in Japanese), Journal of Plasma and Fusion Research, 89(4), pp. 229-233 (2013).
- 3-11) Lou, G., Bao, A., Nishihara, M., Keshav, S., Utkin, Y.G., Rich, J.W., Lempert, W.R., Adamovich, I.V.: "Ignition of Premixed Hydrocarbon-Air Flows by Repetitively Pulsed, Nanosecond Pulse Duration Plasma," Proc. Combust. Inst., 31(2), pp.3327-3334 (2007).
- 3-12) Tanoue, K., Ushimaru, K., Suga, M., Kuboyama, T., Moriyoshi, Y., Watanabe, M., and Hotta, E.: "Study of Ignition Characteristics of Repetitive Nano-Pulse Discharges Plasma - Ignition Characteristics of Non-thermal Plasma -" (in Japanese), Journal of the Combustion

- Society of Japan, 56(175), pp. 59-66 (2014).
- 3-13) Cathey, Cain, J., Wang, H., Gunderson, M.A., Carter, C., Ryan, M.: "OH Production by Transient Plasma and Mechanism of Flame Ignition and Propagation in Quiescent Methane-Air Mixtures," *Combustion and Flame*, 154(4) pp.7150727 (2008).
- 3-14) Ohtori, S. and Watanabe, Y.: "On Arc Discharges During the Opening of Electric Contacts" (in Japanese), *Journal of the Institute of Electrical Engineers of Japan*, 81(875), pp. 1331-1337 (1961).
- 3-15) Hayata, K. and Ikegami, T.: "Measurement of Arcs Between Relay Contacts" (in Japanese), *Collection of Preprints for the Year 2005 Kyushu-section Joint Convention of Institutes of Electrical Engineering*, p.138, https://www.jstage.jst.go.jp/article/jceek/2005/0/2005_0_138/pdf-char/ja (2005).
- 3-16) Xuebo Dong: "An Experiment Concerning Influence of Surrounding Gases and Their Pressure on Various Characteristics of Electrical Contact" (in Japanese), *Nippon Institute of Technology Research Report*, 46(1), pp. 105-108 (2016).
- 3-17) Fujitsu Corporation Website: "Relay Technology Manual" (in Japanese), <http://www.fujitsu.com/downloads/MICRO/fcl/relays/relay-technology.pdf> (2019).
- 3-18) Isato, M.: "Commutation Phenomena and Brush Wear of DC Motor at High-Speed Rotation" (in Japanese), *Nippon Institute of Technology Research Report*, 47(1), pp. 154-157 (2017).
- 3-19) List of Voltages Around the World (in Japanese): <https://henatuki.aimary.com/> (last viewed on Mar. 18, 2020).
- 3-20) JSRAE: Risk Assessment of Mildly Flammable Refrigerants Final Report 2016, Tables 2-9, p. 41, (2017).
- 3-21) IEC60947-1: Low-voltage switchgear and controlgear - Part 1: General rules, (2007).
- 3-22) Imamura T., Aoki, M., and Haruyama, T.: "Properties of Ignition of Retained Propane Due to Plugging in and Unplugging" (in Japanese), *Collection of Lecture Preprints for the 52nd Safety Engineering Research Presentation Conference*, pp.173-176, (2019).
- 3-23) National Institute of Occupational Safety and Health: Technical recommendations of National Institute of Occupational Safety and Health Recommendations for Requirements for Avoiding Electrostatic Hazards in Industry, 2007, JNIOOSH-TR-No.42, pp. 18-27, (2007).
- 3-24) National Institute of Occupational Safety and Health: Technical recommendations of National Institute of Occupational Safety and Health Recommendations for Requirements for Avoiding Electrostatic Hazards in Industry 2007, JNIOOSH-TR-No.42, p.39, (2007).
- 3-25) K's Memo-Random: "I Repaired My Vacuum Cleaner Early in the Morning" (blog post in Japanese): http://kenshi.airnifty.com/ks_memorandom/2009/04/post-9deb.html (2019).
- 3-26) Engineer's Blog: Episode about the Breakdown of My Washing Machine: Alpha Wave (blog post in Japanese): <https://blog.alphawave.co.jp/eng/index.php?itemid=1744> (2019).
- 3-27) Tom's Blog: First Dehumidifier Maintenance in Six Years - Part 1 - (blog post in Japanese): <http://d.hatena.ne.jp/tomtom1ono/20130128/1359321525> (2019).
- 3-28) Phony Engineer's Ups and Downs Diary: Quick Disassembly: Hair Dryer [Electronic Circuit]: <https://rifle.blog.so-net.ne.jp/2014-02-18> (2019).
- 3-29) KEISUKE TABOGAMI KICHIJOJI, TOKYO: [Must See Tips for Beauticians] How to Troubleshoot Hair Dryer (Nobby) Disassembly and Reassembly Gone Wrong: <http://www.tabogami.tokyo/archives/1284> (2019).
- 3-30) JapaneseClass: Electrolysis (web dictionary page in Japanese): <https://japaneseclass.jp/dictionary/%E9%9B%BB%E6%B0%97%E5%88%86%E8%A7%A3> (2019).
- 3-31) Middle-aged Guy's Diary: Photographic Report of the Disassembly of SR-SS18A (National/Panasonic IH Rice Cooker) (blog post in Japanese): <https://incomprehensiveness.blogspot.com/2014/09/sr-ss18a-nationalpanasonic-ih.html> (2019).
- 3-32) Disassembling a Heated Floor Mat [Toolbox] (blog post in Japanese): <https://insertyourname.blog.so-net.ne.jp/2015-04-09> (2019).
- 3-33) Nakazawa, M., Kariya, H., Shimomura, R., Kuwana, K., and Imamura T.: "Effects of Heated Wall Ignition Energy and Fuel Concentration on a Circulating Flow of Propane-Air Mixed Gas" (in Japanese), *Collection of Abstracts for the Year 2020 Research Presentation Conference of Japan Association for Fire Science and Engineering* (presentation due in May 2020)
- 3-34) Iizuka, H., Kuwana, K., and Imamura T.: "Ignition Conditions for a Premixed Stagnant Flow Colliding Into a Heated Wall" (in Japanese), *Journal of JAFSE "KASAI,"* 70(1), 1-8, (2020).
- 3-35) Imamura, T., Uehara, K., Nakata, K., Maruyama, S., Kuwana, K.: Quasi-steady Characteristics of Flowing Propane/Air Mixture Ignited by a Heated Surface, *Proceedings of 13th International Symposium on Fire and Safety Science*, Waterloo, Canada, (2020, accepted).
- 3-36) Kuwana, K. and Imamura T.: Similarity Law of Hot-Surface Ignition of Flammable Premixed Gases - Cases of Stagnant Flows Colliding into Heated Walls - (in Japanese), *Journal of the Japanese Society for Experimental Mechanics*, 20(4), 254-257 (2020).

Chapter 4 Progress achieved at the Research Institute of Science for Safety and Sustainability, AIST

4.1 Introduction

The research under the charge of the AIST Research Institute of Science for Safety and Sustainability can be divided into the following themes: (1) ignitability evaluation aiming to investigate whether household appliances and other devices in a room can become an ignition source when flammable refrigerant leaks in the room and forms a flammable concentration region and (2) full-scale physical hazard evaluation of room air conditioner indoor units and reach-in refrigerated display cabinets in relation to refrigerant-leakage fire accidents. The subsequent sections present summary reports on the following investigations conducted in accordance with the conditions for full-scale experiments: ignitability evaluation of real devices present in flammable concentration regions, diffusion behavior measurement and full-scale physical hazard evaluation of room air conditioner indoor units, and diffusion behavior measurement and full-scale physical hazard evaluation of reach-in display cabinets.

4.2 Ignitability evaluation of real devices present in flammable concentration regions

To obtain basic data for risk assessment, namely the probability of ignition arising from the accidental leakage of refrigerant from devices charged with propane (R290), a flammable gas regarded as one of the next-generation refrigerant candidates with a low GWP, we repeatedly operated, via remote control, electrical equipment placed in a container filled with approximately 5.2% propane-air pre-mixed gas, which is regarded as the most prone to electrostatic ignition, to observe whether ignition occurred.

4.2.1 Appliances selected for evaluation and experimental method

The models used for evaluation were determined through discussion with the Suwa University of Science (in charge of screening electrical parts as potential ignition sources) and the Japan Refrigeration and Air Conditioning Industry Association (in charge of conducting risk assessments of A3 refrigerants). So far, we have conducted evaluation experiments of laser printers, hairdryers, electric vacuum cleaners, electric screwdrivers, cooking hot plates, and kerosene fan heaters.

Except for the evaluation experiment of kerosene fan heaters, we conducted our experiments using an acrylic chamber (1.00 m³) consisting of four acrylic walls, a steel floor, and a plastic sheet stretched over the ceiling. Considering that the explosion accompanying ignition might blow off some parts of the equipment in all directions, we conducted the experiments with the acrylic chamber installed in the AIST explosion pit. In the experiments using the acrylic chamber, we first placed in the chamber the equipment mounted with an air actuator for remote control and then introduced propane and air into the chamber via flow control. The propane concentration was adjusted and maintained at approximately 5.2% via a concentration sensor, and the equipment was operated from outside the explosion pit via remote control. We used a high-speed infrared camera to observe ignition.

4.2.2 Results of ignitability evaluation experiments

Laser printers

For the evaluation of laser printers, we selected a model with a high operating power from among those whose construction is generally accepted as standard. Two specimens of the same model underwent an experiment of color-printing 250 sheets. Neither specimen showed any anomalies.

Hairdryers

For the evaluation of hairdryers, we selected a model with a high operating power and a brush motor from among those whose construction is generally accepted as standard. In our experiment, we used four specimens of the same model. From the four specimens, we picked two and turned on and off their power from outside the chamber with their

main body switch set to hot blowing. During 100 cycles of 10-s ON and 5-s OFF, no ignition was observed to occur in either of the two specimens. Additionally, when the main body switches of the three selected specimens were operated in the chamber via the air actuator to turn hot blowing on and off, ignition was observed to occur in all three specimens during one to two ON/OFF cycles. In one specimen among the three, ignition was observed to occur during the first OFF operation when the duration of the ON/OFF cycle was longer (Fig. 4-1). These results suggest that in the case of hairdryers, the OFF operation of the main body switch may be a potential ignition source.

Electric vacuum cleaners

For the evaluation of electric vacuum cleaners, we selected a model with a high operating power from among the types that use an inside paper vac bag. In our experiment, we used two specimens of the same model. One of the two specimens produced smoke after five to six cycles of 7-s “High Power” mode operation and 5-s OFF. For practical reasons, we started to dilute the propane-air mixed gas with nitrogen approximately 10 s after the emission of smoke. At that time, neither flame propagation nor explosions occurred with the propane-air mixed gas. The other specimen showed no anomaly during 500 cycles of 7-s “High Power” mode operation and 5-s OFF or during 5-min continuous “High Power” mode operation. A post-experiment look identified burned and melted plastic parts from the motor to the air outlet section of the specimen that emitted smoke earlier (Fig. 4-2).

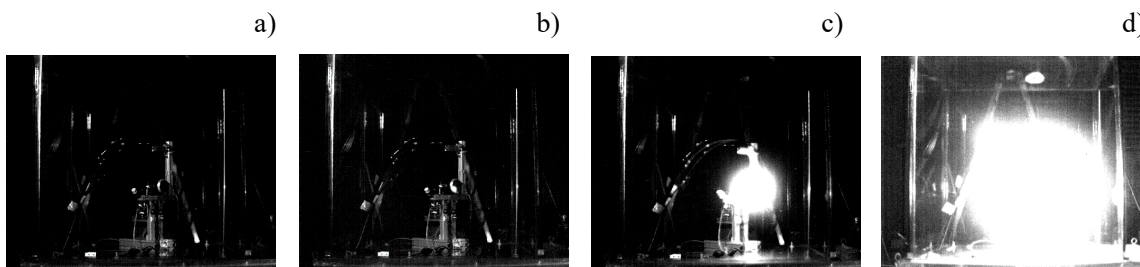


Fig. 4-1 Images taken using a near-infrared high-speed video camera.



Fig. 4-2 Vacuum cleaner emitted smoke.

Electric drill

For the evaluation of electric drills, we selected a model with a high operating power and a brush motor from among those whose construction is generally accepted as standard. In our experiment, we used one specimen. From outside the chamber via the air actuator, the specimen was operated in the three different operating modes of “high-speed revolution with load,” “high-speed revolution without load,” and “low-speed revolution without load.” Irrespective of the operating mode, no ignition was observed to occur during 100 cycles of 6-s revolution ON and 4-s OFF.

Cooking hot plates

For the evaluation of cooking hot plates, we selected a model with a body containing an integrated power supply switch with a temperature control bimetal thermostat. In our experiment, we used one specimen. Ignition was observed to occur at the end of 20-odd cycles of 5-s ON and OFF operation of the slide power switch controlled remotely via the air actuator.

Kerosene fan heaters

For the evaluation of kerosene fan heaters, we evaluated the heater's ignitability during its operation rather than at its ignition. In other words, the chamber requires a continuous supply of fuel-burning air. Hence, for our experiment, we set up a plastic greenhouse-like experimental chamber in the outdoor laboratory on the accumulation grounds of a defunct mine. This chamber (1.00 m³) consisted of a stainless steel frame and a steel floor with plastic sheets stretched over its four walls and ceiling. We selected a small-bodied model to reduce the temperature rise in the plastic greenhouse-like experimental chamber. In our experiment, we used two specimens of the same model. After confirming that the internal temperature of the chamber started to rise following the self-timed ignition of the kerosene fan heater installed in the chamber continuously supplied with fuel-burning air, we operated an air motor valve via remote control to introduce propane into the chamber. We observed ignition and rupture of the plastic sheet when 300 g of propane was supplied rapidly and when 150 g of propane was supplied at a lower flow rate.

Fig. 4-3 shows still images at intervals of 100 ms of the fan heater rapidly supplied with 300 g of propane; the images were obtained using a high-speed camera. When ignition and plastic-sheet rupture occurred during propane discharge (Fig. 4-3 b), the flame was difficult to identify by sight, indicating that fire was caught at a low propane concentration. One of the images shows the propane outlet after it transitioned to releasing and diffusing flames after the ignition and sheet rupture (Fig. 4-3c).

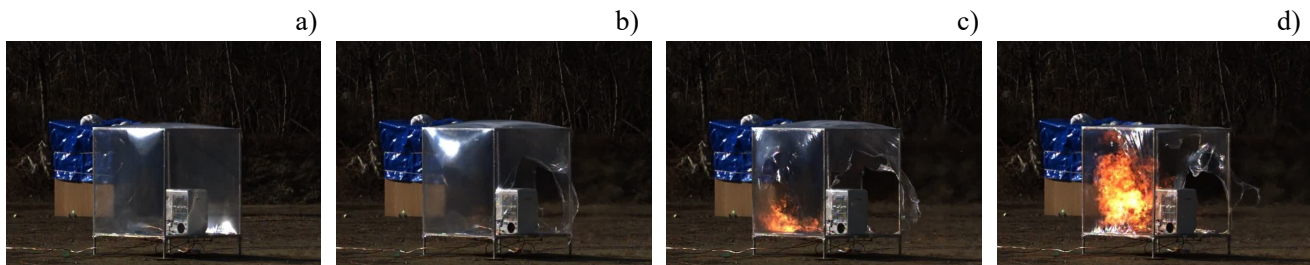


Fig. 4-3 Kerosene fan heater ignites propane.

4.2.3 Summary and plan for ignitability evaluation

The hair dryer, electric vacuum cleaner, electric cooking hot plate, and kerosene fan heater were used to catch fire. Although the experimental results were obtained using a single model, we considered that the risk assessment of the probability of ignition due to operation in a flammable concentration region should be unity. For any identified model that may not catch fire depending on such factors as operating power or structural differences, an additional test will be considered.

No ignition was observed to occur in the laser printers and the electric drill. With a limited number of models or number of repeat experiments, a risk assessment rating of zero ignition probability cannot be assigned to structurally non-explosion-proof devices. Nevertheless, if the non-occurrence of ignition is confirmed with a certain number of models or number of repeat experiments, a lower risk assessment rating for ignition probability will be assigned as appropriate for the required number of repeats. For devices expected to improve in the risk assessment rating for ignition probability, we will consider a repeat experiment using multiple models.

4.3 Diffusion behavior measurement and physical hazard evaluation of room air-conditioner indoor unit

We evaluated the combustion effects of refrigerant-leakage fire accidents to define the risk assessment rating for the harm severity of a leakage accident from a room air conditioner indoor unit using propane (R290) as the refrigerant. This combustion effect evaluation assumes real use conditions. Hence, we installed a room air conditioner indoor unit in a full-scale simulated room, measured the leakage and diffusion behaviors under several probable leakage conditions, and conducted ignition experiments for conditions expected to result in high severity. Consequently, we evaluated the effects of combustion.

4.3.1 Case studies of refrigerant leakage accidents and determination of leakage conditions

Currently, no room air conditioners using flammable natural refrigerants are sold in Japan, and few cases of leakage accidents have been reported. Therefore, we determined the leakage conditions from those for indoor units using mildly flammable refrigerants. The Risk Assessment Report on Building-Multi-Air Conditioners Using Mildly Flammable Refrigerants⁴⁻¹⁾ contains information on reported leakage accidents relating to building-multi-air conditioners using R32, including leaky points/holes, their forms, and equivalent diameters. Entire surface corrosion of the heat exchanger tube in a home-use indoor unit often leads to a leaky hole; the largest equivalent diameter of this hole, among the reported cases, is 0.174 mm. The liquid leak rate at 63 °C is 67 g min⁻¹, which is approximately the same as the discharge rate for the 4-min full-amount discharge used for the risk assessment of rapid leakage. Additionally, most of the reported leaky points were located in heat exchanger tubes and electronic expansion valves. Therefore, the present study adopted the condition of discharging the full charge amount in 4 min as the primary leakage condition for home-use room air conditioner indoor units. Considering cases requiring other time limits for discharge, we included in our experiment a case of discharge at 30 °C under own pressure from a tube with a bore size equivalent to the diameter of the ruptured hole in the tubing. The leaky points adopted were the following three locations: the center of the heat exchanger, the vicinity of the junction between the heat exchanger and its mating tube, and the tubing joint for routing the refrigerant tubing inside the indoor unit. Experiments conducted as part of a 2016 project indicated that when direct discharge into the indoor space occurs from a pinhole or the like, the jet effect promotes the stirring of indoor air, thereby preventing the formation of any flammable concentration region.

4.3.2 Experimental method for the measurement of leakage and diffusion behaviors in the room air conditioner indoor unit

We set up a 2.7 × 5.4 × 2.4 m wooden simulated room in a large indoor space at the Detonation Tube Laboratory of the National Institute of Occupational Safety and Health, Japan. We added an indoor partition wall in another space measuring 2.7 × 2.7 × 2.4 m. At the center of the short side of the 2.7 × 5.4 m space, we installed the indoor unit of a split-type room air conditioner with its bottom part positioned at a distance of 2.00 m from the floor surface. The room air conditioner used was typical in size for a room unit and had an air blowing mechanism generally adopted in Japan. Two modeled door undercuts measuring 800 mm × 4 mm were provided, one in each 2.7 m × 2.7 m space, sealed with aluminum tape, if not in use, to check for any effects on the concentration distribution time history.

The propane concentration was measured using catalytic combustion-type gas sensors. We installed a total of 28 sensors. There were 14 sensors with a measurement range of 0 to 6.6 vol% installed at locations immediately below the air conditioner indoor unit, on the floor, and up to 25 cm above the floor. The other 14 sensors with a measurement range of 0 to 2.2 vol% were installed at other locations.

We used the following two propane discharge amounts: the maximum allowable charge amount determined using Kataoka's formula (4-1) for air blowing and similar purposes without safety measures, adopted in IEC60335-2-40:2018⁴⁻²⁾, and the allowable charge amount (4-2) under consideration for adoption on the premise that air blows with a sufficient flow rate. The calculations in our experiment were made using a room height of 2.4 m. The propane discharge amounts thus obtained for the simulated room measuring 2.7 m × 2.7 m × 2.4 m high were approximately 230 g and 340 g. Meanwhile, the amounts obtained for the simulated room measuring 2.7 m × 5.4 m × 2.4 m high were approximately 330 g and 680 g:

$$m_{max} = 2.5 \times LFL^{5/4} \times A^{1/2} \times h_0 \quad (4-1)$$

$$m_{max} = 0.5 \times LFL \times A \times h \quad (4-2)$$

where m_{max} is the maximum allowable charge amount, LFL is the lower flammability limit, A is the floor area, h_0 is the equipment bottom height, and h is the room height (maximum of 2.2 m).

To discharge each of these charge amounts completely in 4 min, we left a propane-filled cylinder (20 kg) in a water bath at 30 °C for degassing, then controlled the flow rate of the degassed propane via a needle valve, and finally discharged the propane from the indoor unit's discharge tube while checking the flow rate using a mass flow meter.

Additionally, to simulate leakage in a compressed liquefied form, a cylinder (5 kg) filled with the maximum allowable charge amount of propane was placed in a constant temperature bath adjusted to 30°C and was then allowed to discharge the full amount.

We performed the discharge operation and all other experimental operations via remote control from the measurement room outside the large space while checking images from security surveillance video cameras or concentration sensor readings to ensure safety.

4.3.3 Experimental results of the measurement of leakage and diffusion behaviors in the room air conditioner indoor unit

While changing the conditions, namely, the size of the indoor space, the discharge amount (assumed charge amount), the discharge point, the discharge rate, the air conditioner's air blowing conditions, and the use or non-use of door undercut(s), we measured the concentration distribution time history to consider the conditions for evaluating combustion effects through ignition experiments.

In all the experiments that discharged the maximum allowable charge amounts calculated using Eq. 4-1, no flammable concentration region of propane was observed after discharge completion. In addition, with the air distribution function of the air conditioner in operation during all the experiments, no flammable concentration region was observed. In other words, only when the allowable charge amount was relaxed on the premise of air blowing, a flammable concentration region was observed after the completion of discharge.

2.7 m × 2.7 m simulated room experiment

In the experiment using the 2.7 m × 2.7 m simulated room, we measured the concentration distribution time history while changing the conditions, namely, the discharge amount (assumed charge amount), the discharge point, the discharge method, the air conditioner's air blowing conditions, and the use or non-use of door undercut(s).

In the experiment using the 2.7 m × 2.7 m simulated room, the ratio of the discharge amounts calculated using Eqs. 4-1 and 4-2 was as small as approximately 1.5. Consequently, almost no flammable concentration region was formed depending on the discharge point, even when 340 g was discharged without air blowing. When the full amount was discharged in the gas form within 4 min at the center of the heat exchanger, a flammable concentration region was formed and remained near the floor surface for approximately 10 min. In the case of discharge at 30 °C under own pressure from a 1.5 mm-diameter pinhole provided in the junction between the heat exchanger and the tubing, flammable concentration regions were formed immediately below the air conditioner during the discharge and on the floor within 5 min after the start of discharge.

2.7 m × 5.4 m simulated room experiment

In the experiment using the 2.7 m × 5.4 m simulated room, we measured the concentration distribution time history while changing the conditions, namely, the discharge amount (assumed charge amount), the discharge method, the discharge point, the discharge rate, the air conditioner's air blowing conditions, and the use/non-use of the door undercuts.

When the maximum allowable charge amount calculated using Eq. 4-1 was discharged, flammable concentration regions were observed only below the indoor unit during discharge. No flammable concentration region of propane was observed after discharge completion (Fig. 4-4b).

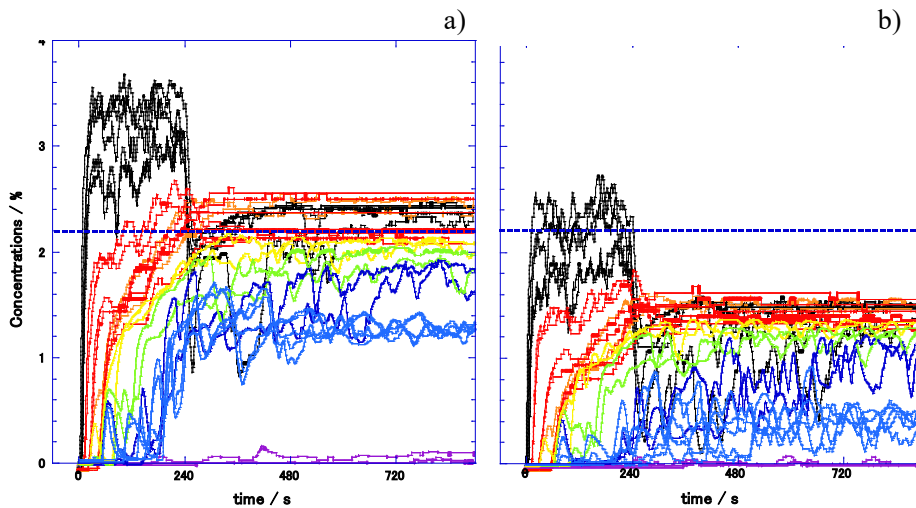


Fig. 4-4 Time profile of propane concentrations: a) 680 g and b) 330 g of propane.

(Conditions: $2.7 \text{ m} \times 5.4 \text{ m} \times \text{h}2.4 \text{ m}$, no airflow, no under door slit, center of heat exchanger discharge, gas phase, 4 min.)

2.7 m × 5.4 m simulated room/Eq. 4-2 charge amount experiment (effects of discharge point/door undercuts)

We performed measurements under the discharge condition of a full-amount discharge within 4 min from each of the three discharge points: the center of the heat exchanger, the junction between the heat exchanger and the tubing, and the tubing connector inside the indoor unit. Under these conditions, a flammable concentration region was observed only at the center of the heat exchanger, even after discharge completion. With no door undercuts in use, flammable concentration regions were observed for approximately 80 min. The duration was reduced to approximately 55 min with an $800 \text{ mm} \times 4 \text{ mm}$ door undercut in use and approximately 40 min with two door undercuts in use. Nevertheless, no significant change was observed in the diffusion behavior during discharge or immediately after the completion of discharge. The reason is that the propane-air mixed gas discharged from the door undercut(s) had a concentration of approximately 2 to 3%, as shown by the measurement, and almost the same volume as that of the 100% propane discharged from near the indoor unit.

2.7 m × 5.4 m simulated room/Eq. 4-2 charge amount experiment (effects of discharge method/discharge time)

We performed this experiment with the center of the heat exchanger used as the discharge point while varying the discharge time for uniform full-amount discharge from 3 min through 4, 5, 6, 8, and 12 min up to 16 min. No significant difference was observed in the indoor propane diffusion behavior between when the full amount was discharged in 4 min and 5 min. When the other discharge times were selected, the propane concentrations during discharge and after discharge completion were further lower. Additionally, flammable concentration regions disappeared in a shorter time. When the discharge time was 12 min, no flammable concentration region was observed after the completion of discharge. When the discharge method selected was rapid discharge at $30 \text{ }^\circ\text{C}$, under own pressure, and from the same discharge point, the propane concentration remained high during discharge. However, no flammable concentration region was observed after the completion of discharge, probably because the jet of propane gas promoted the stirring of the indoor air. These results confirmed that the 4-min full-amount discharge condition widely used for refrigerant leakage risk assessment is the worst-case condition that maximizes the space-time product of the flammable concentration region to be formed.

2.7 m × 5.4 m simulated room/Eq. 4-2 charge amount experiment (effects of air blowing)

When the charge amount calculated using Eq. 4-2 was completely discharged in 4 min with the center of the heat exchanger as the discharge point, propane was diffused in the room during the continuous operation of the air conditioner with its air blowing function set to “Weak/Horizontal.” No flammable concentration of propane was detected at any measurement point during and after discharge. Fig. 4-5 shows the differences in the propane diffusion

behavior during the 4-min full-amount discharge of 680 g of propane with and without air blowing.

Fig. 4-6 shows the propane concentration diffusion behavior 30 s, 1 min, and 2 min after the start of discharge during the 4-min full-volume discharge after the air conditioner started air blowing in the “Strongest/Downward” mode. The flammable concentration region below the indoor unit disappeared within approximately 10 to 20 s after the start of air blowing.

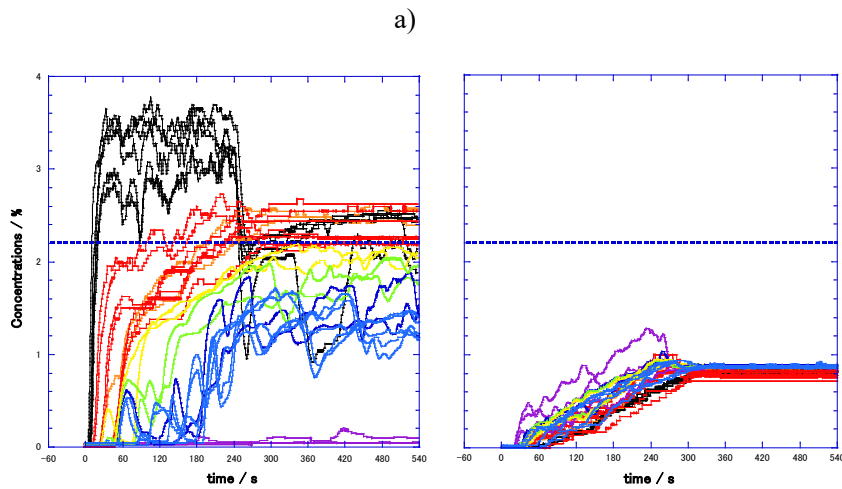


Fig. 4-5 Time profile of propane concentrations: a) no airflow and b) minimum horizontal airflow continuously. (Conditions: 2.7 m × 5.4 m × h2.4 m, no under door slit, center of heat exchanger discharge, 680 g propane, gas phase, 4 min.)

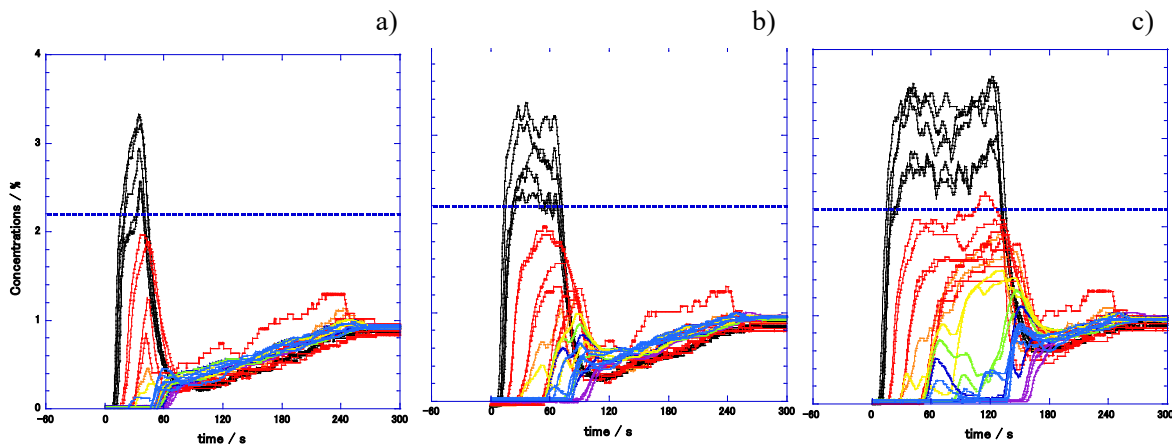


Fig. 4-6 Time profile of propane concentrations: a) maximum airflow started 30 s after discharge, b) 1 min after discharge, and c) 2 min after discharge. (Conditions: 2.7 m × 5.4 m × h2.4 m, no under door slit, center of heat exchanger discharge, 680 g propane, gas phase, 4 min.)

4.3.4 Experimental method for full-scale physical hazard evaluation of the room air conditioner indoor unit

In the outdoor laboratory at the site of the now-defunct Hitachi Cement Taiheida Mine Accumulation Grounds, a 2.7 × 5.4 × 2.4 m steel-made simulated room was set up to conduct a combustion effect assessment experiment by discharging and igniting propane in the same way as that for the diffusion behavior measurement. To observe the combustion effects under conditions close to those of an actual room, we installed a 180 cm-wide, glass-paned sliding sweep window at the center of the wall opposite the 2.7 m × 5.4 m space’s short side mounted with a room air conditioner indoor unit. The ignition source was electric sparks discharged by boosting an alternating current of 100 V from a power generator to 15 kV via a neon-sign transformer.

To evaluate the combustion effects, we installed a total of four radiant heat sensors: two inside the room and two outside. Additionally, we installed a strain gauge pressure sensor indoors, three explosive blast measurement

microphones outdoors on the glass-paned window side, and two more on the rear side. A total of three thermocouples were installed: one above the indoor unit, another above the sidewall, and yet another thereunder.

To observe flame propagation in the room, we installed a 50 mm-thick acrylic window at the center of the 5.4-m sidewall and a visible-range high-speed monochrome camera immediately outside this window. In addition, to observe the flame (if any), we installed a high-speed infrared camera outside at a distance of 40 m from the glass-paned sweep window.

To observe the failure behavior of the glass-paned window, we installed two visible-range high-speed color cameras: one at the 40 m point on the line extended from the wall containing the glass-paned window and the other at the 40 m point on the 45-degree diagonal line.

4.3.5 Experimental results of the full-scale physical hazard evaluation of the room air conditioner indoor unit

No flame resulted from the ignition sparks 2 cm above the center of the floor of the simulated room immediately after the charge amount of 330 g, calculated using Eq. 4-1, was completely discharged in 4 min without the indoor unit blower fan in operation. Additionally, no flame resulted from the ignition sparks 2 cm above the center of the floor of the simulated room immediately after the charge amount of 625 g, calculated using Eq. 4-2, was completely discharged in 4 min with the indoor unit blower fan continuously blowing horizontally.

Using the discharge rate for complete discharging, the charge amount of 330 g, calculated using Eq. 4-1, was discharged in 4 min without the indoor unit blower fan in operation. We observed a flame from the ignition sparks 150 cm above the floor below the indoor unit 210 s after the start of discharge. While no anomaly was found in the glass-paned sweep window in front of the indoor unit and the curtains hung down on the sidewall, the air conditioner indoor unit was completely burned. The maximum value of the measured internal pressure was 2.3 kPa, and that of radiant heat was 7.5 kW m⁻². Fig. 4-4 shows still images of the flame taken every 200 ms immediately after its occurrence.

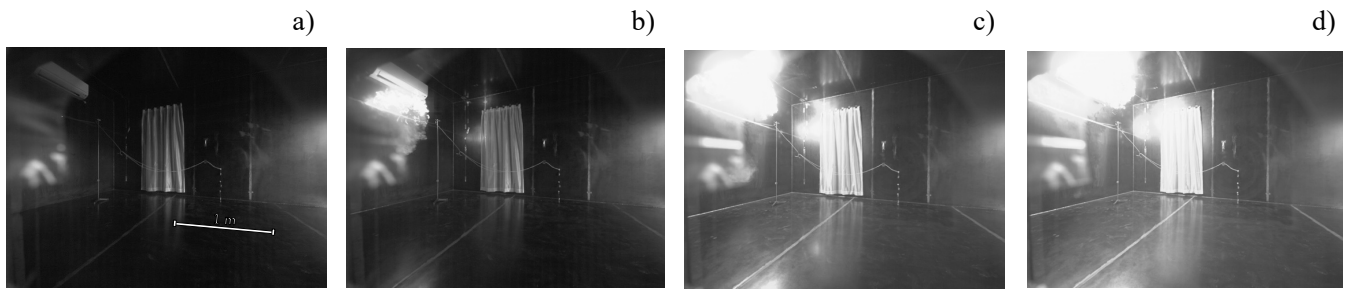


Fig. 4-7 Fire observed after ignition at 30 s before finishing blowout (200 ms interval).

A flame was observed to result from the ignition sparks 2 cm above the center of the floor of the simulated room immediately after the charge amount of 625 g, calculated using Eq. 4-2, was discharged in 4 min without the indoor unit blower fan in operation. Both the frame and the glass of the glass-paned sweep window in front of the indoor unit were broken and blown off in pieces. The maximum value of the measured internal pressure was 5.6 kPa, whereas that of radiant heat was 6.1 kW m⁻². The explosive blast pressure measured at 10 m outside the sweep window had a maximum value of 36 Pa. Fig. 4-5 shows still images of the flame taken every 200 ms immediately after its occurrence.

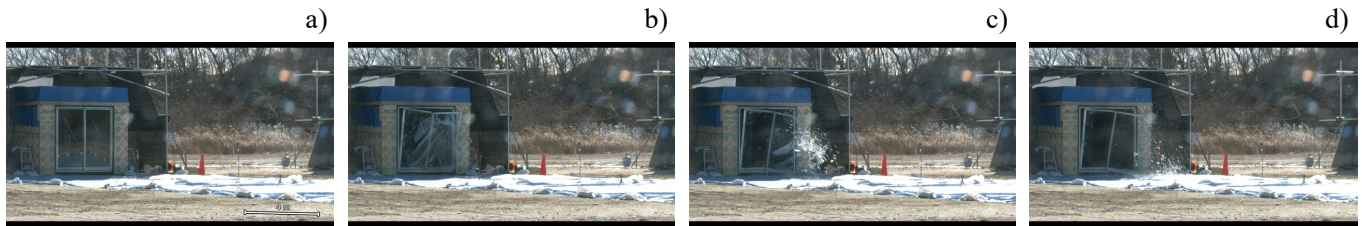


Fig. 4-8 Fire observed after ignition at 30 s before finishing blowout (200 ms interval).

4.3.6 Summary of the full-scale physical hazard evaluation of the room air conditioner indoor unit

When the allowable charge amount calculated using Kataoka’s formula (4-1) was discharged, no flame occurred after

the full discharge amount was reached. Additionally, no flame was observed in a room containing few obstacles with the air conditioner blower fan in operation, even in the case of discharging the relaxed charge amount (Eq. 4-2) currently under consideration on the premise of indoor air stirring.

It turns out that the resin-made main body of the indoor unit may be burned, spreading fire if a flame occurs during leakage, even when the allowable charge amount calculated using Kataoka's formula (4-1) is discharged.

The occurrence of a flame after the completion of discharge result in conditions severe enough to break a glass-paned window if the air blowing function is not used during leakage of the relaxed charge amount (Eq. 4-2) currently under consideration on the premise of indoor air stirring. If the increase in internal pressure is limited because of a damaged glass-paned window, combustion will not significantly affect the human body.

4.4 Diffusion behavior measurement and physical hazard evaluation of reach-in display cabinet

We evaluated the combustion effects of refrigerant-leakage fire accidents to define the risk assessment rating for the harm severity of a leakage accident from a reach-in refrigerated display cabinet using propane (R290) as the refrigerant. This combustion effect evaluation assumes real use conditions. Hence, we installed a reach-in display cabinet in a full-scale simulated room, measured the leakage and diffusion behaviors under several probable leak conditions, and conducted ignition experiments for conditions expected to result in high severity in the event that a fire breaks out to evaluate the combustion effects.

4.4.1 Experimental method for the measurement of leakage and diffusion behaviors in the reach-in refrigerated display cabinet

In the Indoor Large Space of the Detonation Tube Laboratory of the National Institute of Occupational Safety and Health, we set up a wooden simulated room measuring 4.9 m × 4.9 m × 2.8 m high and performed measurements. We installed a reach-in refrigerated display cabinet measuring 120 cm wide, 85 cm deep, and approximately 200 cm high at the center of a wall of the simulated room. The reach-in display cabinet was a double-doored type with the compressor and other mechanical components in the lower part of the display cabinet.

The propane was leaked, assuming that the full amount of propane charged as the refrigerant first leaks and spreads into the display cabinet and that the doors open when the full amount of propane is uniformly distributed inside the cabinet. This leak method probably leads to the worst-case condition because it maximizes the indoor propane concentration with the charge amount. The propane charge amounts used were the three measurements of 100 g, 500 g, and 1000 g. Both doors of the double-doored display cabinet were opened simultaneously for 3 s up to an angle of 60° via remote operation of the air actuators fitted on the doors from the measurement room outside the large experimental space.

The propane concentration was measured using gas thermal conductivity sensors with a measurement range of 0 to 100 vol% and catalytic combustion type sensors with measurement ranges of 0 to 2.2 vol% and 0 to 6.6 vol%. The gas thermal conductivity sensors were installed at a total of 14 points where high concentrations were likely: two points inside the display cabinet; five points 5 cm above the floor near the display cabinet; and a total of seven points 5 cm, 25 cm, and 50 cm above the floor in front of the display cabinet door. The catalytic combustion type gas sensors were installed at a total of 28 points: six points 5 cm above the floor in front of both sidewalls; another six points 25 cm above the floor in front of both sidewalls; and 16 points 50 cm, 100 cm, 200 cm, and 280 cm above the floor at the cross-sectional center of the simulated room.

4.4.2 Experimental results of the measurement of leakage and diffusion behaviors in the reach-in refrigerated display cabinet

We measured the diffusion behavior with variable conditions including the charge amount, the use/non-use of the fan, and the presence/absence of products inside the cabinet. In most cases, the evaporator cooling fan at the bottom of the display cabinet was in operation. We used the charge amount of 500 g, which is currently under consideration as a relaxed amount on the premise of indoor air stirring, by such methods as air blowing. When the condenser fan was in operation, 500 g of refrigerant charge leaked into the cabinet, and approximately 5 min after the doors were opened, the combustible concentration region in the simulated room disappeared (Fig. 4-9a). When a refrigerant charge of 500 g

leaked into the cabinet and the doors were opened without operating the condenser fan, a flammable concentration region continued to form in the simulated room for 90 min. Even when the condenser fan was not in operation, the flammable concentration region disappeared within 1 min when the refrigerant charge was 100 g (Fig. 4-9b). The effect of the simulated refrigerated bottle placed in the cabinet was not significant.

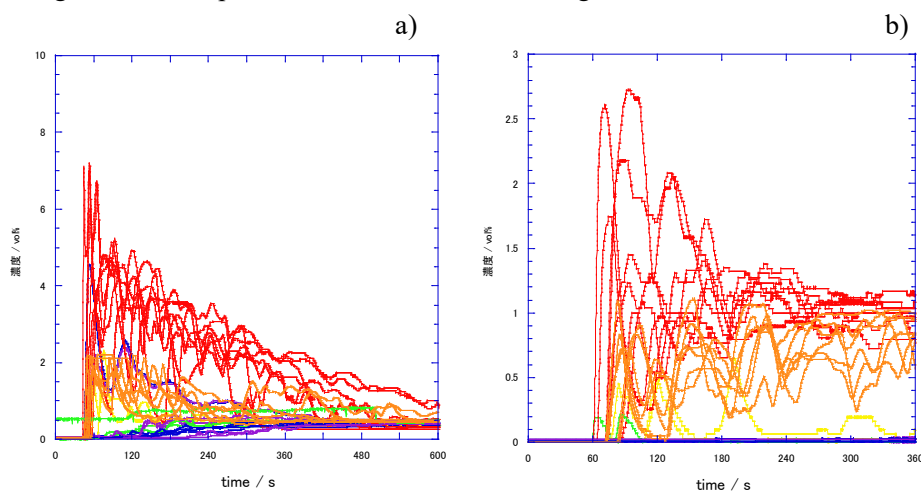


Fig. 4-9 Time profile of propane concentrations: a) 500 g propane with cooling fan in operation and b) 100 g propane without cooling fan.

(Conditions: 4.9 m × 4.9 m × h2.8 m)

4.4.3 Experimental method for the full-scale physical hazard evaluation of the reach-in refrigerated display cabinet

In the outdoor laboratory in the accumulation grounds on the site of the now-defunct Hitachi Cement Taiheida Mine, we set up a steel simulated room measuring 4.9 m × 4.9 m × 2.8 m high to conduct combustion effect evaluation experiments by discharging and igniting propane using the same method as in the diffusion behavior measurements above. To observe the combustion effects under conditions close to those of an actual room, we installed a 240 cm wide, double-sliding glass-paned door simulating an automated door in the wall opposite the wall with the mounted display cabinet. The ignition source was electric sparks discharged by boosting an alternating current of 100 V from a power generator to 15 kV via a neon-sign transformer.

To evaluate the combustion effects, we installed a total of four radiant heat sensors, two inside and two outside the room. Additionally, we installed a strain gauge pressure sensor indoors, three explosive blast measurement microphones outdoors on the glass-paned door side, and two more on the rear side. A total of four thermocouples were installed, one inside the display cabinet, one above the display cabinet, one above the sidewall, and one thereunder.

To observe flame propagation in the room, we installed a 50 mm-thick acrylic window at the center of one sidewall and a visible-range high-speed monochrome camera immediately outside this window. Additionally, to observe the flame (if any), we installed a high-speed infrared camera outside at a distance of 40 m from the glass-paned door.

To observe the failure behavior of the glass-paned door, we installed two visible-range high-speed color cameras: one at the 40 m point on the line extended from the wall containing the glass-paned door and the other at the 40 m point on the 45-degree diagonal line.

4.4.4 Experimental results of the full-scale physical hazard evaluation of the reach-in refrigerated display cabinet

Assuming that all 500 g of propane leaked into the refrigerated compartment of a reach-in display cabinet (the same type as the one used for the leakage and diffusion behavior measurements) with the condenser cooling fan in operation at the bottom of the refrigerated compartment, we adjusted the internal propane concentration of the compartment to 26%, opened the cabinet door via remote control, and provided discharge sparks for ignition. Combustion did not occur when ignited at 2 cm above the floor in the center of the room and 5 min after the showcase door was opened. When ignited at 50 cm in front of the showcase door, 2 cm above the floor, and 40 s after the showcase door was opened,

combustion was confirmed, but the simulated room glass door was not damaged. When ignition occurred 2 cm above the floor and 50 cm in front of the display cabinet door at a time of 0 s after the display cabinet door was opened, we observed a flame and both the frame and glass of the simulated room’s glass-paned window were broken and blown off in pieces.

Fig. 4-9 shows still images of the indoor flame propagation process taken every 100 ms immediately after the flame occurred. Probably, the propane-air mixed gas with a large specific gravity leaked out from inside the cabinet to the downward area and reached the ignition device, resulting in a flame. Additionally, Fig. 4-10 shows still images of the failure behavior of the simulated room’s glass-paned door every 200 ms immediately after the flame occurred. These images show that the glass-paned door was left with broken glass after it was blown off into pieces due to the increased internal pressure in the simulated room.

The maximum value of the measured internal pressure increase was 5.0 kPa, and the maximum blast pressure at 10 m outside the sweep window was 29 Pa. The increase in internal pressure was limited to approximately 5 kPa because of damage to the glass-paned window. Because the burning velocity of propane is not large, the explosive blast pressure transferred to the outside of the room had only minor effects.

The maximum value of the measured radiant heat was approximately 160 kW m⁻², both indoors and outdoors. Although short in duration, the radiant heat was so intense, it caused burn injury.

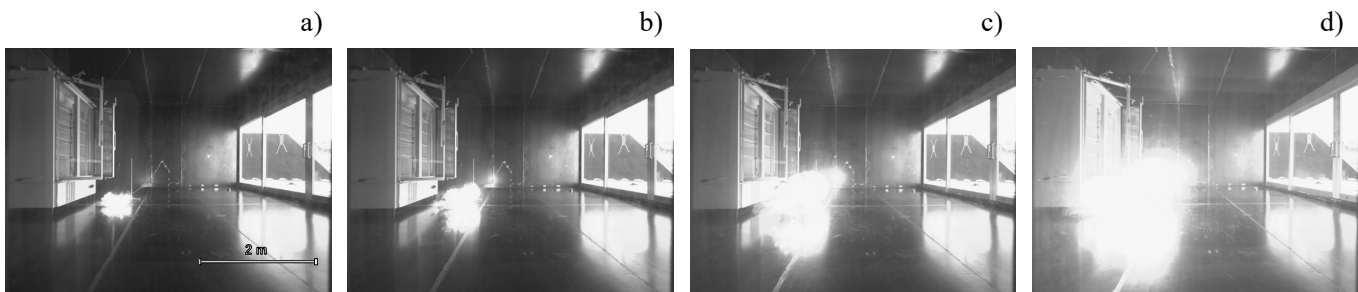


Fig. 4-10 Fire observed after opening door with continuous ignition (100 ms interval).

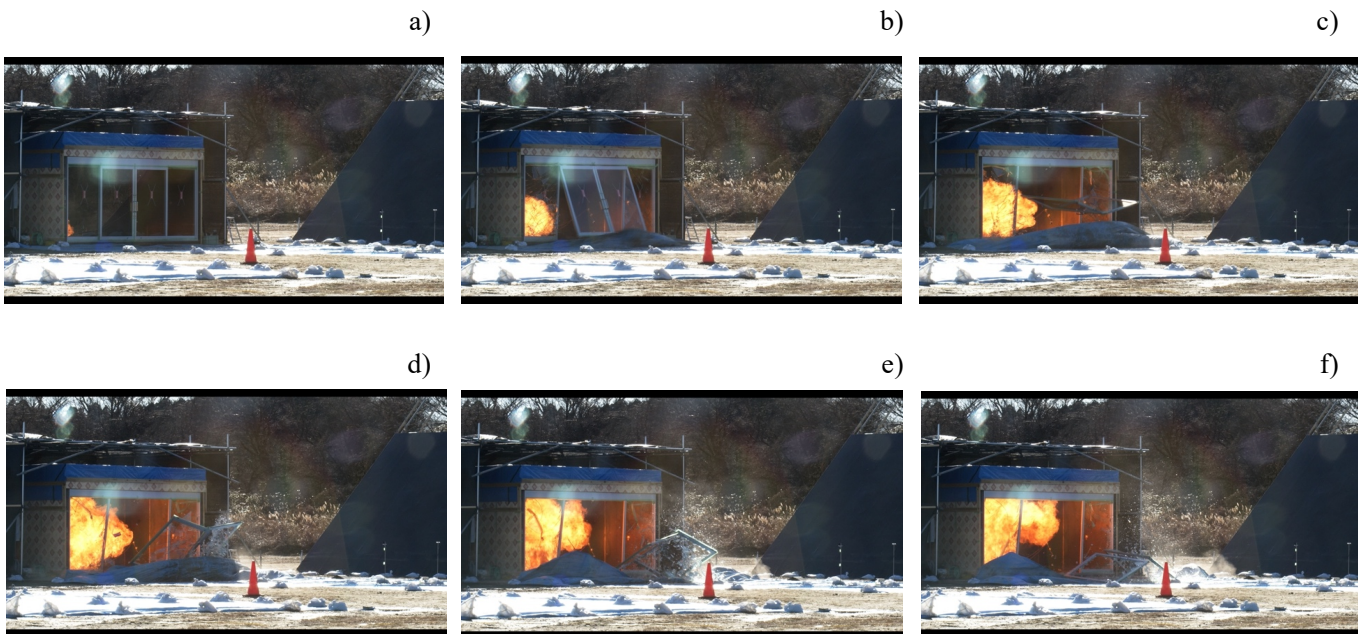


Fig. 4-11 Glass door behavior observed after propane gas ignition (200 ms interval).

Moreover, assuming that all 100 g of propane leaked into the display cabinet’s refrigerated compartment without the evaporator cooling fan in operation at the bottom of the compartment, we adjusted the internal propane concentration of the compartment to 5.2%, opened the cabinet door by remote control, and provided discharge sparks 2 cm above the

floor and 50 cm in front of the display cabinet. We observed fire and damage on the frame of the glass-paned door of the simulated room without any scattering of glass shards. The maximum value of the internal pressure was 4.4 kPa, and the maximum value of the radiant heat was 8.7 kW m⁻². The explosive blast pressure measured at 10 m outside the sweep window had a maximum value of 26 Pa. Fig. 4-12 shows still images of the indoor flame propagation taken every 100 ms immediately after the flame occurred. The emitted light appears small, probably due to the low propane concentration. Fig. 4-13 shows still images of the failure behavior of the simulated room's glass-paned door every 400 ms immediately after the flame occurred. The glass-paned door was blown off but without its glass broken.

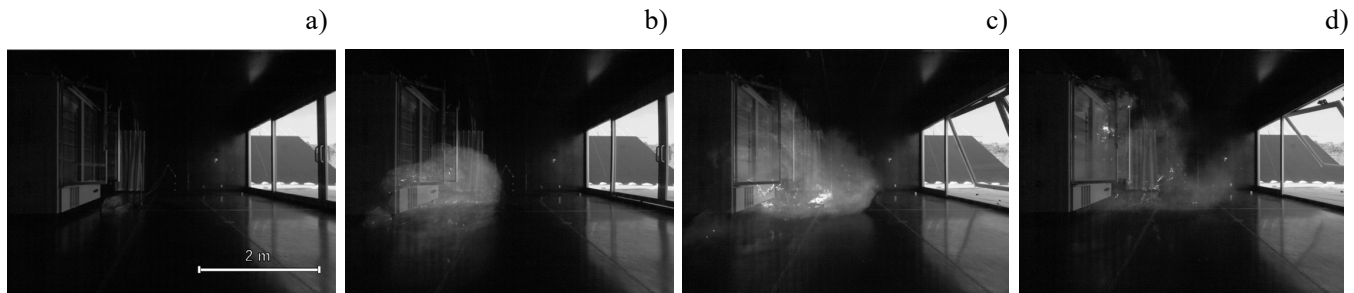


Fig. 4-12 Fire observed after opening door with continuous ignition (100 ms interval).

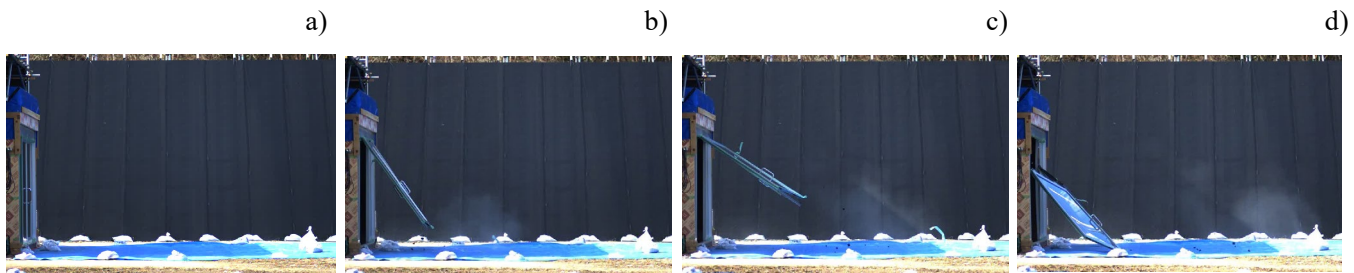


Fig. 4-13 Glass door behavior observed after propane gas ignition (400 ms interval).

4.4.5 Summary of the full-scale physical hazard evaluation of the reach-in refrigerated display cabinet

For the charge amount of 500 g, a relaxed amount currently under consideration on the premise of indoor air stirring, no flammable concentration region should exist from 5 min after the start of leakage. For the investigated reach-in display cabinet, with the evaporator cooling fan in operation, no flame was observed 5 min after the door was opened, following refrigerant leakage into the refrigerated compartment. However, a flame occurred immediately after or 40 s after the opening of the door. When a flame occurred, in particular, immediately after the opening of the door, it resulted in a broken glass-paned door and harmful radiant heat. If the relaxed charge amount currently under consideration on the premise of indoor air stirring is discharged without indoor air stirring, harm severity will increase further.

Although no mandatory safety measures are currently specified for the charge amount of 100 g, a broken glass-paned door or the like will occur despite a relatively low harm severity of combustion if a flame occurs immediately after the door is open following refrigerant leakage into the refrigerated compartment.

References

- 4-1) Risk Assessment Report on Building-Multi-Air Conditioners Using Mildly Flammable Refrigerants, Japan Refrigeration and Air Conditioning Industry Association (2017)
- 4-2) IEC 60335-2-40: 2018. Household and similar electrical appliance - Safety - Part 2-40: Particular requirements for electrical heat pumps, air-conditioners and dehumidifiers. I.E.C

Chapter 5 Progress achieved at the Research Institute for Sustainable Chemistry, AIST

5.1 Introduction

This research and development project aims to clarify the effects of blending fluorine-based refrigerants on safety performance, including flammability, to support the development and spread of low-GWP, high-safety refrigerants. We mainly consider combinations of flammable low GWP and low-flammability refrigerants to determine the mixture composition range that produces refrigerants with safety performance that meets the refrigerant safety standards currently under study at home and abroad, for example, the “Low Flammability Class (Class 2L)” in the International Standard ISO817 and the “Specific Inert Gases” specified in the Japanese High-Pressure Gas Safety Act. Additionally, to facilitate future practical use of low GWP refrigerants, we evaluated the effects of temperature, humidity, refrigerant concentration distribution, and other factors on their flammability to establish practical criteria for fire safety.

In the year 2020, to accumulate data on blend refrigerants, in particular, blend composition, we performed flammability evaluations of an R32/1234yf blend system as a new low-GWP blend refrigerant and an R32/152a blend system as a conventional blend refrigerant and evaluated their flammability limits (burning velocity, and quenching distance) under standard conditions and various temperature and humidity conditions. The results thus obtained revealed that the new low-GWP blend refrigerant in any given mixture composition under practical temperature and humidity conditions showed lower flammability than some existing “specific inert gases” (R1234yf and R32). For the conventional blend refrigerant, we identified a blend composition that allow it to be rated as a low flammability refrigerant with a maximum burning velocity equivalent to or below that of the specific inert gases under standard conditions.

5.2 Evaluation of flammability limits of low GWP blend refrigerant

Until the year 2019, we performed flammability limits evaluations by taking measurements according to the EN1839B method⁵⁻¹⁾, proven effective in obtaining results closest to the full-scale flammability limits for various refrigerants, and using the pressure rise rate $100 \times (P_{\max} - P_0)/P_0 \geq 30(\%)$ as the judgment criterion. Fig. 5-1 shows the results of the pressure rise rate and the temperature rise measurements taken during the combustion of R32 and R1234yf at concentrations near the flammability limit (lower flammability limit, LFL). The flammability limit value was specified as the average value $(B_1 + A_1)/2$ of the highest concentration B_1 among the three consecutive concentrations of B_3 , B_2 , and B_1 , for the pressure rise rate to remain constantly below 30%, and the lowest concentration A_1 among the three consecutive concentrations of A_1 , A_2 , and A_3 , for the pressure rise rate to remain constantly above 30%. As shown in Fig. 5-1(a), the flammability limit value for R32, estimated from the pressure rise rate, was $LFL = (13.75 + 13.65)/2 = 13.7$ vol%. As shown in Fig. 5-1(b), the LFL for R1234yf was $(7.15 + 6.50)/2 = 6.8$ vol%, despite the considerable variation in the pressure rise rate data.

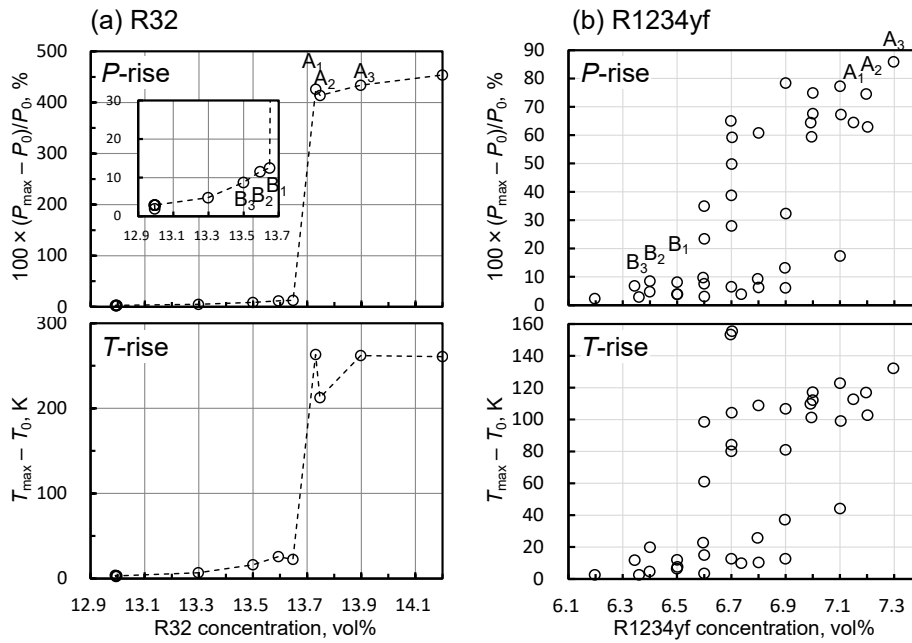


Fig. 5-1 LFL measurement using EN1839 B method for (a) R32 and (b) R1234yf. All tests were conducted at 25 ± 2 °C and $101.3 \text{ kPa} \pm 1\%$.

We investigated the effects of temperature and humidity on the flammability limits of the single-component refrigerant gases R32 and R1234yf. The results showed that the flammability limits usually did not change significantly in the practical temperature range of 15 to 60 °C. The flammability limits showed a tendency to change more markedly in the high-temperature range than in the low-temperature range. The results obtained for the LFL of R1234yf disagreed with the temperature dependence predicted using White’s law. Furthermore, we measured the effect of humidity on the flammability limits of R32 and R1234yf. It turned out it was possible to express the flammability limits as a function of the molar ratio $\text{H}_2\text{O}/\text{sample}$ as well as of relative humidity.

Next, we measured the temperature dependence of the flammability limits for the R32/1234yf blend system at various molar mixing ratios (temperature range = 15 to 60 °C; humidity = 0% RH). The results are shown in Fig. 5-2. In this graph, the ordinate-axis intercepts represent the flammability limits for the single gases R32 and R1234yf. Thus, the results obtained for the blend system confirmed that the flammability limits did not change significantly in the investigated temperature range, similar to the results for the single gases. We found that both the upper (UFL) and lower (LFL) flammability limit in dry air increased monotonically as the molar mixing ratio of R32 increased, which was almost in agreement with Le Chatlier’s formula, and this trend could be approximated using a simple quadratic equation.

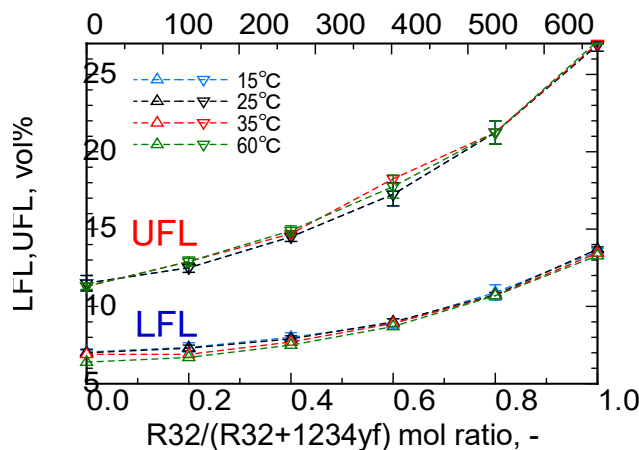


Fig. 5-2 Effect of temperature on the flammability limits of R32/1234yf blends at 0% RH.

Moreover, we investigated the effect of humidity on the flammability limits of the R32/1234yf blend. The measurement temperature was 35 °C throughout. For both the LFL and UFL measurements, the relative humidity were 10%, 35%, and 63% RH. The results are shown in Fig. 5-3. Both Calc1 and Calc2 curves were calculated using Le Chatelier's formula. The H₂O/Sample molar ratio was adjusted to remain at the same value for each measured value. The Calc1 and 2 results did not show very significant differences in this system.

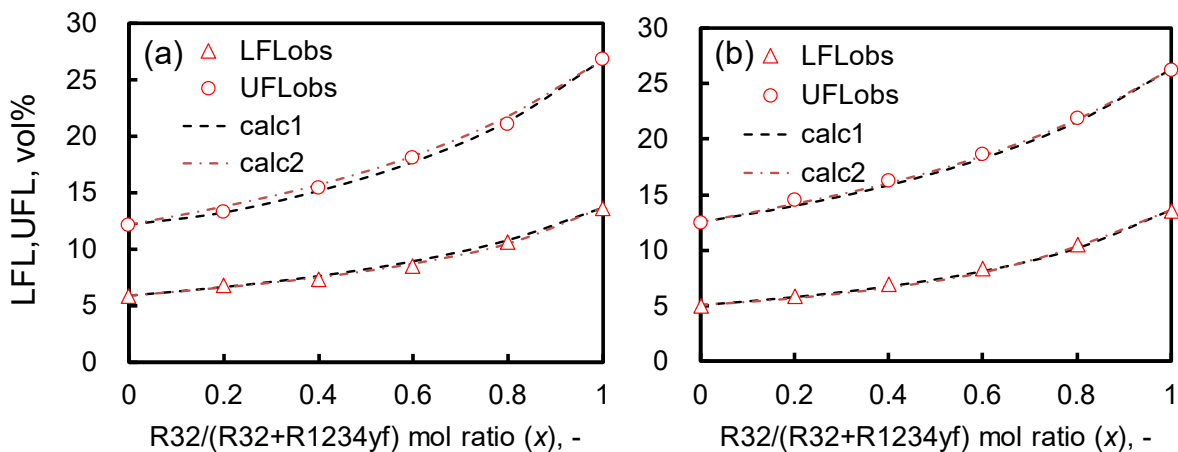


Fig. 5-3 Effect of humidity on the flammability limits of R32/1234yf blends measured at (a) 35 °C and 10% RH and (b) 35 °C and 63% RH.

As explained above, the flammability limits were measured at 35 °C under the respective constant humidity conditions (35°C-equivalents of 0%, 10%, 35%, and 63% RH). In each case, it was found that the flammability limit value (y) for the R32 mol mixing ratio (x) could be well approximated using a quadratic equation in the form of $y = ax^2 + bx + c$. Quadratic equations in terms of the relative humidity ($r = \%RH/100$) were obtained by applying the least-squares method to the values of coefficients a, b, and c, depending on the mixing ratio obtained for each of the LFL and UFL. Table 5-1 shows a summary of these coefficients. If, for example, $r = 0.50$ is substituted for the equation thus obtained, the LFL and UFL can be predicted for an arbitrary mixing composition at a relative humidity of 50% RH. To verify this expectation, we used the values obtained for coefficients a, b, and c to predict and then compare the LFL and UFL values with the measured values at each composition. As shown in Fig. 5-4, the predicted values basically agree with the measured values within the margin of error, thus suggesting the predictability of the flammability limits for the R32/1234yf blend system, at any given mixing ratio and humidity, within the practical temperature range.

Table 5-1 Coefficients for the flammability limits of R32/1234yf blends at relative humidity r

LFL	0%RH	10%RH	35%RH	63%RH		r dependency of each coefficient		$r=0.5$ (50%RH)
a	6.85	7.47	7.15	7.24	→	$y_a = -1.95r^2 + 1.49r + 7.03$	→	7.29
b	-0.074	-0.072	0.965	0.961	→	$y_b = -3.85r^2 + 4.36r - 0.22$	→	0.995
c	6.72	6.07	5.31	5.27	→	$y_c = 6.37r^2 - 6.25r + 6.69$	→	5.155
UFL	0%RH	10%RH	35%RH	63%RH		r dependency of each coefficient		$r=0.5$ (50%RH)
a	12.68	10.85	9.26	7.83	→	$z_a = 8.84r^2 - 12.80r + 12.44$	→	8.25
b	2.76	3.61	4.4	5.44	→	$z_b = -2.28r^2 + 5.45r + 2.88$	→	5.04
c	11.59	11.94	12.55	12.74	→	$z_c = -3.26r^2 + 3.89r + 11.59$	→	12.715

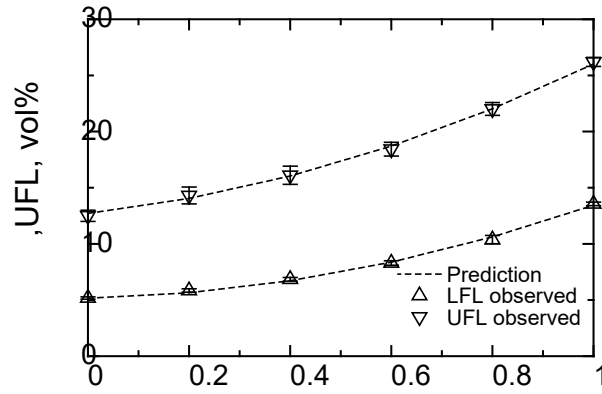


Fig. 5-4 Comparison between prediction and experiment for the flammability limits of R32/1234yf blends at 35 °C and 50% RH.

5.3 Evaluation of burning velocity of low GWP blend refrigerant

The overall combustion reaction rate can be expressed by the Arrhenius equation. Hence, the mass burning rate ($\rho_u S_u$) is expressed as in Eq. (5-1):

$$(\rho_u S_u)^2 \propto \exp(-E_a/RT_b) \quad (5-1)$$

where ρ_u is the unburned gas density, S_u is the burning velocity, E_a is the overall activation energy, R is the gas constant, and T_b is the flame temperature represented by the adiabatic flame temperature. Under the condition that the chemical reaction of the reaction system does not change significantly, the burning velocity exponentially depends on the flame temperature. Accordingly, we first calculated the flame temperature of the blend system. For example, Fig. 5-5 shows the concentration dependence of the flame temperature (initial temperature = 298 K; pressure = 1 atm) of the R32/1234yf (50/50 v/v) blend system, and Fig. 5-6 shows the mixture ratio dependence (equivalence ratio $\phi = 1.0$) of the flame temperature of the R32/1234yf blend system. Both figures also show the values calculated from the flame temperatures of the single components and various Le Chatelier's equations. A comparison of these relationships revealed that none of Le Chatelier's equations could express the remarkably low flame temperature of this blend system in any concentration range and mixture composition, thus suggesting the possibility of the contribution of the interaction between the components.

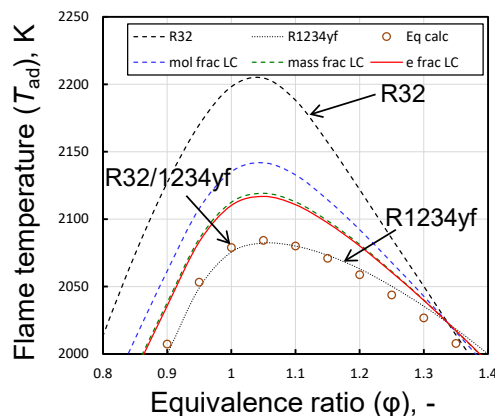


Fig. 5-5 Flame temperature for R32/1234yf (50/50 v/v) blend at $T_0 = 298$ K and $P_0 = 1$ atm.

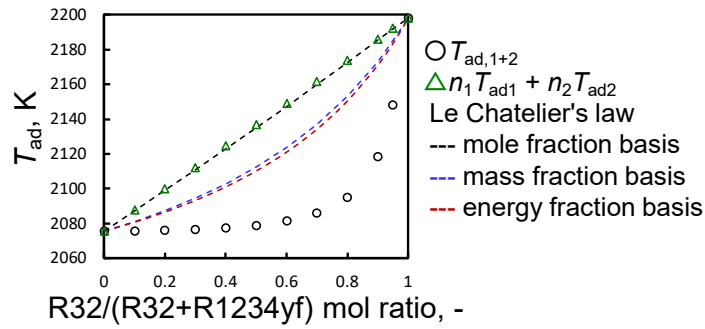


Fig. 5-6 Flame temperatures of R32/1234yf blends as a function of mixing rate at $\phi = 1.0$, $T_0 = 298$ K, and $P_0 = 1$ atm.

On the basis of the above findings, we evaluated the R32/1234yf blend system in terms of the mixture ratio dependence of its burning velocity under various temperature and humidity conditions, using the Schlieren visualization technique. First, we performed measurements over a wide range of temperatures for the entire range of mixing ratios at a humidity of 0% RH. Fig. 5-7 shows an example of the results. We did not find the significant difference in the maximum burning velocity ($S_{u,max}$) within the practical temperature range, similar to the case of the flammability limits. In addition, the burning velocity monotonically increased as the R32 mol mixing ratio increased in the dry air condition, and a significant increase in the burning velocity was not observed until the R32 mixing ratio exceeded approximately 0.5, similar to the tendency of the flame temperature. As shown by the curves in Fig. 5-7, Le Chatelier's equation cannot express the maximum burning velocity of this blend system very well on the molar fraction basis, but it can on the weight fraction or energy fraction basis.

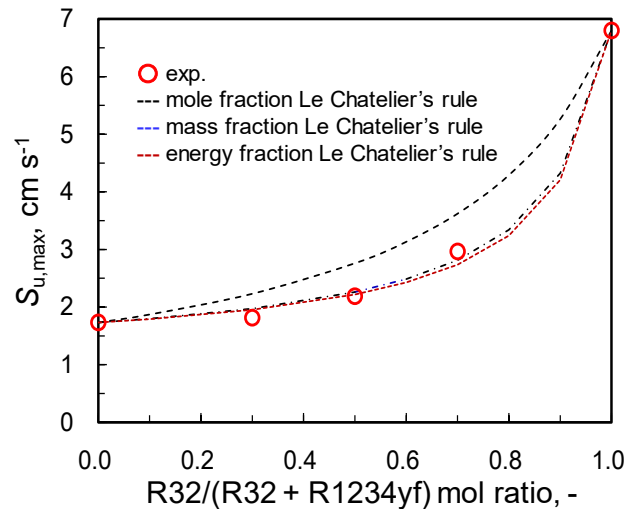


Fig. 5-7 Maximum burning velocities as a function of mixing rate for R32/1234yf blends at 35 °C, 1 atm, and 0% RH.

Additionally, we evaluated the R32/1234yf blend system in terms of the humidity effect of its burning velocity at 35 °C. Fig. 5-8 shows a summary of the results. Because the burning velocity of R1234yf on its own increased as the humidity increased, the burning velocity of the blend system showed a reduced mixture ratio dependence. This blend system turned out to show a lower burning velocity at any given mixture composition under the practical temperature and humidity conditions used this time for evaluation, i.e., 35°C/63%RH or less, than R1234yf and R32 on their own under the same conditions.

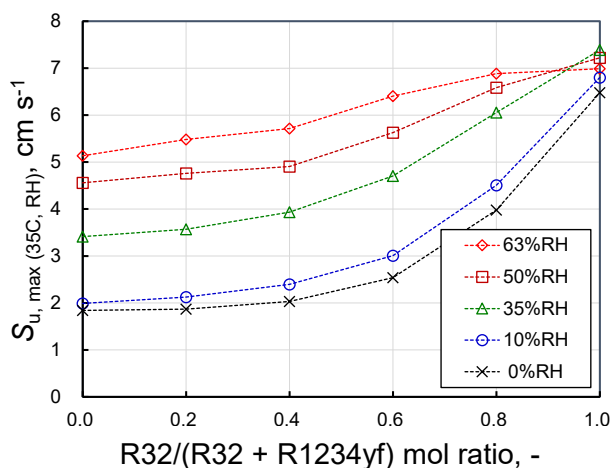


Fig. 5-8 Effect of humidity on $S_{u,max}$ of R32/1234yf blends measured at $T_0 = 308$ K and $P_0 = 1$ atm.

5.4 Evaluation of the quenching distance for low-GWP blend refrigerants

In measuring the quenching distance (d_q) for the very mildly flammable refrigerant covered by the present study, the significant effects of buoyancy on flame propagation, in addition to the large distance between the parallel flat plates, are problematic. Hence, direct measurement of the quenching distance (d_q) requires a special buoyancy removal apparatus, such as a microgravity experimental apparatus. The findings obtained so far showed that higher temperatures and pressures reduce the quenching distance. It follows then that the quenching distance may become easier to quantify with an ordinary instrument, as an indirect result of reducing it through the use of its temperature-pressure dependence. On the other hand, the required voltage for dielectric breakdown due to spark discharges follows Paschen's law and positively correlates with the gas pressure and the distance between the electrodes. Therefore, it must be noted that increased gas pressure increases the required discharge voltage. From the perspective of estimating quenching distance for the very mildly flammable refrigerant, apart from the importance of the quenching distance itself and the purpose of flame extinction diameter estimation, we measured and analyzed the temperature-pressure dependence of the quenching distance. First, we measured the initial pressure dependence of the quenching distance (at the measurement temperature and humidity of 25 °C and 0% RH).

The initial pressure dependence of the quenching distance for the mildly flammable R32 decreased approximately in the form of P_0^β relative to the increase in the initial pressure P_0 , whereby the quenching distance under 5 atm decreased to approximately 1/4 of the value under 1 atm. The quenching distance for the very mildly flammable R1234yf radically decreased relative to the increase in pressure until it became immeasurable under normal gravity. We observed that although the initial pressure dependence of R1234yf was significantly shifted in the low-pressure region from the tendency shown by R32, the former and the latter substantially agreed with each other under 2 atm or higher. We estimated the burning velocity $S_{u0,max}$ under standard conditions, using the quenching distance ($d_{q(T,P)}$) measured under various pressures and the correlation equation⁵⁻²⁾ of the mildly flammable refrigerant's quenching distance and burning velocity $S_{u,max(T,P)}$. Using this method, we obtained $S_{u0,max} = 6.7$ cm s⁻¹ for R32 and $S_{u0,max} = 1.5$ cm s⁻¹ for R1234yf. These estimated values substantially agreed with the measured burning velocity values reported in the past. Moreover, we observed that the quenching distance values under high-pressure conditions were a good fit with the correlation equation of the quenching distance and the burning velocity.

Hence, we performed measurements for the R32/1234yf blend system and examined if it was possible to estimate the quenching distance for the blend system from the results obtained above for the respective components on their own. We evaluated the R32/1234yf blend system in terms of the effects of the mixing ratio on the quenching distance under the initial pressures of 2 atm and 3 atm (measurement temperature = 25 °C; humidity = 0% RH). Fig. 5-9 shows the experimental results and the estimation results obtained using various Le Chatelier's equations. The quenching distance of the mixtures can be well expressed by Le Chatelier's formula for the mass fraction or energy fraction using the result of each single substance. Thus, the use of high-pressure conditions allows accurate measurement of the quenching

distance for a very mildly flammable refrigerant, thereby revealing that the mixture ratio dependence of its quenching distance can be estimated similarly to that of its burning velocity.

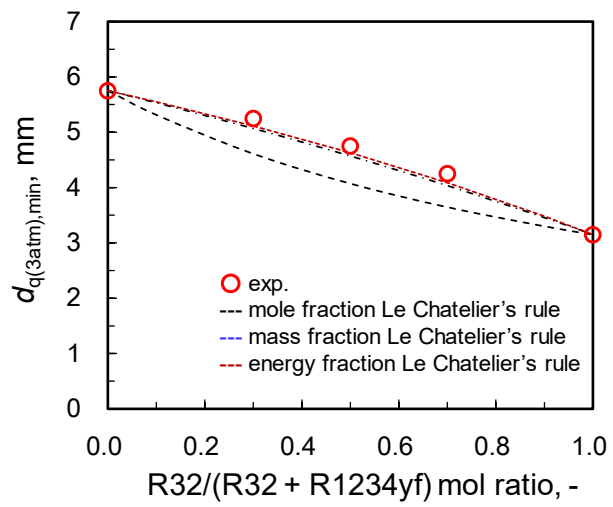


Fig. 5-9 Quenching distances of R32/1234yf blends measured at 3 atm, 25 °C, and 0% RH.

Next, we evaluated the R32/1234yf blend system in terms of the temperature, humidity, and mixture ratio dependence of the quenching distance. Figs. 5-10 and 5-11 show the results. Similar to the results for the burning velocity, the quenching distance for the evaluated mixture composition showed a higher dependence under practical conditions than that for R32 or R1234yf on its own under the same conditions, thereby revealing a low ignition possibility for the mixture composition. Additionally, it turned out that, for the most part, the quenching distance for this blend system under high humidity conditions can be expressed according to various Le Chatelier's equations.

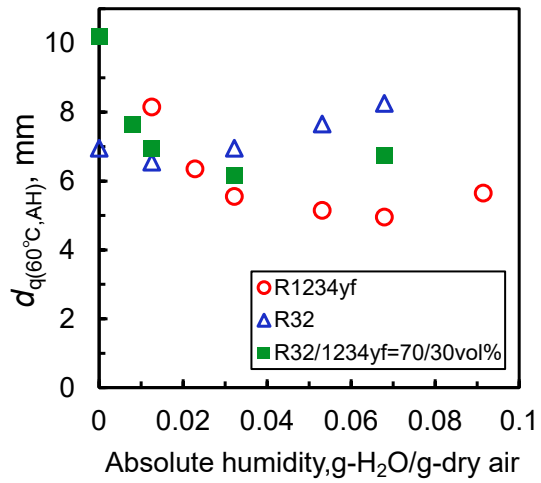


Fig. 5-10 Effect of humidity on d_q of R32, R1234yf, and R32/1234yf (70/30 v/v) blends at $T_0 = 333$ K and $P_0 = 1$ atm.

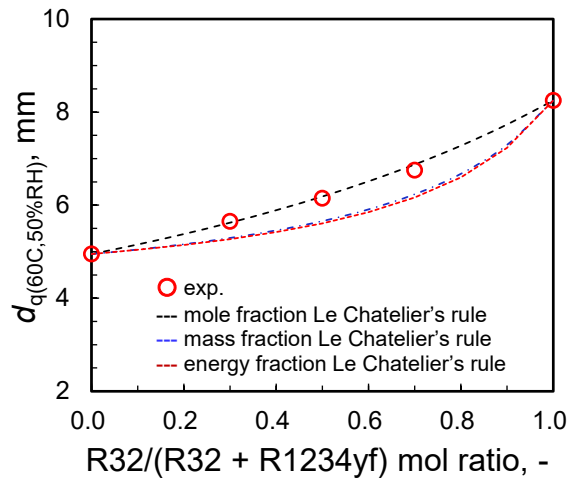


Fig. 5-11 d_q of R32/1234yf blends under high humidity ($T_0 = 333$ K and 50%RH).

5.5 Evaluation of the fundamental flammability of conventional blend refrigerants

The conventional blend refrigerant we selected for comparison with the new refrigerants was an R32/152a blend system, which is versatile enough to allow extensive adjustment of flammability. We evaluated several mixture compositions in terms of the flame temperature, burning velocity, and quenching distance under standard conditions (temperature = 25 °C; pressure = 101.3 kPa; humidity = 0).⁵⁻³⁾ First, we calculated the flame temperature of the blend system and compared it with the values calculated from the flame temperatures of its components on their own according to various Le Chatelier's principles. As an example, Fig. 5-12 shows the concentration dependence of the flame temperature of the R32/152a (50/50 v/v) blend system, and Fig. 5-13 shows the mixture ratio dependence of the flame temperature of R32/152a (equivalence ratio $\phi = 1.0$). These observations suggest that the flame temperature will show only a minor change due to this mixture. Additionally, Le Chatelier's principles on the energy fraction basis best reproduced the flame temperature of the blend system for all concentration ranges and mixture compositions. It turned out that Le Chatelier's principles on other bases also approximately reproduced the flame temperature of the blend system.

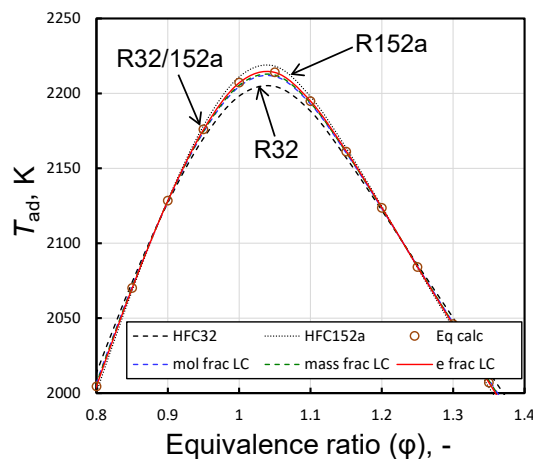


Fig. 5-12 Flame temperatures of R32/152a (50/50 v/v) blend at $T_0 = 298$ K and $P_0 = 1$ atm.

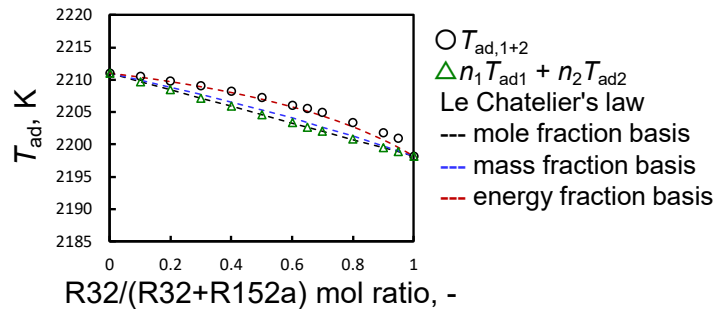


Fig. 5-13 Flame temperatures of R32/152a blends as a function of mixing rate at $\phi = 1.0$, $T_0 = 298$ K, and $P_0 = 1$ atm.

On the basis of the above findings, we evaluated the R32/152a blend system in terms of the mixture ratio dependence of the burning velocity (S_{u0}) under standard conditions using the spherical-vessel (constant-volume) method. Figs. 5-14 and 5-15 show the results. The blend system turned out to have a maximum burning velocity of 10 cm s^{-1} or less (“Specific Inert Gas” under the High-Pressure Gas Safety Act) when the molar mixing ratio of R32 exceeded 0.86. It turned out that various Le Chatelier’s equations failed to express the mixture ratio dependence of the maximum burning velocity and underestimated the experimental values.

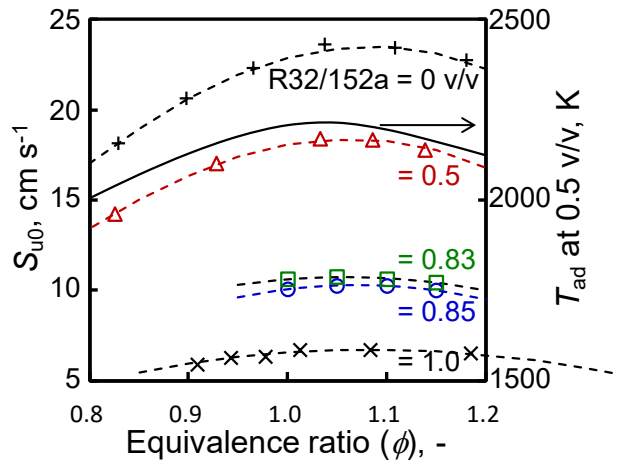


Fig. 5-14 Burning velocities of R32/152a blends at $T_0 = 298$ K and $P_0 = 1$ atm.

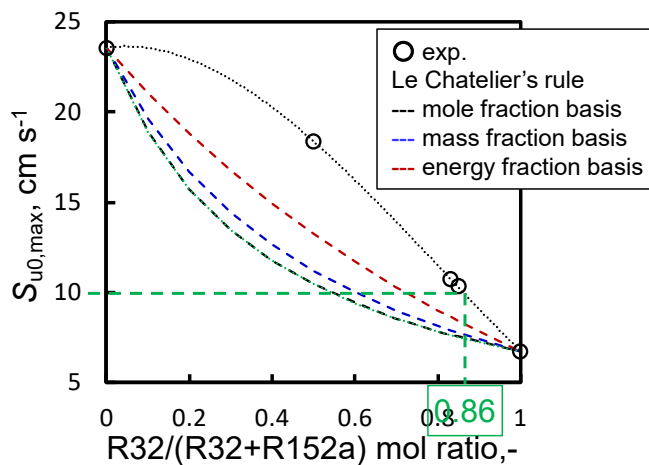


Fig. 5-15 Maximum burning velocities of R32/152a blends at $T_0 = 298$ K and $P_0 = 1$ atm.

Then, we evaluated the R32/152a blend system in terms of the quenching distance (d_{q0}) under standard conditions. Figs. 5-16 and 5-17 show the results. These results, together with those for the burning velocity, revealed that this blend system fell into the category of “specific inert gases” when its quenching distance exceeded 5 mm, and that it has the same boundary value as conventional single-component refrigerants. Additionally, the quenching distance of this blend system was approximately expressed according to Le Chatelier’s principles on the energy fraction basis, thereby confirming that the correlation equation obtained from the conventional refrigerants held for its correlation with burning velocity. Thus, it turned out that the quenching distance values (known) for single-component refrigerants allow the estimation of the quenching distance and burning velocity for any given mixture composition.

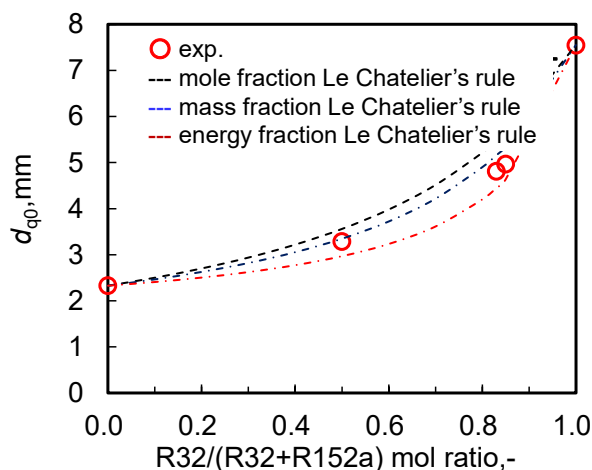


Fig. 5-16 d_{q0} of R32/152a blends at $T_0 = 298$ K and $P_0 = 1$ atm.

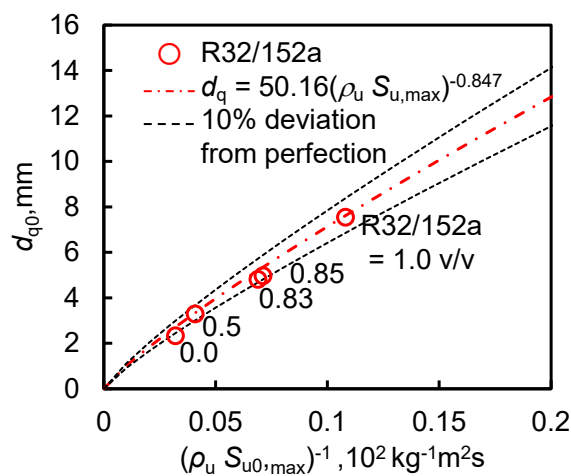


Fig. 5-17 Relationship between maximum burning velocity and d_{q0} for R32/152a blends.

References

- 5-1) EN 1839:2017, “Determination of the explosion limits and the limiting oxygen concentration (LOC) for flammable gases and vapours (2017).
- 5-2) K. Takizawa, N. Igarashi, K. Tokuhashi, and S. Kondo: Sci. Tech. Built Environ., 24(1), 97(2018).
- 5-3) K. Takizawa, N. Igarashi, K. Tokuhashi, and S. Kondo: Int. J. Refrig., 120, 370(2020).

Chapter 6 Progress of risk assessment of mini-split air conditioners using A3 refrigerant conducted by JRAIA

6.1 Introduction

In July 2016, the Japan Refrigeration and Air Conditioning Industry Association (JRAIA) launched a new working group to conduct risk assessment of low GWP A3 refrigerants, aiming to achieve stepwise conversion to low GWP refrigerants as a global warming countermeasure. Regarding the risk assessment of A3 refrigerants, demand increased for the establishment of a framework involving members of the government, academia, and industry, similar to the one established to consider A2L refrigerants. In response, a framework was established and a study project started in the latter half of 2018 as a NEDO Project.

This report mainly presents excerpts of the reports prepared by JRAIA Mini-Split Risk Assessment WG3 for international conferences over the past three years using the results of the risk assessment studies of the WG. Therefore, this report does not systematically describe the risk assessment results and inherits minute discrepancies in certain values and terminology from reports published at different times for international conferences. However, we (hereafter “we” refers to WG3 members of the JRAIA) did not make corrections to avoid discrepancies between each past report. The contents presented herein are up-to-date results at the time each report was written for each international conference. Therefore, the reader of this report is expected to understand this background and refer to the contents properly at his/her discretion.

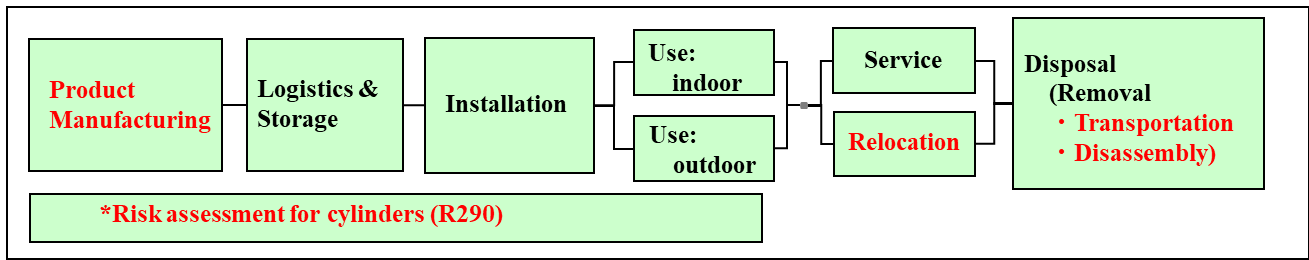
We will correct the aforementioned discrepancies in certain values and terminology in this report and make a new presentation at the JRAIA International Symposium in October 2021.

6.2 The risk assessment outline

6.2.1 Scope of the risk assessment

Usually, a product risk assessment covers the processes from manufacturing to disposal. Fig. 6-1 shows the product life stages covered in the mini-split air conditioner risk assessment studied by JRAIA. As shown in the figure, there are six stages of the life cycle, including “logistics and storage,” “installation,” “usage indoors and outdoors,” “repair,” and “disposal.” “Product manufacturing” was excluded from the scope of this assessment on account of the confidentiality of individual manufacturer’s know-how. Additionally, the “disposal” stage consists of the substages of air conditioner removal, transportation to the recycling factory, and disassembly at the recycling factory. At the “disposal” stage, only removal was considered in this risk assessment. Air conditioner relocation was excluded from the scope of the present risk assessment because this stage was considered a combination of the “transportation” and “installation” stages, neglecting minor technical differences.

The risk assessment considerations at each stage were made by JRAIA members as air conditioner manufacturers within a reasonably foreseeable range, estimating risks on the basis of typical conditions. An example of such conditions are workers having reasonable knowledge about their job (logistics, installation, repair, and removal of air conditioners) through training and lectures. Criminally or intentionally committed cases and extremely severe scenarios were excluded. The ignition probability at each stage was calculated on the basis of “work method and procedure usually expected.” Accordingly, “work method and procedure usually not expected” were placed beyond the scope of assumption. In addition, no detailed study was made of refrigerant cylinder handling, although it relates to a few life stages.



Note: The stages in red are not included in the JRAIA risk assessment.

Fig. 6-1 Life stages covered by risk assessment.

6.2.2 The structure of this report

It is preferable to present the achievements as of today after briefly outlining the six stages, including “logistics and storage,” “installation,” “usage indoors and outdoors,” “repair”, and “disposal,” in relation to the aforementioned scope of risk assessment. However, discussions are still underway regarding the differences and evidence for the fault tree analysis (FTA) at each stage. Therefore, this report is structured to list and address the following topics without pursuing consistency. It first describes “accident occurrence probabilities,” focusing on the results obtained by reconsidering the temporal encounter probability. Then, the contents of the published papers prepared by the working group for international conferences over the past three years are explained, specifically “indoor ignition source” and “outdoor refrigerant leak simulation”. The part on “indoor ignition sources” identifies many ignition sources present indoors and considers simulated encounters with flammable regions. On the other hand, because not many ignition sources exist outdoors, the part on outdoor sources focuses on simulated refrigerant diffusion behaviors in terms of factors contributing to flammable region generation. In particular, the installation conditions of the air conditioner, the effects of operating outdoor fans, the effects of the gap of balcony walls, and the effects of natural winds are significant to flammable region generation and ignition probability. Although the approaches for indoor units and outdoor units are apparently very different, the two parts are in accordance with the basic procedure of risk assessment, that is, the evaluation of factors that has more significant impacts on the accident probability are prioritized. In other words, ignition sources are considered to be the major factors that vary indoor ignition probability, whereas the formation of flammable region is the major factor for outdoors. A last section presents suggestions of “unassumed events” that would be a problem after the completion of the present risk assessment. Moreover, considering the “security and safety” mindset characteristic of the Japanese, another section was added to ensure risk communication, which is indispensable before R290 refrigerant is commercialized.

6.2.3 Risk assessment method

The risk assessment method used in this study for R290 is FTA, which is the same method used by the JRAIA in the study on A2L refrigerants. More specifically, the procedure is in accordance with the risk assessment flow shown in Fig. 6-2 and is based on the iterative improvement process specified in ISO/IEC Guide 51.⁶⁻¹⁾ For more detailed information on the risk assessment method, refer to the R32-related risk assessment reports located at the website of the Japan Society of Refrigerating and Air Conditioning Engineers [JSRAE] and the website of JRAIA.

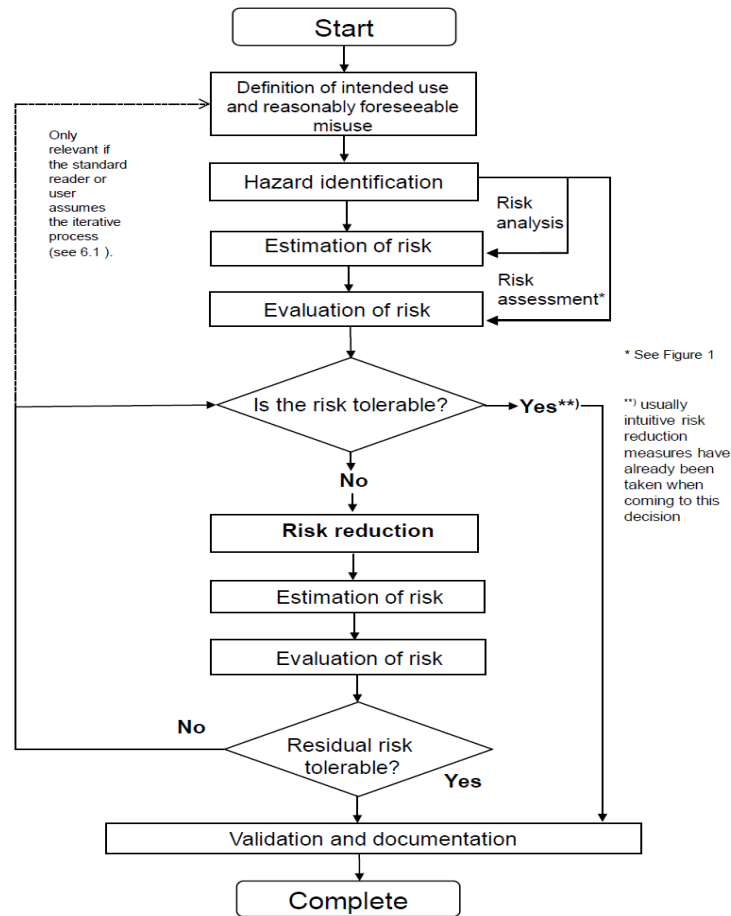


Fig. 6-2 Iterative process of risk assessment and risk reduction.

The present risk assessment concerns the use of higher flammable refrigerants. Hence, we focused on the existence probabilities of ignition sources and those of refrigerant leakage events as a factor of flammable region formation. For this report, we decided to show ignition sources' existence, refrigerant leakage events, and their relationship using FTA and derive the probabilities of burn injuries and fire accidents from the existence probability of ignition sources, the probability of leakage, the degree of a flammable region generation resulting from a leakage, and the probability of encountering them simultaneously. Additionally, assuming the considered accident events are mutually independent, their probabilities are totaled and presented as a per-annum probability of accidents per unit.

In any case, a risk assessment requires the following steps: “identify the tolerable level of risk for its termination,” “plan safety measures to reduce frequency and degree of risk” to the required level, and “determine them as safety measures.” However, because safety measures reduce risk to a tolerable level, but are not perfect, a text intended to inform the residual risks to the users must be included for conformity with Guide 51.

6.2.4 Air conditioners covered by the risk assessment

The air conditioners covered by the present risk assessment are wall-mounted mini-split-type air conditioners, used mainly in households, with a rated cooling capacity of 2.2 kW to 5.0 kW.

The refrigerant charge amount of air conditioner has the most significant impact on the risk assessment of leaked refrigerant ignition. The first charge amount used was 200 g, which is below the amount specified by IEC 60335-2-40 for a 7-m² room (typically, the smallest room with an AC in Japan) and seems to be safe. The second charge amount used was 500 g. A refrigerant charge of 1000 g is typical for the so-called energy-saving model of air conditioners with R32. However, the density of R290 is approximately half of that of R32. Thus, the required charge amount for R290 is halved, which is 500 g.

6.2.5 Tolerable values of the risk assessment

In the risk assessment performed around 2015 on A2L refrigerants for residential air conditioners by JRAIA, the report of the National Institute of Technology and Evaluation (NITE) was used to determine the tolerable value of the accident occurrence rate that was used as the judgment criterion. More specifically, the target tolerable value (indoors and outdoors) in the usage stage of life for products on the market on the order of 1 million units is specified as 10^{-8} units/year or less, which means one or fewer accident occurrences per 100 years. The total number of residential air conditioners used in the Japanese market amounts to 100 million units, which equates to a target tolerable value for the usage stage of 10^{-10} times/units/year. For stages other than usage, i.e., logistics and storage, installation, repair, and removal, we determined that a tolerable value approximately ten times larger than the value for the usage stage, i.e., 10^{-9} times/unit/year or less, is acceptable, assuming that the degree of tolerance increases due to factors, such as the sense of professional obligation.

The present risk assessment for A3 refrigerant (R290) follows the above idea and finds that the tolerable value for the usage stage is 10^{-10} times/units/year and that for the other stages is 10^{-9} times/units/year or less.

6.3 Accident occurrence probability

6.3.1 Temporal encounter probability

For leaked refrigerant to ignite, an ignition source and a flammable region must exist simultaneously. Using the probability of their concurrence in time as the temporal encounter probability, while consulting the book authored by Okabe⁽⁶⁻²⁾ and the specialist website hosted by Takakura for public access,⁽⁶⁻³⁾ we derived calculation formulae by using geometric probability applied to the duration of the ignition source, the duration of the flammable region, and other relevant values. Then, the obtained formulae were used for risk assessment. Note that the calculation formulae were considered for each stage because of the differences in the reference time period and other criteria between the usage stage and the work stages (logistics and storage, installation, repair, and removal).

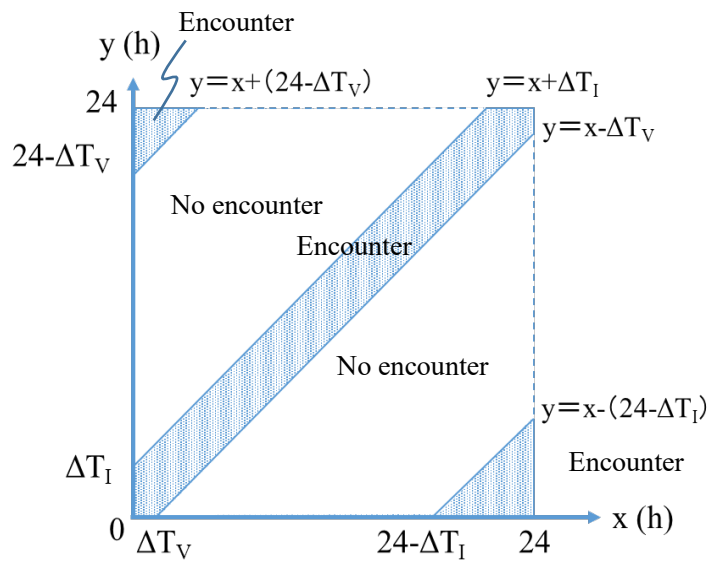


Fig. 6-3 Statistical encounter between ignition source and flammable volume.

(1) Temporal encounter probability at the usage stage

First, we consider the temporal encounter probability, P_1 , when the frequency of the ignition source operating at the usage stage is once/day.^{(6-2), (6-2)} Assuming that the occurrence time of the ignition source is x and that the occurrence time of the flammable region is y , the non-encounter condition for the ignition source and flammable region falls within the range defined by Eqs. (6-1) and (6-2). Their relationship is shown in Fig. 6-3.

$$\Delta T_V < x - y < 24 - \Delta T_I \quad (x \geq y) \quad (6-1)$$

$$\Delta T_I < y - x < 24 - \Delta T_V \quad (x < y) \quad (6-2)$$

where ΔT_V is the duration of the flammable region (h) and ΔT_I is the duration of the ignition source (h).

As shown in Eq. (6-3), P_1 is derived from the area ratio between the encounter region and the non-encounter region in Fig. 6-3. From this equation, it turns out that the temporal encounter probability can be calculated by dividing the sum of the duration of the ignition source and the duration of the flammable region by the reference time period (24 h for the usage stage).

$$P_1 = \frac{\frac{\Delta T_I^2 + \Delta T_V^2}{2} + 24^2 \cdot \frac{(24 - \Delta T_I)^2 + (24 - \Delta T_V)^2}{2}}{24^2} = \frac{\Delta T_I + \Delta T_V}{24}$$

Next, we consider P_n , the temporal encounter probability with an ignition source with multiple occurrences per day. Assuming that the frequency of the ignition source is n times/day, the probability of non-encounter per day is $(1 - P_1)^n$. Therefore, P_n can be expressed in the form shown in Eq. (6-4). Although the temporal encounter probability must be calculated as a per-annum value, the denominator is 24 h, i.e., the duration of a day; the assumption here is that the ignition source invariably occurs every day (365 days/year).

$$P_n = 1 - (1 - P_1)^n = 1 - \left(1 - \frac{\Delta T_I + \Delta T_V}{24}\right)^n \quad (6-4)$$

where n is the frequency of the ignition source (times/day).

Additionally, we consider P_{tn} , the temporal encounter probability with an ignition source with multiple occurrences per day concentrated in a specific time band. The assumption here is that the ignition source can exist in multiple time bands and operates multiple times during a specific time band. An example of such an ignition source is a smoking implement that exists intensively in smoking break times and operates multiple times per smoking break time. P_{tn} can be obtained as the product of “the encounter probability of the ignition source and the flammable region on the premise of the encounter between the ignition source’s potential duration and the flammable region” and “the encounter probability of the ignition source’s potential duration and flammable region.” Note that the duration of the ignition source present intensively in ΔT_I is ΔT_{IC} , the frequency of the ignition source in ΔT_I is n , and the frequency of the ignition source in a specific time band is n_c . Eq. (6-5) can be obtained by applying the same method described above to each encounter probability.

Eq. (6-5) is used to calculate the temporal encounter probability at the usage stage. Where the ignition source does not exist intensively in a specific time band, as with a stove, $\Delta T_{IC} = \Delta T_I$ and $n_c = 1$ hold, whereby Eq. (6-5) is equal to Eq. (6-4).

$$P_{tn} = \left\{1 - \left(1 - \frac{\Delta T_{IC} + \Delta T_V}{\Delta T_I + \Delta T_V}\right)^{n_c}\right\} \left\{1 - \left(1 - \frac{\Delta T_I + \Delta T_V}{24}\right)^n\right\} \quad (6-5)$$

where ΔT_{IC} is the duration of the ignition source in a specific time band (h) and n_c is the frequency of the ignition source in a specific time band (n times/day).

(2) Temporal encounter probability at the work stages of logistics and storage, installation, repair, and removal

The temporal encounter probability at the work stages (logistics and storage, installation, repair, and removal), P_s , is obtained as the product of the following:

- (i) The encounter probability of the work and leaked refrigerant,
- (ii) The encounter probability of the work and the ignition source, and
- (iii) The encounter probability of the ignition source and the leaked refrigerant on the premise of the concurrence of the ignition source and leakage during the work.

It is possible, at the work stages, that the ignition source and leakage occur due to or not due to the work. Therefore, consideration of P_s was divided into Cases (I) to (IV) on the basis of the following:

- (a) When the leakage is not caused by work (e.g., leakage during usage), the leak probability is a value obtained as the per-annum leakage likelihood for products on the market. Hence, this probability must be converted into the leakage likelihood within the work time by multiplication with $\Delta T_s / (24 \times 365)$ represented as (i).
- (b) When the ignition source is not caused by work (e.g., indoor electrical devices), the duration of the ignition source is calculated using the reference time period of 24 (h). Hence, this duration must be converted into the duration of the ignition source within the work time by multiplication with $[1 - \{1 - (\Delta T_I + \Delta T_s) / 24\}^n]$ represented as (ii).

If the leakage is not caused by work and the ignition source is caused by work, (ii) = 1 holds because the ignition source always occurs during the work. Hence, Eq. (6-6) holds, in which the 24 (h) in Eq. (6-5) for the usage stage is replaced with the work time ΔT_S (h). Each encounter probability was calculated similarly to that in the usage stage. When an ignition source occurs multiple times per day but not due to the work, it does not follow that all of its occurrences concentrate in the work time. Hence, the frequency n is multiplied by the ratio of the work time ΔT_S (h) and the 24 (h) of the day to obtain the number of encounters: $n \times \Delta T_S/24$. In cases where the frequency n is large and the duration of the ignition source ΔT_I is short, this calculation method is probably close to reality. In cases where the frequency n is small and the duration of the ignition source ΔT_I is long, a more realistic value can probably be obtained by multiplying the duration of the ignition source ΔT_I , instead of the frequency n , by $\Delta T_S/24$. However, considering the difficulty in the separate handling of cases, we chose to multiply the frequency n by $\Delta T_S/24$ in all cases. Eqs. (6-6) to (6-9) show the instances of P_S thus derived:

(I) Both the leakage and the ignition source are caused by work (= (iii)):

$$P_S = \left\{ 1 - \left(1 - \frac{\Delta T_{IC} + \Delta T_V}{\Delta T_I + \Delta T_V} \right)^{nc} \right\} \left\{ 1 - \left(1 - \frac{\Delta T_I + \Delta T_V}{\Delta T_S} \right)^n \right\} \quad (6-6)$$

(II) The leakage is not caused by work and the ignition source is caused by work (= (i) \times (iii)):

$$P_S = \left(\frac{\Delta T_S}{24 \times 365} \right) \left\{ 1 - \left(1 - \frac{\Delta T_{IC} + \Delta T_V}{\Delta T_I + \Delta T_V} \right)^{nc} \right\} \left\{ 1 - \left(1 - \frac{\Delta T_I + \Delta T_V}{\Delta T_S} \right)^n \right\} \quad (6-7)$$

(III) Neither the leakage nor the ignition source is caused by work (= (i) \times (ii) \times (iii)):

$$P_S = \left(\frac{\Delta T_S}{24 \times 365} \right) \left\{ 1 - \left(1 - \frac{\Delta T_I + \Delta T_S}{24} \right)^n \right\} \left\{ 1 - \left(1 - \frac{\Delta T_{IC} + \Delta T_V}{\Delta T_I + \Delta T_V} \right)^{nc} \right\} \left\{ 1 - \left(1 - \frac{\Delta T_I + \Delta T_V}{\Delta T_S} \right)^{n \times \frac{\Delta T_S}{24}} \right\} \quad (6-8)$$

(IV) The leakage is caused by work and the ignition source is not caused by work (= (ii) \times (iii)):

$$P_S = \left\{ 1 - \left(1 - \frac{\Delta T_I + \Delta T_S}{24} \right)^n \right\} \left\{ 1 - \left(1 - \frac{\Delta T_{IC} + \Delta T_V}{\Delta T_I + \Delta T_V} \right)^{nc} \right\} \left\{ 1 - \left(1 - \frac{\Delta T_I + \Delta T_V}{\Delta T_S} \right)^{n \times \frac{\Delta T_S}{24}} \right\} \quad (6-9)$$

where ΔT_S is the work time (h).

The symbols used so far are summarized below:

- P_1 : Temporal encounter probability when the frequency of an ignition source is once per day, -
- P_n : Temporal encounter probability with an ignition source with multiple occurrences per day, -
- P_{tn} : Temporal encounter probability with an ignition source with multiple occurrences per day concentrated in a specific time band, -
- ΔT_V : Duration of a flammable region, h
- ΔT_I : Duration of an ignition source, h
- ΔT_{IC} : Duration of an ignition source intensively present in ΔT_I , h
- ΔT_S : Work time, h
- n : Frequency of an ignition source, n times/day
- nc : Frequency of the ignition source in a specific time band, n times/day

6.3.2 Summary about accident occurrence probabilities

In the risk assessment for A3 refrigerant currently carried out by the JRAIA, the study is underway on the accident occurrence probability when the leaked refrigerant ignites. As explained in the previous subsection, we derived the calculation formulae for the temporal encounter probability between an ignition source and a flammable region, i.e., the

probability of both existing and occurring simultaneously in time, using geometric probability.

Although the usage stage and the work stages (logistics and storage, installation, repair, and removal) differ in the reference time period and other criteria, the derived formulae can be applied because the ignition probabilities during these stages are based on common factors.

6.4 Indoor ignition sources

6.4.1 Foreseeable indoor ignition sources

Ignition sources for A3 refrigerants can be categorized into open flames, high-temperature surfaces, and sparks. As shown in Table 6-1, open flames include cigarette lighters, candles, and gas cooktops, and they are sure to ignite both A2L and A3 refrigerants upon contact. High-temperature surfaces are typically electric heaters or cooking hot plates. These devices are quite likely to ignite A3 refrigerants, which have a low auto ignition temperature, although such factors as air convection may have an effect to some extent. Sparks are divided into electrostatic sparks and electric sparks from electrical devices. Electric sparks are further categorized according to their origin: brush motors of vacuum cleaners and the like, thermostats of irons and the like, relay contacts of electrical appliances, and plugging in and unplugging or light switch ON/OFF operations. Note that these ignition sources are just study candidates and have not been demonstrated to ignite A3 refrigerants.

These potential ignition sources exist indoors in large numbers. Open flames, high-temperature surfaces, and sparks were examined one by one to see if they would be a potential ignition source with A3 refrigerants. In Japan, most people maintain the custom of sitting on the floor. Hence, our investigation took into consideration such factors as life habits and location of ignition sources.

We used the propane auto ignition temperature (470 °C or more) and the minimum ignition energy of propane (0.25 mJ or more) as reference conditions to judge whether a high-temperature surface or a spark would be a potential ignition source, respectively.

When the same ignition source as in the present chapter exists in other stages, the contents of the present chapter were adopted to that stage. Otherwise, individual studies were undertaken at each stage.

6.4.2 Open flames

Table 6-1 enumerates the results of our considerations on smoking, candles, and other open flames assumed to be potential ignition sources:

(1) Smoking

A cigarette lighter is obviously an ignition source when it is used to light up a cigarette. Meanwhile, according to Li and Kashimura et al., the burning tip of a cigarette is a potential ignition source because it becomes as hot as 650 to 800 °C, reaching or exceeding the propane auto ignition temperature when a deep puff is taken from the cigarette.^{6-4),6-5)} The results of a fact-finding

survey conducted by the JRAIA on actual smokers' puffing behavior found that the smoking break time per occasion was typically 5 min, including 5 s for lighting with a cigarette lighter and 40 s of puffing from the cigarette (2 s × 20 drags). Hence, our risk assessment adopted these values. However, Nakayama et al. reported that even when a puff was taken from a cigarette in an atmosphere containing propane, no ignition occurred, thus suggesting the need for further consideration of other factors, such as the effects of surface shapes and ashes.⁶⁻⁶⁾

Table 6-1 Comparison of ignition sources

Ignition source	R410A; A1	R32; A2L	R290;A3 (Propane)
Open flame (smoking, candle)	No ignition	Ignition	Ignition
High-temperature surfaces	No ignition	Rare ignition	Occasional ignition
Electric spark	No ignition	No ignition under 15 kVA	Occasional ignition

energy of propane of 0.25 mJ.

$$E=(1/2)CV^2 \quad (6-10)$$

where E is the electrostatic energy (J), C is the capacitance (pF), and Vs is the human body electrostatic voltage (V).

The study by Okukubo et al.⁶⁻¹⁰⁾ indicated that human body charge in everyday life reaches 4.0 kV or more through such activities as standing up from furniture (e.g., sofa) or undressing. It follows that static electricity generated in everyday life by doorknob touching or undressing has sufficient energy to ignite propane. However, according to the above-mentioned “Recommendations for Requirements for Avoiding Electrostatic Hazards in Industry,” the discharge caused by undressing is a brush discharge, which means that with a human body electrostatic potential of approximately 4.0 to 5.0 kV, the discharge energy is as low as less than 10^{-5} J and hence falls short of ignition. From the foregoing, we find that discharge from undressing does not cause ignition, although discharge from doorknob touching may be a potential ignition source. Typically, a doorknob is touched when someone leaves a room. A person may have a human body electrostatic potential exceeding 4.0 kV when they stand up from a sofa. Then, considering the daily activity patterns of a four-person household, the average number of such discharges per person per day was estimated to be approximately three discharges. If this number increases to 5 discharges per day for a full-time homemaker, a typical household’s total discharge number per day becomes 14. The discharge duration (1 μ s) used in our risk assessment is based on the results reported by Yoshida et al.⁶⁻¹¹⁾

(2) Other electrostatic charges

Printers are among the electrical appliances that require consideration for electrostatic charges apart from static electricity. The operation of a laser printer for household use entails the process of electrostatic charging to the photoconductor drum. First, the printer applies voltage to a thin wire to induce a corona discharge. This energy is less than 0.1 mJ and hence falls short of ignition. However, the electrostatically charged photoconductor drum has its whole surface charged with static electricity. Therefore, there is a possibility of ignition. Furthermore, the printer must perform discharging twice per sheet printed because the printing process involves an electrostatic charging process and a transfer process. Both electrostatic discharges are a concern, especially if a printer typically prints ten sheets per use. Although the electrostatic discharge duration of the printer was unclear, our risk assessment assumed a discharge duration of 1 μ s, the same as for human body electrostatic charges.

(3) Brush motors

A brush motor contains brushes. These brushes serve as mechanical contacts and produce sparks during operation. Examples of indoor-use electrical appliances equipped with a brush motor include vacuum cleaners, hairdryers, electric shavers, and printers. Among these appliances, vacuum cleaners and hairdryers fall short of ignition because the fan blows out air during operation and causes the air around the brush motor to flow at a rate sufficiently faster than the burning velocity of propane. In contrast, electric shavers and printers may be a potential ignition source because they lack a fan. In assessing the market share of the four major manufacturers in Japan, electric shavers with a brush motor account for 70% of the whole number. Meanwhile, their average time per use was approximately 3 min.

(4) Thermostats

A thermostat operates by opening and closing two contacts when the bimetal warps with temperature changes and has the possibility of producing sparks from its contacts. Therefore, thermostats must be regarded as ignition sources. Examples of electrical appliances using a thermostat include electric *kotatsu* (a table with electric feet warmers), electric radiant heaters, irons, toasters, and hairdryers. These products have a considerably high possibility of ignition. To estimate the time per use for *kotatsu* and electric radiant heaters, the same numbers of usage days and hours as the above-mentioned kerosene space heaters were adopted. For both, the frequency of use per day was set to two, assuming their use in a living room. However, some electric radiant heaters are used in kitchens. For such cases, the number of cooking events per household each day (breakfast, lunch, and supper) was assumed to be three. For irons, toasters, and hairdryers, our risk assessment took into consideration the family composition, the frequency of use per day, and the time per use.

(5) Relays

Relays are divided into contact relays and non-contact relays. A contact relay has mechanical contacts from which sparks may be produced and therefore must be regarded as an ignition source. Conversely, a non-contact relay contains no

mechanical moving parts and consists mainly of semiconductors and other electronic parts, posing no possibility of spark generation. For safety's sake, our consideration here assumed the inclusion of contact relays in all electrical appliances.

Relays used for motor control or heater control pass a large amount of high electric energy. Hence, it is assumed that with such built-in controls, electrical appliances (air purifiers, dehumidifiers, vacuum cleaners, washing machines, hairdryers, electronic carpets, and rice cookers) might be a potential ignition source. Regarding frequency of use, assuming that an air purifier is used for six months per year and remains in operation all day once powered on, its relay is estimated to operate twice per day, once at power-ON and again at power-OFF. Dehumidifiers are presumably used four months per year from April until July, and their relays are estimated to operate twice per day, as for air purifiers. Likewise, assuming that a vacuum cleaner remains powered on until one whole room has been vacuum-cleaned, its relay is estimated to operate twice per use, once at power-ON and one more time at power-OFF. For washing machines, the frequency of operation for their motor and water supply valve was considered. For hairdryers, electric carpet, and rice cookers, in the same way, their frequency of use was factored in.

(6) Plugging in and unplugging

Some electrical appliances basically remain plugged in, and others are unplugged after each use. If its use requires plugging in and unplugging, an appliance may be a possible ignition source due to sparks from plugging in and unplugging. Appliances are plugged in and unplugged with the power ON sometimes. Others retain some current even with the switched OFF condition. These appliances must be carefully examined one by one. These points are under investigation and this study is to be continued.

(7) Wall-mounted switches for lighting

Wall-mounted switches for lighting are supposed to produce spark energy exceeding the minimum ignition energy when switched from ON to OFF. Hence, these switches were considered to be a potential ignition source. These switches are presumably operated twice per day in everyday life, with a discharge duration of 5 ms. Incidentally, a small number of lights are still operated with a string instead of a wall-mounted switch. Our risk assessment assumed that string-operated lights account for 20% of the whole number.

6.4.5 Summary of potential ignition sources

Table 6-2 shows the potential indoor ignition sources identified as a result of our consideration of open flames, high-temperature surfaces, and sparks. These items are a potential ignition source for R290 refrigerant. Their chance of encountering a flammable region must be elucidated for them to be definitively identified as ignition sources. What follows presents our consideration of the height of presence of ignition sources.

Table 6-2 Potential indoor ignition sources

Ignition source types		Potential ignition sources
Open flames		Cigarettes during smoking (including lighters), candles (for religious events and aromatherapy)
		Kerosene space heaters, gas cooktops, portable butane stoves
High-temperature surfaces		Electric radiant heaters
Sparks	Charges	Static electricity, laser printers
	Brush motors	Electric shavers, printers
	Thermostats	Kotatsu (tables with electric feet warmers), electric radiant heaters, irons, toasters, hairdryers
	Relays	Air purifiers, dehumidifiers, vacuum cleaners, dryers, electric carpets, rice cookers, microwave ovens
	Others	Plugging in/unplugging of power plugs, ON/OFF of lighting switches

6.4.6 Ignition-source heights

Ignition sources are divided into those that are hand held, such as cigarettes or hairdryers, and those placed on a floor or a mounting platform, such as combustion room heaters or household cooking appliances. We estimated the height of presence of ignition sources of the former type using the average body size of the Japanese population. For ignition sources

of the latter type, we estimated this parameter using the height of the mounting platform.

(1) Height of presence of ignition sources for hand-held use

Examples of ignition sources for hand-held use include cigarettes, electric shavers, and hairdryers. These ignition sources can be used both in a standing position and sitting position. Because the difference in the height of ignition sources between the two positions, both height conditions were considered.

Cigarettes or electric shavers are used near the mouth or the chin. The usage position for hairdryers is assumed to be approximately 10 cm above the top of the head. The following statistical data was used to derive the estimated height of presence of ignition sources: Ministry of Health, Labour and Welfare (2019) for the average heights of the Japanese population; Ministry of Education, Culture, Sports, Science and Technology (2016) for the sitting heights; and the numerical data stored in the human body dimensions database (National Institute of Advanced Industrial Science and Technology (2001) and Research Institute of Human Engineering for Quality Life (2001)) for shoulder heights and the other physical dimensions. The estimation results thus obtained of the height of presence of ignition sources are shown in Table 6-3.

(2) Height of presence of other ignition sources

(2.1) Gas cooktops and portable butane stoves

Table 6-3 Height of potential indoor ignition sources.

Ignition source	Position of use	Standing position	Sit-down position
Cigarettes	Around the mouth	About 155 cm	About 65 cm
Electric shavers			
Hairdryers	Between shoulders and 10 cm above the top of head	About 180 cm	About 55 cm

A typical kitchen worktop is positioned at a height of 80 to 90 cm. A typical gas cooktop is operated at a height similar to that for the kitchen worktop. Portable butane stoves are used not only in the kitchen but on a *kotatsu* tabletop in the living room, depending on the situation. When used in the kitchen, the height of presence of this ignition source is 80 to 90 cm, as with a gas cooktop. For its usage height in the living room, 35 cm was taken as a conservative estimate of the height of a *kotatsu* because a typical *kotatsu* has a tabletop height of approximately 37 to 60 cm. Additionally, assuming that the stove itself is approximately 5 cm high, the flame height of a portable butane stove is estimated to be 40 cm above the floor level.



Fig. 6-5 Configuration of floor-standing and shelf-top type household Buddhist altars

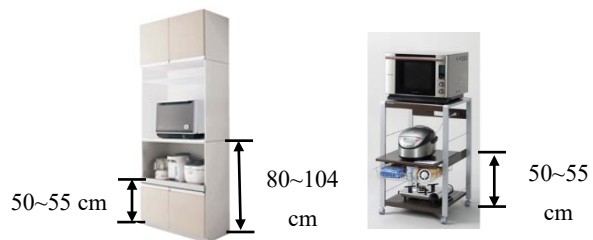


Fig. 6-6 Kitchen cabinet and dedicated racks

(2.2) Kerosene space heaters

A typical kerosene space heater has an open flame-equivalent heat chamber and a spark-generating ignition device, both of which can be said to be positioned at a height of approximately 20 to 35 cm.

(2.3) Candles for household Buddhist altars and aromatherapy

Candlesticks on a household floor-standing type Buddhist altar are placed on the bottom part of the altar's upper stand, as shown in Fig. 6-5. They are positioned at an estimated height ranging from 50 to 100 cm above floor level. Some household Buddhist altars are of the shelf top type and generally placed on the top of a household Buddhist altar chest or a household Buddhist altar cabinet, both approximately 44 to 100 cm high. Then, assuming that candles are held approximately 30 cm from the bottom of the shelf-top type household Buddhist altar, their estimated height falls in the range of 74 to 130 cm. In many cases, aroma candles are placed on a bedside table or the inner side of a bay window. The estimated heights of these locations are approximately 40 to 50 cm and 70 cm, respectively.

Table 6-4 Heights of ignition sources

Ignition source types		Potential ignition sources	Heights of ignition sources	Remarks
Open flames		Cigarettes	155 cm/65 cm	In the state of standing/ being seated
		Candles for religious events	74–130 cm	
		Aroma candles	40–50 cm/70 cm	Bedside/bay window
		Kerosene space heaters	20–35 cm	
		Gas cooktops	80–90 cm	
		Portable butane stoves	80–90 cm/40 cm	Used in the kitchen/ living room
High-temperature surfaces		Electric radiant heaters	30 cm or less	
Sparks	Charges	Doorknobs (Static electricity)	90–130 cm	
		Laser printers	74–150 cm	
	Brush motors	Electric shavers	155 cm/65 cm	
	Thermostats	Kotatsu (tables with electric foot warmers), electric radiant heaters, irons	30 cm or less	
		Toasters	80–104 cm	
		Hairdryers	180 cm/55 cm	In the state of standing/ being seated
	Relays	Air purifiers, dehumidifiers, vacuum cleaners, electric carpets	30 cm or less	
		Microwave ovens	80–104 cm	
		Rice cookers	50–100 cm	
	Other	Plugging in/unplugging of power plugs	25 cm or less	
ON/OFF of lighting switches		110–120 cm		

(2.4) Sparks

Household cooking appliances, such as microwave ovens, rice cookers, and toasters, are usually placed on a kitchen cabinet or a dedicated rack. Fig. 6-6 shows a typical kitchen cabinet and a typical dedicated rack. In general, microwave ovens or toasters are placed on a kitchen cabinet or an upper shelf of a kitchen rack. Meanwhile, rice cookers are usually stored on a sliding shelf in the lower part of the kitchen cabinet or the kitchen rack. Additionally, in single-person households, it is also likely that toasters or rice cookers are placed on the top of a small refrigerator of approximately 100 cm in height. Based on these findings from our survey on commercially available products, the estimated installation heights for household cooking appliances are as follows: 80 to 104 cm for microwave ovens and toasters and 50 to 100 cm for rice cookers. The doorknob height assumed here is 90 to 130 cm, with the average height of the Japanese male population (170 cm) and workability taken into consideration. Household-use printers are generally placed on a desk (80 to 85 cm), the upper shelf of a personal computer rack (140 to 150 cm), or a dedicated rack (74 to 95 cm). Hence, the assumed installed height here for printers is 74 to 150 cm. Power plug sockets are provided at a height of approximately 25 cm. Those at the end of an extension cord are used near the floor surface, depending on the situation. For wall-mounted switches, an installed height of 110 to 120 cm above floor level is recommended as ergonomically best suited for easy operation. Accordingly, the installed height assumed here for wall-mounted switches is 110 to 120 cm.

(3) Summary of the height of presence of ignition sources

Table 6-4 on the preceding page shows the results of our consideration of the height of presence for each ignition source type. Although not taken up in Subsection 6.4.6, appliances such as electric radiant heaters, electric *kotatsu* tables, irons, air purifiers, dehumidifiers, vacuum cleaners, and electronic carpets are used at near-floor height, whereby we estimated their heights of presence to be equivalent to the height of a typical *kotatsu* tabletop on which a portable butane stove is used, as explained in 6.4.6-(2.1).

6.4.7 Indoor flammable region due to refrigerant leakage

It is necessary to determine the flammable region formed due to refrigerant leakage to identify ignition sources. Hence, CFD analysis was used to obtain the height of presence of the flammable region due to refrigerant leakage. Before

performing the leakage simulation, we first determined the floor area and the refrigerant charge amount.

The floor area of a room with 4.5 *tatami* floor mats (7.0 m²), a room size still adopted for nearly half of the dwellings built by the Urban Development Corporation, was used for the simulation. According to Eq. (6-11), an R290 refrigerant amount of 200 g is equivalent to the maximum refrigerant amount that requires no safety measures for the floor area of 7.0 m² under the IEC Standard (IEC 60335-2-40:2018). Additionally, assuming that the current HFC refrigerant amount for residential air conditioners is 1000 g and that the R290 refrigerant amount expected to provide equivalent performance is 500 g, another leakage simulation was conducted for this amount of R290 with a floor area of 11.8 m², which was derived using Eq. (6-12) on the premise of mandatory indoor air circulation safety measures for the floor area involved.

$$m_{\max} \leq 2.5 \times LFL^{5/4} \times h_0 \times A^{1/2} \quad (6-11)$$

$$m_{\max} \leq 0.5 \times H \times A \times LFL \quad (6-12)$$

The spatial model analyzed is shown in Fig. 6-7. Calculations for two conditions were performed: one with the air conditioner stopped (without indoor air circulation) and another with the air conditioner operating (with indoor air circulation). The refrigerant leakage rate assumed for each refrigerant amount was for full-amount leakage within 4 min. The circulated air flow rate during operation was calculated according to Eq. (6-13), which was proposed by Colbourne et al. ⁶⁻¹² Eqs. (6-11) and (6-12) take into consideration the content to be adopted for the draft of the 7th edition of IEC60335-2-40. The assumption here is that the refrigerant leaks horizontally from the indoor unit at a uniform flow velocity of approximately 1 m/s (for the refrigerant amount of 200 g) and approximately 2 m/s (for the refrigerant amount of 500 g).

$$Q = \frac{8Y\sqrt{A_0}}{240} \left(\frac{m_C}{LFL}\right)^{3/4} \left(\frac{F^{1/4}}{1-F}\right) \quad (6-13)$$

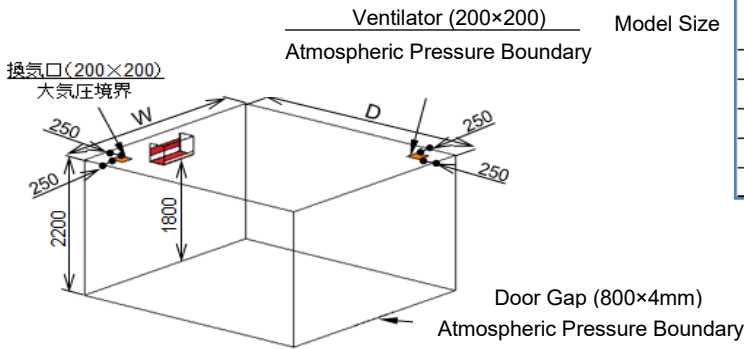


Fig. 6-7 Analyzed spatial model

		Refrigerant Amount	
		200g	500g
W	m	2.5	3.3
D	m	2.8	3.6
H	m	2.2	2.2
Installation Height	m	1.8	1.8
Floor Area	m ²	7.00	11.88

Table 6-5 Flammable gas height

	Heights of flammable gas	
	Refrigerant 200 g	Refrigerant 500 g
Operating	1.705 m	1.510 m
Stopped	0.008 m	0.326 m

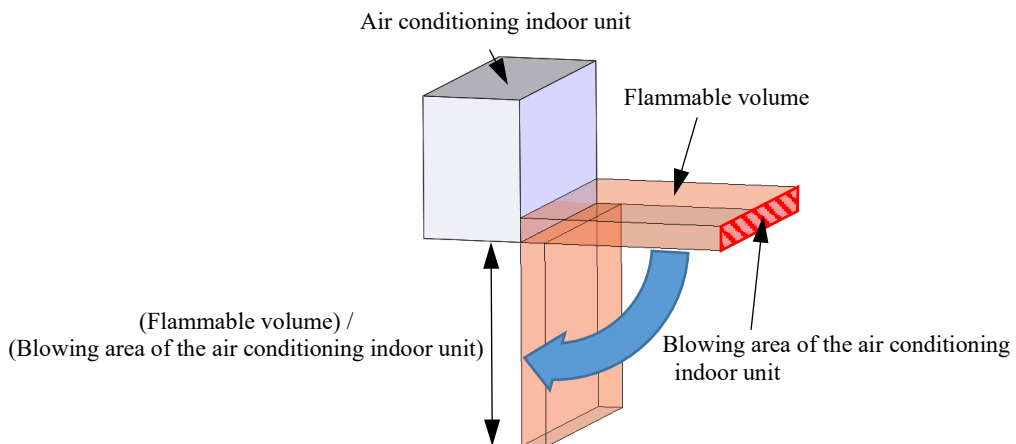


Fig. 6-8 Height of presence of the flammable region during air conditioning operation.

From the calculated results, the estimated heights of presence of the flammable region are presented in Table 6-5. “Operating” values indicate that a flammable region exists in the range between the installed height of the wall-mounted indoor unit (1.8 m) and the numerical values in the table, whereas the “stopped” values indicate the heights up to which a flammable region extends from the floor surface. During operation, the refrigerant leaking from the indoor unit moves with the blown air. Therefore, as shown in Fig. 6-8, the value of the flammable volume divided by the air outlet area of the indoor unit corresponds to the length along which the flammable region exists. Here, it must also be taken into consideration that the air outlet is oriented downward, e.g., during space heating operation. The chance of an encounter

with an ignition source becomes more challenging with the air outlet oriented downward. Accordingly, the above-mentioned length was reoriented to downward and this length was subtracted from the installed height of the wall-mounted indoor unit (1.8 m) to obtain the numerical values shown in Table 6-5. Fig. 6-9 shows the refrigerant concentration distribution at the end of leakage (4 min elapsed). For both the refrigerant amounts of 200 g and 500 g, flammable region exists only near the indoor unit’s air outlet during the air conditioner’s operation, as can be seen from the concentration distribution. Note that because the results shown here are for space cooling operation, flammable region exists to the front of the indoor unit’s air outlet. Conversely, as shown in Fig. 6-9, with the air conditioner stopped, the refrigerant leaks from the indoor unit to immediately thereunder, thereby forming a flammable region layered from the floor upward. Therefore, the value of the flammable region volume divided by the floor area is the height of presence of the flammable region from the floor surface. It must be borne in mind that the refrigerant amount of 500 g is 2.5 times greater than the refrigerant amount of 200 g, whereby the spreadability of the flammable region increases by the power law, and the severity of an explosion from ignition increases exponentially relative to the ratio of increase in the charge amount.⁶⁻¹³⁾

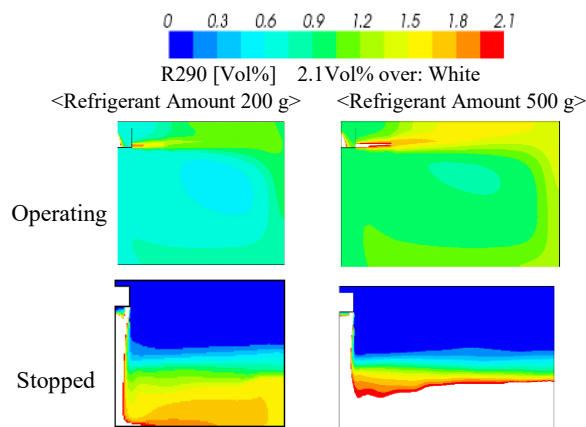


Fig. 6-9 Refrigerant concentration distribution after 4 min.

6.4.8 Identification of ignition sources

Ignition does not occur until an ignition source comes into contact with a flammable region. Hence, ignition sources were identified by checking one by one the positional relationships between the flammable regions obtained by CFD analysis (Table 6-6) and the presumed height of presence of ignition sources arising from our examination. As shown in Fig. 6-9, with the air conditioner stopped, a flammable region forming immediately below the air conditioner must be taken into consideration. Accordingly, we adopted 10% as an assumed probability of an ignition source used immediately below the indoor unit. Table 6-6 shows the ignition sources finally identified as the results of the above.

6.4.9 Summary of indoor ignition sources

A summary of the background and considerations leading up to the identification of ignition sources were compiled for the ignition sources considered in the risk assessment of A3 refrigerants currently undertaken by the JRAIA. Everyday usage situations for each individual ignition source were factored in to estimate ignition-source heights. The height of presence of flammable regions was quantified under the condition of full-amount leakage within 4 min. As a result, we identified the following potential ignition sources by considering their height of presence: from among open flames, cigarettes and kerosene space heaters; from among high-temperature surfaces, electric radiant heaters; from among sparks, laser printers, electric shavers, electric *kotatsu*, electric radiant heaters, irons, hairdryers, air purifiers, dehumidifiers, vacuum cleaners, electronic floor mats, and plugging in and unplugging. Conversely, examples found not to pose a risk as an ignition source by considering their height of presence include candles, cooktops, cooking appliances, static electricity generated from doorknob touching, and light switch ON/OFF operations. However, candles, cooking appliances, and light switches are deemed ignition sources because they may exist immediately below the indoor unit. Hereafter, we will examine the measure for the ignition risk sources, taking the results of the research by NEDO into consideration.

Table 6-6 Identification of ignition sources

Ignition Source types	Potential ignition sources	Heights of ignition sources		Height of flammable gas (during operation/stop)		Ignition or no ignition (during operation/stop)	
				Refrigerant 200 g	Refrigerant 500 g	Refrigerant 200 g	Refrigerant 500 g
Open flames	Cigarettes	155 cm	Standing	1.705 m /0.008 m	1.510 m /0.326 m	No/Yes*	Yes/Yes*
		65 cm	Seated			No/Yes*	No/Yes*
	Candles for religious events	74–130 cm				No/Yes*	No/Yes*
	Aroma candles	40–50 cm	Bedside			No/Yes*	No/Yes*
		70 cm	Bay window			No/Yes*	No/Yes*
	Kerosene space heaters	20–35 cm				No/No	No/Yes
	Gas cooktops	80–90 cm				No/No	No/No
	Portable butane stoves	80–90 cm	Kitchen			No/No	No/No
40 cm		Living room	No/No	No/No			
High-temperature surfaces	Electric radiant heaters	30 cm or less		No/No	No/Yes		
Sparks	Charges	Doorknobs (Static electricity)	90–130 cm		No/No	No/No	
		Laser printers	74–150 cm		No/No	No/Yes	
	Brush motors	Electric shavers	155 cm	Standing	No/Yes*	Yes/Yes*	
			65 cm	Seated	No/Yes*	No/Yes*	
	Thermostats	Kotatsu (tables with electric foot warmers), electric radiant heaters, irons	30 cm or less		No/No	No/Yes	
		Toasters	80–104 cm		No/Yes*	No/Yes*	
		Hairdryers	180 cm	Standing	No/Yes*	Yes/Yes*	
	55 cm		Seated	No/Yes*	No/Yes*		
	Relays	Air purifiers, dehumidifiers, vacuum cleaners, electric carpets	30 cm or less		No/No	No/Yes	
		Microwave ovens	80–104 cm		No/Yes*	No/Yes*	
		Rice cookers	50–100 cm		No/Yes*	No/Yes*	
	Others	Plugging in/unplugging of power plugs	25 cm or less		No/No	No/Yes	
		ON/OFF of lighting switches	110–120 cm		No/Yes*	No/Yes*	

Yes*. If the ignition source is directly under the air conditioner, it is considered to be ignited.

6.5 Simulation of outdoor refrigerant leak

6.5.1 Installation condition of outdoor unit

There are two main types of housing in Japan: detached house and apartment. In the former, an outdoor unit is usually installed on a balcony, on the ground, on an outer wall surface, or on the roof. In the latter, an outdoor unit is usually installed on a balcony, in a common corridor, or at a dedicated installation place. Among these outdoor unit installations, it is in floor-mounted installations on ill-ventilated balconies surrounded by walls that leaked refrigerant is most easily accumulated. They are rarely seen in high-rise apartments, but considering the worst-case scenario, a balcony with such features was selected as the installation environment for outdoor units

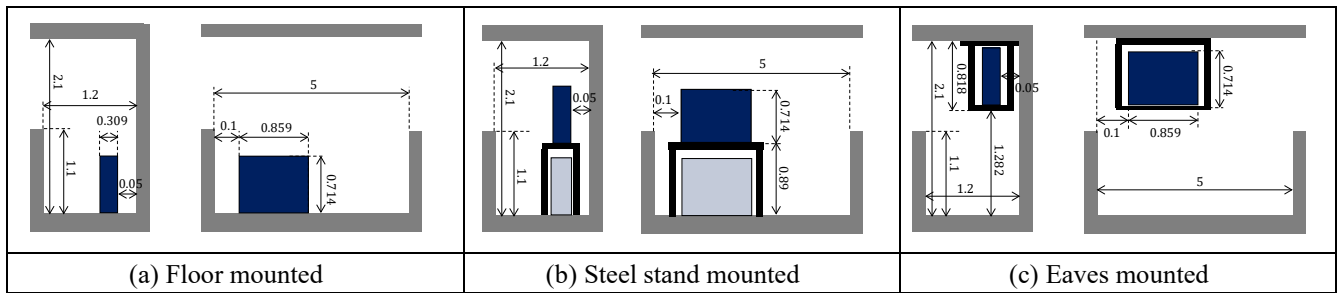


Fig. 6-10 Three installation conditions of an outdoor unit on a balcony

Fig. 6-10 shows typical installation patterns of an outdoor unit on the balcony. Considering the worst-case, a drainage hole was not provided with the balcony in our simulations. The outdoor unit is with the cooling capacity of 4.0 kW. As an installation pattern, the floor-mounted, the steel stand-mounted, and the eaves-mounted were considered.

6.5.2 Simulation of outdoor refrigerant leakage

(1) Analysis model and leakage condition

Table 6-7 shows the leakage conditions of R290. The leakage amount of 200 g is the maximum allowable amount stipulated by IEC Standards for an indoor floor area of 7 m². The leakage amount of 500 g is the estimated refrigerant amount that can achieve the performance equivalent to a 4.0kW R410A air conditioner, and 1000 g corresponds to m₂ of R290 in IEC Standards. The whole amount of refrigerant for each condition was assumed to leak in 4 min, as adopted in IEC standards. In our simulations, refrigerant leaked during stoppage of equipment was assumed to flow evenly through the air suction surface of its outdoor heat exchanger into the balcony. The concentration of R290 was set to 100 vol% as the boundary condition.

Table 6-7 R290 leakage conditions

Leakage amount	g	200	500	1000
Leak rate	kg/s	8.3×10^{-4}	2.1×10^{-3}	4.2×10^{-3}
R290 density (25 °C)	kg/m ³	1.832		
Leakage area	m ²	0.834		
Leakage concentration	vol%	100		

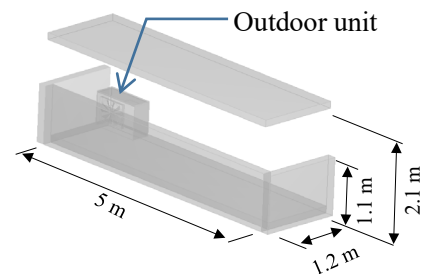


Fig. 6-11 CFD model of balcony.

Fig. 6-11 shows our CFD model. To simulate leaked refrigerant dispersion, the three-dimensional CFD analysis of mixed fluid consisting of air and R290 was performed using three equations for conservation of mass, momentum, and chemical species. Because the temperatures of the air-R290 mixture were fixed at 25 °C, no energy conservation equation was used. To consider the density change due to the mixing of air and R290, compressible fluid CFD simulations were carried out. Furthermore, a turbulent flow model using the standard k-ε model was used in consideration of the Reynolds number, which was calculated from the leak rates of R290, its free fall speeds, its kinematic viscosity coefficient, and the distance between the outdoor heat exchanger and the wall of the balcony.

(2) Flammable region for each installation

Fig. 6-12 shows our simulation results. When a refrigerant amount of 1000 g leaked from a floor-mounted outdoor unit, the duration of the flammable region reached 3546 s. For each of the leakage amounts, the duration of flammable region decreased as the installation height increased. The floor-mounted installation made little difference on the time-averaged flammable volume between the leaked refrigerant amounts of 1000 g and 500 g. This may be due to the fact that regions with concentrations above the UFL of R290 formed in the vicinity of the floor. The minimum air flow rate of the outdoor unit fan could not entirely prevent the flammable region from occurring for the leaked refrigerant amount of 1000 g.

Installation Condition	Leakage Amount	200 g		500 g		1000 g	
		Time	Time	Time	Time	Time	Time
Floor mounted	Concentration distribution						
	Duration	776 s		1900 s		3546 s	
	Averaged volume	1.22 m ³		2.96 m ³		2.73 m ³	
Steel stand mounted	Concentration distribution						
	Duration	292 s		1206 s		2126 s	
	Averaged volume	0.20 m ³		2.83 m ³		3.87 m ³	
Eaves mounted	Concentration distribution						
	Duration	260 s		939 s		1711 s	
	Averaged volume	0.05 m ³		2.47 m ³		3.73 m ³	

Fig. 6-12 Concentration distribution, duration, and time averaged volume of the flammable region within the balcony for different installation conditions.

(3) Effect of gap

Fig. 6-13 shows the layout of a typical apartment balcony in Japan. A partition plate is used when the two balconies are directly adjacent to each other. There is a gap between the partition and the floor, and the partition can be broken by kicking to secure an evacuation route. From our investigation, the height of the gap was set to 0.1 m.

Fig. 6-14 shows the simulation results for the concentration distribution of R290, the duration of the flammable region, and the time-averaged volume for each condition. The duration of the flammable region for the leakage amount of 1000 g was 1211 s, which was almost one third the duration (3546 s) for the situation without the gaps (Fig. 6-12). This indicates that the gap under the partition reduced the duration of the flammable region and its time-averaged volume in the balcony where the outdoor unit is installed. In other words, the leaked refrigerant flowed through the gap under the partition plate into the adjacent balcony.

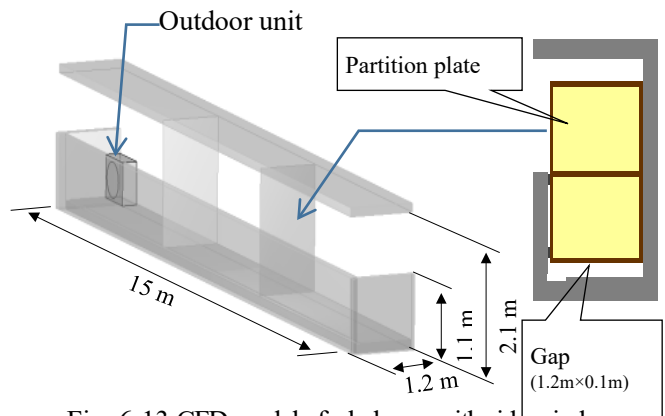


Fig. 6-13 CFD model of a balcony with side wind.

Although the refrigerant leakage amount of 200 g generated a tiny flammable region with a short duration and small time-averaged volume in the adjacent balcony, the two other leakage amounts formed a flammable region in a farther balcony: the one next to the adjacent balcony.

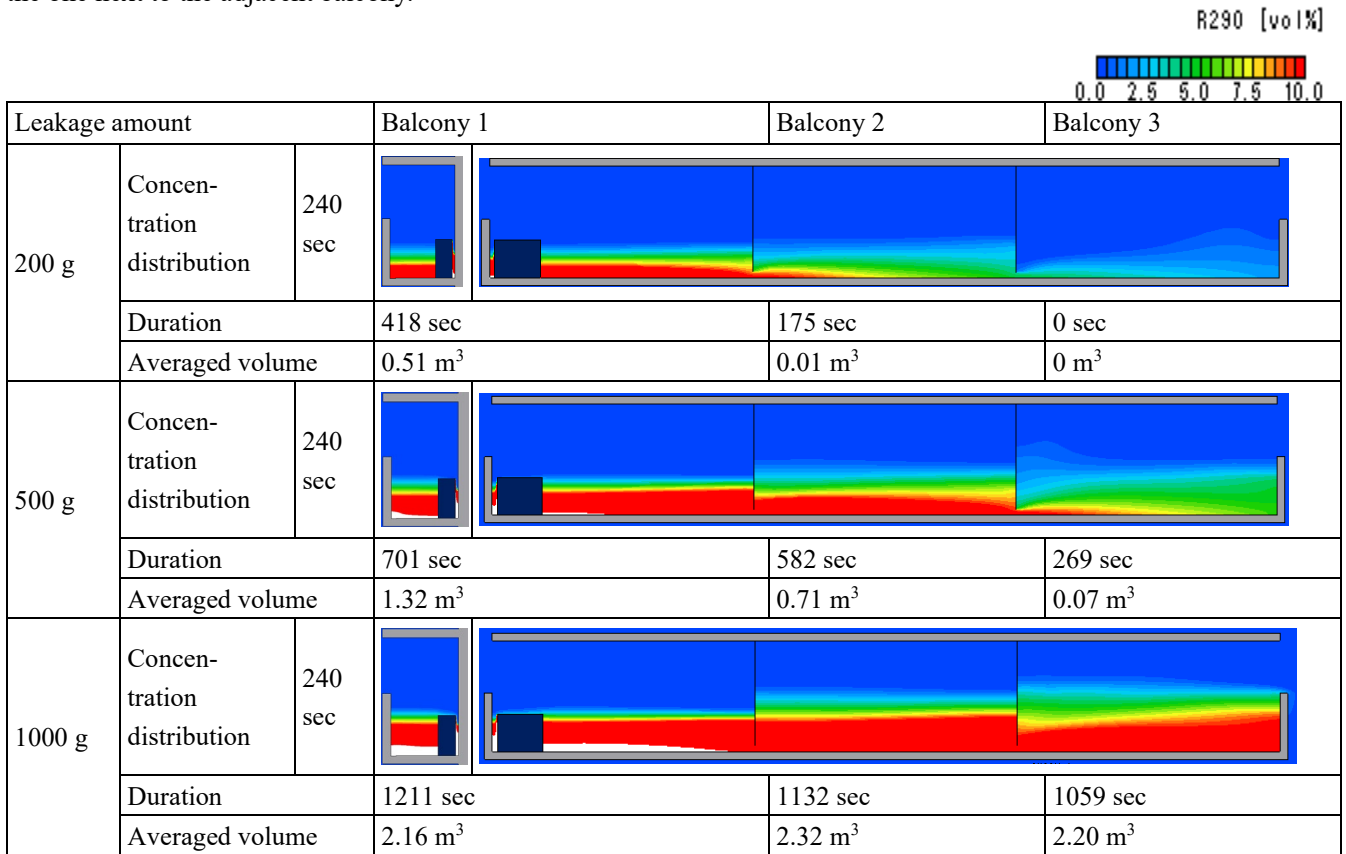


Fig. 6-14 Concentration distribution, duration, and time averaged volume of flammable regions within each balcony with partition plates.

(4) Effect of natural wind

Outdoor units are usually exposed to natural wind. Fig. 6-15 shows the relationship between the velocity of natural wind and its annual cumulative occurrence in hours in some major cities of Japan. Although there are some differences between cities, natural wind blows most frequently at velocities between 1.0 m/s and 2.0 m/s. These data also indicate that the probability of windless weather is 0.5 %. Therefore, the probability of natural wind blowing is 99.5 % during the year. This means that it is important to consider balcony environments with natural wind in refrigerant leakage simulations. By incorporating the frequency probability of wind velocity, the weight-averaged ignition probability decreased to approximately 1/100 of the ignition probabilities under no natural wind for the refrigerant leakage amounts of 500 g and 1000 g.

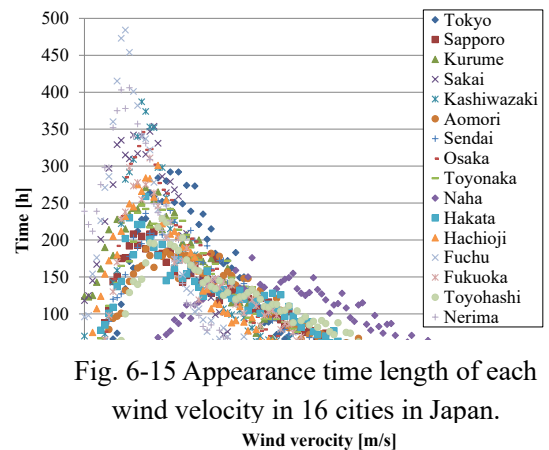


Fig. 6-15 Appearance time length of each wind velocity in 16 cities in Japan.

(5) Effect of analysis model

The turbulence model described above was selected, considering the leak rates of R290 and its velocities near the floor in free fall during refrigerant leakage. In windless weather, however, the turbulence in the balcony disappears sometime after the end of the leakage and then the flow state reverts to a laminar state. Therefore, CFD simulations using a laminar flow model was performed for the refrigerant leakage amount of 500 g in the floor-mounted installation on the balcony without any gap. The results showed that the flammable region lingered for a very long time. The duration of the flammable region using the turbulence model was 1900 s, whereas the duration using the laminar flow model was as long as 60,740 s (16 hours, 52 minutes, and 20 seconds). This is due to the difference in the diffusion coefficient. The turbulent diffusion coefficient is intrinsically at least one to two orders of magnitude larger than the

molecular diffusion coefficient. Although it is almost impossible that balcony airflows remain laminar for a long time, this significant difference should be contemplated with the utmost care.

6.5.3 Outdoor ignition sources

Table 6-8 shows various potential ignition sources and their duration and heights in outdoor installations. Smoking by users, the open flames of gas/oil water heaters, and electric spark generated by switching ON/OFF another outdoor unit were considered as potential ignition sources. Static electricity was excluded because it is mainly generated by undressing of clothes and contact of the human body with a metal doorknob and consequently rarely occurs outdoors. The height and duration of each ignition source were determined by considering its actual usage and its operating principle. On the other hand, some Japanese researchers contend that electric sparks by switching ON/OFF as well as smoking by users are not ignition sources of R290. In addition, ordinary gas/oil appliances, including water heaters, can be estimated not to cause the ignition of leaked refrigerants because their combustion fans operate before ignition sources activate. It is necessary to obtain ignition probability by constituting an FTA tree that reflects these advances in our understanding as to sources of ignition.

Table 6-8 Typical duration and location height of each ignition source

Name	Ignition sources	Duration T_s (sec)	Height h_s (m)
Smoking by users	Open flame	4.5×10^1	≤ 1.72
Gas/oil water heater (stationary type)	Open flame	3.0×10^2	≤ 0.6
Outdoor unit of AC	Electric spark	5.0×10^{-3}	≤ 0.714
Static electricity	Electrostatic spark	1.0×10^{-6}	-

6.5.4 Study results of outdoor unit risk from refrigerant leakage simulations

The following conclusions were obtained from the refrigerant leakage simulations and their related risk assessment:

- i. Among outdoor unit installations, it is in floor-mounted installations on ill-ventilated balconies surrounded by walls that leaked refrigerant is most easily accumulated, which can be viewed as the worst-case for high-rise apartments.
- ii. Higher installations, such as steel stand-mounted and eaves-mounted, on a balcony led to shorter durations of the flammable region. However, the time-averaged volume of the flammable region did not always decrease. This can be linked to the formation of a region with concentrations above the UFL of R290 near the floor. When there was a gap under a partition plate between adjacent balconies, the duration and volume of the flammable region decreased in the balcony where an outdoor unit is installed. If the leaked refrigerant amount is large, another flammable region can form in the adjacent balcony and even in a farther balcony (next to the adjacent balcony).
- iii. Our investigation shows that the probability of natural wind blowing in balconies during the year is 99.5 %. Natural wind considerations make the ignition probability of R290 decrease to 1/100 of that in windless weather.
- iv. Installation heights greater than floor level, appropriate gaps between walls and the floor, and natural wind are factors that can reduce the ignition risk of R290.
- v. Potential outdoor ignition sources in Japan are smoking, gas/oil appliances, and outdoor units of air conditioners using non-flammable refrigerants. Considering that the risk of ignition caused by these ignition sources is almost tolerable, attaching warning labels to outdoor units for the benefit of product users is a practical safety measure. However, since it is a measure based on risk assessment that is only applicable to the Japanese market, different safety measures should be formulated in other countries, especially ones where a lot of outdoor ignition sources exist.

6.5.5 Possible safety measures for outdoor unit

Our risk assessment results have underlined the need for installation heights greater than floor level, appropriate gaps between walls and the floor, and natural wind in order to reduce the ignition risk of R290. Although most outdoor unit installations satisfy these constraints, the assumption that all installation conditions satisfy them is unrealistic.

For air conditioners using flammable refrigerants, the IEC 60335-2-40 stipulates that warning labels with flame symbols

should be attached to their outdoor units and that flammability-related precautions should be described in their operation manuals. The former is intended for service personnel, while the latter is targeted at product users. Product users cannot, however, be expected to look through the precautions in order to merely operate their air conditioners. On the other hand, our risk assessment reveals that the ignition risk that might ensue is almost tolerable. As a result, attaching warning labels that are instantly recognizable to product users is the most practical safety measure.

6.6 Consideration and proposal for events beyond the assumptions of the risk assessment

6.6.1 Beyond the assumptions in the risk assessment

This risk assessment, including calculations of ignition probability at each stage, is based on authorized “work and process.” Therefore, “work and process other than authorized ones are not considered” and are handled as beyond the scope of assumption.

i. Disposal and recovery

A typical example of an event beyond the scope of assumption is the recovery of refrigerants from a household air conditioner that is handled via unauthorized ways at the time of the disposal. According to the press release from the Ministry of Economy, Trade and Industry (METI) and the Ministry of Environment of Japan, the rate of recovery via the authorized ways stipulated in the Home Appliance Recycling Law and Waste Disposal Law is only 35.4%. Therefore, most refrigerants (more than 60% of air conditioners) are recovered via unauthorized ways, possibly to recover valuable metals, such as iron, copper, and aluminum. Thus, whether refrigerants are recovered and treated is unclear.

When performing scrap metal treatment while trying to recover the valuable metals in air conditioners, the possibility of an increase in ignition accidents cannot be refuted in the case of higher flammable (A3) refrigerants if the refrigerant is emitted to the atmosphere to avoid high treatment costs. In addition, when waste material recovery companies treat air conditioners and perform scrap metal treatment for recycling in towns in Japan, the same risk arises.

Even if unauthorized waste material recovery companies are registered as secondhand goods dealers, the scrap metal treatment is illegal when they have no license, as required by the Waste Disposal Law. The Home Appliance Recycling Law stipulates that the recycling rate of valuables, obtained by recycling the iron, copper, aluminum, plastics, etc. of scrapped air conditioners, should be 80 % or more. In addition, the law also stipulates that the recovery and the proper treatment of refrigerants are mandatory. Manufacturers should ensure that they fulfil their duty to achieve the recycling ratio, including DfE (Design for Environment), and collaborate with recycling plants.

The metal (iron, copper, and aluminum) composition in air conditioners is approximately 70%. It is much higher than that of other products (refrigerators, televisions, and washing machines). This high value is a significant factor to which operators in unauthorized ways pay attention and are probably working on.

In contrast, the recycling rate in authorized ways is much higher with other home appliance that includes copper and aluminum heat exchangers, such as heat pumps, washing and drying machines, and bathroom dehumidifiers. It is considered that the operators in unauthorized ways are not tempted by the low weight ratio of copper and aluminum that can be easily recovered.

We examined the actual status and challenges at the time of refrigerant disposal and recovery above and highlighted the increase in ignition probability from the atmospheric emission of refrigerants via unauthorized routes. However, these matters were not considered in this risk assessment because of the difficulties related to quantification and process details. In other words, it is beyond the current assumption.

ii. Installation and repair

For this risk assessment, we assumed that workers received training (knowledge and techniques) on the installation and repair of air conditioners. However, in the case of a moving company relocating an air conditioner, such training is questionable. In those cases, workers may not have received sufficient training to perform these jobs. In some recent cases, we were informed that workers performed the installation of air conditioners without knowledge of flammable refrigerants or the installation, which resulted in failure of the units because of mistakes made with poor knowledge. Although such information is available, these matters were not considered in this risk assessment because the total number based on actual status has not been clarified. This is also beyond the assumption of the risk assessment.

Other than the above, we assumed that installation and repair are conducted by workers in a mentally normal and relaxed state in this risk assessment, as described by Hashimoto et al.⁶⁻¹⁴⁾ However, in reality the workers’ mental state is not always

normal and relaxed. For instance, they may feel hurried or stressed on busy hot summer days or when a work quota is imposed to increase sales. In this mental state, the error rate increases, leading to accidents. Since mental state is not easily identifiable, it is also assumed to be beyond the scope of assumption.

iii. Unassumed accident phenomena

Finally although it is needless to state, the arson and theft of an air conditioner outdoor unit, in use or otherwise, are also not assumed.

In the above, the unassumed items of this risk assessment were enumerated, and it can be easily imagined that these items will increase the actual ignition probability. However, it is very difficult to prepare precise FTA of these items, calculate their exact ignition probabilities, and quantify their risks.

6.6.2 Proposal for unassumed events in risk assessment

The unassumed cases explained in previous subclauses were also not considered in the risk assessments of air conditioners using the R32 (classification A2L) refrigerant by JRAIA. Nevertheless, ignition accidents have not been reported. There are two main reasons: First, R32 has far fewer ignition sources than A3 refrigerants because the former has a much higher minimum ignition energy. Second, the formation of a flammable region is quite unlikely because the LFL of R32 (13.5%) is very high. These factors make an ignition accident with R32 extremely unlikely to occur both in assumed and unassumed cases in the risk assessment as well as the in the market. In contrast, the R290 (classification A3) refrigerant has many types and numbers of ignition sources because of its low minimum ignition energy (1/80 of R32), and a flammable region can easily form because of its LFL is as low as 2.02 %. Furthermore, the burning velocity of R32 is so low, flashing cannot be observed in standard flash point tests. In contrast, propane does flash.

Therefore, concerning R290, it is necessary to study the unassumed risks of this risk assessment further and to eliminate the risks caused by such works and procedures.

Before commercializing R290 as a refrigerant, the following points are recommended and needed.

i. Enhancement or guarantee of the recovery and/or treatment scheme of air conditioner refrigerant

We recommend that consumers and companies dispose of air conditioners in a manner that further promotes social responsibility and is in accordance with the Home Appliance Recycling Law. We further recommend that authorities (government and industrial association) investigate and clarify the unauthorized ways of recycling and improve the situation by performing proper investigations if illegal actions are presumed. Considering the current social system, we recommend that disposal is performed through the home appliance recycling route to ensure recovery of refrigerants, and this route should be enforced. First, studies on infrastructure improvement for the recovery and treatment of refrigerants in air conditioners, including the home appliance recycling system, is necessary. In particular, ensuring the safety of a person who intervenes is essential in the case of A3 refrigerant. In the worst case, if the effect of the above-mentioned is not sufficient, the “study of a new social system” should be instigated.

ii. License system for workers who install and repair air conditioners

We consider that it necessary to study a new mechanism in which the industry association related to refrigeration and air conditioning develops a qualification system for workers handling flammable refrigerants, including seminars and practical training, or establishes a license system within a legal framework. In addition to the development of a qualification and/or license system, it is required to strengthen the punishment when a worker without qualification or license is involved in installation or services.

Although the above measures are to avoid any unsafe work and action that should be eliminated, risk assessment for labor safety and machinery safety requires that safety is ensured on the assumption that “humans always make mistakes” and “machinery failure always occurs”, as described in the international standard ISO 45001 and ISO 12100, as well as in JIS Z8115. In the case of adopting R290 as a refrigerant, it is necessary to return to this origin and consider measures that will not harm people even if an ignition accident occurs or consider measures so that an ignition concentration region will not form even if the refrigerant leaks.

To realize a better society for dealing with global warming, we should implement the above measures as well as various political proposals and innovate the social system in the middle-term period, which invariably requires alignment of viewpoints. Furthermore, returning to the original ideas of safety in studies may also be necessary. We consider that R290 may safely be used for air conditioners by reducing the unassumed events of this risk assessment to achieve an ignition probability below once per 100 years, which is the allowable level chosen by this WG.

6.7 Summary

The activities of the Mini-split Working Group in JRAIA started on July 2016. This report summarized the following items that were studied over three years (FY2018–2020) in collaboration with the NEDO project. Academic clarification concerning “calculation of the accident probability” was achieved. In addition, discussions were carried out about “indoor ignition sources” and “simulation of refrigerant leak outdoors,” which were made public. Furthermore, most of the measures described in each Subsection are still under study, but they are reported here as interim results, and their effectiveness are confirmed through FTA quantification and so on. Regarding the measures considered in this study, we will incorporate them to the JRAIA standard as needed. Moreover, we provide a new Subsection on “Consideration and proposal for events beyond the assumption of the risk assessment” that would be important while reviewing the risk assessment this time. Fundamentally, product risk assessment is performed for the purpose of investigating the magnitude of the risk when a company plans to manufacture a novel product and for the purpose of minimizing product risk in the stage of finally launching the product. However, this risk assessment of residential air conditioners using R290 as the refrigerant was implemented under the condition that no specific product exists, and thus the risk assessment is fundamentally one for the planning stage. Therefore, “Assumed and unassumed events in the risk assessment” and “Proposal” described in Subsection 6.6 are hereafter important. In addition, concerning “Security and safety” that is characteristic of Japanese people, we also described that correct risk communication is essential when we are going to use R290 refrigerant. Anyway, solutions for the global warming issue are urgently needed. We consider that refrigeration and air conditioning engineers should make the best effort to solve this problem based on their knowledge, experience, and inspiration, and that we industry should also accelerate collaborations with the government and academia.

References

- 6-1) ISO/IEC Guide 51 (2014).
- 6-2) Y. Okabe: “Probability and statistics – Model solution of sentence problem –,” Asakura Publishing, pp. 131-133, Tokyo (2010). (in Japanese)
- 6-3) W. Takakura: “Teaching material concerning geometric probability,” http://izumi-math.jp/W_Takakura/k_kakuritu/k_kakuritu.pdf. (in Japanese)
- 6-4) B. Li, H.R. Pang, J. Xing, B. Wang, C. Liu, K.G. McAdam, J.P. Xie: “Effect of reduced ignition propensity paper bands on cigarette burning temperatures”, *Thermochimica Acta*, 579, pp. 93–99, Amsterdam (2014).
- 6-5) T. Kashimura, S. Goto, A. Fushimi: “Ignition mechanism by cigarette”, Report of Fire Science Laboratory of Tokyo Fire Department, 7, pp. 34-45, Tokyo (1970). (in Japanese)
- 6-6) T. Nakayama, H. Nakada, M. Mochizuki, S. Toriya: “Study on the Ignition Properties of Various Types of Flammable Gas”, Report of Fire Technology and Safety Laboratory of Tokyo Fire Department, 53, pp. 86-94, Tokyo (2016). (in Japanese)
- 6-7) M. Kotani: “Actual state of ritual for deceased,” Life Design REPORT, Tokyo (2010). (in Japanese)
- 6-8) Japan Industrial Standard JIS S 2073: “Standard use conditions, standard acceleration mode and test conditions for domestic direct vent type oil burning space heater.” (in Japanese)
- 6-9) National Institute of Occupational Safety and Health, Japan Technical Guide: Technical Electricity Safety Guide 2007, published by National Institute of Occupational Safety and Health, Japan, p. 47, p.20, pp. 23-24, Tokyo (2007). (in Japanese)
- 6-10) A. Okukubo, T. Sakai: “Textile product consumption science,” Vol. 15, No. 10, Tokyo (1974). (in Japanese)
- 6-11) T. Yoshida, K. Kubota, T. Sawai, N. Matsui: “Time-Frequency Analysis of Discharge Current from Charged Human Body”, Journal of the Institute of Electrostatics Japan, Tokyo (2007).
- 6-12) D. Colbourne, K. O. Suen: “ASSESSMENT OF FACTORS AFFECTING R290 CONCENTRATIONS ARISING FROM LEAKS IN ROOM AIR CONDITIONERS”, Proc. 13th IIR Gustav Lorentzen Conference on Natural Refrigerants, 1103, Valencia (2018).
- 6-13) R. Tsuchihashi: “Journal of Combustion Society of Japan,” Vol. 56, No. 177, pp. 234-240, Tokyo (2014). (in Japanese)
- 6-14) K. Hashimoto: “Safety Ergonomics,” edited by Japan Industrial Safety & Health Association, Tokyo (1984) (in Japanese)

Chapter 7 Progress of risk assessment of refrigerated display cabinets using A3 refrigerant conducted by JRAIA

7.1 Introduction

Refrigerated display cabinets with a built-in condensing unit (built-in refrigerated display cabinet) are used in restaurants, food stores, supermarkets, and other venues. Although HFC refrigerants with a large GWP, such as R404A and R134a, are currently used, the shift to low GWP refrigerants is desired to prevent warming in response to the Kigali Amendment to the Montreal Protocol. The refrigerant amount in a built-in refrigerated display cabinet is ~10 g to more than 1 kg. Studies on A3 refrigerants (higher flammable refrigerant), including propane (R290, GWP: 3) and isobutane (R600a, GWP: 4), for built-in refrigerated display cabinets are mainly carried out in Europe because the cabinet is a hermetically sealed appliance and the refrigerant amount is comparatively small. Following this situation, International Standard IEC 60335-2-89⁷⁻¹⁾ was revised to Edition 3.0 on June 2019, and the maximum refrigerant charge of A3 refrigerant was relaxed from the conventional 0.15 kg to about 0.5 kg (in case of R290). However, the contents are not necessarily capable of sufficiently ensuring safety because the International Standard tends to prioritize usability and the timing of the revision this time cannot be postponed considering the state of refrigerant regulation in each country.

The Japan Refrigeration and Air Conditioning Industry Association (JRAIA) has been conducting evaluations of the safety of built-in refrigerated display cabinets using A3 refrigerants, such as R290, since July 2016. Refrigerant leak analyses assuming leakage from inside and outside the refrigerated space of the refrigerated display cabinet and risk assessments have been performed, and methods for the safe operation of display cabinets using A3 refrigerants have been studied. On the basis of these study results, JRAIA established JRA standards and performed activities to propose necessary deviations (amendments from the International Standard) to JIS C 9335-2-89, which is the Japanese Standard based on IEC 60335-2-89.

Here, we summarize the study results and the current state of the International Standard, the refrigerant leak analyses, the risk assessments, Japanese Standards and Japanese laws concerning built-in refrigerated display cabinet using A3 refrigerants, such as R290.

7.2 Main revision points of International Standard IEC60335-2-89

7.2.1 Maximum refrigerant charge

According to the conventional IEC Standard, the maximum charge of flammable refrigerants (A3 refrigerant, A2 refrigerant, and A2L refrigerant) in a refrigerant circuit was 0.15 kg (the upper limit). The IEC Standard after revision stipulated that the flammable refrigerant can be charged up to 13 times the LFL (lower flammability limit) or 1.2 kg, whichever is smaller. In the case of R290, since LFL is 0.038 kg/m³, the charge amount is up to 0.494 kg. However, in the case of R1234yf, an A2L refrigerant, since LFL is 0.289 kg/m³, 13 times LFL is 3.757 kg, but the maximum refrigerant charge is 1.2 kg because the upper limit of the refrigerant charge is limited.

7.2.2 Minimum room floor area

Relaxation of the maximum refrigerant charge makes it important to reduce the ignition risk at the time of flammable refrigerant leakage from the appliance for safety. Therefore, the Standard also stipulates that the installation of appliances using flammable refrigerants is limited to rooms not smaller than the minimum room floor area of A_{min} m², calculated using Eq. (7-1), and this value must be marked on the product. In Eq. (7-1), H is the ceiling height (2.2 m fixed value), 0.25 is a safety factor, LFL is LFL kg/m³ of the refrigerant used, and M is the refrigerant charge in kg. For example, in case of an appliance charged with 0.494 kg of R290, the appliance must be installed in a location with a floor area of 23.7 m² or more.

$$A_{min} = M / (H \times 0.25 \times LFL) \quad (7-1)$$

7.2.3 Refrigerant leak test

When 0.15 kg or more of the refrigerant is charged in the refrigerant circuit, it should be verified that no flammable

region is generated around the appliance by conducting a refrigerant leak test. At this time, leakage from the location producing the most unfavorable result shall be assumed. The refrigerant amount released during the test shall be equal to the refrigerant charge in the refrigerant circuit. The refrigerant leak rate w g/min is obtained using Eq. (7-2). For example, when the refrigerant is R290 and the refrigerant charge M is 0.494 kg, the mass flux q is 281 g/min/mm² (higher pressure side; 134 g/min/mm² for the lower pressure side), and the refrigerant leak rate w is 44.4 g/min (2.66 kg/h).

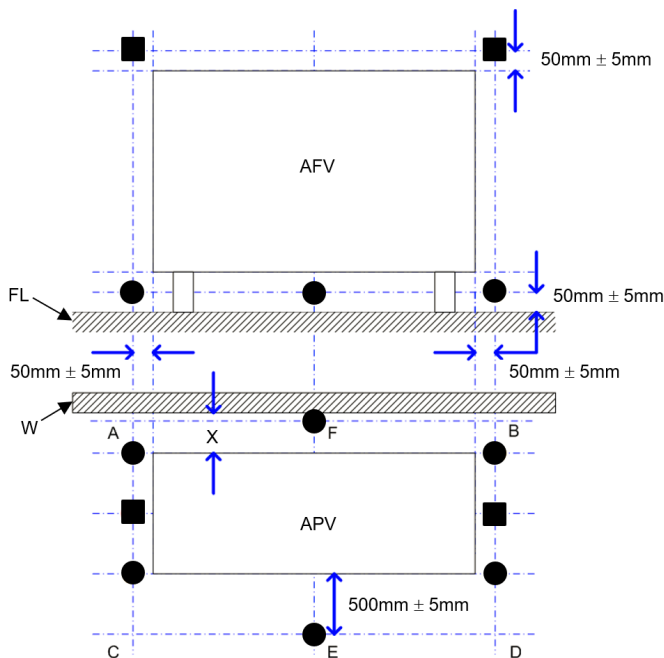


Fig. 7-1 Schematic illustration of the refrigerant concentration sampling points.¹⁾

For a reach-in refrigerated display cabinet, etc., the door or the lid shall be opened after leakage of the total refrigerant amount into the refrigerated space. The refrigerant concentration shall be measured with an interval of 5 s or less, and the duration of the test shall be twice or more the time required to release the total refrigerant amount (t_c min, Eq. (7-3)). The refrigerant concentration shall be measured at the points shown by black squares and black circles in Fig. 7-1, and 1/2 of LFL shall not be exceeded at all measuring points after 5 min from measurement start (that is to say, even if a large flammable cloud is generated within 5 min, it is regarded that no flammable region is generated).

$$w = q \times 0.32 \times M \times (476 / \rho) \tag{7-2}$$

$$t_c = 10^3 \times M / w \tag{7-3}$$

7.3 Refrigerant leak analysis

7.3.1 Leakage from the refrigerated space of a reach-in refrigerated display cabinet

(1) Analysis model

Analyses were performed assuming rapid opening of the door after refrigerant leakage into the refrigerated space of a reach-in refrigerated display cabinet. The analysis model is shown in Fig. 7-2. The external dimensions of the reach-in refrigerated display cabinet were 2.0 m in height, 1.542 m in width, 0.7 m in depth, and the refrigerated volume was 1.08 m³. A condensing unit consisting of a compressor, a condenser, and a fan was installed at the bottom of the display cabinet. The air was sucked in from the front, passed through the rear side, and exhausted from the top of the refrigerated display cabinet. The area of the air inlet opening of the condensing unit was 8.3×10^{-2} m² (1.206 m in width × 0.0689 m in height) and the air flow rate was varied from 0 to 0.249 m³/s (air velocity of 0 to 3 m/s). The refrigerated display cabinet was installed at the center of the wall in a store with a square-shaped floor, and pressure boundaries of 0.4 m × 0.4 m were defined at both corners of the ceiling on the opposite side of the refrigerated display cabinet. The analysis started from the state in which the refrigerant concentration equivalent to the total refrigerant amount was uniformly distributed inside the refrigerated space, and it was performed assuming no door. This analysis emulates the behavior in the refrigerated display cabinet with sliding doors. The air curtain flowing from the top to the bottom of the front of the refrigerated space had an

opening area of $6.59 \times 10^{-2} \text{ m}^2$ and an air flow rate of $0.137 \text{ m}^3/\text{s}$ (air velocity of 2.08 m/s), and the analysis was performed with and without the air curtain. The floor area inside the store was varied: 17.14 m^2 ($4.14 \text{ m} \times 4.14 \text{ m}$), 24.01 m^2 ($4.9 \text{ m} \times 4.9 \text{ m}$), 36.0 m^2 ($6.0 \text{ m} \times 6.0 \text{ m}$), 64.0 m^2 ($8.0 \text{ m} \times 8.0 \text{ m}$) and 100.0 m^2 ($10.0 \text{ m} \times 10.0 \text{ m}$). The refrigerant amount was set to either 0.358 kg or 0.5 kg . The ceiling height inside the store was 2.2 m .

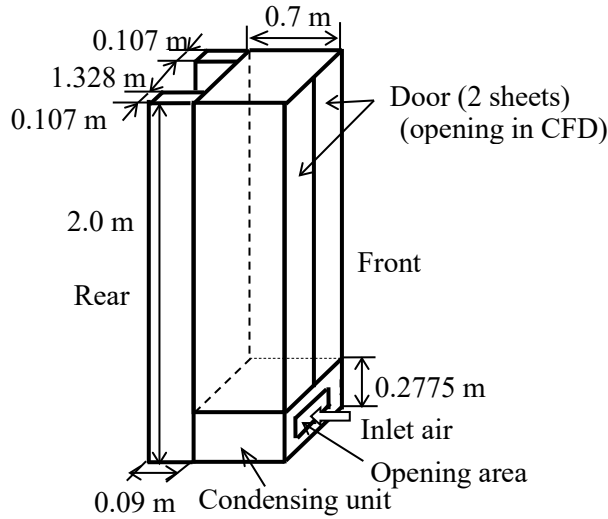


Fig. 7-2 CFD model of a reach-in refrigerated display cabinet.

(2) Analysis results

The refrigerant concentration distribution at the center of the refrigerated display cabinet in a store at times 5 s and 10 s after the door was opened in the case of a refrigerant amount of 0.5 kg and a floor area of 24.01 m^2 is shown in Figs. 7-3 and 7-4. Fig. 7-3 shows the case without the air curtain and an air flow rate in the condensing unit of $0 \text{ m}^3/\text{s}$, and Fig. 7-4 shows the case with the air curtain and the condenser air flow rate of $0.166 \text{ m}^3/\text{s}$ (air velocity of 2 m/s). With an air flow rate of $0 \text{ m}^3/\text{s}$, the leaked refrigerant linearly moves from the refrigerated display cabinet to the facing wall and collides with the wall. In all cases, the flammable region spreads over a wide area of the floor surface or the ceiling surface, irrespective of the air curtain (absence or presence) and its air velocity (air flow rate). The cause is considered to be the high leak rate resulting in a low residence time for the refrigerant to diffuse, i.e., all the refrigerant that leaked into the refrigerated space of the reach-in refrigerated display cabinet immediately leaks to the outside when the door is opened.

The flammable volume as a function of time upon changing the air flow rate in the condensing unit and the floor area, with and without the air curtain at the refrigerant amount of 0.5 kg , is shown in Fig. 7-5. Fig. 7-5 (a) shows the case without the air curtain and with a floor area of 24.01 m^2 , (b) shows the case with the air curtain and a floor area of 24.01 m^2 , (c) shows the case without the air curtain and with a floor area of 100 m^2 , and (d) shows the case with the air curtain and a floor area of 100 m^2 . The duration of the flammable region (the time from the generation of the flammable region to its disappearance) is shorter in the cases with the air curtain than in the cases without the air curtain, and the reduction in flammable volume is small. However, the difference in the values due to the existence or the non-existence of the air curtain is not so large in all the cases other than in the case of the condenser air flow rate of $0 \text{ m}^3/\text{s}$. When the condenser air flow rate is increased, although the duration of the flammable region is reduced (irrespective of the absence/presence of the air curtain), the maximum value of the flammable volume is hardly reduced.

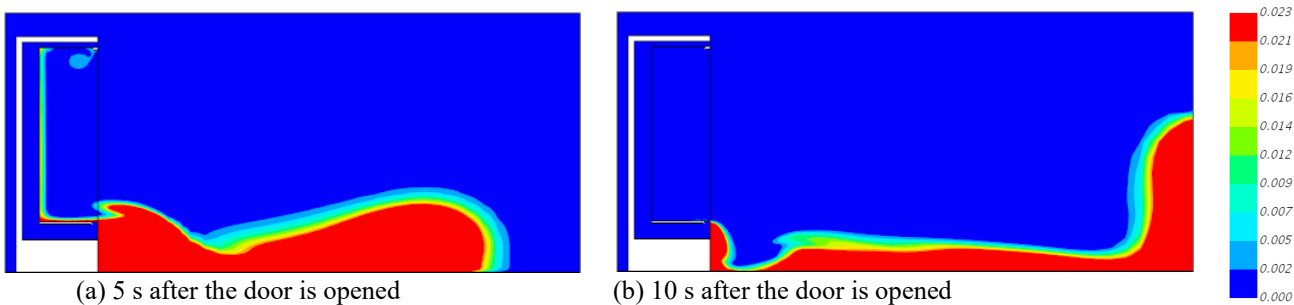


Fig. 7-3 Concentration distribution at air flow rate $0 \text{ m}^3/\text{s}$ without air curtain (refrigerant 0.5 kg , floor area 24.01 m^2).

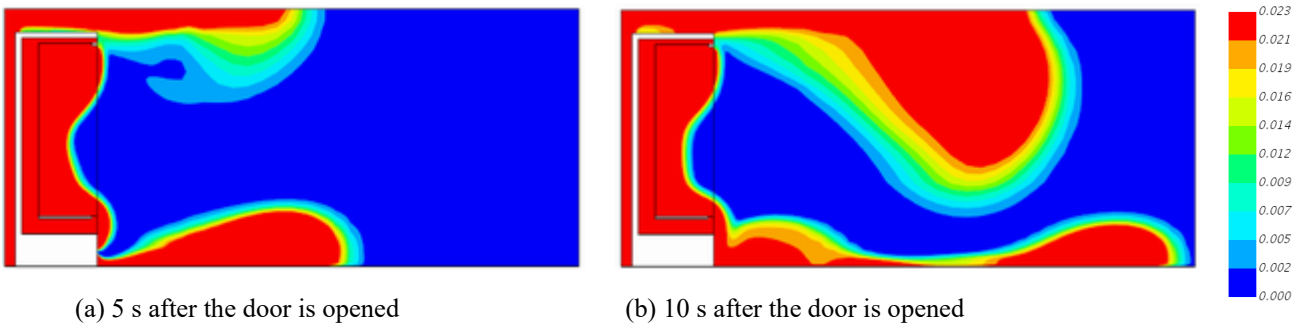
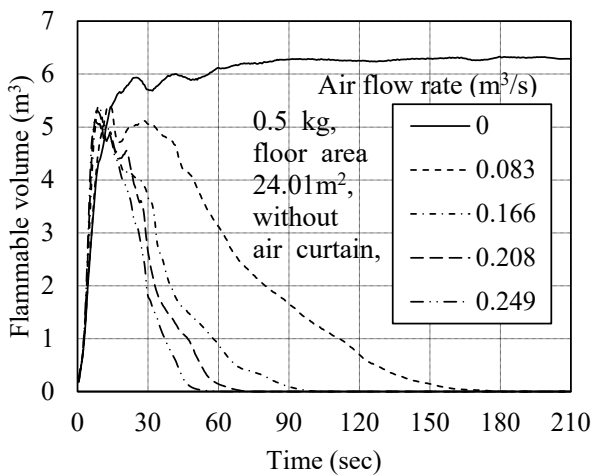
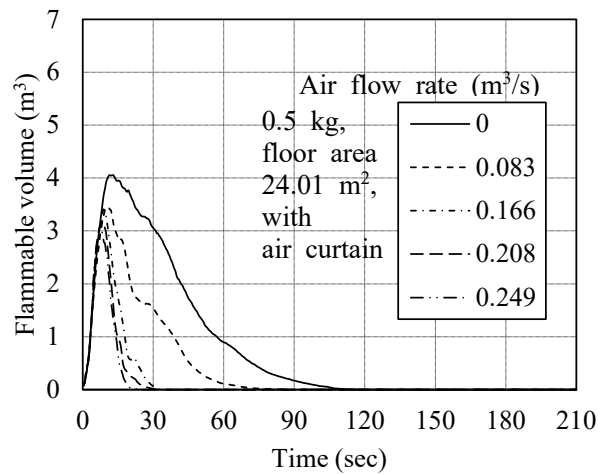


Fig. 7-4 Concentration distribution at air flow rate 0.166 m³/s with air curtain (refrigerant 0.5 kg, floor area 24.01 m²).

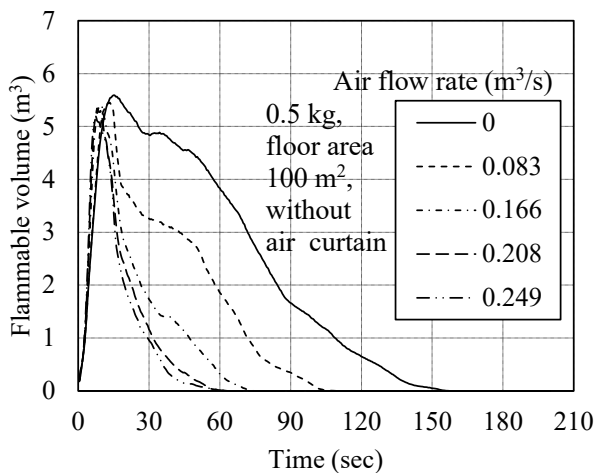
In addition, although the change in flammable volume with time is highly dependent on the floor area when the air flow rate is 0 m³/s, this effect is not so large when the air flow rate is 0.083 m³/s (air velocity of 1 m/s) or more. The maximum value of the flammable volume hardly changes irrespective of the absence/presence of the air curtain, the value of the floor area, and the value of the air flow rate. In the cases other than the floor area of 24.01 m² and the condenser air flow rate of 0 m³/s, the duration of the flammable region is within 5 min (300 s). Therefore, according to International Standard IEC 60335-2-89, no flammable region is generated. However, the flammable region spreads over the wide area of the floor surface or the ceiling surface, as shown in Figs. 7-3 and 7-4. Since static electricity, a relay of the electrical device in a store, etc. are ignition sources in case of A3 refrigerants, such as R290, there is a



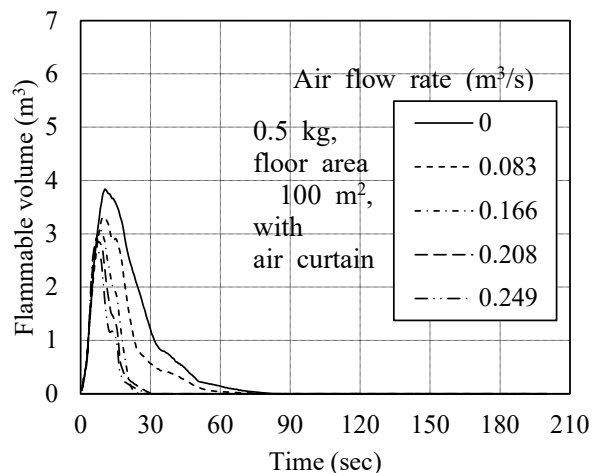
(a) 0.5 kg and floor area 24.01 m² without air curtain



(b) 0.5 kg and floor area 24.01 m² with air curtain

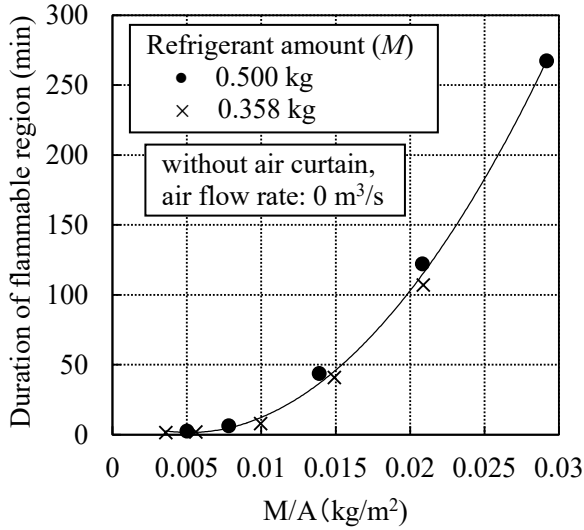


(c) 0.5 kg and floor area 100 m² without air curtain

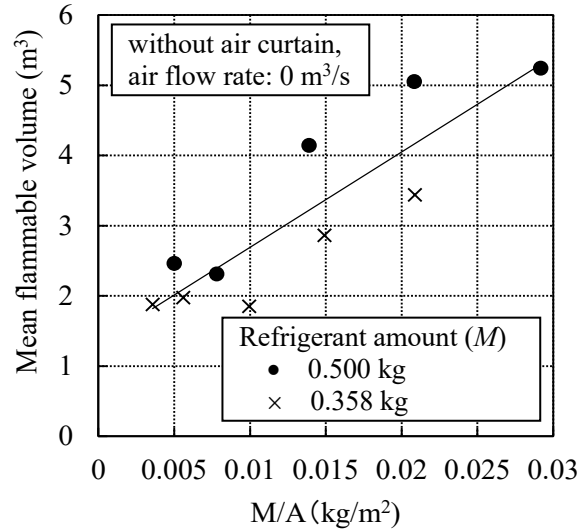


(d) 0.5 kg and floor area 100 m² with air curtain

Fig. 7-5 Change in flammable volume with time when the floor area and condenser air flow rate is varied.

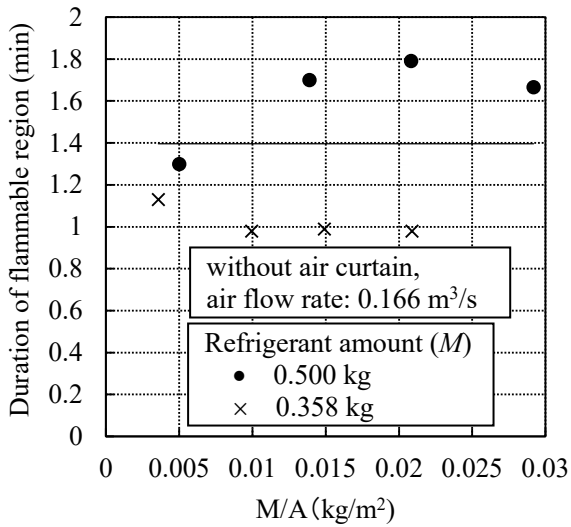


(a) Duration of the flammable region

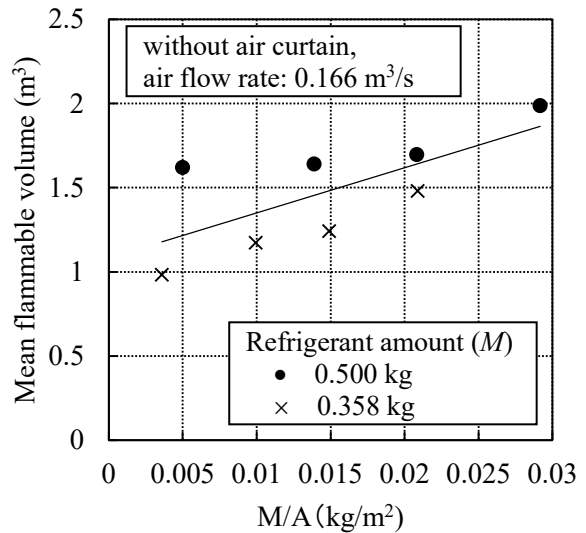


(b) Mean flammable volume

Fig. 7-6 Duration and volume of flammable region for air flow rate 0 m³/s without air curtain.



(a) Duration of the flammable region



(b) Mean flammable volume

Fig. 7-7 Duration and volume of flammable region for air flow rate 0.166 m³/s without air curtain.

$$T_v = 4.61 \times 10^5 \times \left(\frac{M}{A}\right)^2 - 4.76 \times 10^3 \times \left(\frac{M}{A}\right) + 1.38 \times 10^1 \quad (\text{air flow rate: } 0 \text{ m}^3/\text{s}) \quad (7-4)$$

$$V_v = 1.36 \times 10^2 \times \left(\frac{M}{A}\right) + 1.34 \quad (\text{air flow rate: } 0 \text{ m}^3/\text{s}) \quad (7-5)$$

$$T_v = 1.40 \times 10^1 \quad (\text{air flow rate: } 0.166 \text{ m}^3/\text{s}) \quad (7-6)$$

$$V_v = 2.68 \times 10^1 \times \left(\frac{M}{A}\right) + 1.08 \quad (\text{air flow rate: } 0.166 \text{ m}^3/\text{s}) \quad (7-7)$$

possibility that the existence of the ignition source causes ignition and danger even if the flammable region is generated only for a short time.

The analysis results of the duration of the flammable region (T_v) and the mean flammable volume (V_v) (mean value of flammable volume in the duration of the flammable region) are shown in Figs. 7-6 and 7-7. The figures show the cases for the air flow rate of 0 m³/s and 0.166 m³/s (air velocity of 2.0 m/s), and the horizontal axis is the value of the refrigerant amount (M) divided by the floor area (A). Both the duration of the flammable region and the mean flammable volume can be expressed in terms of M/A , and the obtained least square approximate equations are shown in Eqs. (7-4) to (7-7) and in

Figs.7-6 and 7-7 with solid lines. In the leakage from the refrigerated space of the reach-in refrigerated display cabinet, the flammable region outside the refrigerated display cabinet persisted even when the air flow rate of the condensing unit was increased. Similar results were obtained for the cases with the air curtain in front of the refrigerated space of the refrigerated display cabinet.

Two methods were applied to provide several types of different air flows in the refrigerated space of the reach-in refrigerated display cabinet: the air curtain method in which air flow is formed from the upper side to the lower side in front of the refrigerated space of the refrigerated display cabinet and the rear exhaust method in which air flow is formed from the rear to the front of the refrigerated space of the refrigerated display. Therefore, in the risk assessment of JRAIA, the analysis results without the air curtain were used as the worst-case scenario, and the values with and without the air flow rate of the condensing unit were used as the value during operation and stoppage, respectively.

7.3.2 Leakage from outside the refrigerated space of a horizontal refrigerated display cabinet

(1) Analysis model

Refrigerant leakage from the condensing unit at the bottom of a horizontal refrigerated display cabinet was analyzed. The analysis model is shown in Fig. 7-8. The external dimensions of the horizontal refrigerated display cabinet were 0.81 m in height, 1.8 m in width and 1.09 m in depth. The bottom of the refrigerated display cabinet was installed with a condensing unit, and air was sucked in from one opening and exhausted from the other opening. The opening area of the condensing unit was $6.89 \times 10^{-2} \text{ m}^2$ (0.733 m in width \times 0.094 m in height) for both the inlet and the outlet, and the air flow rate was varied in the range from 0 to 0.207 m^3/s (air velocity of 0 to 3 m/s). The refrigerated display cabinet was installed at the center of the store with a square-shaped floor, and pressure boundaries of $0.4 \text{ m} \times 0.4 \text{ m}$ were defined at the two corners of the ceiling above a store wall. The refrigerant concentration at the opening of the condensing unit at the air flow rate of $0 \text{ m}^3/\text{s}$ was set to 100%, and the calculated value was used for the refrigerant concentration at the air flow rate of more than $0 \text{ m}^3/\text{s}$. The refrigerant was allowed to leak evenly from the inlet and the outlet with an air flow rate of $0 \text{ m}^3/\text{s}$, and it was allowed to leak from the outlet with an air flow rate of more than $0 \text{ m}^3/\text{s}$. The ceiling height inside the store was 2.2 m, and the floor area was varied: 15.21 m^2 ($3.9 \text{ m} \times 3.9 \text{ m}$), 24.01 m^2 ($4.9 \text{ m} \times 4.9 \text{ m}$), 36.0 m^2 ($6.0 \text{ m} \times 6.0 \text{ m}$), 64.0 m^2 ($8.0 \text{ m} \times 8.0 \text{ m}$) and 100.0 m^2 ($10.0 \text{ m} \times 10.0 \text{ m}$). The refrigerant amount was 0.358 kg or 0.5 kg. The leak rate was the value at which the total refrigerant amount leaked in 4 min (*leak rate of total amount in 4 min*), and it was 5.37 kg/h and 7.5 kg/h for the amounts of 0.358 kg and 0.5 kg, respectively.

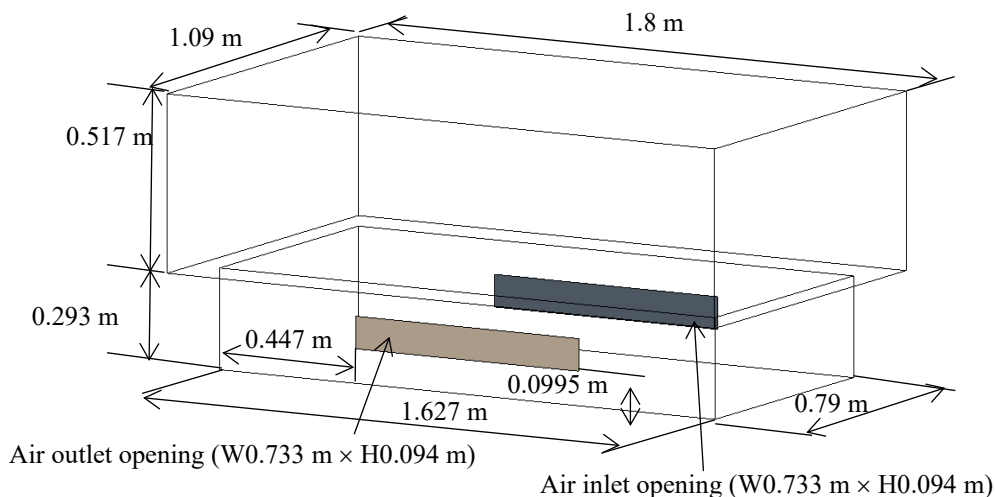


Fig. 7-8 CFD model of horizontal refrigerated display cabinet.

(2) Analysis results

Fig.7-9 shows the analysis results for the duration of the flammable region (T_v) and the mean flammable volume (V_v) at the condenser air flow rate of $0 \text{ m}^3/\text{s}$. The horizontal axis is the value of the refrigerant amount (M) divided by the floor area (A). Both the duration of the flammable region and the mean flammable volume can be expressed in terms of M/A , and the obtained least square approximate equations are shown in Eqs. (7-8) and (7-9) and with solid lines in Fig.7-9.

$$T_V = 4.41 \times 10^5 \times \left(\frac{M}{A}\right)^2 - 1.42 \times 10^3 \times \left(\frac{M}{A}\right) + 3.94 \quad (\text{air flow rate: } 0 \text{ m}^3/\text{s}) \quad (7-8)$$

$$V_V = 8.90 \times 10^1 \times \left(\frac{M}{A}\right) + 2.58 \quad (\text{air flow rate: } 0 \text{ m}^3/\text{s}) \quad (7-9)$$

For air circulation of the refrigerant leaked from the condensing unit, Eq. (7-10) was used to calculate the air flow rate that does not generate a flammable region⁷⁻²⁾. Here, A_0 is the area of the air outlet in m^2 , F is a safety factor of 0.25, G is LFL kg/m^3 , h_0 is the height of the centerline of the air outlet in m, Q is the air flow rate of outlet air in m^3/min , and w is the leak rate in kg/h .

$$Q = 60 \times \frac{5 \times \sqrt{A_0} \times (w/3600)^{3/4}}{h_0^{1/8} \times [G \times (1 - F)]^{5/8}} \quad (7-10)$$

When the floor area is 24.01 m^2 , the amount of R290 is 0.5 kg, and the leak rate is $7.5 \text{ kg}/\text{h}$, the calculated air flow rate using Eq. (7-10) is $0.150 \text{ m}^3/\text{s}$ (air velocity of $2.182 \text{ m}/\text{s}$). Refrigerant leak analyses under this condition did not recognize the generation of the flammable region. In addition, a flammable region was not generated even with the air flow rate of $0.1378 \text{ m}^3/\text{s}$ (air velocity of $2.0 \text{ m}/\text{s}$), which is lower than the above by 8.4%. Additionally, as results of similar analyses using R600a (an A3 refrigerant) and R152a (an A2 refrigerant), the flammable region was not generated at the air flow rate calculated using Eq. (7-10), and the flammable region was not generated even at an air flow rate lower than the calculated value by 8 to 20%.

Analyses were performed with the floor area of 24.01 m^2 , refrigerant amount of 0.5 kg, and condenser air flow rate of $0 \text{ m}^3/\text{s}$ by changing the leak rate in the range from 0.1 to $40.71 \text{ kg}/\text{h}$. The calculation results of the mean flammable volume and the flammable volume-time integration are shown in Figs. 7-10. The flammable volume-time integration is the value of the duration of the flammable region multiplied by the mean flammable volume. When the leak rate is $2 \text{ kg}/\text{h}$ or more, the calculation results of the mean flammable volume and the flammable volume-time integration are almost the same. When the leak rate as reduced from $2 \text{ kg}/\text{h}$, the mean flammable volume reduced gradually, specifically by approximately 60% at the leak rate of $0.2 \text{ kg}/\text{h}$ and by approximately 25% at the leak rate of $0.1 \text{ kg}/\text{h}$ in comparison with the value at the leak rate of $2 \text{ kg}/\text{h}$. However, since the refrigerant amount is the same, reducing the leak rate increases the time until the end of the leakage and also increases the duration of the flammable region. Consequently, the flammable volume-time integration scarcely changes at the leak rate of $0.54 \text{ kg}/\text{h}$ or more, and when the leak rate is lower than that, the value decreases: it has a value approximately 50% of that at the high leak rate, even when the leak rate is $0.1 \text{ kg}/\text{h}$.

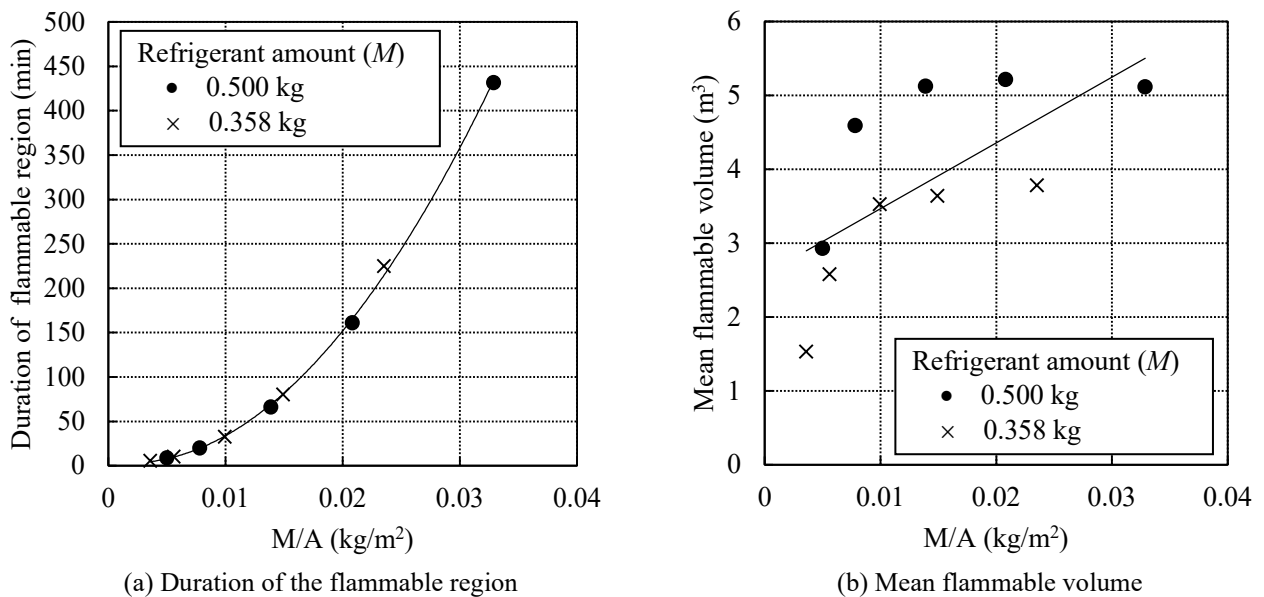


Fig. 7-9 Calculation results for a horizontal refrigerated display cabinet at air flow rate $0 \text{ m}^3/\text{s}$.

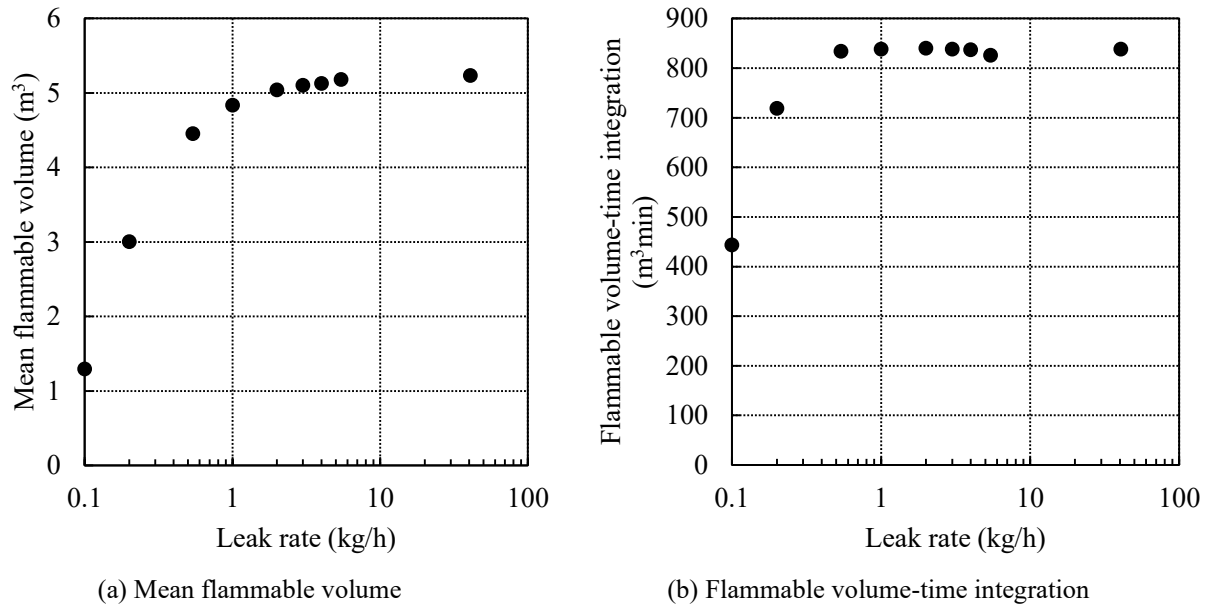


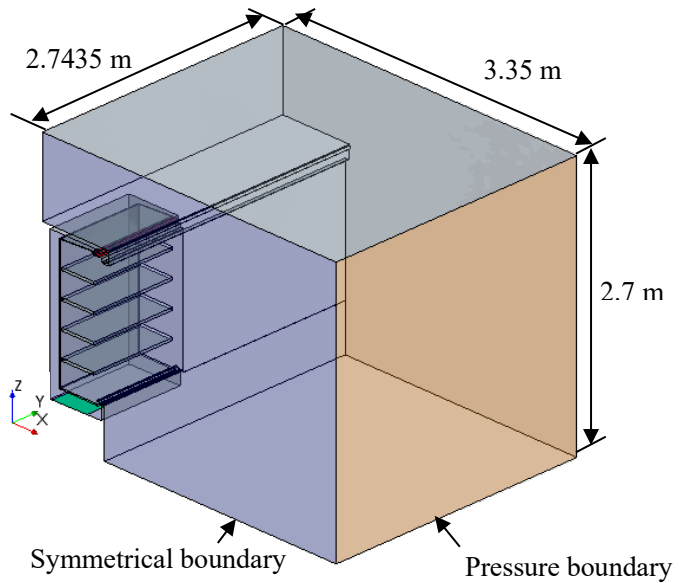
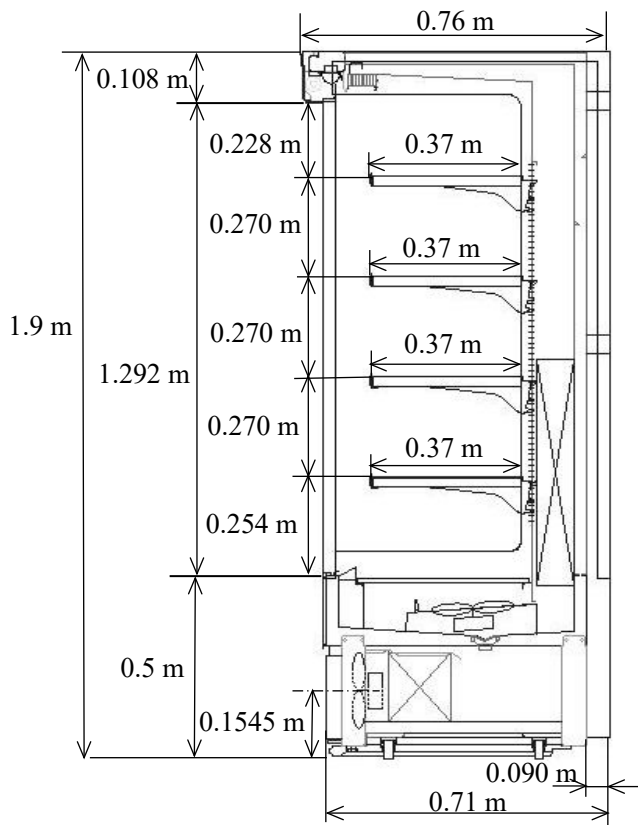
Fig. 7-10 Calculation results at different leak rates.

In the case of R290, a slow leak occurs at 0.54 kg/h or less (see Table 7-1 in 7.4.5), which results in the generation of a sufficiently large flammable cloud. In the risk assessment of A3 refrigerant, it was found that the ignition probability should be calculated by considering all leaks, including the slow leak. Furthermore, the risk assessment should be carried out using the flammable volume-time integration at the *leak rate of total amount in 4 min* (7.5 kg/h for R290) for safety.

7.3.3 Leakage from the refrigerated space of a vertical open refrigerated display cabinet

(1) Analysis model

The analysis model of a vertical open refrigerated display cabinet when refrigerant leaks from the refrigerated space and a store model (half model) are shown in Fig. 7-11. The external dimensions of the refrigerated display cabinet were 1.9 m in height, 1.8 m in width and 0.76 m in depth. A condensing unit was installed at the bottom, and air was sucked in from the front, passed through the rear side, and exhausted from the top of the refrigerated display cabinet. The opening area of the condensing unit was $9.66 \times 10^{-2} \text{ m}^2$, the height of the center of the opening was 0.1545 m, and the air flow rate was varied from 0 to 0.290 m³/s (air velocity of 0 to 3 m/s). The outlet of the air curtain flowing from the top to the bottom of the front face in the refrigerated space of the refrigerated display cabinet was for a single air curtain; the opening area was 0.1296 m² (1.8 m in width \times 0.072 m in depth) and the air flow rate is 0.114 m³/s (air velocity of 0.88 m/s). The store model was a half model 2.7 m in height \times 5.487 m in width \times 3.35 m in depth; the refrigerated display cabinet was installed at the center of a wall of the store, the symmetry boundary was set at the center of the refrigerated display cabinet, and the wall surface of the opposite face was set as the pressure boundary. The refrigerant amount was 0.5 kg and the leak rate was 7.5 kg/h, which is the *leak rate of total amount in 4 min*.



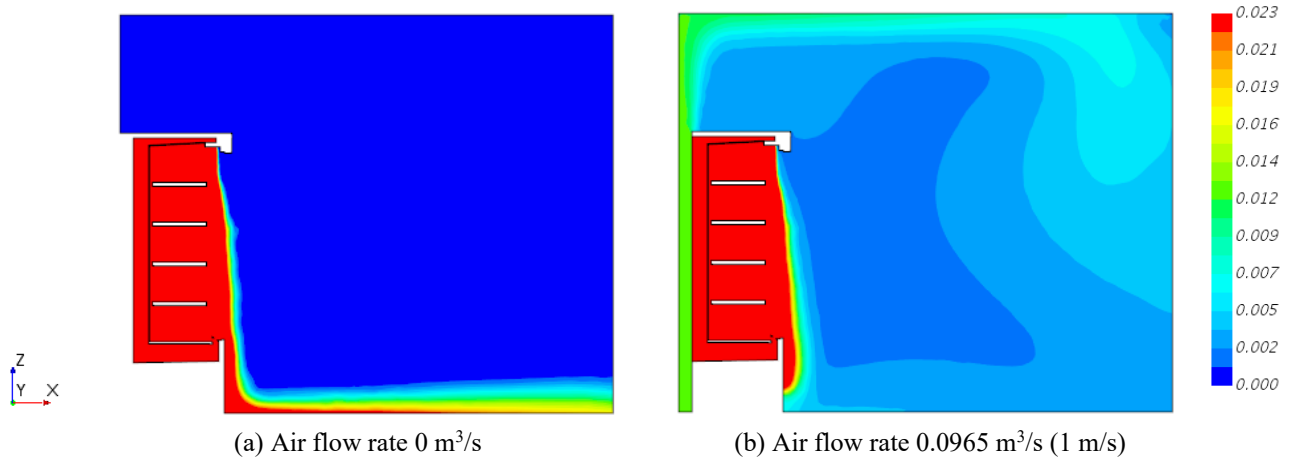
(a) CFD model of vertical refrigerated display cabinet

(b) CFD model of store (half model)

Fig. 7-11 CFD model of vertical refrigerated display cabinet and store (half model).

(2) Analysis results

Fig. 7-12 shows the concentration distribution at 240 s (4 min from the start of leakage) with a condenser air flow rate of $0 \text{ m}^3/\text{s}$ and $0.0965 \text{ m}^3/\text{s}$ (air velocity of 1 m/s). When the condenser air flow rate was $0 \text{ m}^3/\text{s}$, a flammable region was generated on the floor surface. When the air flow rate was $0.0965 \text{ m}^3/\text{s}$ (air velocity of 1 m/s) or more, a flammable region was scarcely generated outside the cabinet and slightly generated between the bottom of the air curtain in the refrigerated space and the air inlet of the condensing unit. This is not a problem because no ignition source exists. Therefore, with internal leakage of the refrigerant in a vertical open refrigerated display cabinet, a significant flammable region leading to ignition is not generated outside the refrigerated space only if the air flow rate of the condensing unit installed at the bottom is sufficiently high. In addition, similar results were obtained for R600a (an A3 refrigerant) and R152a (an A2 refrigerant).



(a) Air flow rate $0 \text{ m}^3/\text{s}$

(b) Air flow rate $0.0965 \text{ m}^3/\text{s}$ (1 m/s)

Fig. 7-12 Concentration distribution at 240 s after leakage.

7.4 Condition and method for risk assessment

International Standard IEC 60335-2-89 relaxed (increased) the maximum refrigerant charge of flammable refrigerants and provided the floor area limit corresponding to the refrigerant amount, along with the methods of refrigerant leak tests to ensure minimum safety. However, since the International Standard tended to prioritize usability over safety and risk assessment was not carried out, the Standard does not necessarily provide contents capable of sufficiently ensuring safety. Therefore, JRAIA carried out risk assessments concerning the ignition of refrigerants leaked from built-in refrigerated display cabinets using the A3 refrigerant and studied safety measures to reduce the risk. Contents extracted from these studies will be proposed to the IEC Standard.

7.4.1 Process of risk assessment and calculation of ignition probability

The ignition probability of an appliance using a flammable refrigerant is calculated by multiplying the temporal encounter probability, which is the time rate of encounter between the ignition source and the flammable region, with the spatial encounter probability representing the space distribution of the flammable region and the refrigerant leak probability.

The temporal encounter probability (P_t) is calculated using the concept of geometric probability^{7-3), 7-4)}. Since the detail is described in Chapter 6, a brief image is given here. The temporal encounter probability is calculated with Eq. (7-11) using the total time (T_a) of the targeted stage, the duration of the flammable region (T_v), the duration of the ignition source (T_i), and the frequency of ignition source (n). Coefficient k is determined by considering the abundance ratio of the potential ignition source (dissemination rate of electrical devices, etc.) and the concentration degree when the ignition source is concentrated on the specific time zone. The spatial encounter probability (P_s) is calculated with Eq. (7-12) using the mean flammable volume (V_v) and the targeted space volume (V_a), and the ignition probability (P) is calculated with Eq. (7-13) using the temporal encounter probability (P_t), the spatial encounter probability (P_s) and the refrigerant leak probability (P_r). Among these, the value (approximate equation) obtained from refrigerant leak analyses (see 7.3) is used for the duration of the flammable region (T_v) and the mean flammable volume (V_v). Other values are set at the value corresponding to the setting in each life stage and the characteristic of the ignition source.

$$P_t = k [1 - \{1 - (T_i + T_v) / T_a\}^n] \quad (7-11)$$

$$P_s = V_v / V_a \quad (7-12)$$

$$P = P_t \cdot P_s \cdot P_r \quad (7-13)$$

The ignition probability at usage is obtained by weight-averaging the ignition probability during the operation and stoppage (failure, etc.) of the fan in the condensing unit by the operation factor. Eqs. (7-4) and (7-5) and Eqs. (7-6) and (7-7) are used for leakage from the refrigerated space of a reach-in refrigerated display cabinet during stoppage and operation, respectively. The equation for the horizontal refrigerated display cabinet is applied to leakage from the condensing unit, Eqs. (7-8) and (7-9) are used during stoppage, and the flammable region is not generated because the air flow rate satisfies Eq. (7-10) during operation. The value during work is obtained using the equation for stoppage.

7.4.2 Setting of risk model for built-in refrigerated display cabinet

The model store in which the risk assessment was carried out is a convenience store capable of simple cooking, such as frying. Since there are a large number of convenience stores (approx. 55,000), and A3 refrigerant can be ignited even by static electricity or the relay of an electrical device, the convenience store is assumed to have the largest number of ignition sources among the venues with a built-in refrigerated display cabinet installed. The refrigerated display cabinets shown in Fig. 7-13 are installed inside the convenience store.

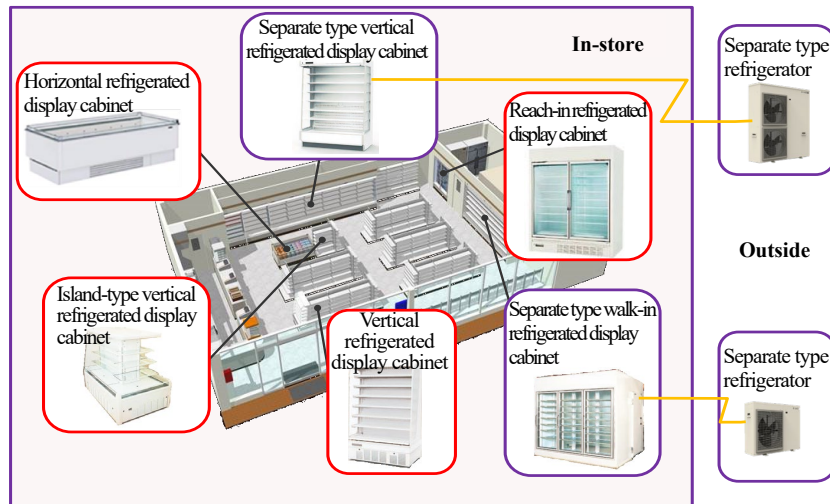


Fig. 7-13 Refrigerated display cabinets installed in convenience store.

In the risk assessment, it was assumed that the refrigerant amount in the refrigerant circuit of a display cabinet is 0.5 kg, and the floor area in the store is 84.7 m². This floor area is based on the standard dimensions of the store and exclude the separate type closed refrigerated display cabinet, the office, and the lavatory in the store.

7.4.3 Life stage of built-in refrigerated display cabinet and scenario for each stage

Generally, a built-in refrigerated display cabinet is produced in a factory, temporarily stored in a warehouse, transported to a store for use, installed in a proper location in the store, and then used. When a problem occurs during use, the refrigerated display cabinet is repaired at the installation place, or, when it is judged that sufficient work cannot be performed there, the refrigerated display cabinet is taken back to a service agent, etc. of the manufacturer, and is installed again after repair. When the refrigerated display cabinet is no longer in use, it is removed from the installation location, temporarily stored in a warehouse and disposed of, or some display cabinets may be installed again after recycling or maintenance as a secondhand product.

Among these, the risk assessment carried out by JRAIA sets transportation, storage, installation, usage, repair, and removal as the life stage.

(1) Transportation stage

The transportation of a built-in refrigerated display cabinet to be installed in a convenience store is generally performed using a truck, and ignition sources do not exist in the freight compartment at the back of the truck. Therefore, in the risk assessment during transportation, transportation using a minivan in which the cargo compartment and the driver cab exist in the same space is assumed.

Transportation using a minivan is performed when the condensing unit is replaced during on-site repair. For the outbound trip, it was assumed that unused product is packed in a wooden crate, and for the return trip, used product is not packed in a wooden crate, and only the condensing unit charged with the refrigerant is transported. When failure requiring brazing occurs, replacement work is performed. The probability of requiring minivan transportation was decided to be 8.39×10^{-4} , which is the investigation result of the number of repairs involving brazing divided by the number of appliances in the market. The frequency of minivan transportation was decided to be 4.2×10^{-6} by multiplying this by the value 5×10^{-3} , which is the estimated value of the probability of replacing condensing units containing refrigerants.

It was assumed that the internal volume of the minivan is 2.9 m³, the number of persons on board required for loading and unloading appliances is 2, the maximum transportation time is 12 h, and the average transportation time is 2 h. The ignition source at the transportation stage was set assuming this scenario.

(2) Storage stage

The warehouses for storing the refrigerated display cabinets are classified into the middle-sized warehouse that

temporarily stores the refrigerated display cabinets brought in after production in a factory or from an overseas production factory and the small-sized warehouse that stores them at each sales location. The areas of a middle-sized warehouse and a small-sized warehouse are 1,000 m² and 15 m², respectively.

Carrying of the refrigerated display cabinets is performed using a transport device, such as a forklift or a trolley, directly operated by a worker. The working time is 8 hours a day, 20 days a month with 5 persons in a middle-sized warehouse, and 2 hours a day, 20 days a month with 2 persons in a small-sized warehouse. Unused and secondhand refrigerated display cabinets are stored in a warehouse, and an unused appliance is assumed to be wrapped in plastic or in plastic plus wooden crate. Air moves to the outside through an opening at the bottom of the plastic sheet packing. Secondhand refrigerated display cabinets are assumed to be without packing or wrapped in plastic. Furthermore, unused or secondhand reach-in refrigerated display cabinets with doors should be in the closed and fixed state so as not to unintentionally open during transportation and storage. The ignition source at the storage stage was set assuming this scenario.

(3) Installation stage

The refrigerated display cabinet before installation is assumed to be an unused or secondhand product. The unused product is in the factory condition and in plastic packaging or plastic packaging plus wooden crate, while the secondhand product is unpackaged or wrapped in plastic packaging.

Installation work consists of the unloading work (bringing the refrigerated display cabinet from the freight compartment of a truck onto the ground), the carrying work (carrying the unloaded refrigerated display cabinet to the installation location inside the store), and the emplacement work (performing unpacking, attaching accessories, etc.) These works take approximately about one hour with two workers for one refrigerated display cabinet. This time consists of 0.2 h for unloading, 0.1 h for carrying, and 0.7 h for emplacement. The installation ratio of the refrigerated display cabinets per year was assumed to be 1.67×10^{-1} considering the life span of display shelves and display cases. The ignition source at installation stage was set assuming this scenario. Installation in a new store construction and installation in a store in operation were assumed as the installation condition. When installation takes place in a store in operation, the ignition source at the usage stage should be considered because the store has electrical devices in operation.

(4) Usage stage

A refrigerated display cabinet using a flammable refrigerant installed as an appliance inside a convenience store is not an ignition source because it is designed considering safety. Since all other equipment have the possibility of being an ignition source, the structure of the appliance should be studied in detail. For A3 refrigerants, such as R290, open flame, electric spark, static electricity, and hot surface may be the ignition source. Among these, the electric spark may be generated by a relay and a thermostat of the electrical device in the store, turning switches for lighting ON/OFF, and plugging in and unplugging from a power outlet for an electrical device. Static electricity was assumed to be discharged by a person contacting the metal part of a refrigerated display cabinet in the store.

i) Electric spark

The discharge time of an electric spark was assumed to be 5 ms. The scenario of electric spark generation is as follows:

A coffee machine (Fig. 7-14 (a)) has a boiler and a motor. Since the boiler is protected with an excessive temperature rise switch or fuse, which prevents empty heating, and a brush motor is not used, neither is an ignition source. Electric discharge was assumed to be generated when an internal relay of the coffee machine is actuated. The number of times of internal relay actuation is set by obtaining the number of times of annual sales per store from the number of times of coffee sales in the whole number of convenience store chains and the number of convenience stores.

Although a deep frying machine (Fig. 7-14 (b)) has a heater, it is not an ignition source because the temperature of both the oil and plate is controlled at 250 °C or less. Electric discharge was assumed to be generated when the switch of a deep frying machine is turned ON/OFF. Since the freshness date of deep-fried food cooked and sold by a convenience store is 4 h, it was assumed that deep-fried food is cooked every 4 h from 4 o'clock in the morning to 0 o'clock at night, and the number of switch ON/OFF times is set.

Although a Chinese-style buns steamer (Fig. 7-14 (c)) and a heating appliance for "Oden" (Fig. 7-14 (d)) have heaters, they are not ignition sources because they are protected with an excessive temperature rise switch or fuse. Electric discharge

was assumed to be generated when each of their switches is turned ON/OFF.

A copier (Fig. 7-14 (e)) consists of a writing section using laser beam, charging roller that generates corona electric discharge, toner fixing section that fixes toner on a sheet of paper using heater, etc. Since the difference between a household printer and a commercial copier is unclear, they were assumed for safety to always be an ignition source during use. Assuming the number of times of use and the time spent copying per day, it was assumed that copying always induces ignition.

Since the use of flammable refrigerants was not assumed in a refrigerated display cabinet other than “a refrigerated display cabinet using flammable refrigerant” installed in the same store, the electric discharge from the built-in brush motor was assumed to be an ignition source. The dissemination rate of brush motors was assumed to be 1%. Since air flows at a velocity sufficiently higher than the burning velocity during motor operation, it was assumed that the motor is not an ignition source and electric discharge occurs at motor start.

Electric discharge produced by unplugging a vacuum cleaner and turning a lighting switch ON/OFF in the store was assumed. The probability that unplugging of a vacuum cleaner for cleaning inside the store is performed twice a day and unplugging without operating the switch of the cleaner itself is performed was assumed. The lighting switch in the store was assumed to be turned from ON to OFF twice a day.

Since a ventilating fan in a store is generally in continuous operation without being turned ON/OFF, the switch is not an ignition source.

Additionally, ignition due to an ignition accident of each electric appliance was assumed. The number of each piece of appliance per store was assumed, the number of annual accidents was investigated from the data of NITE (National Institute of Technology and Evaluation), and the generation probability of the ignition accident was calculated based on the number of appliances in the market.



Fig. 7-14 Typical equipment in the store.

ii) Static electricity

Static electricity generated when someone holds the door handle of a reach-in refrigerated display cabinet for opening or closing or when a shopper contacts the handrail of an open refrigerated display cabinet or metal part of a shelf, etc. was assumed. The number of cups of ice coffee sold per day in a convenience store was investigated, and the number of opening and closing times of a reach-in refrigerated display cabinet for refrigerating and freezing was calculated. Even if the door is opened after leakage into the refrigerated space of the reach-in refrigerated display cabinet, ignition does not occur because the refrigerant is not leaked to the outside from the refrigerated space when the first shopper makes contact with the door. Therefore, the probability that the first shopper opens the door and a second shopper opens the door immediately after the first was assumed. The discharge time of static electricity was assumed to be 1 μ s. Humidity that may cause electrostatic discharge was assumed to be 30% or less, and its generation probability was assumed to be 18.7% as an annual average by converting the weather data of Tokyo to the temperature inside a store.

iii) Hot surface

Since the surface temperature when a fluorescent lamp, LED, or incandescent light bulb is turned ON and the surface temperature of the defrost heater for the refrigerated display cabinet are equal to or less than the auto-ignition temperature

of R290, they are not ignition sources.

iv) Open flame

A case where a shopper performs trial ignition of a cigarette lighter displayed in a store was assumed. Trial use was assumed to be performed by 5 persons per day for 5 s each. No smoking in a store was assumed. In addition, the use of a combustion-type heater was assumed, its dissemination rate was assumed to be 0.01%, and its usage rate was assumed to be 10 h per day.

(5) Repair stage

The repair was assumed to be a take-back repair in which the repair is performed in the manufacturing factory or the service factory of a maintenance agent, an outdoor repair in which the repair is performed by temporarily moving the product outdoors, and an in-store repair in which the repair is performed with the refrigerated display cabinet installed as is inside the store because moving it is difficult due to size.

The probability of a repair for a built-in refrigerated display cabinet was assumed to be 1.00×10^{-2} , which was obtained by dividing the investigation results of the number of repairs by the number of products in the market. In addition, within the generation ratio of work involving the repair of refrigerant circuits, the ratio was assumed to be 8.39×10^{-2} for repairs outside and inside the store. For the working time of the repair, it was assumed that the time for releasing refrigerant to the atmosphere (disposal of refrigerant) is one hour, the time for pipe cutting and the replacement of refrigerant circuit parts is one hour, the time for refrigerant charging is one hour, and working time not related to the refrigerant circuit is one hour.

The ignition source at the repair stage was set by assuming this scenario. Concerning the work inside the store, the ignition source at the usage stage should be considered because electrical devices, etc. exist in the store. Furthermore, refrigerant disposal and refrigerant charging on site in relation to the High Pressure Gas Safety Act will be explained in 7.5.

(6) Removal stage

The removal stage was assumed to be the case that the refrigerated display cabinet installed inside the store is removed from inside the store for disposal. At this time, the built-in refrigerated display cabinet is moved with the refrigerant in the refrigerant circuit.

The removal ratio of the built-in refrigerated display cabinet was assumed to be 1.24×10^{-1} by summing the probability (7.69×10^{-2}) that the refrigerated display cabinet is replaced at the end of service life (13 years) and the probability (4.70×10^{-2}) that the refrigerated display cabinet is removed because the store is closed down. The time required for removal was assumed to be one hour. The ignition source at removal stage was set by assuming this scenario. The removal was assumed to be the case of removal from the closed down store and the case of removal from a store in operation. When removing from a store in operation, the ignition source of the usage stage should be considered because electrical devices, etc. in operation exist inside the store.

7.4.4 Setting of tolerable level

The number of built-in refrigerated display cabinets in the market in Japan was 1.9 million⁷⁻⁵⁾ as of FY 2014. According to the data of JRAIA, since the number of built-in refrigerated display cabinets shipped in and after FY 2014 has scarcely changed, the number of refrigerated display cabinets in the market was decided to be 1.9 million, assuming that the number did not change.

For safety, all the ignition accidents were assumed to be fatal ones. The tolerable value at the usage stage was decided to be 5.26×10^{-9} by assuming that the level is the generation of a fatal accident once in a hundred years for the number of refrigerated display cabinets in the market. Concerning accidents other than at the usage stage, the tolerable value was decided to be 5.26×10^{-8} because dedicated workers who always handle the refrigerated display cabinet and who received technical education concerning the work are involved as professionals and the tolerable probability of accident generation is considered to be able to be raised by one digit compared with that at usage stage.

7.4.5 Refrigerant leak rate

Table 7-1 Comparison of refrigerant leak rates

Refrigerant	Burst leak (kg/h)	Rapid leak (kg/h)	Slow leak (kg/h)
R32 (63 °C saturated liquid)	75	10	1
R290 (63 °C saturated liquid, higher pressure side)	40.71	5.43	0.54
R290 (35 °C saturated liquid, lower pressure side)	31.2	4.16	0.42

The refrigerant leak rate can be categorized as a burst leak, rapid leak, or slow leak depending on the damage condition of the piping. The burst leak generally occurs when piping is broken by the vibration of the compressor and the freezing of the evaporator, and the slow leak arises when corrosion leads to a small hole and from insufficient tightening. The rapid leak is characterized by an intermediate leak rate and the maximum leak rate, which occur when the compressor is not exist and evaporator is not frozen and occur when the piping cracks.

In the case of R32, we assumed the following leak rates: burst leak of 75 kg/h, rapid leak of 10 kg/h, and slow leak of 1 kg/h. These were determined using the investigation results of the parts of air conditioners that generated the refrigerant leak recovered from the market⁽⁷⁻⁶⁾. The leak rates for R290 were obtained by replacing the physical property of R32 with that of R290 using the calculation equation by which these leak rates were calculated, as shown in Table 7-1. At this time, the leak rates of R290 were calculated both for the saturated pressure (saturated liquid, higher pressure side) at 63 °C and for the saturated pressure (saturated liquid, lower pressure side) at 35 °C.

The hole diameter through which the refrigerant leaks varies depending on its origin, such as corrosion. Although it leaks at the maximum leak rate through that hole diameter in the initial period of refrigerant leakage, the leak rate decreases because of the reduction in pressure inside the refrigerant circuit when leakage progresses, and the leakage stops finally. In the built-in refrigerated display cabinet, the reduction in pressure inside the refrigerant circuit due to leakage occurs earlier because of the small amount of refrigerant, and the leak rate decreases earlier. Therefore, the refrigerant leak rate of the built-in refrigerated display cabinet used for the risk assessment was assumed to be the *leak rate of total amount in 4 min*. For 0.5 kg of R290, the *leak rate of total amount in 4 min* is 7.5 kg/h, which is higher than the rapid leak rate and lower than the burst leak rate. Here, the *leak rate of total amount in 4 min* is a concept of International Standard IEC 60335-2-40 for air conditioners. The leak rate is 2.66 kg/h when it was calculated using the other equation (Eq. (7-2)) provided in IEC 60335-2-89. This value is lower than the rapid leak rate, and 1/2.8 of the *leak rate of total amount in 4 min*. JRAIA adopted the *leak rate of total amount in 4 min* used for air conditioners in the risk assessment of the built-in refrigerated display cabinet to enhance safety.

7.4.6 Refrigerant leak probability

(1) Refrigerant leak probability at usage

The refrigerant leak probability at usage was calculated by dividing the investigation results of the number of refrigerant leakage occurrence by the number of products in the market. The results are shown in Table 7-2.

Refrigerant leak analyses in which R290 leaks from the condensing unit at the bottom of the horizontal refrigerated display cabinet were performed by varying the refrigerant leak rate in the range from 0.1 to 40.71 kg/h. As a result, it was found that a sufficiently large flammable region was generated even when the leak rate was 0.1 kg/h (see 7.3.2). Therefore, the value of 1.0×10^{-3} that was obtained by summing all refrigerant leak probabilities including the slow leak, rapid leak, and burst leak was assumed to be the refrigerant leak probability when used in the risk assessment of A3 refrigerants.

As shown in Table 7-2, we found that the slow leak accounts for approximately 98% of all leakage accidents, and the percentage of the leakage accidents leading to a dangerous situation in case of A3 refrigerants is considerably high.

Table 7-2 Annual refrigerant leakage probability

	Refrigerant leak probability	Percentage
Burst leak	5.26×10^{-7}	0.05%
Rapid leak	1.89×10^{-5}	1.89%
Slow leak	9.82×10^{-4}	98.06%
Total	1.00×10^{-3}	—

(2) Refrigerant leak probability until initial installation

The refrigerant leak probability until the initial installation was assumed to be 2.11×10^{-4} by dividing the investigation results of the number of refrigerant leakage occurrence among the initial failures by the number of products in the market. This was assumed to be the refrigerant leak probability from shipment from a factory to installation, and the refrigerant leak probability during transportation and installation was assumed to be 1/3 of the refrigerant leak probability until the initial installation. The refrigerant leak probability until the initial installation was used as the refrigerant leak probability during storage for safety, considering a long period of storage.

In addition, according to the investigation results, the percentages for each type of refrigerated display cabinets were assumed to be 29.7% for reach-in refrigerated display cabinets, 13.3% for horizontal refrigerated display cabinets, and 57.0% for vertical refrigerated display cabinets. Since rapid door opening after internal leakage in the reach-in refrigerated display cabinet was assumed to lead to the most dangerous situation, the percentage of this generation was handled as 29.7% of the case of reach-in refrigerated display cabinets.

(3) Refrigerant leak probability at working

Refrigerant leakage due to work occurs because of a work mistake. The refrigerant leak probability due to work during repair or removal was calculated from the probability of human error assumed from the scenario of each work.

(4) Probability of human error

Although the installation, repair, and removal of refrigerated display cabinets are performed by trained professionals with a high level of technical skill, the work environment is not uniform, and when the refrigerated display cabinet is used for the storage of food, the time of repair work may be limited by the storage temperature of food. Generally, since the risk assessment was carried out under normal conditions, the probability of human error was assumed to be 1.0×10^{-3} assuming the work was performed with a relaxed mental state⁷⁻⁷⁾. For unconventional work, that is, work performed to prevent the ignition of flammable refrigerants, the probability of human error was assumed to be 1.0×10^{-2} to 5.0×10^{-2} because careful work is required⁷⁻⁷⁾. In addition, the probability of human error shall not be lower than 1.0×10^{-4} even after implementing safety measures that reduces human error, such as education or marking on product.

7.5 Japanese law (High Pressure Gas Safety Act)

The High Pressure Gas Safety Act excludes high pressure gas in refrigeration equipment (refrigerant circuit) in which the refrigerating capacity is less than 3 legal tons from application. However, this is concerning the Refrigeration Safety Regulation that covers high pressure gas in the refrigerant circuit. Excluding refrigerants covered by the Refrigeration Safety Regulation, for a refrigerant in which the main component is hydrocarbons with a carbon number of 3 or 4, the Liquefied Petroleum Gas Safety Regulation applies, and for other refrigerants, the General High Pressure Gas Safety Regulation applies. If the General High Pressure Gas Safety Regulation or the Liquefied Petroleum Gas Safety Regulation is applied to the release of refrigerant into the atmosphere from the refrigerant circuit of an appliance (disposal of refrigerant), the recovery of the refrigerant, and the charging of the refrigerant into an appliance, notification reports to regulatory authorities is required 20 days in advance, which makes the repair of an appliance substantially impossible. Therefore, JRAIA repeatedly negotiated with the High Pressure Gas Safety Office of the METI to relax this. Here, we explain the provisions for the disposal of refrigerants, the recovery of refrigerants, and refrigerant charging to equipment.

7.5.1 Disposal of refrigerant

The Refrigeration Safety Regulation, General High Pressure Gas Safety Regulation, and Liquefied Petroleum Gas Safety Regulation stipulate that, when disposing flammable gas (A3 and A2 refrigerants) and particular inert gas (A2L refrigerant), ignition sources should be avoided, and when releasing the gas to the atmosphere, it should be released little by little in a well ventilated place. The Liquefied Petroleum Gas Safety Regulation stipulates that the distance between the equipment and ignition sources should be 8 m or more. Although the General High Pressure Gas Safety Regulation does not stipulate the distance to ignition sources, the Exemplified Standard related to the General High Pressure Gas Safety Regulation stipulates similarly.

However, disposing refrigerant from equipment in which the refrigerating capacity is less than 3 legal tons is the action of moving the refrigerant from the zone that the Refrigeration Safety Regulation applies to the zone that the General High Pressure Gas Safety Regulation or the Liquefied Petroleum Gas Safety Regulation applies. In addition, the disposal of refrigerant on site is performed from the equipment to the atmosphere using the pressure difference. Therefore, in July 2020, the High Pressure Gas Safety Office of METI passed the following judgment:

“Regarding the disposal of refrigerant from refrigerating equipment with refrigerating capacity of less than 3 legal tons due to pressure difference is exempt under the High Pressure Gas Safety Act. At this time, a treatment facility for changing the pressure shall not be used.”

Therefore, since the disposal of refrigerant from equipment in which the refrigerating capacity is less than 3 ton on site is not covered by the High Pressure Gas Safety Act, JRA Standard (JRA GL-21) provides content for the disposal of these refrigerants that when operated in accordance will ensure safety. In addition, since the Act on Rational Use and Proper Management of Fluorocarbons JAPAN prohibits the release of HFC refrigerant to the atmosphere, the disposal of these refrigerants to the atmosphere cannot be performed.

7.5.2 Recovery of refrigerant

The Minister of METI excluded the application of the High Pressure Gas Safety Act to recovery equipment related to inert gases, including fluorocarbons and CO₂, or particular inert gases that satisfies the specific requirements stipulated by the notification and the notice. The specific requirements for particular inert gases include use in a well-ventilated place, non-use near ignition sources, installation of suitable fire extinguishers in a suitable location, and installation of a gas leakage detection alarm system in a suitable location. Furthermore, for particular inert gases, the recovery equipment corresponding to the particular inert gas should be used. However, the provision for recovery equipment does not refer to flammable gas. Therefore, the recovery of flammable gas is not excluded from the application of High Pressure Gas Safety Act, and notification at least 20 days in advance is required. Thus, the recovery of flammable gas cannot substantially be performed. Furthermore, the expansion of the provision for recovery equipment to flammable gas makes it a difficult task.

7.5.3 Refrigerant charge to refrigerating equipment

Concerning facilities for charging refrigerating equipment with high pressure gas, the on-site charging of inert gases, including particular inert gases of which the gas volume is 0.15 m³ (150 L) or less, using the facility concerned is excluded from the application of the High Pressure Gas Safety Act. It is stipulated that “Facilities for charging high pressure gas” are “Facilities such as gauge manifold, pressure reducing valve, valve, hose, etc. (excluding compressor) for charging high pressure gas to refrigerating equipment.” That is to say, refrigerant charging from a refrigerant cylinder to the equipment on site is excluded from the application of the High Pressure Gas Safety Act. However, no provisions for flammable gas were found.

Refrigerant charging to equipment in which the refrigerating capacity is less than 3 legal tons is the action of moving the refrigerant from the zone that the General High Pressure Gas Safety Regulation or the Liquefied Petroleum Gas Safety Regulation applies to the zone that the Refrigeration Safety Regulation applies. In addition, refrigerant charging on site is performed from a refrigerant cylinder to the equipment using pressure difference. Therefore, in July 2020, the High Pressure Gas Safety Office of METI passed the following judgment:

“Regarding refrigerant charge to refrigerating equipment with refrigerating capacity of less than 3 legal tons due to pressure difference are exempt under the High Pressure Gas Safety Act. At this time, a treatment facility for changing the pressure shall not be used.”

Therefore, since refrigerant charging on site to equipment in which the refrigerating capacity is less than 3 legal tons is excluded from the application of the High Pressure Gas Safety Act, JRA Standard (JRA GL-21) provides content for refrigerant charging that when operated in accordance will ensure safety.

7.6 Japanese Standard

JIS C 9335-2-89 is the Japanese Standard established by translating IEC 60335-2-89 and adding the necessary deviation (amendment from the international standard). The draft was prepared by JRAIA, and revisions were made in accordance with Edition 3.0 of IEC 60335-2-89. JRA 4078 and JRA GL-21 are JRA Standards provided by JRAIA on the basis of risk assessments of built-in refrigerated display cabinets, etc. using A3 refrigerants, and their scope covers built-in freezing and refrigerating appliances using A3 and A2 refrigerants. The risk assessments of JRAIA are still in progress. However, since the Act on Rational Use and Proper Management of Fluorocarbons JAPAN has a plan to define the target value of GWP and the target FY year for built-in freezing and refrigerating appliances, including built-in refrigerated display cabinets, the JRA Standards were established on the basis of current study results.

Here, JIS C 9335-2-89 and JRA Standards (JRA 4078 and JRA GL-21) are generically called Japanese Standards, and the main difference in the contents between IEC 60335-2-89 and Japanese Standards are explained.

7.6.1 Maximum refrigerant charge

The flammability of A2L refrigerants is lower than that of A2 and A3 refrigerants. However, because the maximum refrigerant charge is 1.2 kg, according to the provision of IEC 60335-2-89, A2L refrigerants cannot be used for large appliances. On the other hand, in International Standard IEC60335-2-40 for air conditioners, the charge of A2 and A3 refrigerants are allowed by up to 26 times LFL, however, the charge of A2L refrigerants are allowed by up to 52 times LFL because of the difference in flammability. Therefore, the Japanese Standards eliminated the upper limit of 1.2 kg and enabled charging up to 13 times the LFL regardless of the flammability classification of refrigerants. In case of R1234yf, since LFL is 0.289 kg/m³, up to 3.76 kg can be used. We proposed this content to the IEC as DC (Document for Comments) for the next revision.

7.6.2 Surface temperature

The provision of IEC 60335-2-89 prohibits the temperature of a surface exposed to leaked flammable refrigerants to exceed the auto-ignition temperature of the refrigerant reduced by 100 K. However, the International Standard IEC60335-2-40 for air conditioners permits a surface temperature of up to 700 °C for A2L because the refrigerant has a lower flammability. Therefore, the Japanese Standards specifies that the temperature of a surface exposed to A2 and A3 refrigerants should not exceed the auto-ignition temperature of the refrigerant reduced by 100 K, and the temperature of a surface exposed to A2L refrigerant should not exceed 700 °C. We also proposed this content to the IEC as DC toward the next revision.

7.6.3 Measurement exemption time and leakage test exemption

Analysis of the refrigerant leakage clarified that when a door is opened after leakage of the total amount of refrigerant into the refrigerated space of a reach-in refrigerated display cabinet, a large flammable cloud is generated outside the refrigerated display cabinet (see 7.3.1). IEC stipulates the measurement exemption time of 5 min (see 7.2.3) and the generation of the flammable region during this period is ignored. Since static electricity, relays in a store, etc. are the ignition sources for A3 refrigerant, the generation of a flammable region even for a short time may lead to an ignition accident. Therefore, the Japanese Standards eliminates the measurement exemption time of 5 min and stipulates that the generation of the flammable region is not allowed from the start of the test. Furthermore, to prevent the generation of a flammable region outside the refrigerated space, it provides the means for detecting the leakage inside the refrigerated space and the equipment for shutting off the refrigerant circuit, and it also stipulates that the test leaked from the refrigerated space becomes unnecessary when such means are equipped. Moreover, JRA Standards stipulates that concerning the leakage from the condensing unit consisting of a compressor and a condenser, when the air flow rate satisfies the equation of Colbourne et al.⁷⁻²⁾ (Eq. (7-10)), the test leaked from the condensing unit becomes unnecessary. The refrigerant leak analyses already verified that the air flow rate of this equation does not generate a flammable region (see 7.3.2).

7.6.4 Refrigerant leak rate

IEC 60335-2-89 provides a unique equation (Eq. (7-2)) for the refrigerant leak rate. JIS C 9335-2-89 adopts the same provision as IEC 60335-2-89. On the other hand, International Standard IEC 60335-2-40 for air conditioners provides the *leak rate of total amount in 4 min*. The leak rate is from the size of the hole or crack produced caused by various effects, such as corrosion and vibration, and the pressure difference between the inside and the outside of the piping irrespective of the type of appliance. Therefore, the JRA Standards decided to adopt the *leak rate of total amount in 4 min* for safety and to use it for the refrigerant leak test (7.2.3) and the calculation of the air flow rate using Eq. (7-10). For 0.5 kg of R290, the *leak rate of total amount in 4 min* is 7.5 kg/h, which is 2.8 times the value (2.66 kg/h) calculated using the IEC equation.

7.6.5 Ensuring safety while working

IEC 60335-2-89 has no provision for ensuring safety while working. JRA Standard (JRA GL-21) has the provision for reducing the ignition risk, such as wearing gloves to prevent static electricity and carrying a portable leak detector. In addition, it has provisions for the elimination of ignition sources from around the appliance and the allocation of sufficient ventilation during the disposal and the charging of refrigerants at the repair of refrigerant circuits on site.

7.7 Task for risk assessment

The built-in refrigerated display cabinet is handled with refrigerant contained in the refrigerant circuit from the transportation to the removal. The risk assessments of JRAIA assume various causes of refrigerant leakage, such as initial failure, corrosion or vibration during use, and impact from outside the piping during work, set the flammable volume-time integration at the time of the refrigerant leakage to the value assuming the worst-case scenario, and handles unclear ignition source as igniting. It sets the refrigerant leak probability due to the initial failure and corrosion/vibration during use on the basis of investigation results and considers that it is rare to fall into a situation more dangerous than the assumption of the current risk assessment because the impact from outside the piping is hardly considered to directly lead to refrigerant leakage.

The repair in the store is required at a large-size built-in refrigerated display cabinet difficult to carry. While conducting repairs in the store, the following tasks is required and should be performed carefully: disposing refrigerants from the refrigerant circuit, and charging the equipment with refrigerants. In the risk assessment, human error during work is set assuming that work is performed in a relaxed state. However, when the refrigerated display cabinet is used for storing food, a time restriction may be imposed on the repair work because of the storage temperature of food. In this situation, the reduced time for repair work may lead to mistakes and in turn severe accidents. Therefore, concerning in-store repair, it is important that safety measures are implemented to prevent ignition accidents, especially if human error occurs more than when in a relaxed mental state. Thus, JRA Standard (JRA GL-21) provides content (work procedure) on the basis of this viewpoint while referring to the provision of the High Pressure Gas Safety Act.

Compliance with JRA Standards is important to ensure safety. However, since JRA Standards are not the law, the activities to make known is important in relation to contents that should be observed by persons other than those involved in the manufacturer of products.

In addition, the safe disposal of the appliance after removal is also important for the commercialization of the appliances. The built-in refrigerated display cabinets are disposed of according to the Waste Management and Public Cleansing Act. JRAIA proceeds with the preparation of the manual providing the procedure concerning the disposal of the appliances at the stage of delivering the built-in freezing and refrigerating appliances using flammable refrigerants to a disposal company, and proceeds with studies in collaboration with Ministry of Environment concerning the safe disposal method.

7.8 Summary

Concerning built-in refrigerated display cabinets using A3 refrigerants, such as R290, we explained the results of provisions so far and the situation of the studies for International Standard, the refrigerant leak analyses, the risk assessment from transportation to removal, and Japanese Standards and laws for safely operating the appliance. In addition, the tasks concerning the risk assessment were also described. JRAIA provided methods for safely operating the products in the

Japanese Standards on the basis of risk assessments. Furthermore, we are also proceeding with studies for laws and regulations in collaboration with related ministries and agencies. However, since the proposal of study contents will be made to the International Standard Organization for incorporation is important in order to ensure the safety of appliances imported from overseas, further studies are required.

References

- 7-1) IEC 60335-2-89:2019, “Household and similar electrical appliances - Safety - Part 2-89: Particular requirements for commercial refrigerating appliances and ice-makers with an incorporated or remote refrigerant unit or motor-compressor”, (2019.6).
- 7-2) D. Colbourne and K. O. Suen: “Minimum Airflow Rates to Dilute R290 Concentrations Arising from Leaks in Room Air Conditioners”, 13th IIR Gustv Lorentzen Conference, 1104, Valencia (2018).
- 7-3) Y. Okabe: “Probability and statistics — Model solution of sentence problem,” pp. 131-133, Asakura Publishing, Tokyo (2010). (in Japanese)
- 7-4) http://izumi-math.jp/W_Takakura/k_kakuritu/k_kakuritu.pdf: (W. Takakura: “Teaching material concerning geometric probability” (2020). (in Japanese)
- 7-5) Environment and Energy Research Division, Mitsubishi Research Institute, Inc.: “Report of infrastructure establishment project for energy use rationalization promotion in FY 2015 (Investigation related to study of saving energy measures for equipment)” (Jan. 2016). (in Japanese)
- 7-6) “Risk Assessment of Mildly Flammable Refrigerants Final Report 2016”, JSRAE (2017.3).
- 7-7) David J. Smith: “Reliability, Maintainability and Risk 8th Edition: Practical Methods for Engineers”, Eighth Edition, Elsevier, pp. 395-397 (2011).